Clinical Handbook of Cardiac Electrophysiology

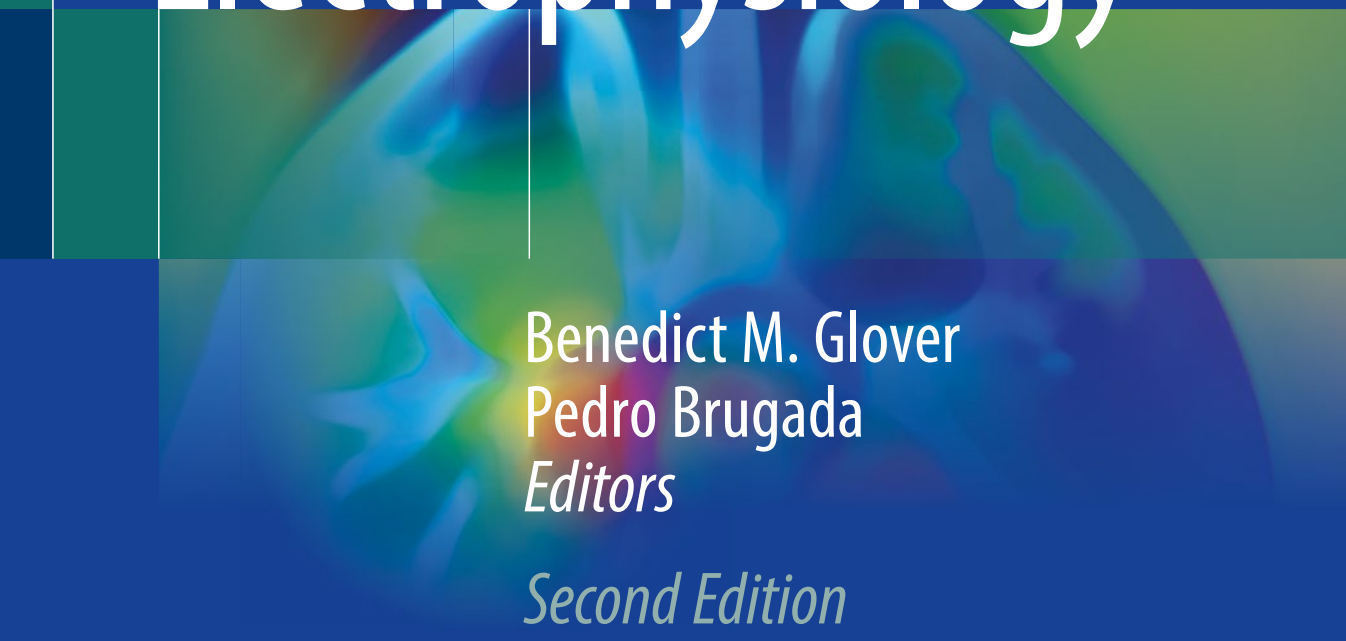

Benedict M. Glover
Pedro Brugada
Editors

Second Edition

Springer

Clinical Handbook of Cardiac Electrophysiology

Benedict M. Glover • Pedro Brugada
Editors

Clinical Handbook of Cardiac Electrophysiology

Second Edition

Springer

Editors
Benedict M. Glover
Division of Cardiology
Department of Medicine
University of Toronto
Toronto, Ontario
Canada

Pedro Brugada
University Hospital of Brussel
Brussels
Belgium

ISBN 978-3-030-74318-5 ISBN 978-3-030-74319-2 (eBook)
https://doi.org/10.1007/978-3-030-74319-2

This Springer imprint is published by the registered company Springer Nature Switzerland AG
The registered company address is: Gewerbestrasse 11, 6330 Cham, Switzerland

Preface

Cardiac arrhythmia management has evolved as one of the most rapidly expanding fields within medicine. The development of catheter ablation has transformed the treatment of many arrhythmias, providing highly effective treatment options for the majority of tachyarrhythmias. There is also considerable research and development of more effective anti-arrhythmic and anticoagulant drugs.

New high-definition mapping technologies and sources of energy have been developed and are discussed widely in this text. Despite these huge technical advances, it is important to understand the basic principles of arrhythmia mechanisms in order to help make a diagnosis and chose an effective treatment strategy.

Although there are many excellent and detailed reference texts in this field, we hope that this provides a practical overview bridging the gap between basic physiology, anatomy, pharmacology and interventional catheter ablations with precise details which should help in the intricate management of the patient.

This book covers all the important aspects of cardiac electrophysiology, presented in an easy-to-use format. For each arrhythmia, the aetiology, classification, clinical presentation, mechanism, electrophysiology set-up (including precise set-up and ablation parameters) and trouble-shooting are presented and demonstrated using illustrations, fluoroscopy images, ECGs and endocavity electrograms.

The overall aim of this book is to provide a logical and practical approach to cardiac arrhythmia management. We hope that this provides a useful resource and, importantly, helps to promote this wonderful sub-specialty.

This book is aimed at cardiac electrophysiologists, fellows, cardiologists, physicians, family practitioners, cardiology trainees, students, allied professionals and nurses. Given its succinct summary of electrophysiology, this should be available as a reference guide in the electrophysiology laboratory. We hope that this reaches a truly international audience and provides an important guide for those studying for heart rhythm exams.

Toronto, Ontario, Canada — Benedict M. Glover
Brussels, Belgium — Pedro Brugada

Success comes from a combination of your heart's passion, your brain's purpose and your body's persistence

KLHBMG2021

Contents

Editors and Contributors

Editors

Benedict M. Glover Division of Cardiology, Department of Medicine, University of Toronto, Toronto, Ontario, Canada

Pedro Brugada University Hospital of Brussel, Brussels, Belgium

Contributors

Jason Andrade Division of Cardiology, University of British Columbia, Vancouver, BC, Canada

Adrian Baranchuk Queens University, Kingston, ON, Canada

Noel G. Boyle University of California, Los Angeles, CA, USA

Jason S. Bradfield UCLA Cardiac Arrhythmia Center, Ronald Reagan UCLA Medical Center, Los Angeles, CA, USA

Duc H. Do University of California, Los Angeles, CA, USA

Paul Dorian Department of Medicine, University of Toronto, Toronto, ON, Canada

Michel Haissaguerre Cardiac Electrophysiology and Cardiac Pacing Department, CHU de Bordeaux, University of Bordeaux, Bordeaux, France

Haris M. Haqqani Faculty of Medicine, University of Queensland, Brisbane, QLD, Australia

Justin Hayase UCLA Cardiac Arrhythmia Center, Ronald Reagan UCLA Medical Center, Los Angeles, CA, USA

Kathryn L. Hong Division of Cardiology, Department of Medicine, University of Toronto, Toronto, Ontario, Canada

Siew Yen Ho Royal Brompton Hospital, London, UK

Henry H. Hsia University of California San Francisco, San Francisco, CA, USA

Jacob Larsen Department of Cardiology, Aalborg University Hospital, Aalborg, Denmark

Adam Lee University of California San Francisco, San Francisco, CA, USA

Damian Sanchez-Quintana Faculty of Medicine, Department of Anatomy and Cell Biology, University of Extremadura, Badajoz, Spain

Melvin M. Scheinman University of California San Francisco, San Francisco, CA, USA

Cardiac Anatomy and Electrophysiology

1

Adrian Baranchuk, Benedict M. Glover, Siew Yen Ho, Damian Sanchez-Quintana, and Pedro Brugada

Abstract

Cardiac electrophysiology has rapidly moved from the mapping and ablation of accessory atrioventricular connections and ectopic foci to more extensive mapping and substrate modification. Training in cardiac electrophysiology requires a detailed knowledge of the anatomy and physiology of the heart. In order to understand the basis of cardiac electrophysiology it is important to discuss the different phases of the cardiac action potential, variability in morphology and duration throughout the heart and the most important ion channels and electrolyte shifts responsible for depolarization and repolarization of the cardiac cells. Electrophysiology continues to rely heavily on an understanding of these basic principles as well as the relevant anatomy of all cardiac chambers and surrounding structures. It is therefore fundamental to have a thorough understanding of cardiac anatomy as visualized on fluoroscopy, echocardiography, CT, MRI and three-dimensional cardiac mapping systems.

A. Baranchuk (✉)
Queens University, Kingston, ON, Canada
e-mail: adrian.baranchuk@kingstonhsc.ca

B. M. Glover
Division of Cardiology, Department of Medicine, University of Toronto, Toronto, Ontario, Canada

S. Y. Ho
Royal Brompton Hospital, London, UK

D. Sanchez-Quintana
Faculty of Medicine, Department of Anatomy and Cell Biology, University of Extremadura, Badajoz, Spain

P. Brugada
University Hospital of Brussel, Brussels, Belgium
e-mail: pedro@brugada.org

The Cardiac Action Potential

Spontaneous depolarization of cells within the sinus node (SN) results in propagation of excitation throughout adjacent cells within the right atrium (RA) and left atrium (LA). The electrical impulse spreads through the atrioventricular (AV) junction into the His bundle, through the Purkinje network and then into the ventricular muscle where activation occurs from the septum spreading through the endocardium, mid-myocardium and finally the epicardium.

Each cardiac cell undergoes a process of depolarization and repolarization, which is recorded across the cell membrane as an action potential and occurs as a result of the relative concentration of ions (predominantly potassium, sodium and calcium) and electrostatic forces across the membrane. As shown in Fig. 1.1 this is composed of five components in atrial and ventricular myocytes and three components in the SN and AV node. The QTc on the surface ECG is an approxi-

B. M. Glover, P. Brugada (eds.), *Clinical Handbook of Cardiac Electrophysiology*,
https://doi.org/10.1007/978-3-030-74319-2_1

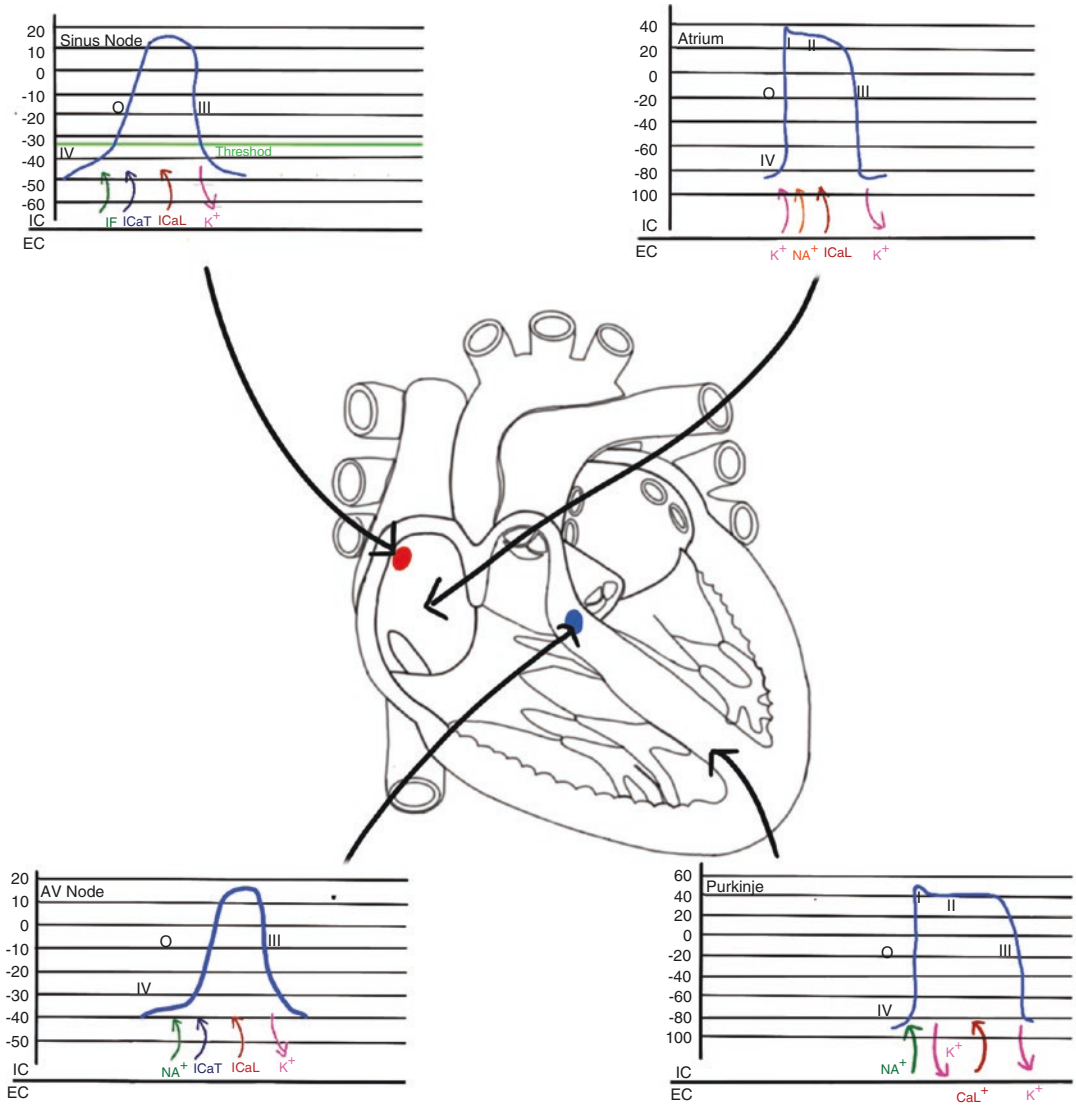

Fig. 1.1 Cardiac action potentials recorded from the sinus node, atrium, AV node and Purkinje network and the predominant ionic currents responsible for these changes in membrane potential (Na^+: Sodium, Ca^{2+}: Calcium, K^+: Potassium, If: funny current)

mation of the mean duration of the ventricular action potential.

Phase 0 is where the membrane potential becomes positive and is therefore known as **rapid depolarization**.

Phase I, also known as **rapid repolarization** occurs in the atrium and ventricle but not in the SN and AV node. It is much more prominent in the Purkinje and epicardial cells.

Phase II is the **plateau phase** where the action potential becomes relatively flat and does not occur in the SN or AV node. It is followed by **Phase III,** which is known as **rapid repolarization** resulting in restoration of the membrane potential to the resting phase.

Finally, **Phase IV** is known as the **resting membrane potential.** This is recorded as −80 to −95 mV in atrial, Purkinje and ventricular cells. It is slightly less negative in the atrium than the ventricle. In the SN it is −50 to −60 mV and the AV node −60 to −70 mV. In both the SN and AV nodes there is a slow spontaneous diastolic depo-

larization which merges with Phase 0 resulting in spontaneous automaticity while Phase IV in other cells is generally more flat.

Phase IV (Resting Phase)

In the atrium and the ventricle this occurs largely as a result of the balance of potassium (K^+) across the cell membrane and is relatively flat with only a very slight slope.

K^+ is found in much higher concentrations in the intracellular space compared with the extracellular space. As a result of this there is an outward motion of K^+ leaving predominantly negative anions inside the cells at baseline.

This is counteracted during the resting phase by the inward rectifying current, (IK1). In general rectifier currents allow current to pass in a preferential direction. In the case of IK1 the transmembrane channel responsible allows the inward movement of K^+ at more negative potentials than the reversal outward K+ potential with less current movement at more positive membrane potentials (Dhamoon and Jalife 2005). This results in a very slight upward curve as the cell becomes less negative.

The resting phases in the SN and AV node are different from those recorded in the atrium and ventricle. As well as being less negative there is a continual slow spontaneous diastolic depolarization. This occurs as a result of the funny current (If) which plays the predominant role in this phase as opposed to the Ik1 current. This current is activated at voltages in the diastolic range resulting in a slow and steady inward Na^+ current (INa) which would normally occur in the depolarization phase in atrial and ventricular cells. There is also a slow outward movement of K^+ with the overall combined effect of a less negative cell membrane potential.

Phase 0 (Depolarization)

In the atrium and ventricle as a result of electrical stimulation from adjacent myocytes, a rapid inward sodium current (INa^+) results in the abrupt initial upstroke in the action potential known as Phase 0.

There are principally two Na^+ gates responsible for depolarization called the **activation** and **deactivation gates**. At the start of depolarization the activation gates are closed while the deactivation gates are open. As the action potential becomes less negative the activation gates tend to open rapidly allowing the inward movement of Na^+ while the deactivation gates tend to close slowly. This continues beyond zero voltage at which point/;the rate of Na^+ entry into the cell slows. As the deactivation gates close the fast Na^+ channels become inactive. These remain closed until Phase III of the action potential.

Depolarization in the SN and AV node does not occur as a result of INa^+ but rather as a result of calcium entry through the L-type calcium channels (ICaL) and T-type calcium channels (ICaT).

Phase I (Early Repolarization)

As the vast majority of the inward current deactivates, a rapid transient outward potassium current (Ito) results in early rapid repolarization. Phase I is much more prominent in Purkinje fibers and in epicardial myocytes and does not occur in the SN or the AV node.

Phase II (Plateau Phase)

The plateau phase occurs in the atrium and ventricles as a result of an inward movement of calcium ions (ICaL) combined with an outward movement of potassium (IKs, IKr and IKUr). As the voltage becomes less negative during depolarization the ICaL and ICaT channels become active.

ICaL channels are the predominant type found in cardiac myocytes and are activated when the voltage reaches −30 mV. ICaT channels which are less common in cardiac myocytes are activated at more negative voltages.

Overall ICaL activation begins in late depolarization. Ca^{2+} crosses from outside the cell where the concentration is higher relative to the inside.

K^+ shift is also partially responsible for the plateau phase. The balance of K^+ across the cell

membrane is similar to that during the resting phase but the voltage is positive rather than negative which results in an outward movement of K^+ from the cell. The overall balance between the inward movement of calcium and the outward movement of K^+ results in the plateau phase. The transient outward current (Ito) is expressed in the atrium more than the ventricle. As a result of this there is a greater outward movement of K^+ versus the inward movement of calcium resulting in a shorter plateau phase.

Phase II does not occur in the SN or the AV node.

Phase III (Repolarization)

As the outward movement of K^+ exceeds the inward movement of Ca^{2+} the voltage becomes more negative resulting in repolarization. Although the delayed rectifier currents Ikr and Iks are activated during depolarization their action tends to be delayed and gradually increases during the plateau phase. Next to Ito the inwardly rectified K^+ current (Ik1) is also responsible for repolarization although this is more active as the voltage across the cell membrane becomes less negative and is responsible for the small bump seen in the action potential during repolarization.

All these K^+ currents are responsible for restoration of the K^+ balance. The Na^+ which entered the cell during depolarization is removed by the Na^+/K^+ ATPase enzyme while calcium which entered the cell during the plateau phase is removed by the Na^+/Ca^{2+} exchanger.

Repolarization in the SN occurs as a result of the rapid outward movement of K^+ as well as inactivation of the inward Ca^{2+} current making the cell more negative.

Refractoriness

Refractoriness describes the period after phase 0 of the cardiac action potential during which a stimulus does not result in a new depolarization.

There are three different types of refractory periods (RP): relative, absolute and effective.

The **relative RP** is the longest coupling interval resulting in local capture therefore marking the end of refractoriness.

The **absolute RP** is the longest coupling interval which does not result in in local capture. The absolute and relative RP's are depicted in Fig. 1.2.

The **effective RP** is the longest coupling interval delivered which fails to propagate through the distal tissue.

In the clinical electrophysiology laboratory the RP is calculated by performing an **extrastimulus test**. In order to perform this the threshold for stimulation is measured in diastole by pacing at a fixed rate and decreasing the intensity of the pacing stimulus until capture fails.

Following a drive of eight beats at a fixed rate (to establish a steady state) a single extrastimulus is introduced at twice the diastolic threshold at shorter intervals until capture no longer occurs. This can be seen in Fig. 1.3 where pacing from the high RA is performed at a cycle length of 600 ms for 8 beats (drivetrain) in order to achieve

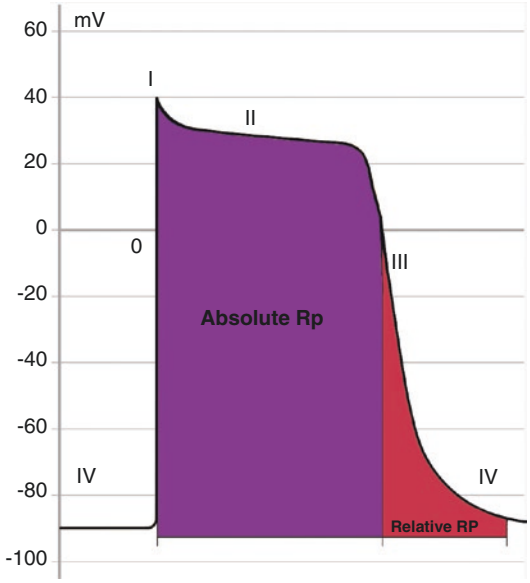

Fig. 1.2 Diagram showing the absolute RP and relative RP during the cardiac action potential. The absolute RP occurs from phase 0 until the transmembrane potential reaches −60 mV during phase III. During this time a stimulus will not result in depolarization. The relative refractory period follows this in which a high voltage stimulus may result in further depolarization

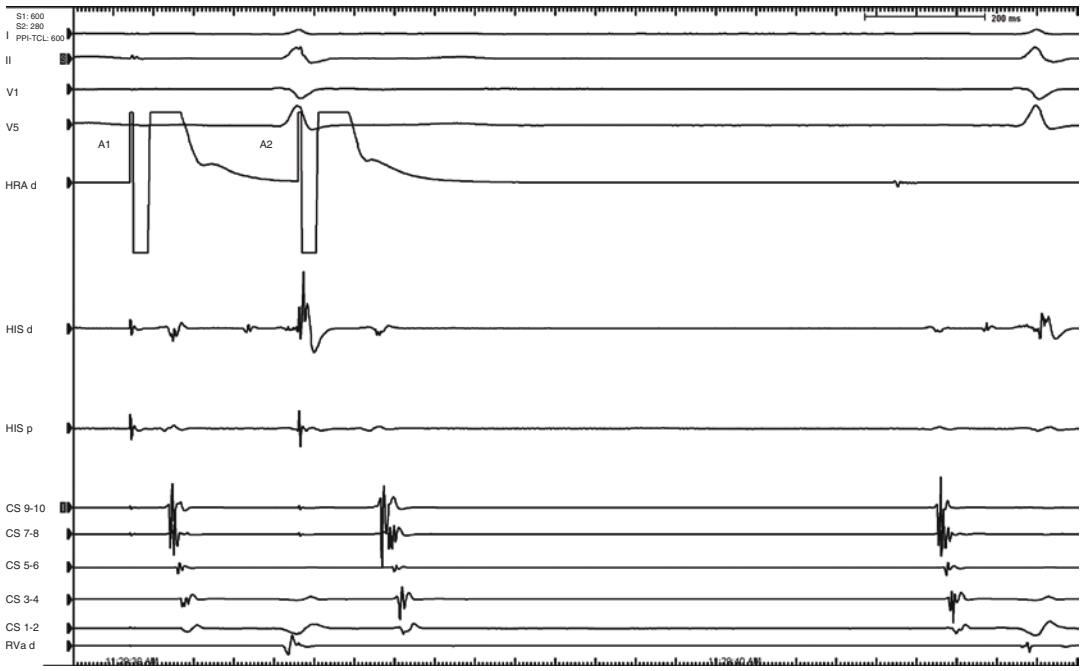

Fig. 1.3 Example of extrastimuli testing by pacing from the high RA (HRA d). The first paced beat on the left of the image is the final beat of the drive train where pacing is performed at 600 ms (A1). This beat conducts through the His to the ventricle via the AVN. This is followed by an extrastimuli which is performed at a progressively shorter cycle length. In this example this occurs at 280 ms (A2). Capture is seen on the high RA (HRA d) and the coronary sinus (CS) with lack of conduction through the AV node. This is considered to represent the AV node refractory period. (CS 9–10 is positioned in the proximal CS while CS 1–2 is in the distal CS, His d is positioned along the distal His, His p along the proximal His and RV a d is positioned in the RV apex)

a steady state followed by a decremental extrastimulus. In this example the first beat on the left is the final beat of the drive train. The extrastimulus occurs at a cycle length of 280 ms and captures the atria but fails to conduct over the AV node. This is considered to be the AV node ERP.

Arrhythmia Mechanisms

Arrhythmias may be classified as either **macro re-entry** or **focal**. Focal arrhythmias may be caused by **micro re-entry, enhanced automaticity, or triggered activity.**

Re-Entry

A very common mechanism of clinical cardiac arrhythmia is re-entry. During re-entry a wave of excitation moves around a circuit which is determined anatomically, functionally or a combination of the two. A macro re-entry circuit which makes understanding of re-entry easy is the circuit during circus movement tachycardia in patients with the Wolf-Parkinson-White (WPW) syndrome (Fig. 1.4).

For re-entry to occur the following conditions have to be fulfilled:

1. There must be two or more pathways for conduction (for example the AV node and accessory pathway in WPW)
2. Unidirectional block in one pathway
3. Alternative conduction over the other pathway with sufficient delay as to retrogradely invade the formerly blocked pathway.

For a re-entry circuit to sustain, the length of the circuit must be greater than or equal to the

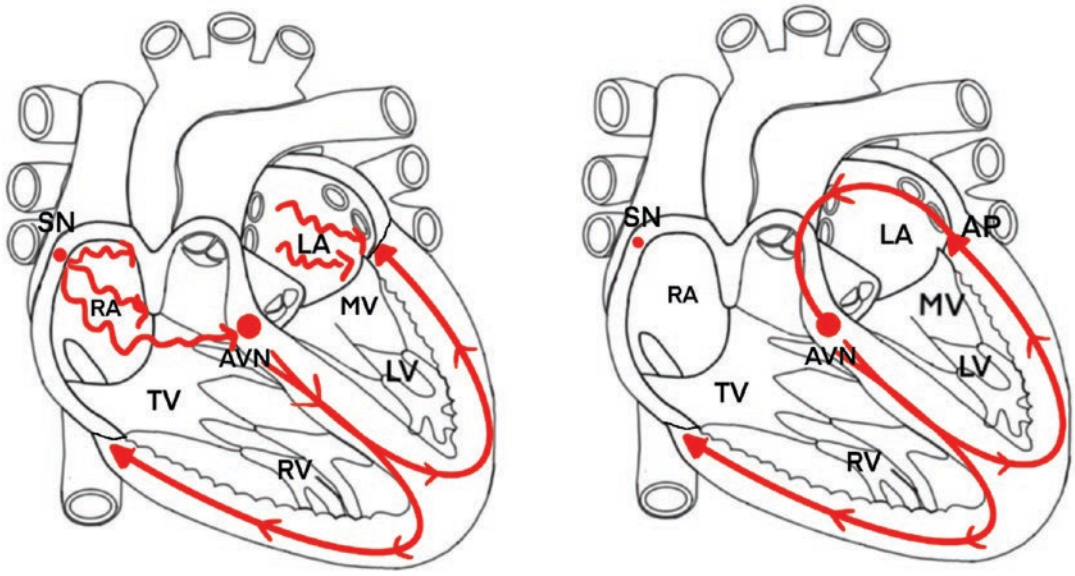

Fig. 1.4 Diagram showing the initiation of circus movement tachycardia (CMT) in a patient with WPW. In the left image conduction occurs antegradely through the AV node and is blocked retrogradely as there is no accessory pathway present. In the right image a re-entry tachycardia is demonstrated utilizing the AV node as the antegrade limb and the AP as the retrograde limb. Arrows indicate the predominant direction of conduction. A denotes atrium, AVN is the AV node, V is ventricle and AP is the accessory pathway

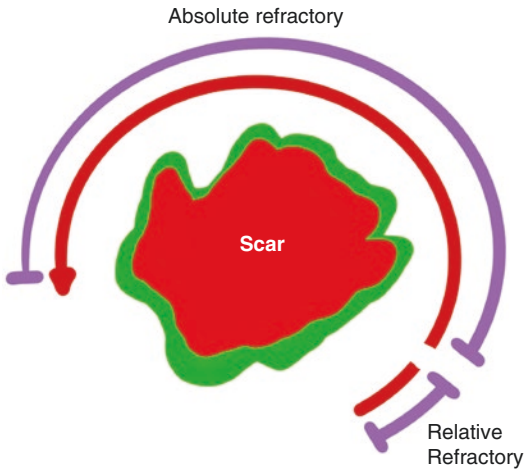

Fig. 1.5 Diagrammatic representation of a re-entry circuit circulating around a conduction barrier in this case scar. The region of tissue where the wavefront is propagating corresponds with tissue during the absolute RP. The tail of the wavefront corresponds with tissue during the relative RP

product of the conduction velocity and the refractory period termed the wavelength of the circuit. The pathways involved in these circuits must therefore have different conduction properties and refractoriness. A slow conduction pathway ensures that the wave of depolarization does not reach tissue which is refractory and thus terminate the arrhythmia.

Another requirement is the existence of a region of conduction block. This may be either anatomical or functional. Anatomical block may be structural such the tissue which exists between the slow and fast pathways in AV nodal re-entry tachycardia (AVNRT) or scar tissue in ischemic VT or functional such as occurs in typical atrial flutter. Functional block occurs as wavelets collide with each other and thus prevents the leading edge of the circuit stimulating refractory tissue resulting in termination of the arrhythmia. Most re-entry circuits involve a combination of structural and functional regions of block. A diagrammatic representation of a re-entry circuit is shown in Fig. 1.5.

The **wavelength of the circuit** is a product of the conduction velocity and the refractory period.

Automaticity

Automaticity results from spontaneous depolarization during phase IV of the AP. Although this

is a feature of automatic cells such as the SN, AV node, His bundle and Purkinje cells, if it occurs in other cells then it is considered to be abnormal (ectopic focus).

Spontaneous depolarization does not normally occur in atrial and ventricular myocytes but may occur as a result of various physiological or pathological changes which on a cellular level may result in a reduction in the expression or function of the IK1 channel (Antzelevitch et al. 2011).

Latent automatic cells are normally suppressed by SN activity and only become functional if the sinus rate becomes slower than the rate of spontaneous discharge of these cells. Some regions of increased automaticity are protected from SN discharge and therefore discharge independently of this. These cells which demonstrate evidence of entrance block with exit conduction are called **parasystolic foci** and tend to result in ectopic beats with intervals which are multiples of each other (Antzelevitch et al. 2011). Incomplete entrance block may also occur resulting in entrainment of the focus at a defined rate resulting in ectopic beats with a fixed coupling interval.

One of the typical features of increased automaticity is the ability to overdrive pace at a rate faster than the tachycardia cycle length. This occurs as a result of an increase in the activity of the Na^+/K^+ ATPase pump resulting in the generation of a hyperpolarizing current which inhibits phase IV of the action potential (Gadsby and Cranefield 1979).

Afterdepolarizations and Triggered Activity

Afterdepolarizations are defined as depolarizations which occur after Phase 0 of the cardiac action potential and may result in a spontaneous action potential known as a triggered response. These are divided into early afterdepolarization (EAD) or delayed afterdepolarization (DAD). These are depicted in Fig. 1.6.

EAD occurs during phase II and phase III while DAD occur after the cardiac action potential is complete. EADs tend to occur when there is an increase in the inward movement of positive ions during the plateau phase of the action potential.

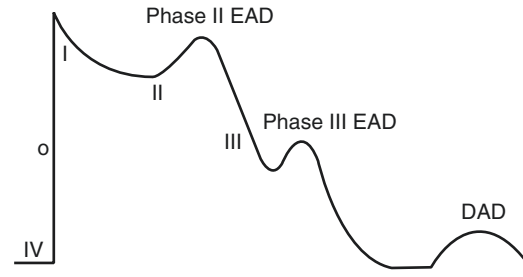

Fig. 1.6 Diagrammatic representation of phase II and phase III early atrial depolarizations (EADs) and delayed atrial depolarizations (DADs) at the end of the cardiac AP

DAD occur as a result of an increase in the inward movement of calcium. This can occur in the setting of digoxin toxicity or in conditions such as catecholamine induced polymorphic ventricular tachycardia (CPVT).

Anatomy of the Cardiac Chambers

The cardiac chambers may be visualized prior to a complex ablation using computed tomography (CT) or magnetic resonance imaging (MRI) or during the procedure using fluoroscopy, echocardiography and electroanatomic mapping (EAM). As shown in Fig. 1.7 the heart lies in an oblique orientation from right and anterior to left and posterior. Posterior to the LA is the esophagus as well as the thoracic aorta.

The majority of procedures rely on a certain amount of fluoroscopic imaging and often our anatomical understanding is based on the locations of the catheters in various views. The most common views in the electrophysiology laboratory are the right anterior oblique (RAO), left anterior oblique (LAO), posterior–anterior (PA) and left lateral (LL). These views are shown in Fig. 1.8.

The RAO projection helps to demonstrate the postero-anterior (PA) location of a catheter within the cardiac chambers and shows the AV groove more clearly than the PA view. In this view the spine is on the left. Moving the catheter to the right results in a more anterior orientation

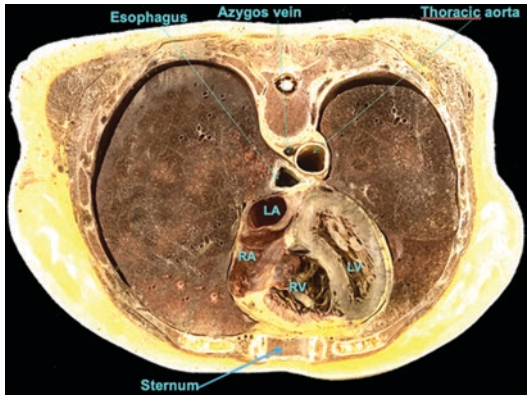

Fig. 1.7 Anatomical location of the heart within the chest wall. The heart is an oblique structure which runs from right anterior to left posterior in which the right atrium (RA) is right and anterior to the left atrium (LA). The right ventricle (RV) is also right and anterior to the left ventricle (LV). Posterior to the heart is the esophagus and the thoracic aorta

while moving to the left is more posterior. The left cardiac border is formed by the RV outflow tract (RVOT) superiorly with the RV superior wall inferior to this and the LV apex at the apex. More steep RAO images result in a greater proportion of the RV being visualized with less LV present. The inferior wall of the RV forms the base of the image while the right cardiac border is formed by the posterior wall of the RA and posterior wall of the LA. The AV annular fat strip is best seen in the RAO projection. This 1 cm thick white line is formed as a result of the overlap of the ring of fat in the right anterior, septal and left posterior annulus and either marks the course of, or is slightly ventricular to the coronary sinus (CS). Any catheter posterior to the fat strip is in the atrium and anterior to this is in the ventricle.

In the LAO view the AV rings are viewed parallel to the image. The left cardiac border is formed by the LA superiorly and the lateral wall of the LV inferiorly. Steeper LAO views image more LA and less LV. The right cardiac border is formed by the right atrial appendage superiorly and the RV free wall inferiorly. In this view the spine is on the right side of the image. In the LAO projection anterior is to the left and posterior to the right.

In the PA view the left cardiac border is formed superiorly by the tip of the left atrial appendage (LAA) and the anterior wall of the left ventricle (LV) more inferiorly and the LV apex at the apex. The right heart border is formed by the superior vena cava (SVC) to right atrial (RA) junction superiorly and the lateral wall of the RA inferior to this. The base is comprised of the inferolateral wall of the RV.

The LL view is very helpful in determining the anterior–posterior location of the catheter. This is useful for trans-septal access as well as for epicardial access in VT ablation.

The RA

The RA lies anterior, inferior and rightward from the LA and is composed of the venous component, appendage and vestibule. The anatomy of the RA and its relationship to aorta and the right and left ventricles is shown in Fig. 1.9.

As shown in Fig. 1.10 the superior and inferior vena cava drain systemic blood into the smooth-walled posterior venous component of the RA. Coronary blood flows through the CS into the RA through the CS os which is located between the inferior vena cava (IVC) and the tricuspid annulus (TA). The CS os is to a variable degree covered by the Thebesian valve which is a thin crescent shaped structure attached at the posterior and inferior boundary of the coronary sinus os. The degree of coverage varies but may practically occlude the CS os in up to 25% of individuals (Hellerstein and Orbison 1951).

The RA appendage is a triangular broad based structure composed of pectinate muscles originating from the **crista terminalis** and is generally where atrial pacemaker leads are positioned for stability. The crista terminalis is one of the most common regions responsible for focal atrial tachycardia's as well as acting as a functional electrical barrier essential for typical atrial flutter. It separates the pectinated appendage from the venous component (or intercaval area) of the atrial body. The latter is posterior whereas the vestibule which surrounds the atrial outlet leading to the tricuspid valve is anterior (Fig. 1.11).

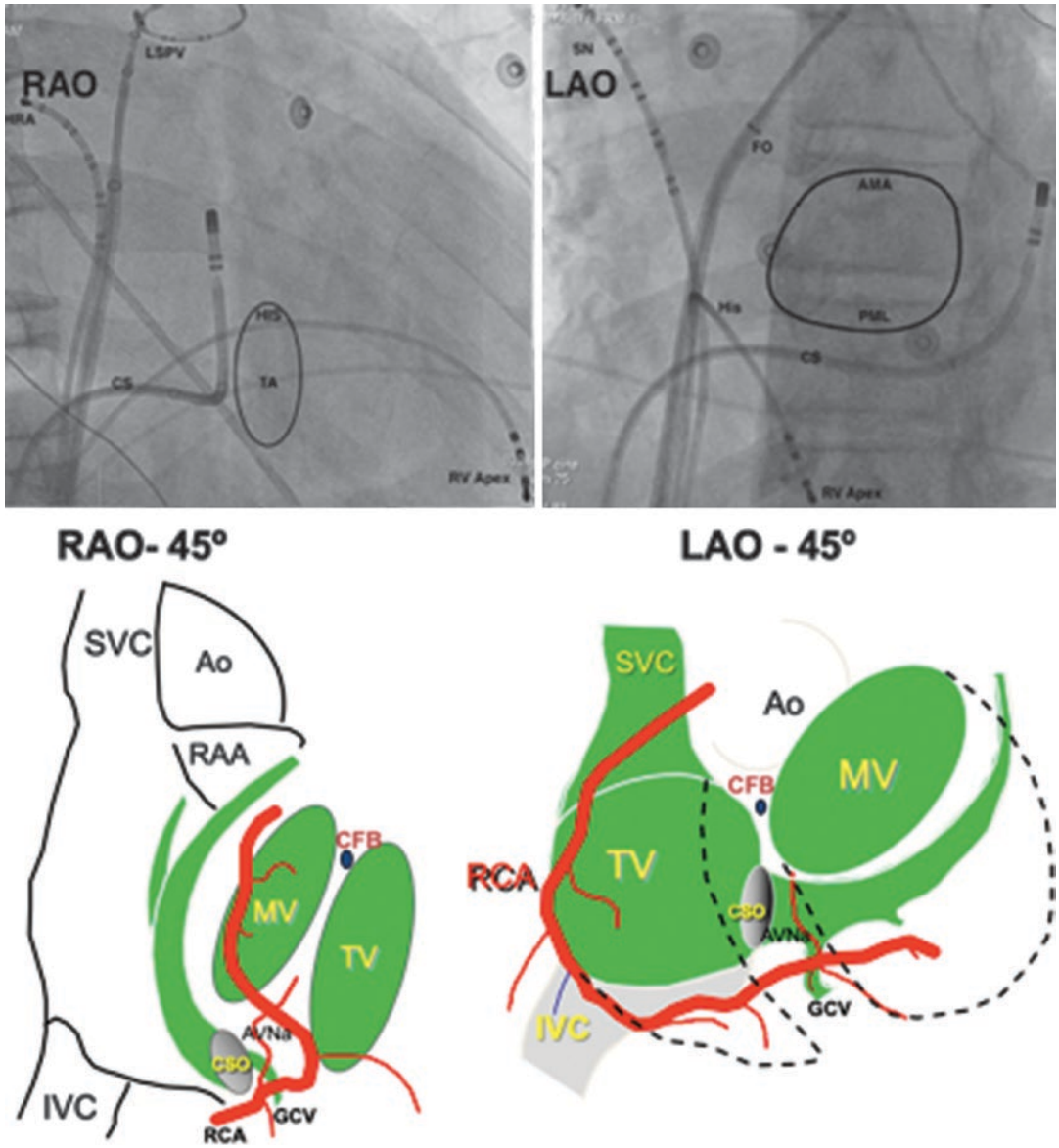

Fig. 1.8 Right anterior oblique (RAO) and left anterior oblique (LAO) views of the heart. Fluroscopic images are at the top and show a catheter positioned in the coronary sinus (CS), RV apex, high right atrium (HRA) close to the sinus node (SN) and a catheter positioned across the fossa ovalis (FO) into the left superior pulmonary vein (LSPV). The location of the His is superimposed on the image. The tricuspid annulus (TA), mitral annulus (MA, anterior mitral annulus (AMA) and posterior mitral annulus (PMA)) and aortic valve (AV) are superimposed

The SN

The SN is a collection of nodal cells within a tough matrix of connective tissue lying just below the epicardium and separated from the endocardium by a layer of atrial myocardium. It is located at the junction between the superior vena cava and the RA, at the antero-lateral quadrant marked by the crista terminalis (CT) and measures 10–20 mm in length, 3 mm in width and 1 mm in depth but there is an enormous anatomical variation between individuals (Opthof 1988) Cells in the SN tend to be much smaller than those in the

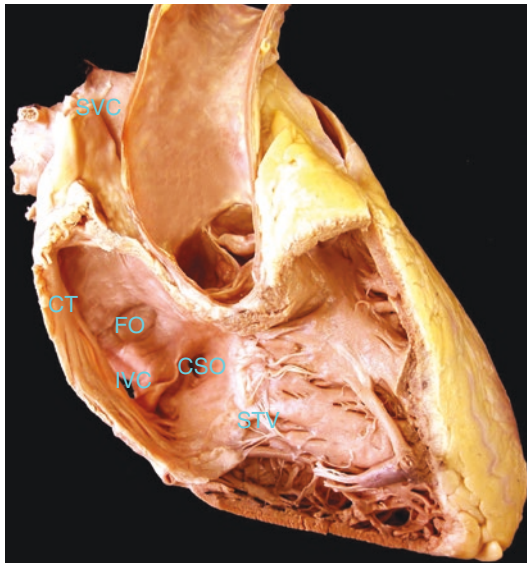

Fig. 1.9 Gross anatomy of the right atrium showing the crista terminalis (CT) along the lateral wall, fossa ovalis (FO) and septum which is posterior to the aorta, inferior vena cava (IVC), superior vena cava (SVC) and septal leaflet of the tricuspid valve

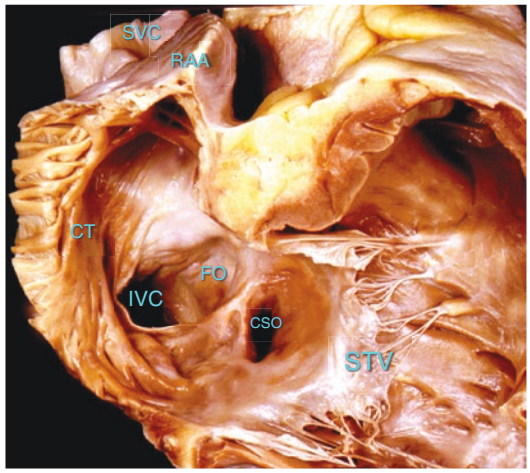

Fig. 1.10 Anatomy of the right atrium showing the superior vena cava (SVC) and inferior vena cava (IVC) entering the smooth wall posterior component of the RA. Blood also flows from the cardiac circulation through the coronary sinus os (CSO) into the RA. The Eustachian valve is seen at the junction with the IVS and the Thebesian valve is seen at the CSO. The pectinate muscles which are predominantly anterior originate from the crista terminalis. The right atrial appendage (RAA) is a muscular structure which is anterior. Also seen is the septal component of the tricuspid valve (STV)

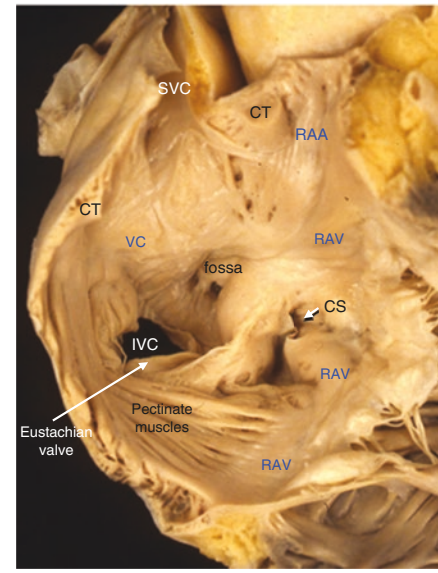

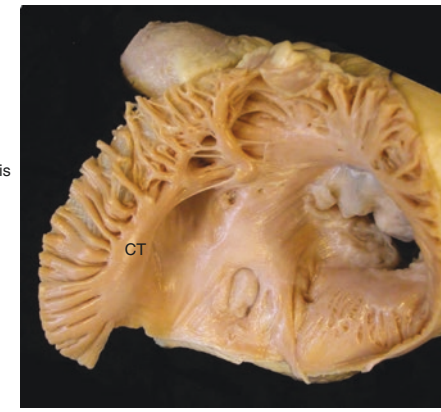

Fig. 1.11 Anatomy of the RA (top image) and the crista terminalis (bottom). The RA is antero-inferior to the LA and is composed of the venous component (VC), RA appendage (RAA) and RA vestibule (RAV). The superior (SVC) and inferior vena cava (IVC) are seen connected posteriorly into the RAV. The RA appendage is an anterior structure composed of pectinate muscles originating from the crista terminalis (CT). The coronary sinus (CS) is inferior and posterior. Superior and slightly posterior on the interatrial septum is the fossa ovalis. In the image below the crista terminalis is seen with pectinate muscles radiating out

RA measuring approximately 5–10 μm. As shown on Fig. 1.12 typical nodal cells known as P cells are located in the centre of the SN and are generally poorly organized myofilaments. There are fibroblasts and collagen fibers interspersed throughout the SN. There is a gradual transition

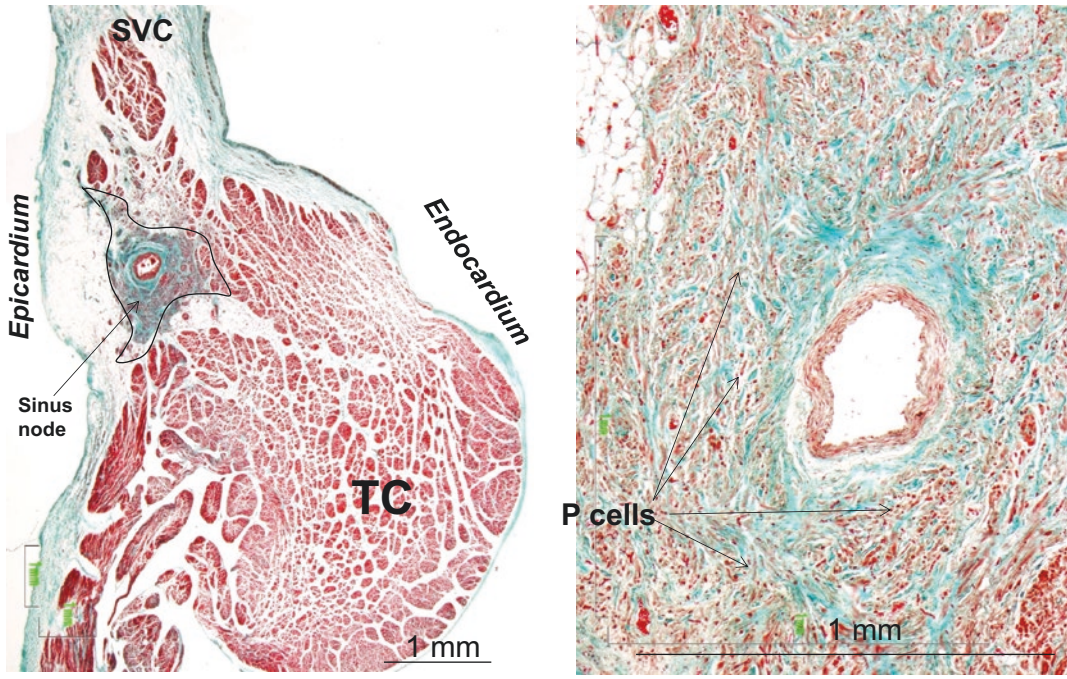

Fig. 1.12 The sinus node is located at the junction between the superior vena cava (SVC) and the lateral border of the right atrium. Its is located close to the epicardial surface and is surrounded by transitional cells which are a mixture of nodal cells and atrial myocytes

between the SN and the RA with a disparity in conduction velocity between the cells thus preventing SN depolarization as a result of atrial depolarization (Boyett et al. 2000).

Spontaneous phase IV diastolic depolarization starts at −65 mV until the activation threshold is reached at −40 mV resulting in rapid depolarization. The action potential of the SN differs from that of a Purkinje myocyte with a more gradual upslope and the absence of a plateau phase. Diastolic depolorization occurs as a result of activation of the If current. This operates in a voltage range more negative than normally occurs in the central pacemaker cells (less than −45 mV). It therefore has maximum activity during hyperpolarization and progressively increases opposing repolarization and then initiating diastolic depolarization (DiFrancesco and Ojeda 1980).

The rate of diastolic depolarization in the SN is affected by both sympathetic adrenergic and parasympathetic muscarinic stimulation. This is predominantly affected by the If channel.

Sympathetic adrenergic stimulation results in an increase in the gradient and duration of diastolic depolarization with minimal effects on the overall action potential duration (DiFrancesco 2010). This occurs as a result of a shift in the activation curve to more positive voltages without a change in the conductance of the If channel as a result of an increase in intracellular cAMP (DiFrancesco and Tortora 1991).

The reverse occurs with parasympathetic muscarinic stimulation (DiFrancesco and Tromba 1988). Slow inward Ca^{2+} channels are involved in the later phase of diastolic depolarization (DiFrancesco 2010). as well as the upslope in the action potential. The transient T type Ca^{2+} channel is activated at more negative voltages and therefore opens first followed by the long lasting L component which opens during the upslope of the action potential (DiFrancesco 2010).

The delayed rectifier Ik channel is the predominant potassium channel in the SN and contributes to repolarization allowing the following depolarization to be initiated.

Respiratory sinus arrhythmia occurs as a result of a reduction in the PP interval with inspiration and a prolongation of the PP interval with expiration. The maximum difference between the longest PP and shortest PP interval should be less than 160 ms. This phenomenon reduces with age.

Ventriculophasic sinus arrhythmia is seen in association with third degree AV block in which the PP interval surrounding a QRS complex is shorter than the PP interval not surrounding a QRS complex.

SN dysfunction encompasses sinus bradycardia, sinus pause, sinoatrial exit block, chronotropic incompetence and inappropriate sinus tachycardia.

Sinus bradycardia is a relatively common finding and in the absence of symptoms is generally of no clinical significance. A sinus pause is defined as the absence of a P wave for greater than or equal to 2 s (although generally not considered clinically significant unless greater than or equal to 3 s while awake or 5 s while asleep). If the duration of the sinus pause is a multiple of the PP interval, then sinoatrial node exit block should be considered. **Chronotropic incompetence** is defined as failure to achieve 70–80% of maximal predicted heart rate (maximal predicted heart rate = 220-age) during peak exercise.

Inappropriate sinus tachycardia is a persistent elevation in heart rate greater than 100 bpm at rest with no obvious precipitating cause. There is an exaggerated increase in sinus rate with minimal activity and a reduction or normalization of sinus rate during sleep. The p wave morphology and axis are unchanged.

It is important to rule out all potential causes as well as other arrhythmias such as right atrial tachycardia close to the SN or SN re-entry tachycardia. Inappropriate sinus tachycardia is most likely multifactorial with a change in the overall autonomic supply to the SN which may include a reduction in the sensitivity to anticholinergic effects or an increased sensitivity to adrenergic activity (Verheijck et al. 1999). Pharmacological options for inappropriate sinus tachycardia include beta adrenergic blockers, nondihydropyridine calcium channel blockers and the selective If channel inhibitor ivabradine. Given the selective nature of ivabradine this has been shown to have a useful role in patients with symptomatic inappropriate sinus tachycardia unresponsive to beta adrenergic blockers and calcium channel blockers (Olshansky and Sullivan 2013). Further data is awaited whether this may be considered as first line treatment in this condition.

Catheter ablation for SN modification is an alternative strategy in select cases of inappropriate sinus tachycardia. The SN is often difficult to modify from the RA endocardium as there are multiple connections with sites of early activation between the SN and the RA. Additionally the bulk of the SN is subepicardial, has a significant amount of connective tissue, is often covered by thick muscle of the CT and there is a significant cooling effect from the SN artery. The usual area to target is the superomedial aspect of the CT targeting areas of local activation 15–60 ms ahead of the surface p wave looking for a reduction in the sinus rate to less than 90 bpm and a 20–25% reduction in the maximum sinus rate with isoprenaline (Cappato et al. 2012). Although acute results are good long term maintenance is less successful (Man et al. 2000). High output pacing should be performed at sites being considered for ablation to avoid phrenic nerve injury. The need for a permanent pacemaker is unusual but a potential complication of this procedure.

Crista Terminalis (CT)

As shown in Fig. 1.11 this is a C-shaped structure which begins septally at the superior aspect becoming more anterior as it traverses the connection with the SVC and then moves posterior and inferior along the lateral wall of the RA towards the junction with the IVC (Sanchez-Quintana et al. 2002). The pectinate muscles which form the right atrial appendage span out from the CT. Approximately two thirds of focal atrial arrhythmias occur along this structure (Ho and Sanchez-Quintana 2009).

RA Conduction

Following discharge from the SN, conduction occurs through the RA using the muscular architecture of the atrial wall that comprises muscle bundles with well aligned working myocytes that preferentially carry the sinus impulse (Kalman et al. 1998). The notion of three specific intermodal tracts is controversial because histologically specialized tissue tracts akin to the insulated ventricular conduction bundles have never been demonstrated anatomically.

Bachmann's bundle, which is also known as the anterior bundle is responsible for right to left atrial conduction (Fig. 1.13). It is not a discrete bundle nor is it insulated with a fibrous sheath. Instead, it is a muscle bundle with well aligned myocytes, superficially located across the anterior interatrial groove. Its rightward extension reaches superiorly to the area of the sinus node and inferiorly toward the right atial vestibule. Usually it is the most prominent interatrial bundle (Ho et al. 2002). It is postulated that epicardial connections between the RA and LA also occur in the Bachamnn's region. This may explain the persistent of inter-atrial conduction even in the presence of advanced inter-atrial block.

Cavotricuspid Isthmus (CTI)

This is the region of slow conduction in typical atrial flutter bounded anteriorly by the septal component of the TA and posteriorly by the Eustachian valve (EV) and the IVC (Fig. 1.14. Conduction in this region is slow due to the criss-cross arrangement of the myocytes and distal ramifications of the crista terminalis relative to the better aligned and circumferential arrangement of myocytes in the vestibule leading to the tricuspid valve (TV) (Cabrera et al. 2005).

In an LAO projection the ablation catheter is generally positioned in the mid isthmus in the 6 o'clock position. In the RAO position the catheter is moved from the right to the left keeping the catheter inferiorly. The EV separates the vestibular inferior RA from the inferior vena cava (IVC). The Eustachian ridge is an elevated region of tissue between the fossa ovalis and the coronary sinus in continuation with the insertion point of the EV. The Tendon of Todaro (TT) runs in this rim towards the AV node (Ho et al. 2002).

The LA is posterior, superior and to the left of the RA. The tip of the left atrial appendage (LAA) contributes to the left side of the cardiac silhouette in a PA image. The LA is a smoother structure with the muscular appendage confined

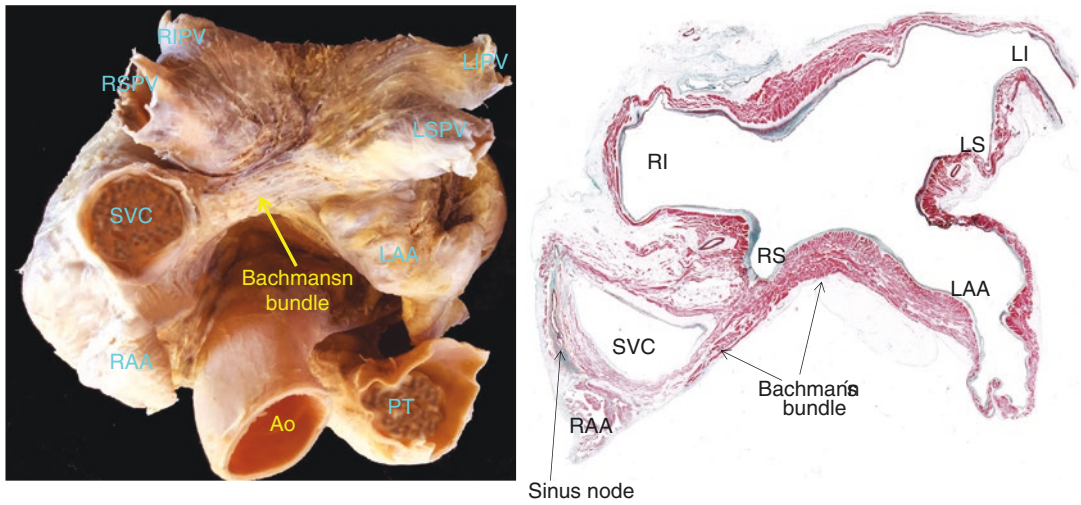

Fig. 1.13 Bachmann's bundle is comprised of parallel atrial myocytes which runs across the interatrial groove and separated from the right atrial wall by fatty tissue. It passes from the region of the sinus node and bifurcates either side of the left atrial appendage (LAA)

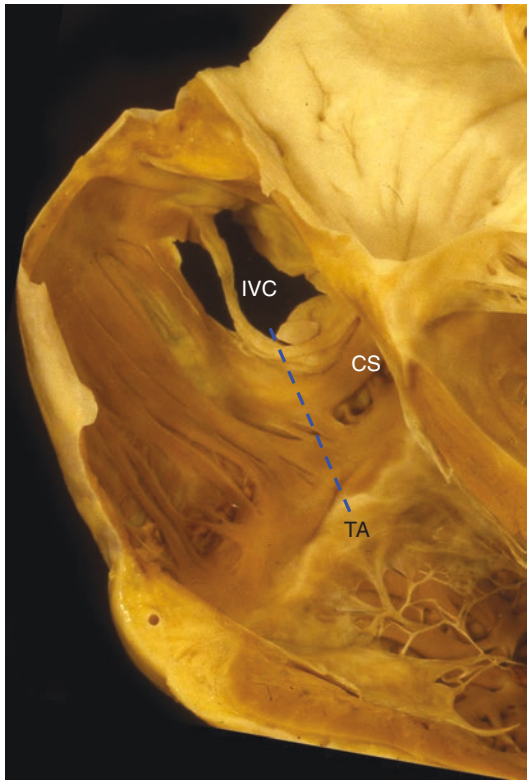

Fig. 1.14 Anatomy of the cavo-tricuspid isthmus (CTI). The CTI runs between the tricuspid annulus (TA) and the inferior vena cava (IVC). The dotted line shows the usual approach taken for catheter ablation of the CTI

to a small tube-like structure arising from the superior and left side of the chamber. As shown in Fig. 1.15 the four pulmonary veins (PV's) drain into the posterior quadrants of the smooth-walled area, which is actually the most posterior region of the heart.

The left sided pulmonary veins are best seen in the LAO projection and are posterior to the left atrial appendage. The right pulmonary veins are best visualized in an RAO projection. The right superior pulmonary vein is posterior to the junction between the right atrium and superior vena cava.

The LA myocardial fibers extend over variable distances into the pulmonary veins. These connections are generally the targets for pulmonary vein isolation.

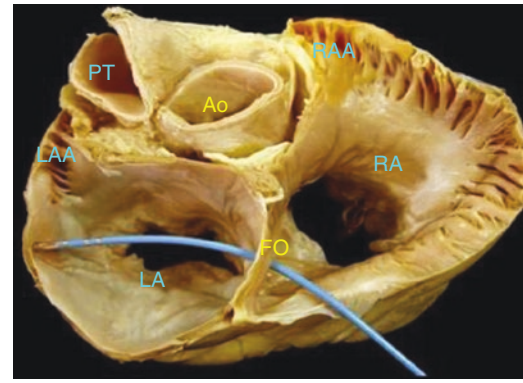

Fig. 1.15 Cross sectional anatomical image (looking from superior) showing that the left atrium (LA) is left and posterior to the right atrium (RA). A catheter is passing through the fossa ovalis (FO) The aorta (Ao) is anterior to the septum whilst the pulmonary trunk (PT) is left and anterior to the aorta. The right atrial appendage (RAA) is right and anterior to the aorta whilst the left atrial appendage (LAA) is left and posterior to the pulmonary trunk

The LA wall is generally a thin structure and therefore care must be taken when manipulating catheters in this region (Fig. 1.16). The lateral wall is approximately 3.9 ± 0.7 mm in thickness, the posterior wall 4.1 ± 0.7 mm, anterior wall 3.3 ± 1.2 mm and the roof 4.5 ± 0.6 mm when measured on cadaver heart specimens (Cabrera et al. 2005).

The LA is anterior to the esophagus. This is of real importance in terms of posterior wall ablation. The esophagus has a variable course in relation to the LA. There is also variability in the thickness of the fibrofatty tissue between the LA and the esophagus. In clinical practice this generally results in the application of lower power (25–30 W) and shorter duration lesion in the posterior left atrial wall in order to attempt to minimize the possibility of esophageal injury. Some operators may monitorized the temperature in the esophagus to reduce power if temperature raises. However, the down side of this approach is delivering sub-optimal lesions in the posterior wall of the LA, which is considered a pro-arrhythmogenic regions.

Anterior to the LA is the ascending aorta which is an important consideration when performing trans septal access.

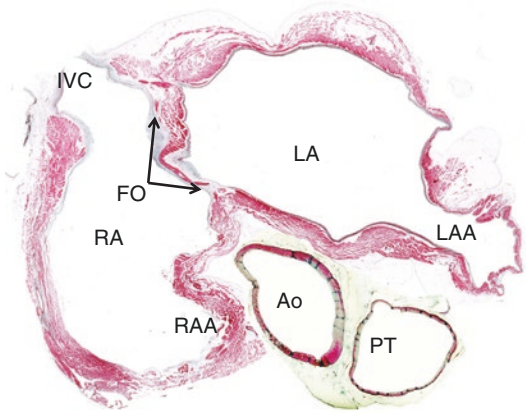

Fig. 1.16 The left atrium (LA) is posterior to the right atrium (RA) and has a much thinner wall. The two chambers share a septum in which the thinnest portion is the fossa ovalis (FO) Although the left atrial appendage (LAA) is much more loculated than the right atrial appendage it has a much thinner wall. The aorta (Ao) is anterior to the septum and posterior and right to the pulmonary trunk (PT)

Atrio-Ventricular (AV) Junction

The compact AV node is the atrial component of the specialized AV junctional area and is located between the coronary sinus os and the septal leaflet of the tricuspid valve (Fig. 1.17). It therefore lies inside the **triangle of Koch (named after Walter Karl Koch)**.

It measures approximately 5 mm in length and is histologically complex. It is not insulated by connective tissue and therefore may potentially be damaged by RF application. The inferior extensions of the compact AV node also run within the triangle of Koch with the rightward extension (fast pathway) parallel to the tricuspid valve and the leftward extension (slow pathway) towards the coronary sinus. These extensions pass either side of the AV nodal artery and also are not protected structures. The histological appearances of these extensions are the same as the compact AV node and are involved in the AVNRT circuit (James 1963). The relationship of the different portions of the His and the compact AV node are shown in Fig. 1.18.

His Bundle

The His bundle is a continuation of the compact AV node and with similar specialized cells although these are more parallel aligned (Ho et al. 1999). It is better insulated than the AV node and therefore is not as easily damaged with RF, although this is still possible. The proximal bundle runs from the distal AV node into the fibrous tissue of the central body where it is termed the penetrating portion. Following this it emerges on the ventricular side of the fibrous body, sandwiched between the membranous septum and the muscular ventricular septum, Taking an initial course usually to the left side of the septum, it then bifurcates into the right bundle (RB) and left bundle (LB) branches, still insulated by fibrous tissue sheaths. The RB tends to have a more anterior origin in the membranous septum.

The CS

The CS is a tubular shaped structure which runs from either the Valve of Vieussens or in its absence the entrance of the vein/ligament of Marshall to the CS os where it enters the RA. It is approximately 7 cm in length (Inoue and Becker 1998) and 6–16 mm in diameter (Sánchez-Quintana and Yen 2003).

As shown in Fig. 1.19 the CS receives blood from the great cardiac vein that channels blood from its tributaries, the anterior interventricular vein, the middle cardiac vein, the left obtuse marginal vein, the right coronary vein and atrial veins of which the most well known is the vein of Marshall. The coronary sinus is generally surrounded by myocardial musculature which extends from the right and left atrial walls (Fig. 1.20) (Chiang et al. 1994). This musculature may extend for a further 2–11 mm along the great cardiac vein (Tschabitscher 1984). Distal to this the venous wall is not surrounded by musculature and therefore perforation through instrumentation is more likely.

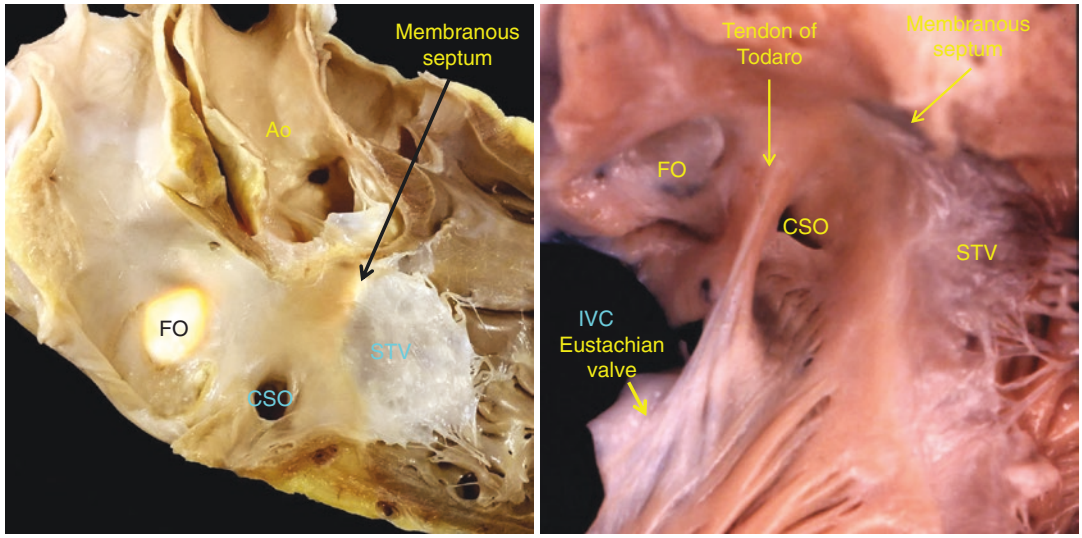

Fig. 1.17 The anatomical location of the AV junction (left) showing the septal leaflet of the tricuspid valve (STV) the membranous septum as well as the proximity to the aorta (Ao), coronary sinus os (CSO) and the fossa ovalis (FO). The boundaries of the triangle of Koch are seen on the right image with the boundaries of the coronary sinus (CS), tendon of Todaro and the septal leaflet of the tricuspid valve (STV). The Eustachian valve is also seen at the junction with the inferior vena cava (IVC)

The Valve of Vieussens rarely causes a significant obstruction to the advancement of a catheter but rather the acute bend in the vein beyond this or an advancement into a side branch are more common causes of cannulation problems. It is therefore better to slowly withdraw and rotate the catheter rather than to try to advance further.

The anterior interventricular vein courses from close to the LV apex and then continues into the great cardiac vein that into the left AV groove under the left atrial appendage (Chauvin et al. 2000). Distally the great cardiac vein receives left atrial veins including the Vein of Marshall and more proximally ventricular veins from the anterior RV and LV and the interventricular septum.

The middle cardiac vein joins the CS close to the os. Occasionally it may also enter the RA directly. As shown in Fig. 1.21 this vein runs along the diaphragmatic surface between the LV and RV with a close proximity to the right coronary artery and in particular the branch to the AV node. It may be used to map accessory pathways in the pyramidal space.

LV Conduction System

The atrioventricular conduction bundle emerges from the central fibrous body to pass below the right and non-coronary cusps and continues into the branching atrioventricular bundle that gives origin to the RB and LB branches (Fig. 1.22).

The LB branch courses along the LV septal surface and divides into three fascicles (Fig. 1.23). The **anterior fascicle** which is **superior** runs towards the base of the anterosuperior papillary muscle, the **posterior fascicle** which is **inferior** runs towards the posteroinferior papillary muscle and in 60% of cases a central or **septal fascicle** which runs to the mid septum. In the remaining 40% of cases this area is supplied by the anterosuperior and posteroinferior fascicles.

Anterior fascicular block is more common than posterior fascicular block and results in a leftward QRS axis deviation poor R wave progression in V1–V3, with a negative QRS in II, III and aVF and positive QRS in lead I. There is also

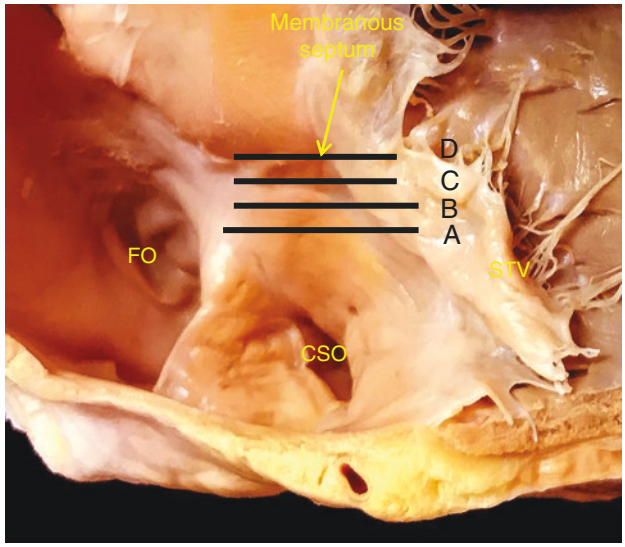

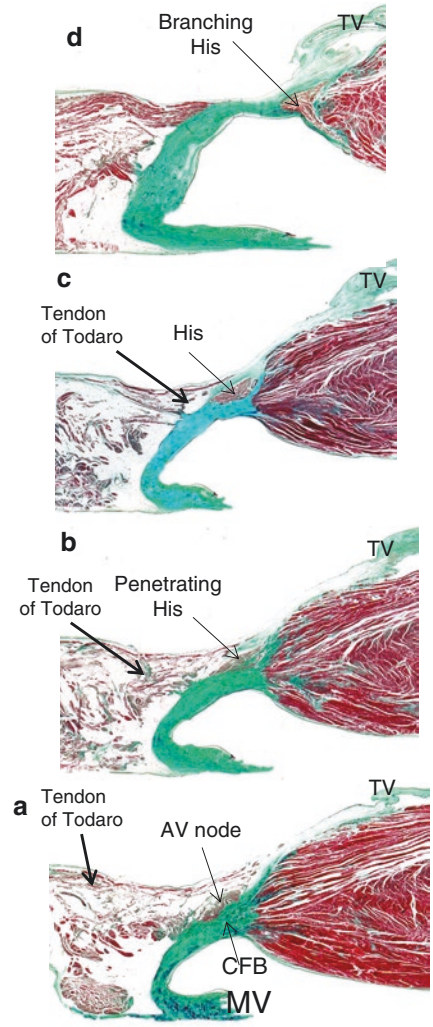

Fig. 1.18 The anatomical location of the compact AV and the bundle of His. The AV node is superior and anterior to the coronary sinus Os (**a**). It penetrates through the central fibrous bosy (CFB) and as it courses superiorly the penetrating His (**b**) continues as the His (**c**) and eventually branches into the right and left bundle

a tall R wave in aVL and aVR. The QRS is not broad.

Posterior fascicular block is less common due to the short and wide nature of this fascicle. The ECG features are a QRS axis greater than 100 degrees with an rS morphology in leads I and aVL; and a qR pattern in leads II, III, and aVF. The QRS is not broad (if not associated to RBBB).

Left septal fascicular block: This remains controversial despite several reports indicating transient block of the septal fibers (midlle fibers). The ECG depicts tall R-waves in lead V2 (>15 mm) in the absence of RVH. There is also loss of q waves in leads V5, V6 and I due to loss or reversal of left to right ventricular septal activation.

Complete bundle branch block occurs as a result of either partial or complete structural or functional block in one of the two bundle branches resulting in a widening of the QRS greater than 120 ms as well as a change in morphology, which generally reflects conduction down the contralateral bundle with secondary repolarisation.

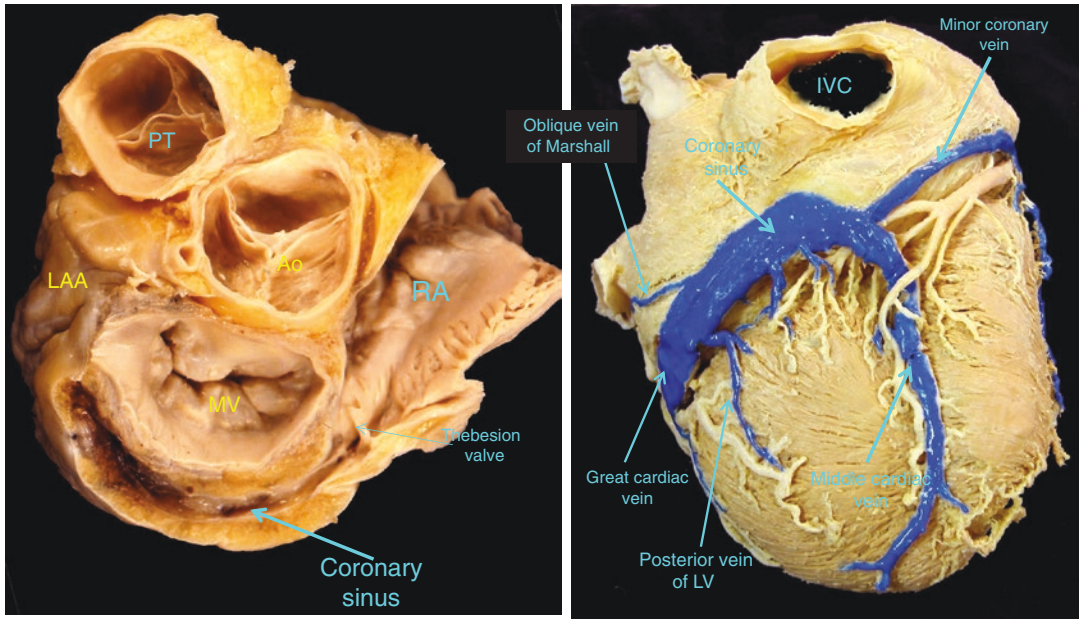

Fig. 1.19 The coronary sinus and its branches. As shown on the image on the left the coronary sinus (CS) runs posterior to the mitral valve (MV) annulus and courses towards the left atrial appendage (LAA) There is often a valve of variable size called the Thebesion valve which is located at the CS Os. As shown on the right the great cardiac vein as well as the posterior veins of the LV and the oblique vein of Marshall drain into the coronary sinus where it joins with the middle cardiac vein and the minor coronary vein

In **left bundle branch block (LBBB)** the initial activation is rightward and anterior resulting in small q waves in I, avL, and V6 with an rS in V2. Following this depolarisation spreads from the apex to the base and to the RV free wall and apex. During this process, septal activation is the pre- dominant force and therefore the vector is anterior and to the left, resulting in a wide slurred QRS in I, aVL and V6 (Fig. 1.24). Depolarization then occurs in a leftward and posterior direction through the LV. Finally, the anterior wall of the LV is depolarized.

RV Conduction System

The RV is anterior to the LV as shown in Fig. 1.25. The RB branch is an insulated bundle of specialized myocytes that runs as a direct continuation of the atrioventricular conduction bundle distal to origin of the left bundle branch. It penetrates the musculature of the ventricular septum toward the midseptum where it becomes subendocardial running along the posterior margin of the septal band. Continuing toward the apex, it divides into several branches one of which courses through the moderator band to the base of the anterior papillary muscle, and then the right ventricular free wall. It gives off septal branches which activate the septum almost immediately after left ventricular activation. Septal activation is generally complete within 35 ms and terminates in Purkinje fibres at the apex.

Right bundle branch block (RBBB) is more common than LBBB and as shown in Fig. 1.24 the initial septal activation is followed by depolarization of the left ventricle, resulting in R waves in I, aVL and V6. Following this, right ventricular free wall and septal depolarization results in S waves in these leads. Overall, the QRS is ≥120 ms in adults with an rsr, rsR, or rSR in leads V1 or V2. The R or r deflection is usually wider than the initial R wave. ST segment deviation is generally discordant to the QRS vector.

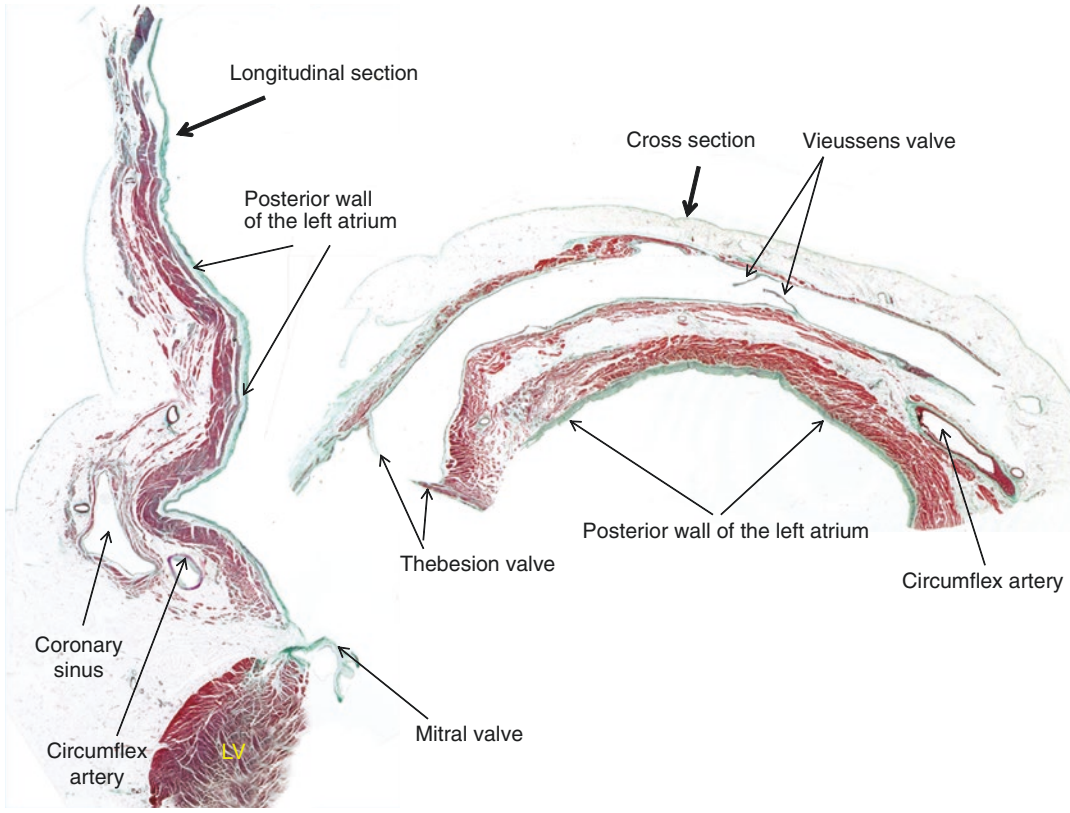

Fig. 1.20 Longitudinal section (left) and cross section (right) of the coronary sinus as it courses around the posterior wall of the left atrium. The opening of the CS into the right atrium often has a Thebesian valve present and the Vieussens valve is more distal. Beyond this valve there is less musculature around the wall of the vein. Also note the proximity of the circumflex coronary artery to the coronary sinus

Aberrant Ventricular Conduction

This occurs when a supraventricular beat conducts rapidly to the His Purkinje system while one of the bundle branches is refractory and then depolarizes the other bundle branch, resulting in a wide QRS complex.

There are four types of aberrancy:

1. Phase III Dependent (Ashman Phenomenon)
   This occurs when a short RR interval follows a longer RR interval. The longer RR interval results in a prolonged action potential in the His and bundle branches. The right bundle usually has a longer action potential duration than the left bundle and therefore the following beat with the shorter RR interval is blocked in the right bundle, which is still refractory and conducts down the left bundle with a RBBB morphology (Fig. 1.26a). This may be seen in AF, where there is a variable cycle length and may be misinterpreted as a PVC.
2. Acceleration Dependent
   This occurs with very slight acceleration of the heart rate (less than 5 ms) at a critical cycle length which is often within normal heart rate ranges. This tends to occur more commonly in the left bundle resulting in a LBBB morphology (Fig. 1.26b). Of note as the rate increases further, the aberrancy often resolves as the action potential duration of the bundles reduces more than that of the AV node. Additionally the action potential dura-

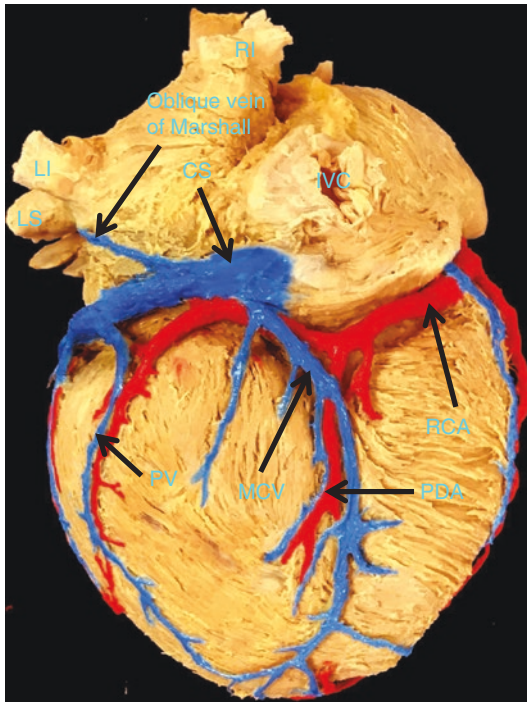

Fig. 1.21 The course of the coronary sinus (CS), the middle cardiac vein (MCV), posterior vein (PV) and the oblique vein of Marshall and its relationship to the right coronary artery (RCA) and posterior descending coronary artery (PDA)

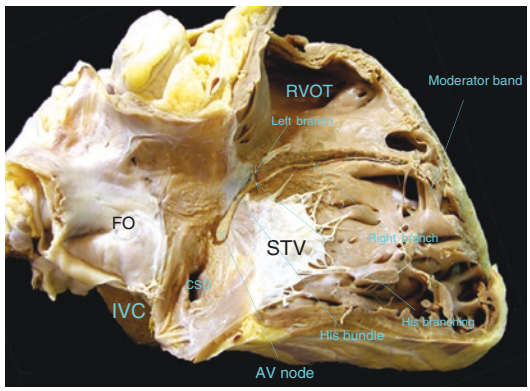

Fig. 1.22 The Compact AV node which is superior and anterior to the coronary sinus os (CSO) continues as the His bundle which then bifurcates into the left and right bundle branches

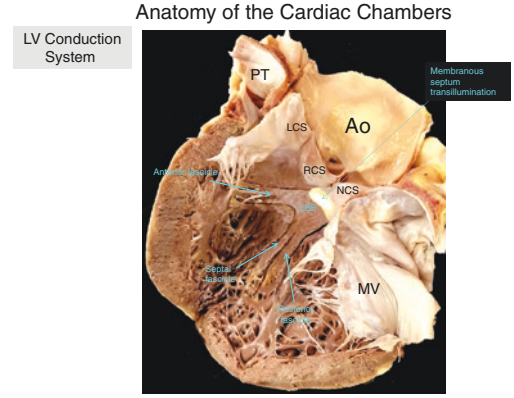

Fig. 1.23 The Left Bundle Branch (LBB) bifurcates on the septum into the anterior, septal and posterior fascicles. (PT pulmonary trunk, LCC left coronary cusp, RCC right coronary cusp, NCC non coronary cusp, MV mitral valve, Ao Aorta)

tion of the bundle branches often reduces in a time dependent manner known as restitution.

3. Deceleration Dependent
   This occurs following a long pause during which a premature atrial beat conducts to the ventricle with a resultant bundle branch block pattern (Fig. 1.26c). This occurs as a result of slow phase IV depolarization of the bundle branches resulting in refractoriness of one of the bundles as the atrial beat results in depolarization. This can be either a RBBB or LBBB pattern,
   An example of deceleration dependent right bundle aberrancy is show in Fig. 1.27. The His catheter is positioned so that the proximal electrogram is recording a His deflection and the distal recording is recording a right bundle potential. The first beat shows a His potential on the proximal electrogram and a right bundle potential on the distal electrogram followed by ventricular activation. Following this a PAC is introduced by pacing the high RA (arrow). The following beat shows a His potential on the proximal electrogram with no right bundle potential on the distal electrogram and a characteristic RBBB pattern on the surface ECG.
4. Concealed Retrograde Conduction
   This occurs when retrograde conduction in one of the bundle branches from a PVC results in refractoriness for the next antegrade beat. As the bundle recovers the next beat which conducts down the contralateral bundle conducts retrogradely up the bundle again. This continues until a different PVC alters the acti-

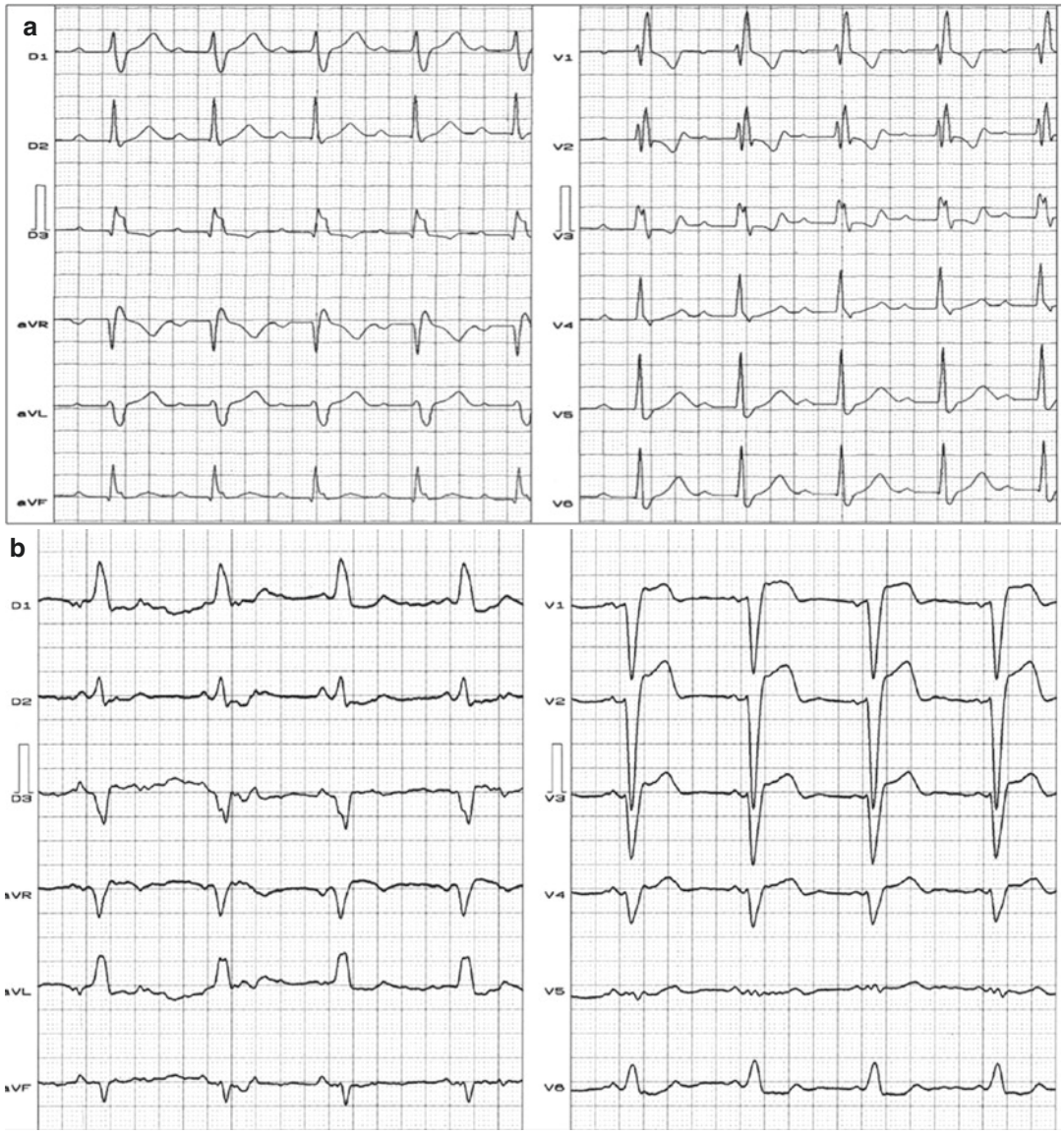

Fig. 1.24 12 lead ECG's showing RBBB (**a**), LBBB (**b**), Left Anterior Fascicular Block (**c**) and Left Posterior Fascicular Block (**d**). The ECG in panel (**a**) shows RBBB with first degree AV block (PR Interval 280 ms). The QRS duration is 120 ms with an rsR pattern in leads V1 and V2. (**b**) This ECG shows a LBBB with a QRS duration of 165 ms. An rS is seen in leads V1 and V2 and a dominant R wave in leads I, aVL and V6. (**c**) This ECG shows a left anterior fasicular block. The QRS duration is within normal range with a leftward axis. There is poor R wave progression V1–V3. The QRS is negative in leads II, III and aVF and positive in lead I. There is also a tall R wave in lead aVL. D: This shows left posterior fasicular block. The QRS axis is in a rightward direction. There is an rS in lead aVL. There is a small q wave in lead III and a dominant R in leads II, III and aVF with the R wave being greater in amplitude in lead III than lead II

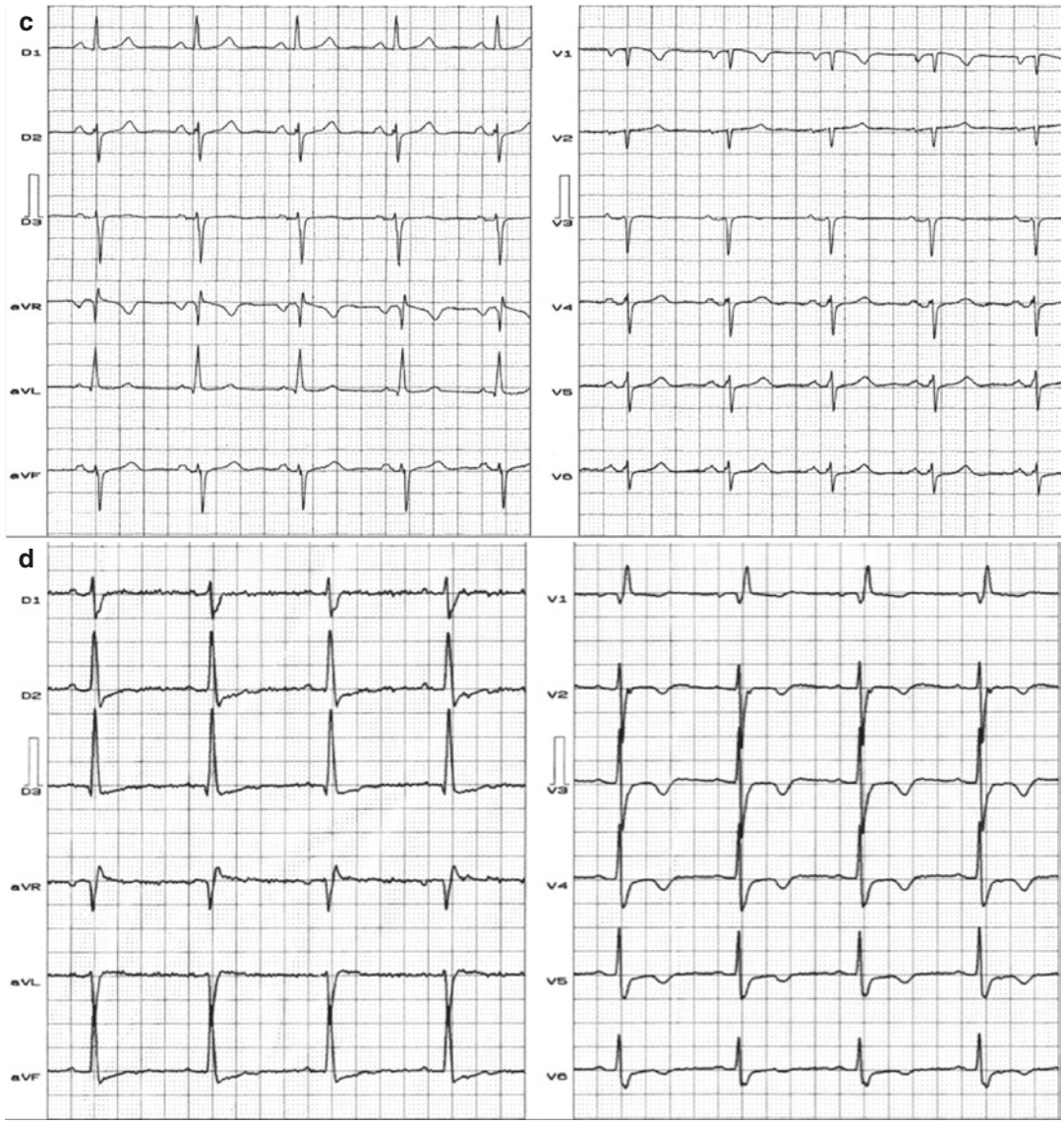

Fig. 1.24 (continued)

vation retrograde activation of the bundle. This is a relatively common cause of aberrancy during SVT.

ECG Signal Acquisition

The ECG is used to record the alterations in electrical potentials during the cardiac action potential. Any number of leads can be recorded in order to electrically visualize the heart from different angles.

The standard 12 lead ECG is composed of six unipolar precordial leads positioned as follows across the anterior chest wall:

V1	4th Intercostal Space Right Parasternal
V2	4th Intercostal Space Left Parasternal
V3	Midway between V2 and V4
V4	5th Intercostal Space Mid Clavicular Line
V5	5th Intercostal Space Anterior Axillary Line
V6	5th Intercostal Space Mid axillary line

The locations of these leads relative to the cardiac chambers can be seen on Fig. 1.28.

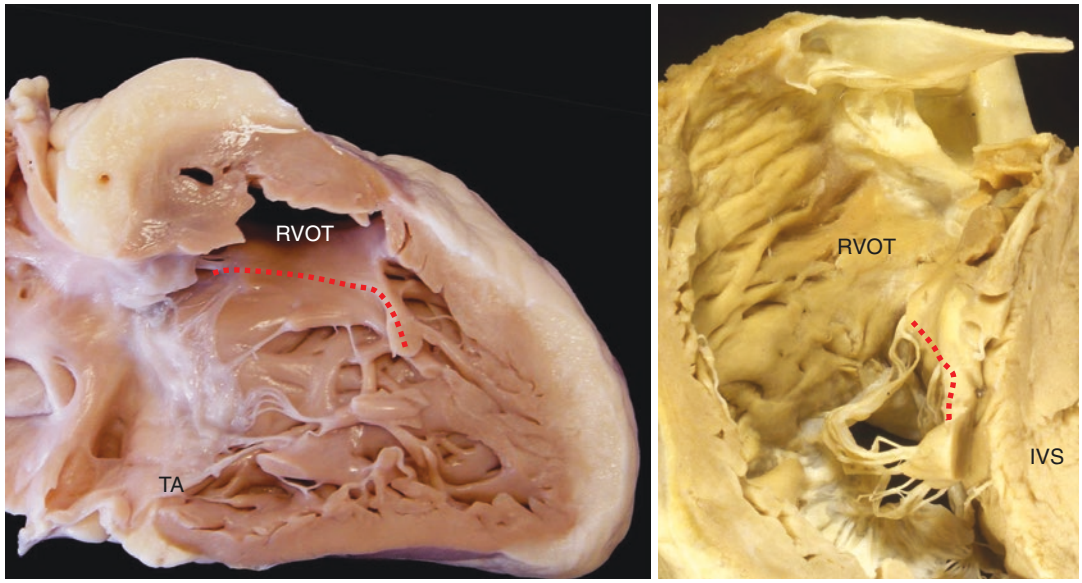

Fig. 1.25 Anatomical image of the Right Ventricle in Right Anterior Oblique (RAO seen on the left) and Left Anterior Oblique (LAO seen on the right) showing the walls of the chamber, interventricular septum (IVS), Tricuspid annulus (TA) right ventricular outflow tract (RVOT)

Each lead records electrical activation between the precordial electrode and **Wilsons Central Terminal** (WCT). This is a theoretical point close to zero potential created from the electrodes between the right arm, left arm and left leg. These vectors create three bipolar leads I (right arm to left arm), II (right arm to left leg) and III (left arm to left leg) through three large resistors. The electrical activation between these three leads therefore cancels out to come close to a zero potential (WCT). The remaining three leads aVR, aVL and aVF are augmented unipolar leads created from the limb electrodes and referenced to **Goldberger's Central Terminal** (GCT) rather than WCT. GCT is created from two of the three limb leads. When aVR is being recorded the GCT is composed of left arm and left leg, for aVL this is formed by right arm and left leg and for aVF is the right arm and left arm.

The right leg lead is used to introduce a current to the patient in order to maintain a voltage equivalent to that of the amplifier. This feeds back an inverse of potential low frequency interference and which increases if this lead is disconnected.

The QRS axis refers to the mean direction of ventricular activation in the frontal plane. In order to calculate the QRS axis the first step is to identify a limb lead where the QRS complex is isoelectric. In theory, the overall direction of electrical activation should be perpendicular to this. As there are two potential perpendicular directions, the leads either side of the isoelectric lead need to be examined and the axis is in the direction of the more positive lead. For example, if the QRS complex is isoelectric in lead I and positive in lead II, the QRS frontal axis is +90. In general principles the QRS axis shifts for several reasons. If there is chamber hypertrophy the QRS axis will shift in the direction of the hypertrophied ventricle as there is a greater component of electrical activation in that direction. In bundle branch block, activation moves from the opposite side to the side with the bundle branch block and

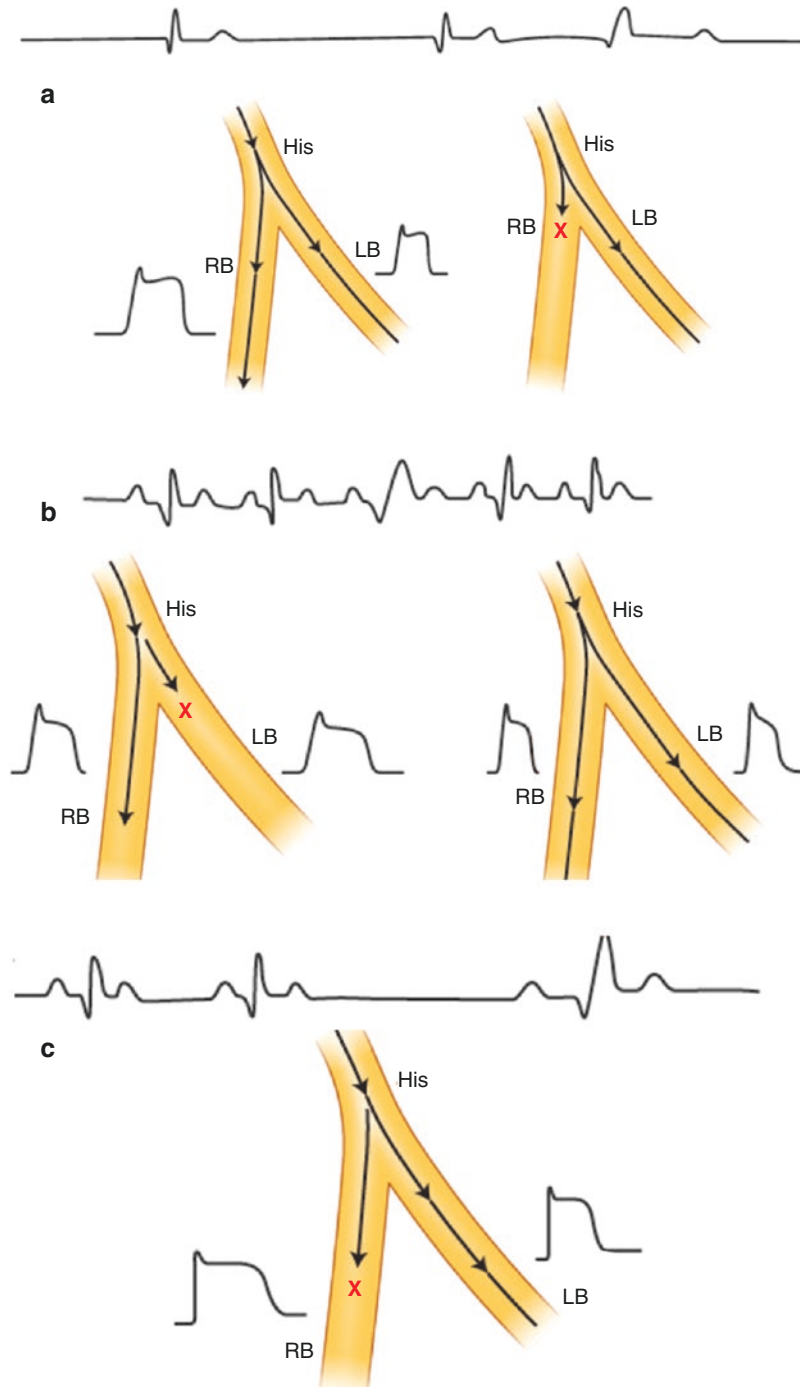

Fig. 1.26 Panel (**a**) demonstrates Phase III dependent aberrant conduction. During AF the longer RR interval on the left results in a prolongation of the action potential in the Right Bundle (RB) and to a lesser extent the Left Bundle (LB). An early activation occurs during phase III of the action potential in the RB resulting in conduction down the LB with a RBBB morphology. In panel (**b**) a very slight acceleration in the RR interval results in antegrade block in the left bundle (LB). An increase in the rate after this results in a narrowing of the action potential duration with normalization of the surface QRS. In panel (**c**) a slow rate with a long pause results in prolongation of the action potential duration in both the right bundle (RB) and left bundle. A premature atrial complex (PAC) conducts through the His and conducts along the LB with block in the RB

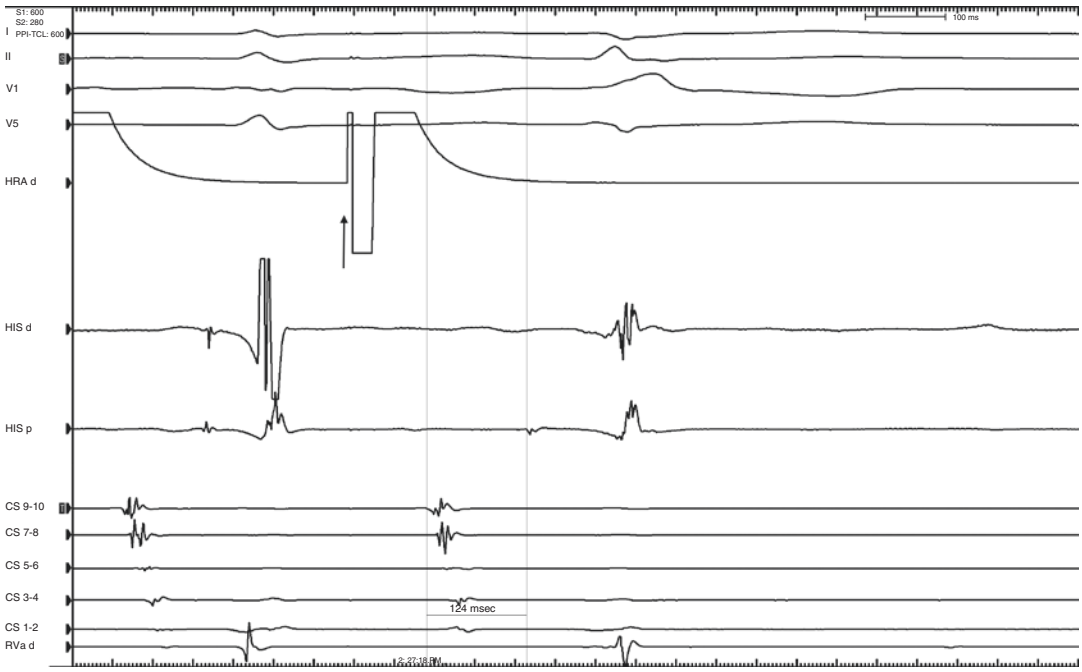

Fig. 1.27 Electrograms showing right bundle abberancy from a PAC (from HRA pacing labeled with an arrow). The HIS d is positioned along the proximal right bundle while the HIS p is positioned along the His. The PAC conducts along the His but does not conduct down the right bundle (no RB potential on HIS d on the second beat) with a RBBB morphology QRS. (CS 9–10 is positioned in the proximal CS with CS 1–2 in the distal CS. RV a is positioned in the RV apex)

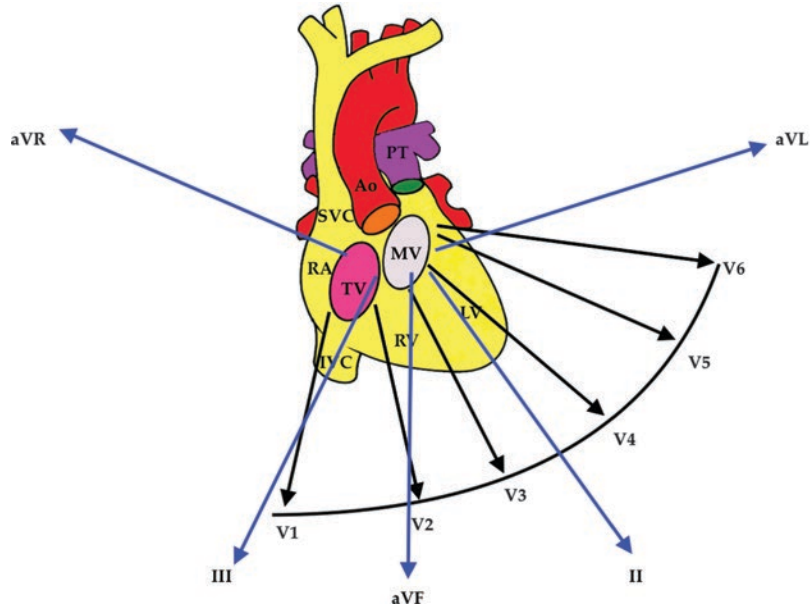

Fig. 1.28 Locations of the precordial and limb lead positions relative to the heart. The precordial leads V1–V6 are seen as well as the augmented leads aVR, aVL, II, III and aVF

therefore the axis will be in the same direction. In cases of myocardial infarction, the axis tends to move in the opposite direction away from the infarcted tissue.

Important Points to Remember

1. The cardiac action potential is composed of four phases.
   Phase IV (resting membrane potential) occurs with a membrane potential of −80 to −95 mV in atrial, purkinje and ventricular cells, −50 to −60 mV in the SN and −60 to −70 mV in the AV node. In both the SN and AV nodes there is a slow spontaneous diastolic depolarization which merges with Phase 0 resulting in spontaneous automaticity while Phase IV in other cells is generally more flat.
   Phase 0 (rapid depolarization) occurs when the membrane potential becomes positive.
   Phase I (rapid repolarization) occurs in the atrium and ventricle but not in the SN and AV node. It is much more prominent in the purkinje and epicardial cells.
   Phase II (plateau phase) occurs when the action potential becomes relatively flat and does not occur in the SN or AV node.
   Phase III (rapid repolarization) occurs when there is restoration of the membrane potential to the resting phase.
2. Refractoriness describes the period during which a stimulus does not result in a new depolarization after phase 0 of the cardiac action potential. There are three different types of refractory periods (RP): relative, absolute and effective.
   The relative RP is the longest coupling interval resulting in local capture therefore marking the end of refractoriness.
   The absolute RP is the longest coupling interval which does not result in in local capture.
   The effective RP is the longest coupling interval delivered which fails to propagate through the distal tissue.
3. Re-Entry occurs when a wave of excitation moves around a circuit which is determined anatomically, functionally or a combination of the two. For re-entry to occur the following conditions have to be fulfilled:
   There must be two or more pathways for conduction
   Unidirectional block in one pathway
   Alternative conduction over the other pathway with sufficient delay as to retrogradely invade the formerly blocked pathway.
4. Automaticity results from spontaneous depolarization during phase IV of the action potential.
5. Afterdepolarizations are defined as depolarizations which occur after Phase 0 of the cardiac action potential and may result in a spontaneous action potential known as a triggered response. These are divided into early afterdepolarization (EAD) or delayed afterdepolarization (DAD).
   EAD occurs during phase II and phase III while DAD occur after the cardiac action potential is complete. EADs tend to occur when there is an increase in the inward movement of positive ions during the plateau phase of the action potential.
   DADs occur as a result of an increase in the inward movement of calcium. This can occur in the setting of digoxin toxicity or in conditions such as catecholamine induced polymorphic ventricular tachycardia (CPVT).
6. The RAO projection helps to demonstrate the postero-anterior (PA) location of a catheter within the cardiac

chambers and shows the AV groove more clearly than the PA view. In this view the spine is on the left.

7. In the LAO view the AV rings are viewed parallel to the image. The left cardiac border is formed by the LA superiorly and the lateral wall of the LV inferiorly.
8. Following discharge from the SN conduction occurs through the RA predominantly utilizing aligned myocytes. Conduction occurs preferentially from the RA to the LA using the Bachmann's bundle.
9. AV conduction occurs through the AV junctional region, the atrial component of which is termed the AV node. This is located between the coronary sinus os and the septal leaflet of the tricuspid valve.
10. The His bundle is a continuation of the compact AV node. Although it has similar cellular components it is better insulated than the AV node and therefore is not as easily damaged with RF. The proximal bundle runs from the distal AV node to the fibrous tissue of the central body where it is termed the penetrating portion. Following this it bifurcates into the right bundle (RB) and left bundle (LB) branches at the level of the septal TV leaflet. The RB tends to have a more anterior origin than the LB.
11. The LB branch originates below the right and non-coronary cusps and then courses along the LV septal surface. It divides into two or three fascicles. The anterior fascicle which is superior runs towards the base of the anterosuperior papillary muscle, the posterior fascicle which is inferior runs towards the posteroinferior papillary muscle and in 60% of cases a central or septal fascicle which runs to the mid septum. In the remaining 40% of cases this area is supplied by the anterosuperior and posteroinferior fascicles.
12. In LBBB the initial activation is rightward and anterior resulting in small q waves in I, avL, and V6 with an rS in V2. Following this depolarisation spreads from the apex to the base and to the RV free wall and apex. During this process, septal activation is the pre- dominant force and therefore the vector is anterior and to the left, resulting in a wide slurred QRS in I, aVL and V6. Depolarization then occurs in a leftward and posterior direction through the LV. Finally, the anterior wall of the LV is depolarized.
13. Anterior fascicular block results in a leftward QRS axis deviation poor R wave progression in V1–V3, with a negative QRS in II, III and aVF, positive in lead I. There is also a tall R wave in aVL and aVR. The QRS is not broad.
14. Posterior fascicular block results in a QRS axis greater than 100 degrees with an rS morphology in leads I and aVL; and a qR pattern in leads II, III, and aVF. The QRS is not broad.
15. Septal fascicular block has a variable ECG appearances. In general the changes noted are Q waves in V1 and V2 as a result of anteriorly directly right ventricular depolarization. This may also cause a qrS in V1 and V2. There is also loss of q waves in leads V5, V6 and I due to loss or reversal of left to right ventricular septal activation. The QRS is not significantly broad because activation of the left ventricular free wall and apex occurs via the anterosuperior and posteroinferior fascicles.
16. The RB branch is an insulated bundle of fibers as a direct continuation of the penetrating atrioventricular bundle. It runs along the RV septum to the apex

where it becomes subendocardial in the mid septum running along the posterior margin of the septal band, courses through the moderator band to the base of the anterior papillary muscle, and then the right ventricular free wall. It gives off septal branches which activate the septum almost immediately after left ventricular activation. Septal activation is generally complete within 35 ms and terminates in Purkinje fibres at the apex.

17. In RBBB the initial septal activation is followed by depolarization of the left ventricle, resulting in R waves in I, aVL and V6. Following this, right ventricular free wall and septal depolarization results in S waves in these leads. Overall, the QRS is ≥120 ms in adults with an rsr, rsR, or rSR in leads V1 or V2. The R or r deflection is usually wider than the initial R wave. ST segment deviation is generally discordant to the QRS vector.
18. Phase III dependent aberrancy also known as Ashman Phenomenon occurs when a short RR interval follows a longer RR interval. The longer RR interval results in a prolonged AP in the His and bundle branches. The right bundle has a longer AP duration than the left bundle and therefore the following beat with the shorter RR interval is blocked in the right bundle which is still refractory and conducts down the left bundle with a RBBB morphology.
19. Acceleration dependent aberrancy occurs with very slight acceleration of the heart rate (less than 5 ms) at a critical cycle length which is often within normal heart rate ranges. This tends to occur more commonly in the left bundle resulting in LBBB.
20. Deceleration dependent aberrancy occurs following a long pause during which a premature atrial beat conducts to the ventricle with a resultant bundle branch block.
21. Aberrancy due to concealed retrograde conduction occurs when retrograde conduction in one of the bundle branches from a PVC results in refractoriness for the next antegrade beat. As the bundle recovers the next beat which conducts down the contralateral bundle conducts retrogradely up the bundle again.

References

Antzelevitch C, Burashnikov A, et al. Overview of basic mechanisms of cardiac arrhythmia. Card Electrophysiol Clin. 2011;3:23–45.

Boyett MR, Honjo H, Kodama I. The sinoatrial node, a heterogeneous pacemaker structure. Cardiovasc Res. 2000;47:658.

Cabrera JA, Sanchez-Quintana D, Farre J, et al. The inferior right atrial isthmus: further architectural insights for surrent and coming ablation technologies. J Cardiovasc Electrophysiol. 2005;16:402–8.

Cappato R, Castelvecchio S, Ricci C, et al. Clinical efficacy of ivabradine in patients with inappropriate sinus tachycardia: a prospective, randomized, placebo-controlled, double-blind, crossover evaluation. J Am Coll Cardiol. 2012;60:1323–9.

Chauvin M, Shah DC, Haissaguerre M, et al. The anatomic basis of connections between the coronary sinus musculature and the left atrium in humans. Circulation. 2000;101:647–52.

Chiang CE, Chen SA, Yang CR, et al. Major coronary sinus abnormalities (identification of occurrence and significance in radiofrequency ablation of supraventricular tachycardia). Am Heart J. 1994;127:1279–89.

Dhamoon AS, Jalife J. The inward rectifier current (IK1) controls cardiac excitability and is involved in arrhythmogenesis. Heart Rhythm. 2005;2:316–24.

DiFrancesco D. The role of the funny current in pacemaker activity. Circ Res. 2010;106:434–46.

DiFrancesco D, Ojeda C. Properties of the current if in the sino-atrial node of the rabbit compared with those of the current IK2, in Purkinje fibres. J Physiol. 1980;308:353.

DiFrancesco D, Tortora P. Direct activation of cardiac pacemaker channels by intracellular cyclic AMP. Nature. 1991;351:145.

DiFrancesco D, Tromba C. Muscarinic control of the hyperpolarization-activated current (If) in rabbit sino-atrial node myocytes. J Physiol. 1988;405:493.

Gadsby DC, Cranefield PF. Electrogenic sodium extrusion in cardiac Purkinje fibers. J Gen Physiol. 1979;73:819–37.

Hellerstein HK, Orbison JL. Anatomic variations of the orifice of the human coronary sinus. Circulation. 1951;3:514–23.

Ho SY, Sanchez-Quintana D. The importance of atrial structure and fibers. Clin Anat. 2009;22:52–63.

Ho SY, Sánchez-Quintana D, Cabrera JA, Anderson RH. Anatomy of the left atrium: implications for radiofrequency ablation of atrial fibrillation. J Cardiovasc Electrophysiol. 1999;10:1525–33.

Ho SY, Anderson RH, Sanchez-Quitana D. Atrial structures and fibers: morphological bases of atrial conduction. Cardiovasc Res. 2002;54:325–36.

Inoue S, Becker AE. Posterior extensions of the human compact atrioventricular node: a neglected anatomic feature of potential clinical significance. Circulation. 1998;97:188–93.

James TN. The connecting pathways between the sinus node and the A–V node and the A–V node and the right and left atrium in the human heart. Am Heart J. 1963;66:498–508.

Kalman JM, Olgin JE, Karch MR, et al. "Cristal tachycardias": origin of right atrial tachycardias from the crista terminalis identified by intracardiac echocardiography. J Am Coll Cardiol. 1998;31:451–9.

Man KC, Knight B, Tse HF, et al. Radiofrequency catheter ablation of inappropriate sinus tachycardia guided by activation mapping. J Am Coll Cardiol. 2000;35:451–7.

Olshansky B, Sullivan RM. Inappropriate sinus tachycardia. J Am Coll Cardiol. 2013;61:793–801.

Opthof T. The mammalian sinoatrial node. Cardiovasc Drugs Ther. 1988;1:573–97.

Sánchez-Quintana D, Yen HS. Anatomy of cardiac nodes and atrioventricular specialized conduction system. Rev Esp Cardiol. 2003;56:1085–92.

Sanchez-Quintana D, Anderson RH, Cabrera JA, et al. The terminal crest: morphological features relevant to electrophysiology. Heart. 2002;88:406–11.

Tschabitscher M. Anatomy of coronary veins (the coronary sinus). In: Mohl W, Wolner E, Glogar D, editors. Proceedings of the 1st International Symposium on Myocardial Protection via the Coronary Sinus. Darmstadt: Steinkopff Verlag; 1984. p. 8–25.

Verheijck EE, van Ginneken AC, Wilders R, Bouman LN. Contribution of L-type Ca^{2+} current to electrical activity in sinoatrial nodal myocytes of rabbits. Am J Phys. 1999;276:1064–77.

2 Cardiac Electrophysiology Study, Diagnostic Maneuvers and Ablation

Kathryn L. Hong, Benedict M. Glover, Siew Yen Ho, Damian Sanchez-Quintana, and Pedro Brugada

Abstract

The overall aim of an invasive electrophysiological (EP) evaluation is to accurately diagnose the mechanism and substrate responsible for a documented or suspected arrhythmia in order to treat the patient's symptoms or improve their prognosis. Significant developments in the understanding of arrhythmias as well as evolving technological advances have allowed electrophysiology studies to be considered as a diagnostic first-line option. This chapter discusses the fundamental principles of invasive electrophysiology and provides an essential guide in terms of establishing the correct diagnosis and ablation strategy.

Indications for an EP Study and Ablation

The overall decision on whether to perform an EP study and ablation depends on the balance between the potential benefits, alternative treatment options, risks as well as the individual patient preference (Fig. 2.1). In general, for symptomatic supraventricular arrhythmias, an EP study and ablation should be considered early as the success rates are high and the results of pharmacological treatment are often suboptimal. The decision for the invasive management of AF and VT is often more complex and requires very careful examination of patient symptoms and potential complications which must be balanced against alternative treatment options. As advancing techniques and technology allow for more complex ablations, the threshold for invasive strategy continues to change with it.

Supraventricular Arrhythmias (SVT)

Ablation can be considered first-line therapy for the treatment of symptomatic SVT due to AV nodal re-entry tachycardia (AVNRT), atrioventricular re-entry tachycardia (AVRT) or atrial tachycardia (AT) (Class I Indication, Level of Evidence B) (Brugada et al. 2020). It is ideal, though not critical, to have inducible tachycardia at the start of the EP study and is entirely reason-

K. L. Hong (✉) · B. M. Glover
Division of Cardiology, Department of Medicine, University of Toronto, Toronto, Ontario, Canada

S. Y. Ho
Royal Brompton Hospital, London, UK

D. Sanchez-Quintana
Faculty of Medicine, Department of Anatomy and Cell Biology, University of Extremadura, Badajoz, Spain

P. Brugada
University Hospital of Brussel, Brussels, Belgium
e-mail: pedro@brugada.org

B. M. Glover, P. Brugada (eds.), *Clinical Handbook of Cardiac Electrophysiology*,
https://doi.org/10.1007/978-3-030-74319-2_2

AVNRT	Documented SVT + Dual AV Nodal Physiology IB
	Inducible AVNRT IB
AVRT	Symptoms or inducible AVRT IB
	Asymptomatic Shortest RR during AF <250 msec or pilot/scuba diver/school bus driver
CTI Flutter	First Symptomatic IIaB
	Recurrent Symptomatic IA

Fig. 2.1 Indications for Ablation for AV Nodal Re-entry Tachycardia (AVNRT), AV Re-entry Tachycardia (AVRT) and Atrial Flutter regarding consideration for Catheter Ablation. SPERRI: Shortest Pre-Excited R-R Interval

able to perform an ablation if either dual AV nodal anatomy or accessory pathway conduction is present in the setting of electrocardiographic evidence of an SVT.

The issue of ablation in the setting of asymptomatic ventricular pre-excitation is somewhat more complex. Ablation is indicated in patients with high-risk occupations such as pilots, scuba divers and school bus drivers (Brugada et al. 2020). Inducibility of AVRT in the absence of symptoms may be considered as an indication for ablation although this decision is not clear-cut and may also depend on patient and physician preference as well as the conduction properties of the pathway. Nonetheless, accessory pathways that can lead to rapid ventricular rates during atrial fibrillation should be ablated.

Atrial pacing may be used to calculate the antegrade refractory period of the action potential with a measurement greater than 250 ms being considered lower risk. The **Shortest Pre-Excited R-R Interval (SPERRI)** may be a more useful measurement with an RR interval greater than 250 ms probably being associated with a lower risk. These measurements may help to guide the decision regarding ablation of an AP.

Typical Atrial Flutter

Typical atrial flutter involving the cavo-tricuspid isthmus (CTI) can be successfully ablated in the majority of cases. An ablation may be considered after a single episode of typical atrial flutter (Class IIa Indication; Level of Evidence B) or following a recurrent episode (Class I Indication; Level of Evidence B) (Brugada et al. 2020). Ablation can also be considered for atypical atrial flutter (Class IIa Indication; Level of Evidence B) although the overall success may not be as high as for typical atrial flutter (Brugada et al. 2020).

Atrial Fibrillation (AF)

In order to consider a catheter ablation for a patient with AF, the patient must have symptoms attributed to the arrhythmia (Fig. 2.2). This is extremely important as symptoms may be non-specific and therefore it is often useful to consider an electrical cardioversion and reassess the patient after sinus rhythm has been achieved. Additionally, all patients who are being considered for a catheter ablation must be able to tolerate anticoagulation therapy at least during and after their ablation (January et al. 2014). There is insufficient data to support routine withdrawal of oral anticoagulation following an AF ablation even if it appears successful, while longer-term decisions regarding oral anticoagulation should be based on the CHADS2VASC score (January et al. 2014). This is because patients may continue to have asymptomatic episodes of AF which continue to pose a thrombo-embolic risk.

For patients with symptomatic paroxysmal AF, catheter ablation can be considered if at least one Class I/III anti-arrhythmic drug has been tried and is ineffective or poorly tolerated. (Class I Indication, Level of Evidence A) (January et al. 2014). Catheter ablation may also be considered prior to commencing a Class I/III antiarrhythmic drug in some patients with symptomatic paroxysmal AF. (Class IIa Indication, Level of Evidence B) (January et al. 2014). Catheter ablation may also be considered in patients with symptomatic persistent AF which is not effectively controlled with at least one Class I/III antiarrhythmic drug. (Class IIa Indication, Level of Evidence A).

The recommendations and evidence for performing catheter ablation for symptomatic persistent AF prior to commencement of a Class I/III

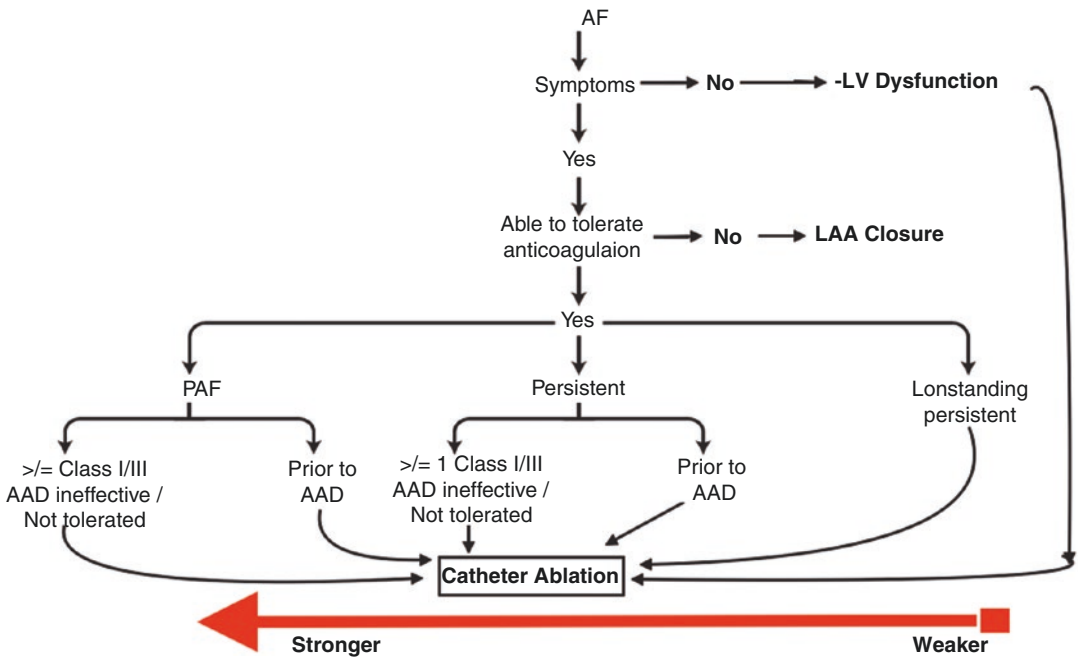

Fig. 2.2 Decision Tree for Consideration for Catheter Ablation for Atrial Fibrillation. *AAD* Anti-arrhythmic drug therapy

antiarrhythmic drug are not as robust. (Class IIb Indication, Level of Evidence C) (January et al. 2014) Likewise, catheter ablation may also be considered for the management of longstanding persistent symptomatic AF (Class IIb Indication, Level of Evidence B), albeit with only a moderate level of success overall. If available at the institution, a hybrid ablation with thoracoscopic approach and closure of the left atrial appendage may be considered for longstanding persistent AF (Pison et al. 2012).

Ventricular Arrhythmias

Catheter ablation is recommended for patients with sustained monomorphic VT, including VT terminated by an ICD, whereby anti-arrhythmic drug therapy is either ineffective or not tolerated as well as the control of incessant VT (Aliot et al. 2009).

It may also be considered when anti-arrhythmic drug therapy has not failed and in particular may be a suitable alternative to amiodarone therapy (Fig. 2.3). Additionally, catheter ablation is recommended for bundle branch re-entry VT and interfascicular VT and for patients with frequent PVC's or non-sustained VT resulting in left ventricular dysfunction. It is, however, not recommended for the treatment of asymptomatic PVC's or non-sustained VT not resulting in left ventricular dysfunction.

EP Study and Ablation: Patient Preparation

The most useful test for any patient prior to an EP Study is an ECG or rhythm strip of the arrhythmia as this may act to guide the entire approach, chamber of access, and threshold for potential ablation.

A baseline ECG and simple blood tests (serum electrolytes and urea) should be performed for all patients, while a full blood count and international normalized ratio (INR) is required in patients taking warfarin. (Haines et al. 2014) Additionally, a pregnancy test in any female of childbearing age

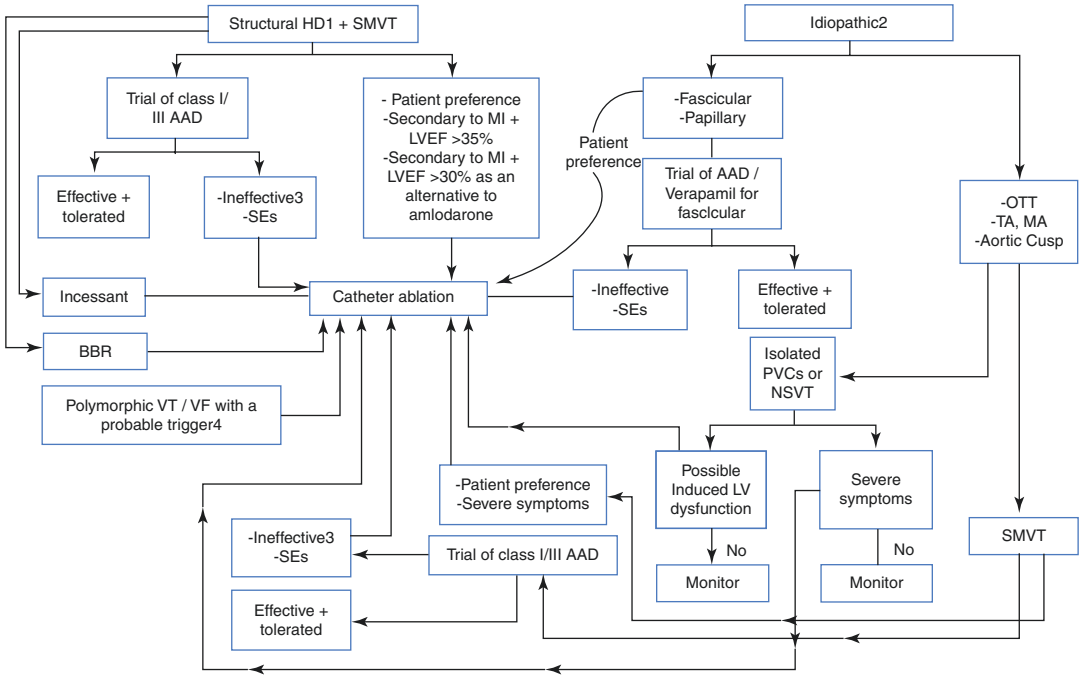

1 Previous Myocardial Infarction; Dilated cardiomyopathy; ARVC; Congenital Heart Disease

2 Outflow Tract Tachycardia; Annular Tachycardia, Aortic Cusp Tachycardia; Fascicular VT; Papillary Muscie VT

3 ≥ 1 episode of MSVT despite the use of ≥ 1 antiarhythmic drug

4 For either structural or Idiopathic VT

Fig. 2.3 Decision tree for the ablation of ventricular arrhythmias. *HD* Heart Disease, *SMVT* sustained monomorphic VT; *SE* side effects, *BBR* bundle branch re-entry, *OTT* outflow tract tachycardia. *TA* tricuspid annulus, *MA* mitral annulus

should be checked within the 2 weeks prior to the procedure (Haines et al. 2014).

For potentially high-risk procedures, a group and crossmatch should be considered.

Generally for most diagnostic studies, antiarrhythmic drugs should be stopped for at least five half lives. This is not required in patients undergoing catheter ablation unless an EP study or rotor mapping is also being performed.

EP Study and Ablation: Potential Risks

The risks associated with EP studies and ablation vary greatly depending on the procedure being performed. General complications include groin hematoma, vascular injury and pericardial effusion, however, more specific complications may occur in AF and VT ablations. Notably, many of these risks can be significantly minimized if the appropriate care and pre-procedural actions are taken. These risks, as well as preventative measures to mitigate these risks, are summarized on Table 2.1.

Collateral Damage During Ablation

Pericardial Effusion

Pericardial effusion may occur as a direct result of catheter, sheath or wire manipulation as well as during or after trans-septal access or as a direct result of catheter ablation. It is, therefore, of critical importance to be gentle with all of the equipment being used, given that some regions within the heart are particularly thin and extra caution should be taken. As demonstrated in

Table 2.1 Reported incidence, features, prevention and management of potential complications associated with EP procedures

Complication	Features	Prevention and management	Reported incidence (%)	
Groin hematoma Pseudoaneurym AV Fistula	Swelling Tenderness Bruit	Careful palpation of femoral artery Medial approach to the vein Careful post procedure groin management	SVT	0.3–0.4 (Scheinman and Huang 2000; Bohnen et al. 2011)
			AF	1.8–2.7 (Shah et al. 2012)
			VTs	2.0–3.6 (Peichl et al. 2014)
			VTsn	0.7–0.8 (Yamada et al. 2008)
AV Block	PR prolongation Loss of AV conduction	Map His prior to ablation If close to compact AV node consider lower energy RF or cryoablation Monitor for Accelerated Junctional rhythm, loss of VA conduction, prolongation of AH or PR interval	SVT	0–1 (Bohnen et al. 2011; Arbelo et al. 2012)
			AF	0.1–0.2 (Shah et al. 2012; Calkins et al. 1999)
			VTs	0–1.6 (Scheinman and Huang 2000; Mallidi et al. 2011)
			VTsn	0–0.4 (Scheinman and Huang 2000; Yamada et al. 2008)
Coronary Artery Injury	ST elevation Chest pain	Careful use of RF in certain locations of the coronary sinus, LVOT, epicardium Do not deliver RF if closer than 5 mm	SVT	0–0.1 (Bohnen et al. 2011; Roberts-Thomson et al. 2009)
			AF	0–0.1 (Bohnen et al. 2011; Chugh et al. 2013)
			VTs	0.6 (epi) (Sacher et al. 2010)
			VTsn	<0.1 (Pons et al. 1997)
Pericardial Effusion	Hypotension Tachycardia Change in left heart border motion in LAO view Accumulation of pericardial effusion on ICE/TEE	Caution when manipulating catheter, sheaths and wires Cautious use of RF in certain areas considered higher risk such as RVOT, RV apex, RV free wall, LAA, LA roof and LA posterior wall Monitor closely during trans-septal access	SVT	0.4–1.0 (Bohnen et al. 2011; Spector et al. 2009)
			AF	1.8–2.5 (Bohnen et al. 2011; Shah et al. 2012)
			VTs	1.4–2.7 (Bohnen et al. 2011; Calkins et al. 2000)
			VTsn	1.3–1.7 (Bohnen et al. 2011; Tokuda et al. 2011)

(continued)

Table 2.1 (continued)

Complication	Features	Prevention and management	Reported incidence (%)	
Thrombo-embolism	TIA/stroke Systemic embolism	Maintain ACT greater than 350 s for left sided ablations Use of heparinized saline through sheaths on left side Careful use of equipment to ensure no air embolism	SVT	0–0.2 (Bohnen et al. 2011; Arbelo et al. 2012)
			AF	0.3–1.0 (Haines et al. 2014; Bohnen et al. 2011)
			VTs	0.8–2.7 (Bohnen et al. 2011; Spector et al. 2009)
			VTsn	0.8 (Bohnen et al. 2011)
Phrenic Nerve Injury	Loss of movement of hemidiaphragm, post procedure dyspnea, pleural effusion, consolidation on CXR	Monitor movement of hemidiaphragm Pacing from ablation catheter to monitor for phrenic nerve capture	SVT	<0.1
			AF	0.2 (Peichl et al. 2014)
			VTs	<0.1
			VTsn	<0.1

VTs VT ablation in the setting of structural heart disease, *VTns* VT ablation in structurally normal ventricle, *Epi* Epicardial

Fig. 2.4, these regions include the RV apex, RV free wall, RVOT, LAA, LA posterior wall and LA roof. A pop and/or sudden rise in impedance during ablation may be associated with perforation, resulting in either a pericardial effusion or tamponade and occurring in approximately 1.3% of all EP procedures (Bohnen et al. 2011). This occurs in approximately 0.2% of SVT ablations, 1.8% of cases amongst patients undergoing catheter ablation for AF, 1.7% of VT ablations in a structurally normal heart (predominantly outflow tract tachycardia) and 1.4% of patients with structural heart disease undergoing VT ablation (Bohnen et al. 2011).

Although the pericardial space can tolerate up to 500 cm^3 of fluid accumulated over a long period of time, decompensation may occur with 50–100 cm^3 when fluid accumulation occurs quickly. This tends to be most evident around chambers with the lowest pressures first; the RA followed by the RV, LA and finally the LV. Accumulation may also be localized and therefore may occur on the left side prior to the right side.

The accumulation of a significant pericardial effusion may be associated with an increase in heart rate with or preceding a drop in blood pressure. However, a drop in blood pressure is a relatively late sign of acute pericardial effusion and it is therefore important to monitor for earlier signs. It must also be noted that an increase in sympathetic drive may initially result in an increase in the blood pressure. Pericardial stretch may occasionally result in an increase in parasympathetic tone with a transient bradycardia and hypotension.

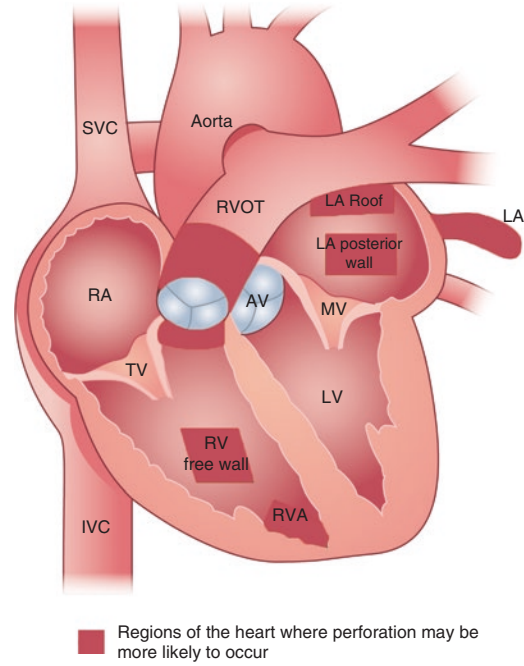

Fig. 2.4 Diagrammatic representation of regions of the heart which are at an increased risk of perforation during instrumentation with catheters and wires; *SVC* superior vena cava, *IVC* inferior vena cava, *RA* right atrium, *TV* tricuspid valve, *RV* right ventricle, *RVOT* right ventricular outflow tract, *LA* left atrium, *LV* left ventricle, *LAA* left atrial appendage

A reduction in the left lateral wall excursion in the LAO fluoroscopic view has been shown to be

associated with pericardial effusion (Nanthakumar et al. 2005). This occurs as the pericardium is relatively fixed to the spine and the sternum and therefore fluid in the pericardial space is more likely to accumulate posterolaterally followed by anterolaterally. The accumulation of pericardial fluid during ablation can easily be observed using Intracardiac Echo (ICE) or Trans-esophageal echo (TEE). The accumulation of a small pericardial effusion detected on ICE during an AF ablation may indicate an increase in the risk of a late post procedure pericardial effusion while no evidence of effusion on ICE indicates a very low post procedural risk.

All EP laboratories should have equipment for emergency pericardiocentesis including rapid access to echocardiography. In order to keep this as simple as possible, the needle used to access the femoral vein and a 0.35 wire should be kept on the table for rapid access. Following confirmation that the wire is within the pericardial space by pushing it as far as possible and ensuring that it is not within one or more cardiac chambers, a short sheath and a pigtail catheter can be used to rapidly drain the effusion.

Phrenic Nerve Injury

The right phrenic nerve runs alongside the SVC and passes laterally along the RA running anteriorly to the right pulmonary veins passing more closely to the superior than the inferior right pulmonary vein (Fig. 2.5). The left phrenic nerve runs over the fibrous pericardium with a variable course over the LA and LV and terminates in the left hemidiaphragm. The incidence of phrenic nerve palsy following an AF ablation is approximately 0.2% (Shah et al. 2012) and more commonly affects the right than the left side. This generally occurs with isolation of the right superior pulmonary vein or the superior vena cava. Left phrenic nerve palsy is less common but may occur during left atrial appendage ablation. Of note, the incidence of phrenic nerve palsy is significantly higher with cryoablation and has been reported to occur in approximately 6% of cases, albeit usually transient (Andrade et al. 2011).

Various techniques may be employed in order to help map the location of the phrenic nerve before or during catheter ablation. Pacing at high output may be performed in order to assess for phrenic nerve capture. However, this should be discussed with the anesthesiologist prior to performing this maneuver as muscle relaxants are often administered which will inhibit the effects of pacing on the phrenic nerve. Additionally, the diaphragm can be monitored using fluoroscopy during ablation in the absence of nerve paralytic agents. More novel techniques such as recording electromyograms from the diaphragm have been described in which either a catheter is positioned in the hepatic vein or modified surface electrodes are positioned over the diaphragm with pacing performed from either subclavian vein.

Phrenic nerve palsy is generally noted on CXR by an elevated hemidiaphragm and may be associated with dyspnea, a cough or hiccups. The majority of phrenic nerve palsy recovery within 9 months.

Esophageal Injury

As shown in Fig. 2.6, the esophagus is immediately posterior to the LA separated by a thin layer of fibrous pericardium and a layer of fibrofatty tissue containing esophageal arteries as well as the vagus plexus. The distance between the posterior wall of the LA and the anterior portion of the esophagus is variable but may be as little as 5 mm (Sánchez-Quintana et al. 2005). The location of the esophagus may run either central to the posterior wall of the left atrium, towards the left pulmonary veins or towards the right pulmonary veins as is generally closer at the atrial pulmonary vein junction and in more inferior locations. Although the esophagus can be clearly visualized on a pre-ablation CT scan the esophagus is a mobile structure and therefore the location may change during the procedure.

Esophageal injury occurs predominantly as a result of direct thermal injury from catheter ablation along the posterior wall of the LA. Other contributing factors may include damage to the arterial flow to the esophagus as well as to the vagus nerve and plexus. This may result in mucosal erythema, esophagitis or atrioesophageal fistula. Discrete mucosal changes have been noted to be present in approximately half of all patients who undergo catheter ablation for AF with almost

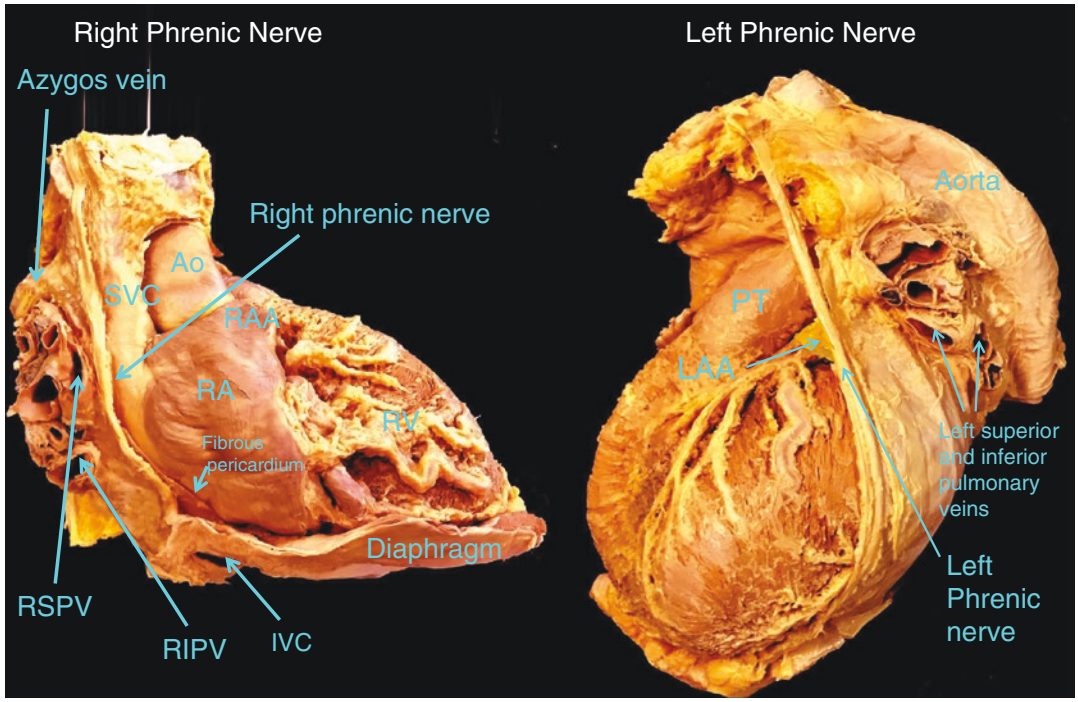

Fig. 2.5 Anatomical images showing the course of the right phrenic nerve (PN) on the left image and the left phrenic nerve (PN) on the right image. *SVC* superior vena cava, *Ao* aorta, *RA* right atrium, *RAA* right atrial appendage, *RV* right ventricle, *RSPV* right superior pulmonary vein, *RIPV* right inferior pulmonary vein, *PT* pulmonary trunk, *LAA* left atrial appendage

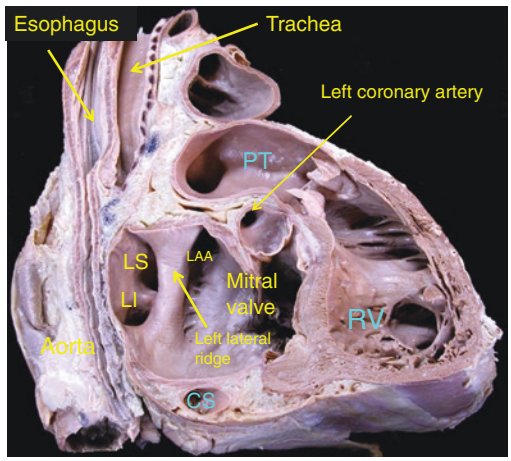

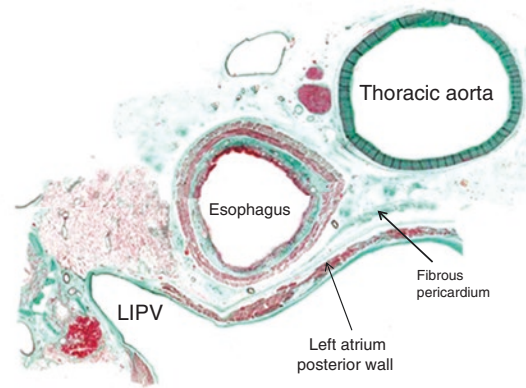

Fig. 2.6 The relationship of the esophagus to the left atrium. The esophagus initially runs posterior to the trachea and as it moves inferior it is posterior to the left atrium. As shown on the left image the esophagus is directly posterior to the left atrium. As shown on the right the left atrial posterior wall is separated from the esophagus by a layer of fibrous pericardium. *LS* left superior pulmonary vein, *LI* left inferior pulmonary vein, *CS* coronary sinus, *LAA* left atrial appendage, *RV* right ventricle, *LIPV* left inferior pulmonary vein

one fifth developing esophageal ulceration (Schmidt et al. 2008).

The incidence of fistula formation between the left atrium and the esophagus as a result of catheter ablation for AF ranges from 0.03% (Ghia et al. 2005) to 0.2% (Dagres et al. 2009) Symptoms relating to atrio-esophageal fistula may occur from 3 days to 6 weeks post-ablation and are often non-specific. The most common is a pyrexia followed by neurological symptoms relating to thrombo-embolism. Other symptoms include chest pain and dysphagia, and in many cases, an elevated white cell count. Management depends on acute recognition of the condition followed by surgical repair.

Although the esophagus can be visualized pre-procedure, this is generally unreliable due to intra-procedural movement. The esophagus can be visualized during ablation using fluoroscopy with a marker such as a naso-gastric tube, a temperature probe or barium paste. This requires fluoroscopy to be performed during ablation along the posterior wall of the left atrium. Although this method marks the lumen of the esophagus, it does not provide an accurate distance from the ablation catheter to the most anterior aspect of the esophagus.

Esophageal temperature monitoring is performed by some operators using a temperature probe. Evidence for the efficacy in preventing esophageal injury is limited and conflicting and overall there is no general consensus as to whether luminal esophageal temperature is a valid predictor of mucosal injury.

It is generally considered reasonable to limit maximum power to 25–30 W and not to spend longer than 30 s on one region when ablating along the posterior wall of the left atrium. It is also common to prescribe proton pump inhibitors post ablation in order to reduce the effects of acid reflux on the esophagus.

Coronary Artery Injury

This may occur if ablation is performed in close proximity to a coronary artery, such as in the aortic cusps. Other regions where ablation may be in close proximity to a coronary artery or one of its branches include: the coronary sinus (as shown in Fig. 2.7), great cardiac vein, CTI, mitral annulus, base of the LAA or in the epicardium.

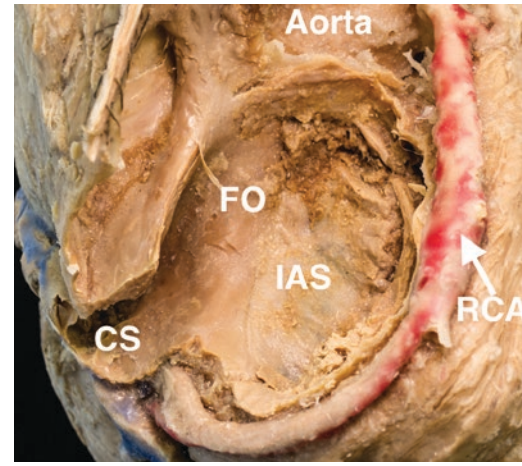

Fig. 2.7 Anatomical images showing proximity of the right coronary artery (RCA) to the coronary sinus (CS). The RCA originates in the right coronary cusp of the aortic root and courses along the right atrioventricular grove anteriorly and inferiorly where it eventually courses towards the proximal coronary sinus (CS). In this region there is close proximity to the CS. Also shown in this image is the right ventricular outflow tract (RVOT) and the fossa ovalis (FO)

Endocardial ablation of accessory pathways along the mitral and tricuspid annulus carries a low risk of coronary artery stenosis. The risk is increased when ablation is performed in the proximal CS, which may be the optimal location for posteroseptal APs and occasionally, the slow pathway and focal atrial tachycardias. The posterolateral branch of the RCA or the circumflex coronary artery often run closely to this location and may be closer to the anterior and inferior walls of the CS. If ablation is being performed in this location a coronary angiogram should be considered and a minimum distance of 5 mm should be maintained between the site of ablation and the coronary artery.

Ablation in the distal cardiac vein for PVCs along the epicardial annulus may also result in coronary artery damage and similar precautions should be taken with regards to distance.

Epicardial ablation is now increasingly performed particularly for non-ischemic VT and to a lesser degree ischemic VT. Coronary CT or

angiography should be performed in these cases prior to ablation.

Ionizing Radiation in Cardiac Electrophysiology

Ionizing radiation may result in molecular injury to the DNA. In the EP laboratory, this is measured in Grays (Gy) or Sieverts (Sv). One gray is defined as the absorption of 1 J of ionizing radiation by 1 Kg of matter. The equivalent dose Sievert is the absorbed dose in Gy multiplied by the radiation weighting factor which varies according to the source of radiation and is 1 for X-rays. This can be further modified in order to calculate the effective dose when the radiation is predominantly exposed to certain regions of the body. It is important to achieve as low as reasonably achievable (ALARA) radiation doses by reducing the frame rate to as low as possible, minimizing the duration of time performing fluoroscopy and not taking cine images. The development of 3 D mapping systems has had a significant impact on reducing the need for fluoroscopy particularly in complex ablations.

Administration of Sedation and Anesthesia

The requirements for sedation and anesthesia vary according to the precise procedure being performed. For EP studies, minimal doses of sedation are given for anxiolytic effects as larger doses may reduce the inducibility of the arrhythmia particularly in adrenaline sensitive focal atrial tachycardia and outflow tract tachycardia. Moderate doses of sedation are often required for ablation and in particular for performing anatomical lesions such as a cavotricuspid isthmus ablation. Ablation for AF and complex VT may be performed with moderate to deep sedation or general anesthesia. There are several potential advantages to the use of general anesthesia in such procedures such as minimizing patient discomfort and movement, thus facilitating more reliable 3D mapping and allowing the use of TEE visualization. Care must be taken in order to minimize the doses of paralytic agents when assessing for phrenic nerve capture.

Benzodiazepines and opioids are used in the EP laboratory for their anxiolytic and partial amnesic effects. If these agents are used, it is ideal to administer low doses before the procedure is performed in order to assess the effect on the individual patient. All patients undergoing any procedure involving the administration of intravenous sedation should have a history and rapid airway assessment performed prior to starting the procedure. Ideally this should also involve an anesthesiologist as well as an individual whose sole purpose is to monitor the patient's respiratory rate, oxygen saturations as well as heart rate and blood pressure throughout the procedure. All patients should be closely monitored post-procedure until their vital parameters have returned to normal limits.

The most common benzodiazepines used in the EP laboratory are midazolam and diazepam. Although either of these agents can be used, midazolam tends to have a shorter duration of action particularly in the elderly or in those with reduced cardiac output, respiratory depression, hepatic and renal impairment.

Midazolam can be administered at a dose of 0.03–0.07 mg/kg over 2 min for most adults adult with additional doses given after 3 min, if required, at 25% of the initial dose. Generally, no more than 10 mg is required for the entire procedure.

Midazolam tends to have less effect on suppression of induction of supraventricular tachycardia compared to diazepam. Routine administration of the benzodiazepine antagonist, flumazenil, should not be performed and instead, should be reserved only for cases of significant over sedation. A dose of 0.2 mg over 15 s with another dose of 0.2 mg after 45 s and then every 1 min up to a maximum dose of 1 mg should be used. The patient should be monitored closely for 2 h in order to ensure that there are no further sedative effects as the drug effects wear off.

Fentanyl is a useful opioid which can be administered at the start of the case at a dose of 0.5 μg/kg if used with a benzodiazepine or 2 μg/

kg if used alone. After 15 min have elapsed, the effects can be re-assessed and an additional 25% of the initial dose may be administered if required. The overall duration of action is approximately 30–60 min. If used in conjunction with a benzodiazepine, fentanyl may result in respiratory depression and therefore monitoring is required. The effects of fentanyl can be partially reversed by naloxone at a dose of 0.1–0.2 mg over 2 min.

Propofol is frequently used in the EP laboratory. The individual responsibility for this depends on the country in which the procedure is being performed. Generally, propofol is administered at a dose of 0.5 mg/kg over a period of 3–5 min, however, further doses may be administered in 5 mg boluses if required. Propofol has no significant electrophysiological effects on arrhythmia induction.

Very occasionally propofol infusion syndrome may occur particularly at higher doses and for longer periods of time. This may occur due to mitochondrial respiratory chain inhibition or impaired fatty acid metabolism and results in acute refractory bradycardia leading to asystole with either metabolic acidosis, rhabdomyolysis, hyperlipidaemia, and or fatty liver. Coved type ST elevtaion with RBBB occurs in the precordial leads. The only effective treatment for this condition is haemodialysis or haemoperfusion with cardiorespiratory support.

Peri-procedural Anticoagulation

For the majority of right sided ablations, anticoagulation is not required. However, some operators may decide to give low dose heparin in order to try to lower the potential risk of deep venous thrombosis and pulmonary embolism. For left sided ablations, intravenous heparin is administered aiming for an Activated Clotting Time (ACT) of greater than 350 s. In patients who are already taking oral anticoagulation, the decision to continue, discontinue or bridge with heparin depends on the risks of thrombo-embolism compared to the risk of bleeding. The main properties of oral anticoagulants are demonstrated on Table 2.2.

Patients undergoing ablation for AF are at an increased risk of thrombo-embolism due to a combination of pre-existing factors involved in Virchow's triad, as well as potential for embolic formation during ablation in the left atrium and possible reversion from AF to normal sinus rhythm. The need for pre-procedural anticoagulation depends on the patients CHA_2DS_2-VASc score. While a score of 0 generally does not warrant anticoagulation pre-ablation, therapeutic anticoagulation is recommended for a minimum period of 4 weeks in all other cases (January et al. 2014).

Even in patients who are considered to have a low baseline CHA_2DS_2-VASc score, there may be an increased risk of thrombo-embolism post-ablation. This occurs as a result of endothelial injury as well as potential mechanical dysfunction of the left atrium post ablation. As shown in Fig. 2.8, manipulation of ablation and mapping catheters and guidewires results in endothelial injury and activation of factor XII which results in the activation of the intrinsic pathway and via tissue factor activation, the extrinsic pathway as well. It is therefore necessary to administer heparin for left sided ablations aiming for an activated clotting time (ACT) of 350 s (January et al. 2014) even in patients who are receiving warfarin. In

Table 2.2 Pharmacological properties of warfarin and direct oral anticoagulants

Drug	Mechanism of action	Time to peak (h)	T1/2 (h)	Renal excretion (%)
Warfarin	Vitamin K antagonist	96–120	40	0
Dabigatran	DTI	1–2	12–17	80
Rivoroxaban	Xa Inhibitor	2–3	7–11	33
Apixaban	Xa Inhibitor	1–2	12	25
Edoxaban	Xa Inhibitor	1–2	10–14	50

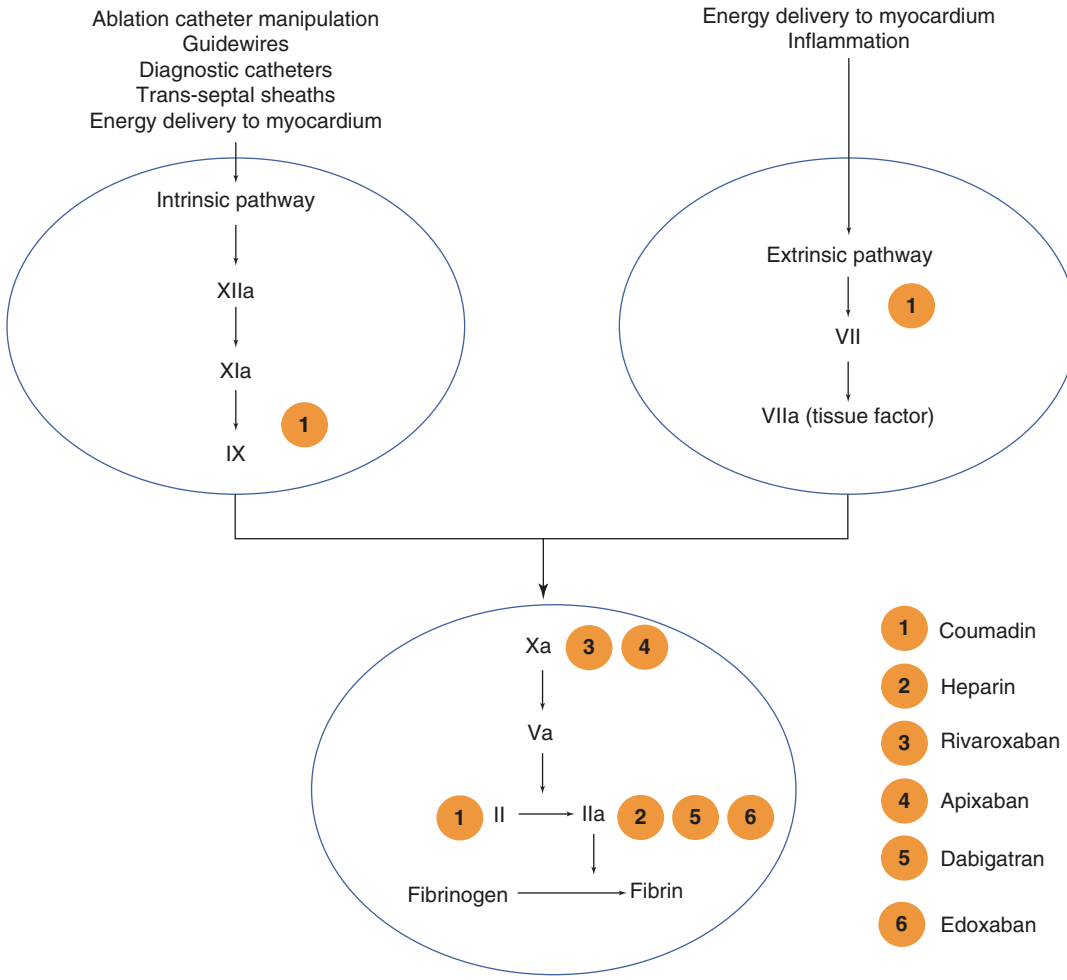

Fig. 2.8 Effect of catheter ablation, sheath and wire manipulation on the coagulation cascade and pharmacological intervention

patients who are allergic to heparin, bivalirudin may be considered.

It is recommended that oral anticoagulation is continued for at least 8 weeks post-ablation in these patients and long-term in patients with a higher risk of thromboembolism (January et al. 2014).

The choice of whether to continue with oral anticoagulation compared with heparin bridging is largely dependent on the individual operator and center experience. However, continuation of warfarin during catheter ablation for AF is likely superior to bridging with heparin with reported lower rates of thrombo-embolism, pericardial effusion and major bleeding (DiBiase et al. 2010).

There is limited data regarding the use of uninterrupted direct oral anticoagulants in AF catheter ablation. Given the shorter half life of the direct oral anticoagulants, minimal interruption can be performed pre-ablation and appears to be effective particularly if a pre-procedure transesophageal echocardiogram (TEE) is performed. Generally, provided the patient has normal renal function, the last dose of oral anticoagulant can be administered 24 h pre ablation with the first dose post procedure administered 4 h after sheath removal.

EP Laboratory Set-Up

The EP lab is composed of an EP recording system, a stimulator, a RF generator with the potential for irrigation, an electroanatomic mapping

(EAM) system, a cryoablation system, and the cables and interfaces which connect these systems (Fig. 2.9). Additionally, EP labs are equipped with resuscitation (at least one defibrillator with rapid access to a second and ventilation equipment) and fluoroscopic equipment for image acquisition.

How Electrograms are Derived: Amplification and Filtering

Electrograms recorded in the heart are generally less than 5 mV in amplitude and often as small as 0.01 mV in scarred tissue. In order to display these signals, they must be amplified and filtered. Signals may be amplified up to 10,000 times prior to being filtered.

The amplified signal then passes through a **high pass filter**. This allows higher frequency signals to pass through while removing signals below a designated frequency. On the **surface ECG** this is set very low at **0.05 Hz**, therefore allowing a larger range of low frequencies to pass through. For **bipolar intracardiac signals** this is set higher at **30 Hz** which therefore filters out a larger range of low frequencies that may occur as a result of catheter movement, electrical farfield or respiratory variability.

For **unipolar intracardiac signals** where the morphology of the signal is more relevant, the setting is similar to the surface ECG at **0.05 Hz** or else switched off.

This signal then passes through an isolation amplifier which isolates the current from the patient and is subsequently transmitted through a **low pass filter**. This allows lower frequency signals to be transmitted while filtering out higher frequencies. This is generally set at **300 Hz for bipolar intracardiac electrograms and filtered and unfiltered unipolar electrograms and 100 Hz for surface ECG signals** (Fig. 2.10).

Additionally, most EP systems have a **notch filter**, which removes signals at a specific frequency range generally in the range of electrical frequency. This is often set at **50 Hz in Europe and 60 Hz in North America** and is designed to reject interference outside of the range around this. This also has several potential disadvantages including a reduction in the amplitude of certain electrograms such as pulmonary vein potentials as well as the potential to add interference.

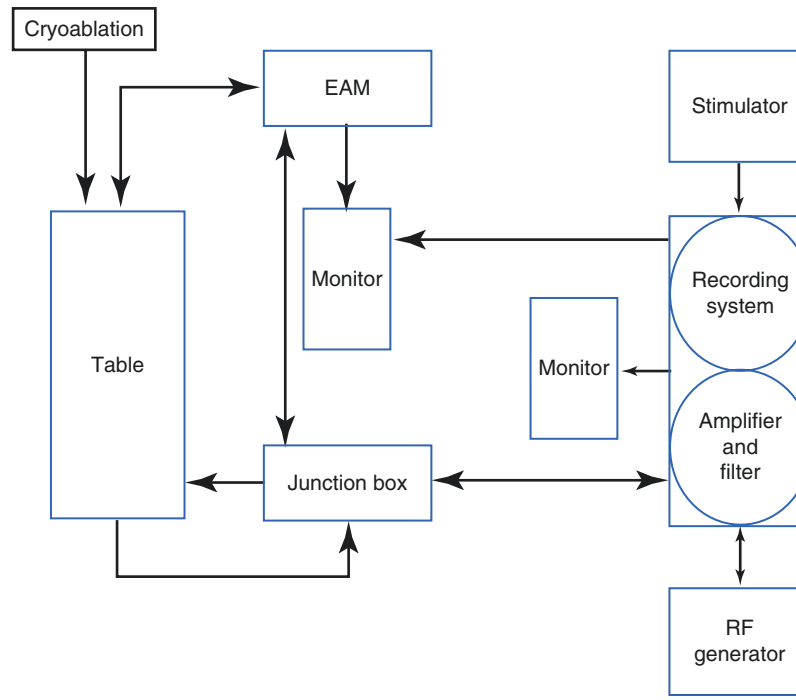

Fig. 2.9 Diagrammatic representation of a typical setup for an EP laboratory. *EAM* electroanatomic mapping system

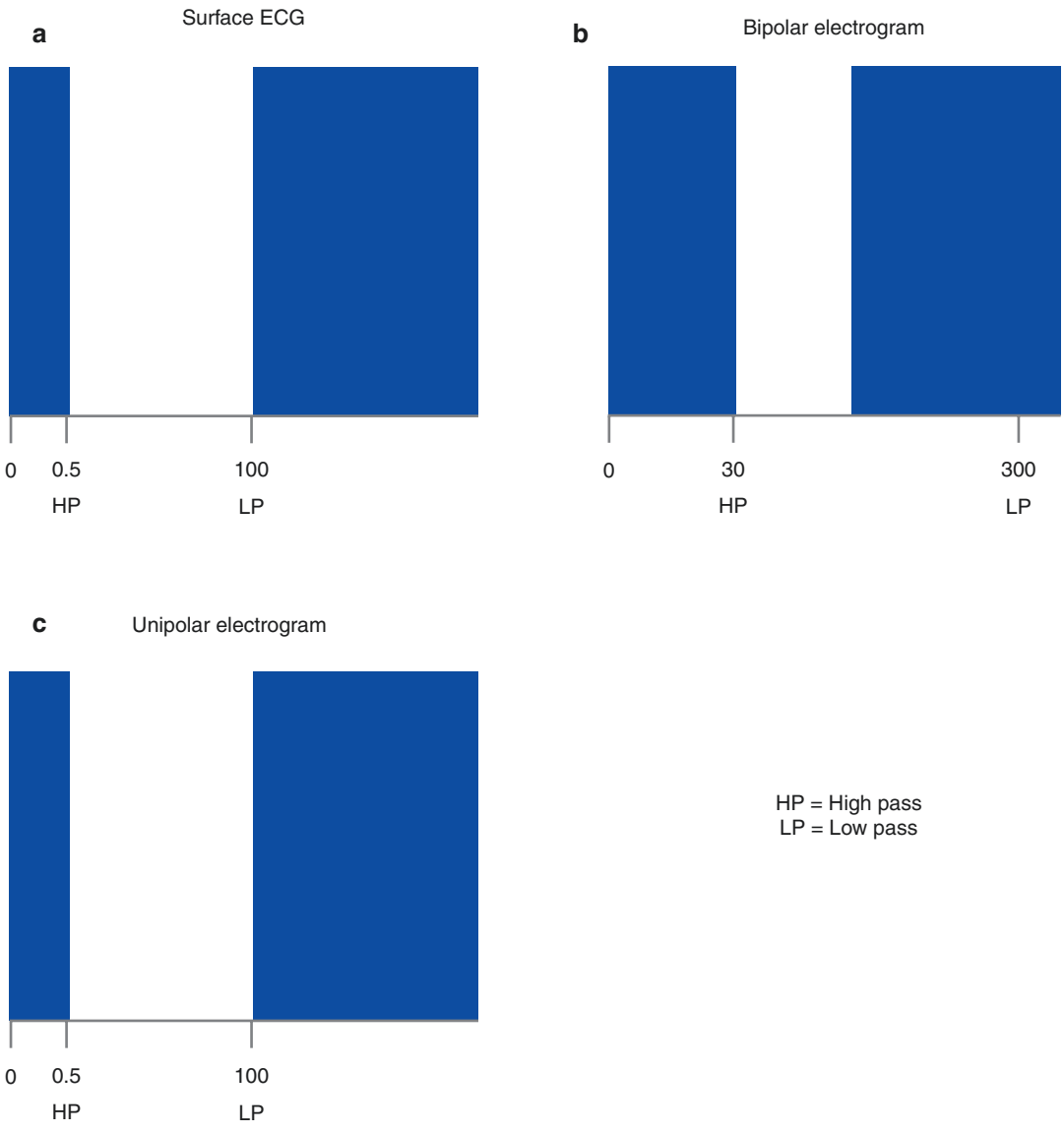

Fig. 2.10 High Pass (HP) and Low Pass (LP) settings for the surface ECG (**a**), bipolar intracardiac electrograms (**b**) and unipolar intracardiac electrograms (**c**)

Electroanatomic mapping systems have their own high pass and low pass filters programmed, but can also be adjusted. These systems are generally set with the range of 30–500 Hz for intracardiac electrograms. For unipolar electrograms, the low pass is either minimized or switched off in order to reduce artifact on the signal. If the standard settings are kept on for unipolar signals, often an artefactual R wave may appear on the signal.

Despite filtering of signals, the best policy is to minimize noise from the onset. This can be due to direct electrical interference from other devices in the lab, leakage current from other devices, as well as electrical cables which may be closely coupled with cables transmitting electrograms. Hence, when designing the EP laboratory, it is critical that electrical cables are not positioned beside cables used for transmitted electrocardiograms. **Leakage current** is the total current from

patient connections through the patient to earth and is required to be less than **10 μA** (ANSI/AAMI 2005). This cumulative current may also result in considerable electrical interference which must be filtered.

Noise which occurs specifically during ablation may often be due to the fact that the pacing function is enabled at the distal electrode at the same time as the ablation function. This is the result of a slight difference in the current between the distal and proximal poles which exists even when pacing is not being performed.

Other potential causes include problems with the ablation catheter or cable, issues with the grounding pad and inadequate gel on the back patch.

Electrogram Signals: Unipolar and Bipolar

Electrogram signals occur as a result of voltage gradients which occur between myocytes at different phases of the cardiac AP. **Unipolar electrograms** are amplified signals which are recorded between the distal pole of the catheter (+) and Wilsons Central Terminal (−) and are in essence bipolar signals between two regions spaced far apart. This, therefore records both near and farfield, the latter of which may distort the local signal.

Bipolar signals are amplified signals recorded from two closely spaced unipoles. In general, the distal pole is negative while the proximal pole is positive. Bipolar recordings are affected by the direction of the wave front with respect to the electrode orientation, electrode spacing and configuration and are generally considered more useful in clinical practice. An example of these two types of signal is shown in Figure 2.11.

Despite these limitations, both types of signal can be used in cardiac mapping, such as in exit site and accessory pathway localization where a deep Q wave with no R wave may indicate proximity to the activation site in unipolar electrograms (Simmers et al. 1994). This is not perfect for localization of the focus. As shown in 2.11, during a PVC originating from the LV inferior wall, there is a deep Q wave with no R wave in the ABL WCT electrogram. However, the electrogram is not significantly earlier than the surface QRS. Although this was the earliest unipolar and bipolar electrogram on the endocardium this focus was found to be located on the epicardial surface.

RF Generation and Ablation

Radiofrequency (RF) energy is the most commonly used energy source using for creating an ablation lesion. The generator produces a continuous sinusoidal waveform at a frequency between **500–1000 kHz** which is then delivered between the catheter tip and a patch electrode placed on the skin. As a result of the difference in the surface area between the tip of the ablation catheter and the dispersive electrode pad the maximum zone of resistive heating, which is directly related to current density, is generally within 2 mm of the catheter tip. The majority of this is lost in the blood flow as blood has a lower resistance than myocardium.

The rest of the lesion, which is in fact the majority, is formed by conductive heat. This diminishes as a function of $1/r^4$ where r is the distance from the point of maximum resistive heating. The size of the lesion increases as the temperature increases. In general, an irreversible lesion occurs at or above 50 °C. Notably, if the temperature at the electrode-tissue interface rises to greater than 100 °C the tissue immediately adjacent to the electrode forms a coagulum and a steam pop is heard.

The actual impedance during RF ablation is dependent on the tissue in contact with the catheter, the temperature, body characteristics, catheter properties, cables and reference patch. In order to create a lesion during the delivery of RF, there is generally a reduction in the impedance of greater than 10 Ohms. As shown in Fig. 2.12, a sudden rise in impedance is often associated with a steam stop and potential perforation.

A thermocouple incorporated into the tip of the ablation catheter measures the temperature. In temperature guided ablation, the temperature of the

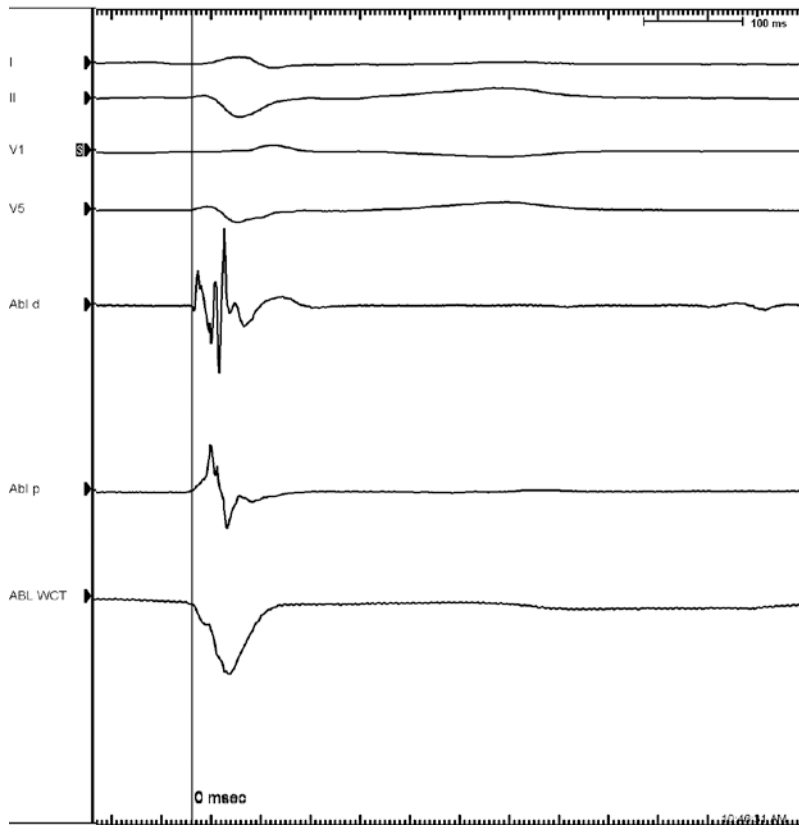

Fig. 2.11 A PVC originating from the inferior LV wall. The bipolar and unipolar electrograms are on time with the onset of the surface QRS. The unipolar electrogram has no R wave and a deep Q wave. Although this indicated activating moving away from the catheter the fact that the signal is not early indicated that this was not the focal site of the PVC. This was mapped to the epicardial surface of the inferior wall of the LV where the local signal was 20 ms ahead. (Abl d is recorded as a bipolar electrogram recorded from the distal electrode on the ablation catheter, Abl p is the bipolar electrogram recorded from the proximal electrode on the ablation catheter, ABL WCT is the unipolar electrogram recorded from the distal electrode on the ablation catheter to Wilson's Central Terminal)

ablation electrode is set at the start of the ablation and automatically adjusts power output to achieve a targeted electrode temperature of between **55** and **70 °C**. Ablation can also be set at a power limit so that RF is delivered until a certain power is achieved.

Lesion sizes are usually 5 mm in diameter but may be increased by the use of a larger diameter ablation catheter or with the addition of irrigation, which aids in flushing the tip of the catheter.

Cryoablation

Cryoablation has been used in the ablation of slow and accessory pathways anatomically close to the compact AV node as well as in pulmonary vein isolation (PVI). There are several potential benefits of using this modality. Following the application of cryoablation, there is an initial degree of reversibility in lesion formation, particularly between −10 and −25 °C. This confers a potential advantage in the case of a nodal or accessory pathway ablation that is close to the compact AV node where the risk of AV block is considered to be significant. Permanent tissue damage occurs at temperatures less than −50 °C.

During the application of cryoablation, the catheter tends to remain lodged to the tissue, resulting in increased catheter stability.

This concept relies on localised hypothermia at the catheter endocardial surface. There are three biophysical phases to this process.

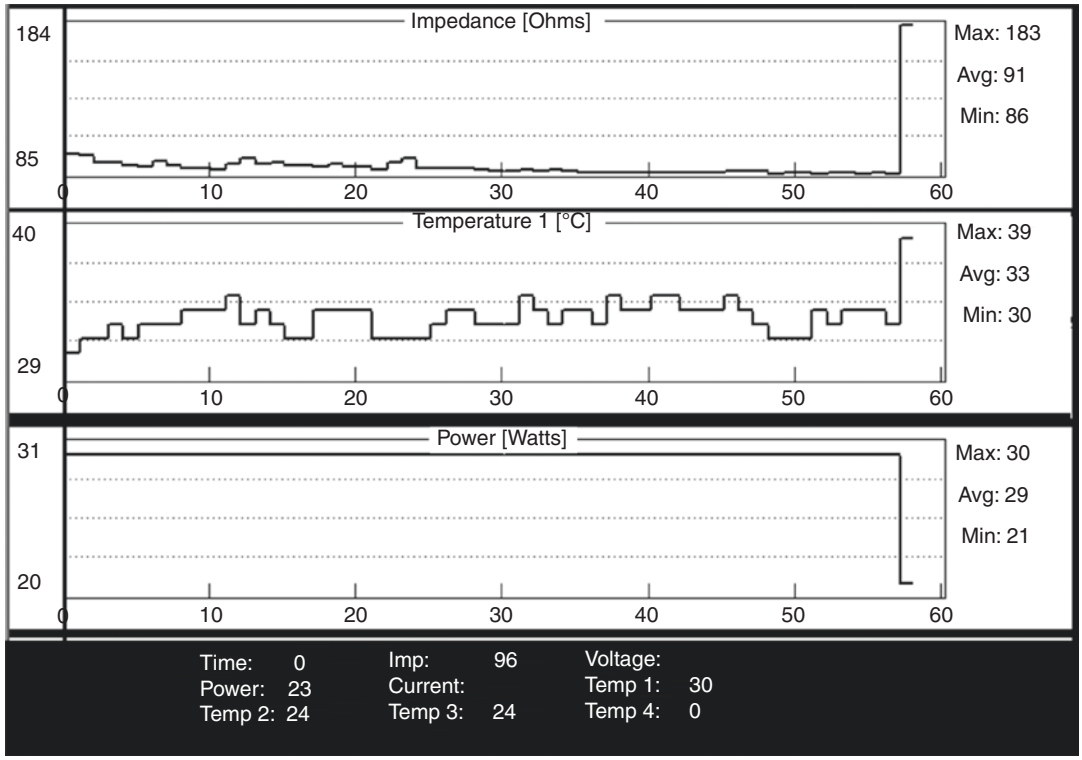

Fig. 2.12 RF ablation in the left atrium using a 4 mm irrigated catheter. There is a sudden rise in impedance and temperature at the interface between the catheter and the endocardium. This results in a steam pop

Freezing: Thawing Phase

This occurs acutely during delivery of cryoablation and may be reversible during the first few minutes. Microscopic extracellular ice formation occurs as the temperature drops below −15 °C and is followed by intracellular ice formation, which occurs as the temperature drops to less than −40 °C. Consequently, there is an increase in ion concentrations in the extracellular space which becomes hypertonic resulting in a shift of fluid from the intracellular space to the extracellular space. This causes a reduction in intracellular pH, leading to mitochondrial damage and progressive microcirculatory vasoconstriction resulting in further localised damage to the local tissue.

Following the completion of localised freezing, passive rewarming, otherwise known as thawing, occurs. This results in the fusion of ice crystals with further cellular damage in addition to microvascular occlusion due to platelet aggregation and microthrombi formation.

Hemorrhagic: Inflammatory Phase

As thawing continues, the changes in the microvasculature result in regional hyperemia and tissue edema with microscopic hemorrhagic changes and inflammation. This tends to occur within 48 h of the thawing process and may continue for up to 1 week.

Replacement: Fibrosis Phase

Replacement fibrosis and apoptosis of cells near the periphery of the lesion occurs within the first week and up to 3 months after the delivery of the lesion. Neovascularisation and collagen remodelling occurs until finally, a fibrotic scar forms.

Electroporation

Both RF and cryoablation techniques use thermal energy transfer to produce local tissue necrosis. Despite their widespread clinical use, there are several limitations associated with thermal-based methods which have the potential to impair proper lesion formation and damage nearby structures (esophagus, phrenic nerve). Electroporation has emerged as an alternative option for the induction of selective cellular death, whereby high electric fields (direct current; DC, alternating current; pulsed DC; or a combination) are applied across the tissue. This results in an increase in cell membrane permeability, leading to either transient cell denaturation or permanent damage leading to cell lysis. In the case of pulsed DC, an increase in cell permeability may be attributed to the formation of nanometric pores in the cell membrane. The successful application of electroporation in cancer therapy has stimulated interest in its use within cardiac electrophysiology. In catheter ablation, its main therapeutic role would be to selectively and permanently disrupt myocytes in order to cause a transmural lesion with no collateral damage. However, precise electrical parameters during ablation (pulse duration, interpulse intervals, levels of electric field) remain unclear, prompting further studies are required in order to achieve tissue-specific death without associated side effects.

Ablation Catheters

Ablation catheters, in their simplest form, delivery energy to the myocardium while providing feedback in the form of tissue temperature and impedance. They vary in the size of the tip electrode as well as ability to delivery irrigation. Some catheters also provide feedback in terms of contact force data. The majority of available catheters tend to have a platinum tip. Other materials such as gold have also been studied and also appear to be efficacious.

Ablation Catheter Size

Larger electrode sizes have a larger percentage of surface area exposed to blood rather than endocardium. Due to the cooling effect of the blood flow a smaller lesion is delivered using similar power with a larger diameter catheter (Fig. 2.13) (Otomo et al. 1998). A higher power is therefore required to achieve the target temperature, thereby producing a larger lesion. Larger tip catheters have been shown to be more effective with a reduced number of RF applications and reduced fluoroscopy time in atrial flutter ablation (Rodriguez et al. 2000).

Conversely, better electrogram resolution is achievable with smaller tip catheters and generally, smaller tip irrigated catheters have been shown to be very effective in atrial flutter ablation. The temperature measured at the tip of the catheter does not accurately estimate tissue temperature.

Irrigation

In open loop irrigation, saline is flushed through the ablation catheter resulting in cooling of the catheter tip with lowering of the catheter tip temperature. This allows for the ability to create deeper lesions with less focal hot spots and a reduced risk of thrombus formation. As shown in Fig. 2.14 a larger lesion is created over a shorter time period using a catheter with irrigation when compared with no irrigation. Using the same power and electrode size a catheter with irrigation tends to result in a larger lesion (Fig. 2.15). Temperature feedback is not reliable and therefore ablation is limited by power.

Although lesion sizes are larger using irrigation, they tend to grow beyond 60 s and therefore a longer application should be considered.

The rate of irrigation should be altered according to the power delivered.

The general recommendations are **2 mL/min during mapping**, **17 mL/min during ablation at a power of less than 30 W** and **30 mL/min at a power of greater than or equal to 30 W**.

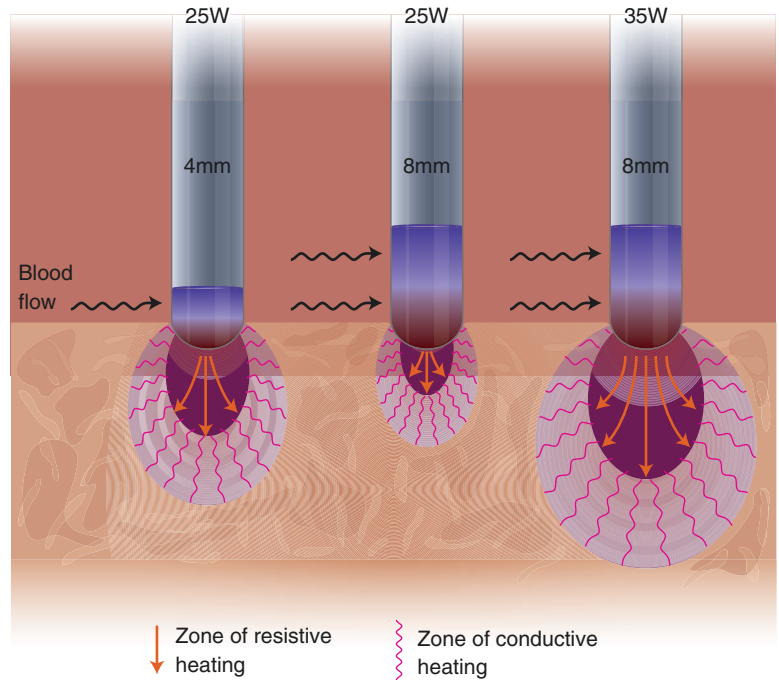

Fig. 2.13 Effect of Ablation Catheter Tip Size on the ablation lesion consisting of the zone of resistive heating and the zone of conductive heating. A higher power is required for a lesion to be created by a larger tip electrode due to an increase in loss of energy through an increase in flow across the larger surface area of the catheter

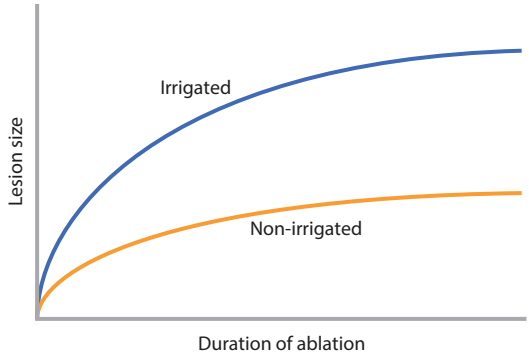

Fig. 2.14 Diagrammatic Representation of lesion size developed over time for irrigated and non-irrigated ablation showing a larger lesion created over a shorter time for an irrigated catheter when compared with a non irrigated catheter

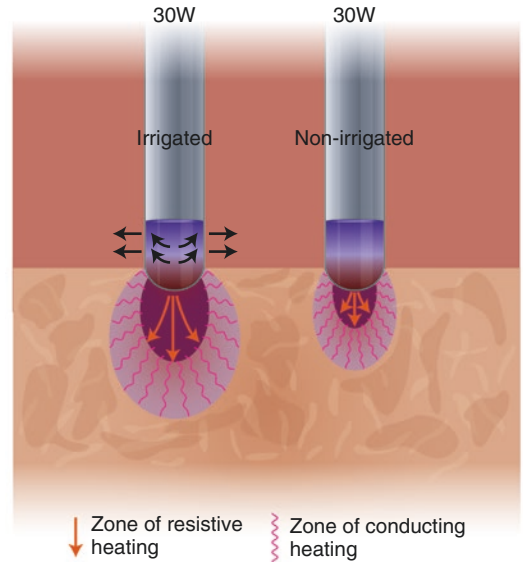

Fig. 2.15 Representation of the effects of irrigation on lesion size using a catheter with the same electrode size and at the same power

Contact Force Catheters

The contact force and orientation between the catheter tip and the endocardial surface provides valuable information on whether RF energy delivery is having any significant impact on the tissue rather than the blood pool. It has been shown that poor tissue contact results in a higher recurrence of AF in patients who undergo a PVI (Reddy et al. 2012; Neuzil et al. 2013), whereas excessive contact force may result in perforation. There are two commercially available contact force catheters which employ different technologies.

The SmartTouch catheter (© Biosense Webster, Inc) is an irrigated 7.5 Fr catheter with an 3.5 mm electrode whereby a magnetic transmitter is connected to the main body of the catheter via a spring. This is able to transmit data regarding the directionality of the electrode tip, relative to the shaft of the catheter, to the processing unit. In order to measure the applied force, three additional sensors are present within the shaft. While this records a minimum change of 1 g every 50 ms, the mean force is displayed every 1 s (Martinek et al. 2012).

Minimum contact force, duration of force as well as catheter stability, power, impedance and temperature changes can all be programmed on in order to set a minimum criteria for display of a lesion using Visitag software on Carto 3. Given the sensitivity of the electrode tip an introducing tool should be used when advancing the catheter through a sheath. A zero baseline reference should also be obtained after the catheter has been in the blood pool for a minimum of 15 min while the catheter is not in contact with any cardiac structure.

The Tacticath catheter (St. Jude Medical, Cardiology Division, Inc., Plymouth, Minnesota) is an irrigated unidirectional 7 Fr catheter with a 3.5 mm tip electrode and a triaxial fibreoptic sensor. Contact force is measured every 100 ms and continually displayed. The force time interval (FTI) can also be displayed and may aid in guiding ablation. Using the Tacticath, a contact force greater than 20 g appeared to generate durable pulmonary vein isolation while a contact force less than 10 g tended to be associated with recurrences (Reddy et al. 2012). A target of 20 g with a minimum greater than 10 g and a minimum force time index greater than 400 g appears to result in a higher likelihood of transmural lesions in the left atrium (Neuzil et al. 2013).

Vascular Access

Electrophysiology catheters are positioned in the heart by gaining access via the central veins; generally the femoral veins for most catheters and occasionally the internal jugular or subclavian veins for coronary sinus catheter placement.

Femoral Cannulation

Femoral vein access is the most commonly used for most EP procedures. The femoral artery is palpated and cannulation is performed medial to the femoral artery while maintaining a position inferior to the inguinal ligament. Superior to the inguinal ligament may result in a difficultly with compression and potential bleeding into the retroperitoneal space. In general, up to three standard EP catheters can be positioned into a femoral vein, provided separate cannulations are performed. However, this is highly dependent on the overall size of the patient. If there are any concerns regarding the potential for vein occlusion, the left femoral vein may also be cannulated.

The femoral artery may be used to access the left ventricle and in particular LVOT focal tachycardias. Additionally, it may be used for LV VTs and left sided accessory pathway ablations. The relationship of the right femoral vein to the femoral artery is shown on the anatomical images in Fig. 2.16. In all cases, it is crucial to maximize the distance between the femoral venous and arterial access points in order to minimize the risk of arteriovenous fistula.

Subclavian/Axillary Vein

The axillary vein combines with the cephalic vein to become the subclavian vein as it passes superficial to and medial to the anterior portion of the first rib. The course of the left axillary and subclavian vein are shown on CT scan in Fig. 2.17. Following infiltration with local anesthesia, the needle is directed towards, and very slightly deep to, the junction of the medial one third of the clavicle with the remainder of the clavicle. This should be superficial to the first rib and can be achieved with the use of fluoroscopy. If venous flow is not obtained a slightly deeper approach should be undertaken. Given that the needle does not pass medial to the first rib or deep

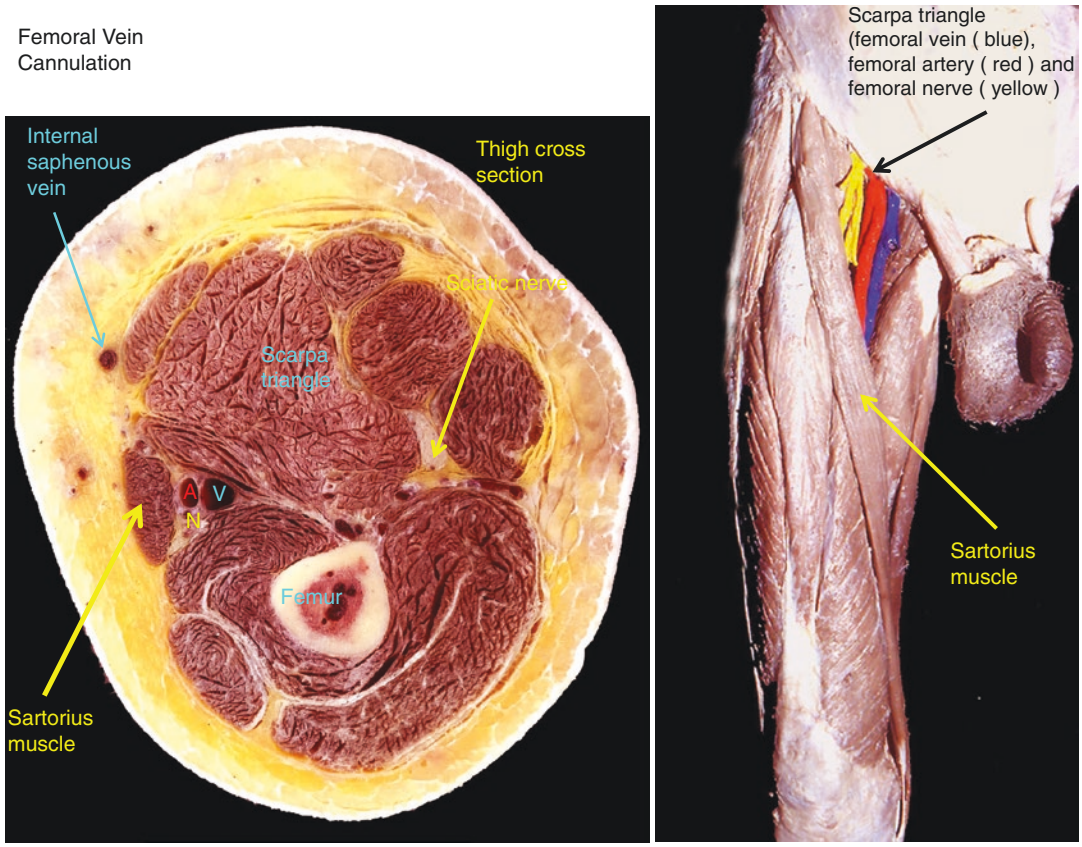

Fig. 2.16 Anatomical images showing the relationship of the femoral vein (blue), the femoral artery (red) and the femoral nerve (yellow) with the Scarpa triangle

to the first rib via the second intercostal space, a pneumothorax should not occur. Alternatively, a venogram can be performed. The advantage of subclavian vein access over internal jugular access lies in the fact that the vein remains patent due to soft tissue attachments with the costoclavicular ligament and the clavicular periosteum, thereby preventing collapse. Hence, while the Trendelenberg position may reduce the incidence of air embolism, it is not required to increase vein patency. At the subclavian axillary junction, the subclavian artery is significantly posterior and slightly superior to the vein. These two structures are separated by the anterior scalene muscle which is 1–1.5 cm thick and reduces the risk of accidental arterial puncture. Since this muscle is not present laterally, the risk of arterial puncture increases in more lateral positions. Traveling more medially towards the juncture of the subclavian and axillary juncture, the apical pleura of the lung is posterior to the vein. It is therefore, imperative to keep the needle as horizontal as possible with only slight increases in depth if a more medial approach is being made. More inferior locations are also more likely to puncture the pleura and lung due to the conical shape of the chest.

Internal Jugular Vein

Cannulation of the internal jugular vein may occasionally facilitate positioning of the coronary sinus catheter. Infiltration of local anaesthesia followed by Seldinger cannulation should be performed at the apex of the triangle of Sedillot. This triangle is formed medially by the sternal head of the sternocleidomastoid, laterally by the

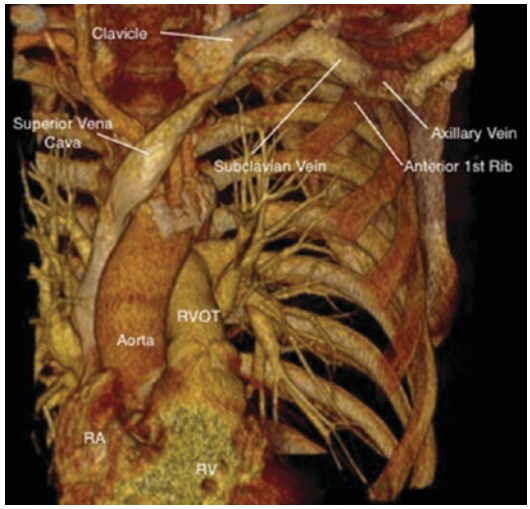

Fig. 2.17 Anatomic course of the left axillary and subclavian vein on a CT scan. The axillary vein runs anterior to the first rib towards the clavicle. Medial to this it becomes the subclavian vein which joins the superior vena cava. Also seen in this image is the ascending aorta. The right ventricular outflow tract (RVOT), the right atrium (RA) and the right ventricle (RV)

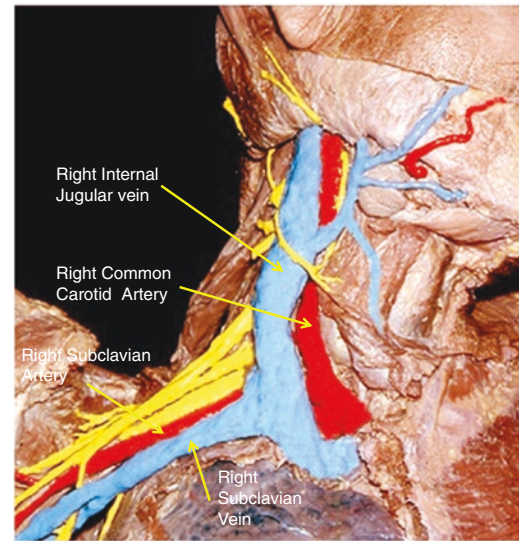

Fig. 2.18 Anatomical image showing the relationship of the right internal jugular vein (blue) which lateral to the right common carotid artery (red). The right internal jugular passes anterior to the right subclavian artery and joins the right subclavian vein where the two become in innominate vein. The right brachial plexus is shown in yellow

clavicular head of the sternocleidomastoid and inferiorly by the medial one third of the clavicle. Transient flexion of the neck should help to accentuate these landmarks in most patients if they are not clear. If the patient is under general anesthesia, palpation of the trachea can be performed while palpating laterally over the sternal head of the sternocleidomastoid into the recess of the triangle. The carotid pulse can also be palpated prior to but not at the same time as cannulation as this often compresses the internal jugular vein. The carotid artery runs medial and posterior to the internal jugular although on occasions may only be posterior. Excessive contralateral rotation of the head beyond a 45°-angle pushes the carotid artery more lateral and posterior to the internal jugular vein.

The internal jugular vein generally lies 1–2 cm deep in the skin at the apex of the triangle and advancing the needle greater than 2 cm increases the risk of a pneumothorax. The needle should be advanced at a 45°-angle. The use of an ultrasound may be helpful to differentiate between vein and artery; however, the artery is generally more medial, deeper, non compressible and has a visible pulsation. The anatomy of the right internal jugular vein is shown on Fig. 2.18.

Electrophysiology Catheters and Positioning

Electrophysiology catheters are generally made of platinum coated electrodes with polyurethane coated shafts. They are categorized according to the diameter of their shaft, the number of poles used to record and pace through, the spacing between electrodes, and the ability to deflect. Ablation catheters are also categorized according to the curve, length of the tip of the catheter, ability for irrigation, and ability to measure contact force.

The external diameter of an EP catheter is measured in **French (Fr)** where **1 Fr is 1/3 mm**. Therefore, in order to convert the French size to mm, the value is simply divided by 3. The majority of diagnostic EP catheters are either 5 Fr or 6 Fr and the number of poles recording and pacing ranges from 2 up to 20. Commonly, quadripolar catheters are positioned in the right atrium,

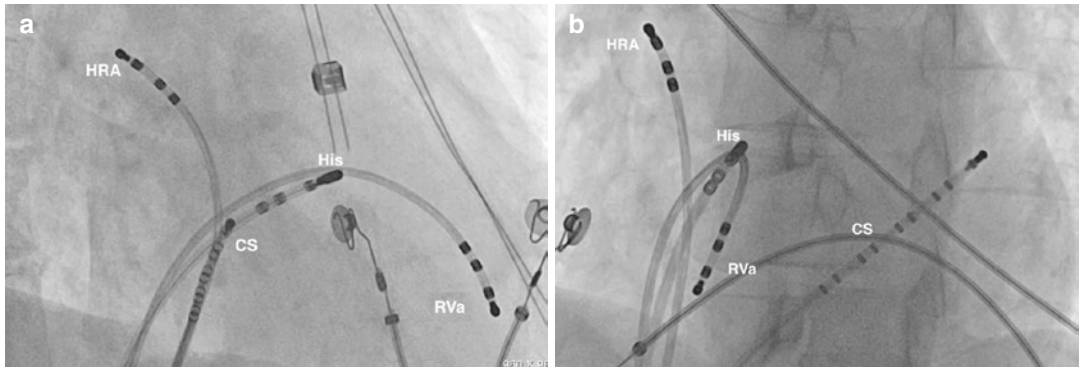

Fig. 2.19 Fluoroscopic image in RAO 30 (top) and LAO 30 (bottom) showing the locations of EP catheters in the high right atrium (HRA), coronary sinus (CS), His and right ventricle apex (RVa)

His bundle and right ventricle while decapolar catheters are positioned in the coronary sinus. A duodecapolar catheter may be used to map right atrial activation during a cavotricuspid isthmus ablation, albeit usually not required.

Catheters that are deflectable are easier to position.

The high right atrium (RA) catheter in an EP study is generally positioned in the high posterolateral wall at the junction of the RA with the superior vena cava close to the sinus node. The catheter can also be positioned in the RA appendage. A non deflectable quadripolar catheter is sufficient for this purpose and can generally be positioned in either the right anterior oblique (RAO) or left anterior oblique (LAO) views.

The RV catheter is generally best placed along the base or septum. It may be positioned close to the His and used to record the His and ventricular signals. This position is achieved in the RAO or LAO projection while withdrawing the catheter from the RV with a clockwise rotation towards the septum.

The coronary sinus catheter is initially positioned in the RA and advanced with a clockwise rotation towards the more posterior CS Os in the LAO projection. Alternatively, it can be positioned in the RV and withdrawn with clockwise rotation in the same view. The general locations of EP catheters are shown in Fig. 2.19.

Baseline Measurements

Sinus Node Recovery Time (SNRT)

SNRT is measured using the principle of overdrive suppression in which pacing is performed close to the sinus node at a rate faster than the sinus rate. This is performed at a cycle length of 600/500/400/300/200 ms for a period of 30 s during each drive train. Subsequently, the time taken from the last paced beat to the first intrinsic sinus beat is measured. As shown in Fig. 2.20 the interval from the last paced beat to the first intrinsic beat is then measured. This is longer than the baseline sinus rate and generally takes 5–6 beats to return to normal after this maneuver is performed. A prolonged sinus node recovery time **greater than 1500 ms** is abnormal. This may not always occur at faster cycle lengths as entry block may intermittently occur in the perinodal cells and therefore not every beat may depolarize the sinus node. The SNRT is also dependent on the baseline sinus cycle length and is prolonged for longer baseline cycle lengths and reduced for shorter cycle lengths. In order to account fot this, the corrected SNRT can be calculated as:

$$\text{cSNRT} = \text{SNRT} - \text{BCL}.$$

A cSNRT of 525 ms or more is considered abnormal.

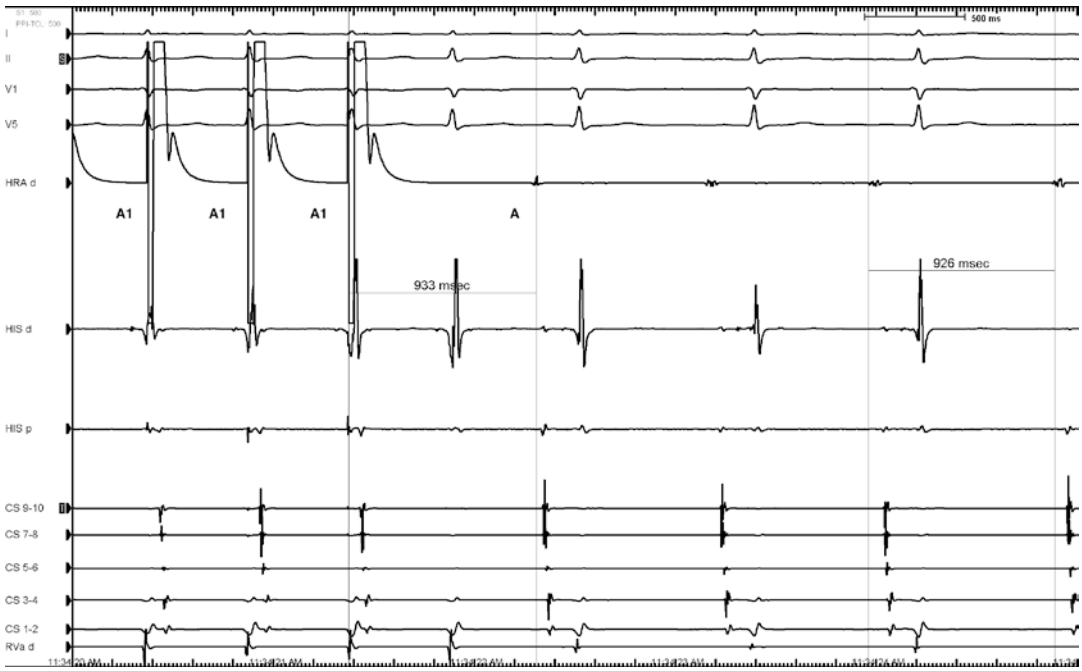

Fig. 2.20 Showing Calculation of the Sinus Node recovery Time (HRA d is positioned in the high right atrium, HIS d in the distal His, HIS p at the proximal component of the His, CS 9–10 is in the proximal CS while CS 1–2 is in the distal CS and RVa d is located in the RV apex) A1 = paced atrial complexes. A = spontaneous sinus beat post pacing

Sinoatrial Conduction Time (SACT)

This is the conduction time from the SN to the RA tissue. This is measured by positioning a catheter close to the sinus node and pacing at a rate slightly faster than the baseline cycle length for a single beat only; hence, to avoid overdrive suppression. As shown in Fig. 2.21, the interval from the last paced beat to the next intrinsic sinus beat is measured and is known as the return cycle length. If the basic cycle length is subtracted from the return cycle the remaining interval is equivalent to the time taken to conduct into and out of the sinus node. This is then divided by two in order to calculate the SACT. **A normal SACT** is considered to be to be **50–125 ms**.

AV Conduction Times (AH and HV Intervals)

The **AH interval** is recorded from the onset of the local atrial electrogram recorded in the His catheter to the onset of the His signal and is considered to represent conduction through the AV node (Fig. 2.22). The normal range is **50–120 ms**. A prolonged AH interval may occur as a result of intrinsic AV nodal dysfunction, as a result of increased vagal tone or a result of antiarrhythmic drugs. A short AH interval can occur spontaneously or under the effect of sympathetic stimulation.

The **HV interval** is measured from the onset of the local His signal to the earliest ventricular signal on the surface ECG (Fig. 2.24). This generally reflects the conduction time through the proximal His, bundle branches and the Purkinje system. The normal range, of which, is considered to be between **30** and **55 ms**. Intrinsic His dysfunction or antiarrhythmic drugs may prolong the HV interval. A short HV interval may be seen with accessory pathway conduction and may even be negative. In the presence of accessory pathway conduction, the HV does not reflect His-Purkinje conduction and instead is represents the true HV interval.

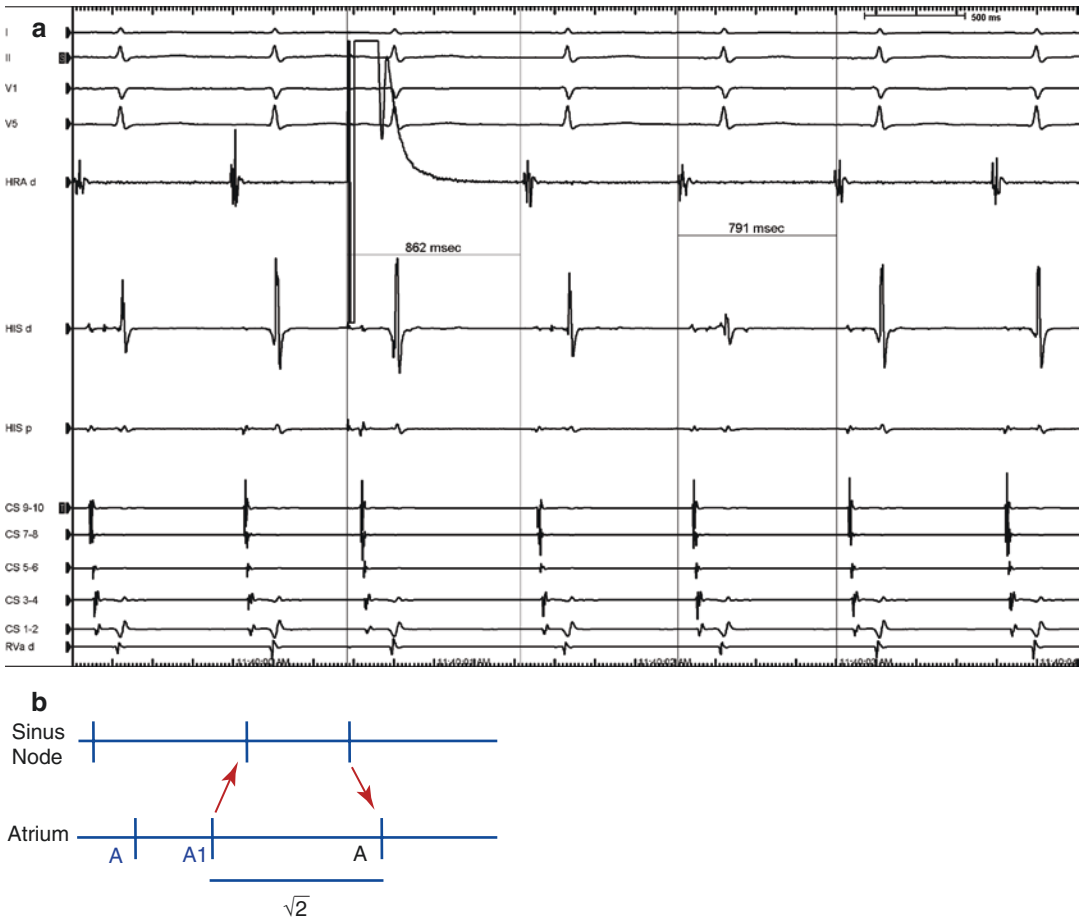

Fig. 2.21 Calculation of Sino Atrial Conduction Time (HRA d is positioned in the high right atrium, HIS d in the distal His, HIS p at the proximal component of the His, CS 9–10 is in the proximal CS while CS 1–2 is in the distal CS and RVa d is located in the RV apex)

Care must be taken not to confuse the right bundle electrogram with the His electrogram as this may artificially lead to a seemingly shorter HV interval.

Refractory Periods (AERP, AVNERP, VERP, VANERP)

During an EP study the **effective refractory period (ERP)** is recorded. This is the longest coupling interval in which the stimulus **fails** to stimulate the myocardium at twice the diastolic threshold.

To calculate the ERP, a drive train of 8 beats followed by a progressively shorter extrastimulus is performed (shown in Fig. 2.23). The **normal atrial ERP is 170–300 ms while the ventricular ERP is 170–290 ms (Josephson** n.d.). In order to evaluate the AVNERP, the atrium is paced in the same way as when the AERP is calculated. During decremental atrial extrastimuli, the AH interval is gradually prolonged while the HV interval remains the same. The **normal AVNERP is 230–425 ms** (Josephson n.d.).

AV Wenckebach Point

As shown in Fig. 2.24, decremental atrial pacing can be performed at progressively shorter cycle lengths until AV block occurs. The AV

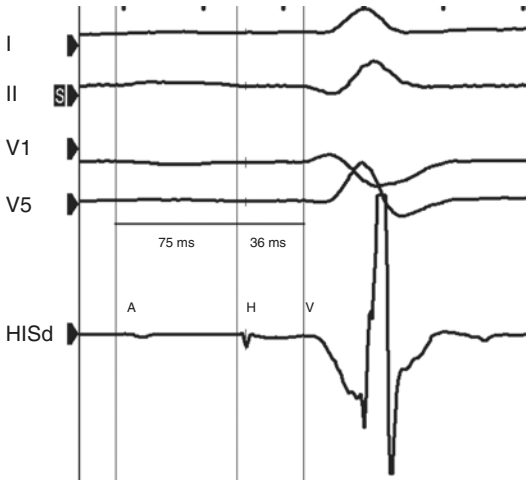

Fig. 2.22 Calculation of the AH interval (75 ms) from the onset of the atrial electrogram on the His recording to the start of the His electrogram and the HV Interval (36 ms) measured from the onset of the His signal to the onset of the ventricular activation on the surface ECG (HIS d is positioned in the distal His)

Wenckeback point is thereby defined as the **longest cycle length which results in AV block**. This provides some data on the functional conduction through the AV node.

Basic EP Study

There is considerable variability that exists with regards to the number of catheters and their positioning. In most diagnostic EP studies, a quadripolar catheter is positioned in the HRA as well as the RV septum and a decapolar catheter is positioned in the coronary sinus. The RV quadripolar catheter can sometimes be used to record the AH and HV intervals.

Pacing is performed from the RV septal catheter at a constant rate, yet faster than the sinus rate. This is to identify the presence of VA conduction and in some cases, the atrial activation sequence. As shown in Fig. 2.25, decremental VA conduction is initially anterior and septal which generally indicates VA nodal conduction. However, this is not always the case and it is important not to disregard an anteroseptal accessory pathway with decremental retrograde conduction. Similarly, a lack of decrement does not always exclude VA conduction as rapid ventricular pacing from the RV may result in infrahisian block.

As shown in Fig. 2.26, pacing from the RV does not always result in VA conduction. Although this may infer that AVRT is not possible, it is generally recommended that pacing is repeated during infusion of isoprenaline as VA conduction may become evident.

A **ventricular extrastimulus test** is performed by pacing at a constant cycle length and adding in an extrastimulus at a progressively shorter cycle length. This pacing mode is used to calculate the VERP and the retrograde conduction properties.

Pacing from the HRA is performed in order to calculate sinus node function. Atrial extrastimulus testing is then performed to examine the AERP and AVNERP, as well as the antegrade conduction properties.

An example of an AH jump, resulting from dual AV nodal pathways, is shown in Fig. 2.27. In panel A conduction occurs antegradely over the fast pathway. In panel B, a sudden reduction in the atrial extrastimulus by 20 ms leads to an increase in the AH interval by more than 50 ms. Antegrade conduction has suddenly shifted from a fast to a slow pathway.

The AV nodal conduction curve in dual AV nodal physiology is shown in Fig. 2.28. A1A2 refers to the interval from the last paced beat of the drive train to the onset of the atrial extrastimulus. A2H2 refers to the interval from the extratimulus (A2) to the His activation, A2H2. As the atrial extrastimulus occurs earlier, the interval to the His is prolonged until there is a sudden increase from 300 to 350 ms. This is most likely indicative of a change in antegrade activation from the fast pathway to the slow pathway.

An example of an AH jump and echo beat are shown in Fig. 2.29. In this example, there is a jump as antegrade conduction occurs along the slow pathway with ventricular activation and retrograde activation up the fast pathway.

Decremental atrial pacing is used to calculate the AV Wenckebach Point.

Further decremental atrial, and sometimes ventricular pacing, may also be used to initiate

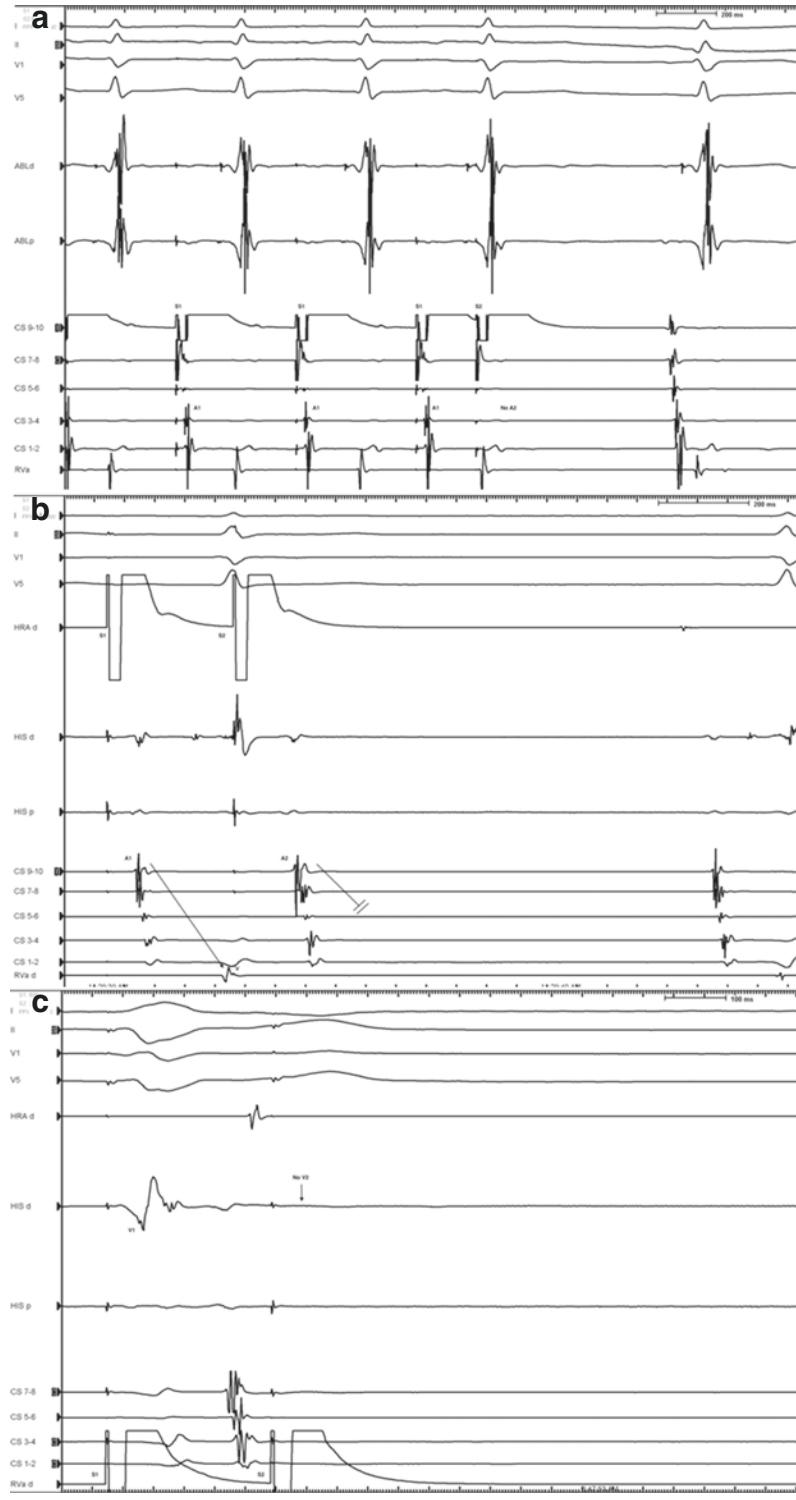

Fig. 2.23 Calculation of the atrial RP (**a**), AV node RP (**b**), and ventricular ERP (**c**). In each case a drive train is performed at a cycle length of 600 ms for 8 beats in order to achieve a steady state. This is followed by a progressively shorter extrastimulus until capture fails to occur. In the case of the atrium and ventricle this is seen as lack of local capture. In the case of the AV node local capture of either the atrium or ventricle occurs with failure of the impulse to propagate through the AV node either antegradely (AV Node ERP) or retrogradely (VA ERP). (HRA d is positioned in the high right atrium, HIS d in the distal His, HIS p at the proximal component of the His, CS 9–10 is in the proximal CS while CS 1–2 is in the distal CS and RVa d is located in the RV apex)

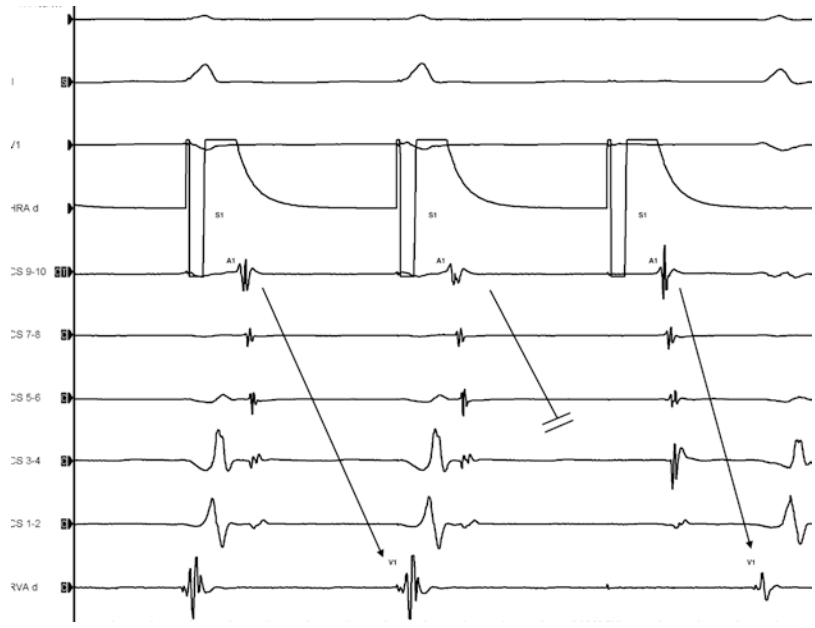

Fig. 2.24 Calculation of AV Wenckeback Point during decremental atrial pacing. (HRA d is positioned in the high right atrium, HIS d in the distal His, HIS p at the proximal component of the His, CS 9–10 is in the proximal CS while CS 1–2 is in the distal CS and RVa d is located in the RV apex)

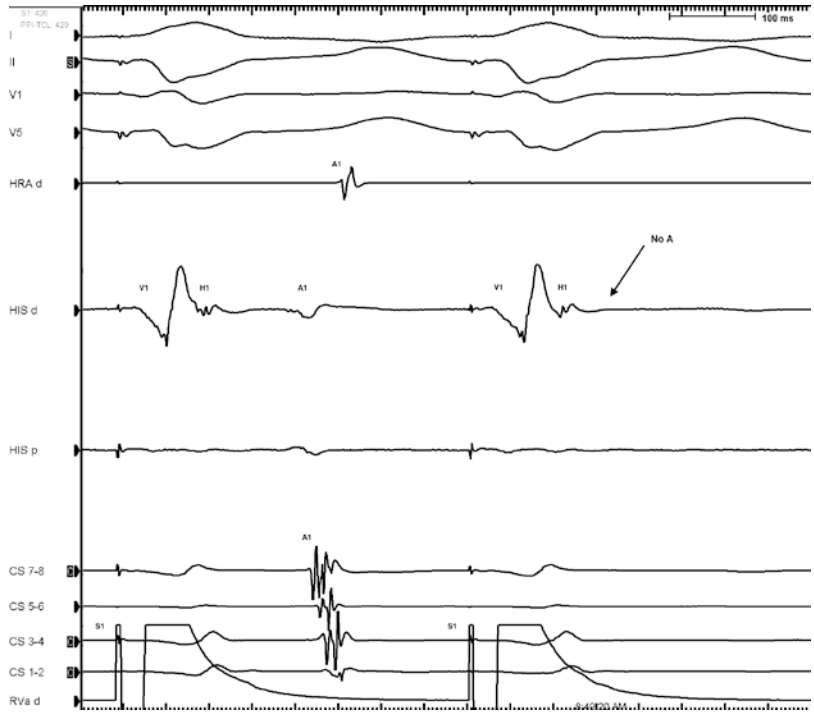

Fig. 2.25 Decremental ventricular pacing (S1) from the RV apex (RVAd). The first paced beat on the left propagates from the RV apex retrogradely up the right bundle and activates the His. A small His deflection (H1) is seen after the ventricular activation (V1) on the distal his (HIS d) channel. Following this there is atrial activation (A1) recorded on the HIS d channel followed shortly thereafter by the proximal his recording (HIS p). Atrial activation (A1) then occurs from the proximal CS (in this case CS 7–8) and spreads distally. The high RA (HRAd) is activated (A1) after the proximal CS. This activation is concentric with the His first followed by proximal to distal CS activation and then the HRAd last). In the following beat there is no conduction from the RV activation followed by His activation and no atrial activation

Fig. 2.26 Pacing from the RV (S1) does not penetrate the His and there is no evidence of VA Conduction. (HRA d is positioned in the high right atrium, HIS d in the distal His, HIS p at the proximal component of the His, CS 9–10 is in the proximal CS while CS 1–2 is in the distal CS and RVa d is located in the RV apex)

tachycardia. If shown to be ineffective, the addition of one or more atrial extrastimuli and the use of incremental doses of atropine or isoprenaline may be required.

In Fig. 2.30, an atrial extrastimulus results in an AH jump in which conduction occurs antegradely along the slow pathway. Following this, tachycardia ensues as retrograde conduction occurs along the fast pathway resulting in a short VA interval. This is most likely in keeping with a typical AVNRT.

VT Stimulation Protocol

The general principle of a VT EP study is to assess the potential risk of VT in a susceptible patient by performing a basic drive train followed by the introduction of extrastimuli at shorter cycle lengths. Typically, this should be performed at the RV apex and the RV outflow tract with a single quadripolar catheter and another catheter in the right atrial appendage. A basic drive train (S1) of 8 beats is introduced at a cycle length of 600 ms followed by an extrastimulus (S2), which is reduced in 10 ms intervals until the ventricular myocardium is refractory. Following this, the S2 pacing rate is brought to 20 ms greater than refractoriness and an S3 introduced in the same manner. S3 is then set 20 ms higher than refractoriness and S1 is reduced to 400 ms. The same protocol is then repeated. In the case that VT is not induced, S1 is brought back to 600 ms and S2 and S3 are set at 20 ms above refractoriness. S4 is then introduced in a similar manner to that described above, and S1 is reduced to 400 ms. If no VT is induced, then the protocol can be reintroduced with an isoprotenolol infusion. Induction of a monomorphic VT using this protocol is considered a significant finding and where possible, this can be compared with clinical VT. An example of a VT stimulation using a drive train at a cycle length of 400 ms with three extrastimuli is shown in Fig. 2.31.

While the initiation of polymorphic VT or VF may be non-specific, this depends on the clinical

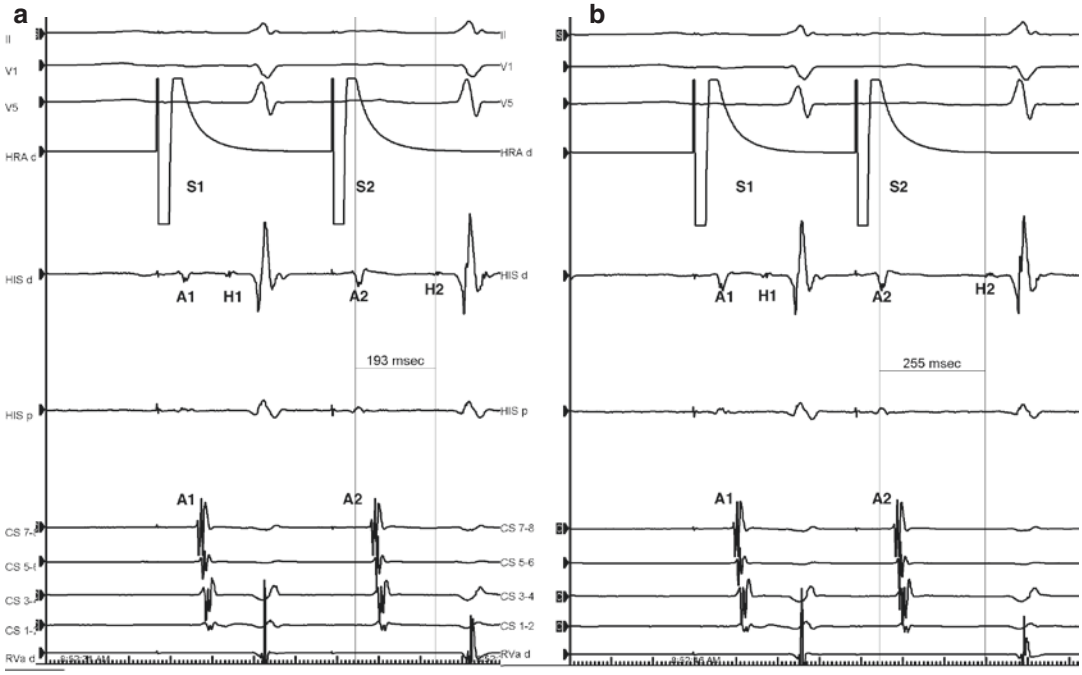

Fig. 2.27 Panel **a**: Atrial extrastimulus testing showing conduction antegradely over the fast pathway. Panel **b**: Antegrade conduction over the slow pathway. Continuous pacing is performed at a cycle length of 600 ms (S1). Following this an extrastimulus (S2) is given after 400 ms on panel **a** with conduction over the fast pathway. In panel **b** the S2 is shortened to 380 ms. The fast pathway is refractory and conduction shifts to the slow pathway. This is evidenced by a sudden prolongation in the AH interval by more than 50 ms. (HRA d is positioned in the high right atrium, HIS d in the distal His, HIS p at the proximal component of the His, CS 9–10 is in the proximal CS while CS 1–2 is in the distal CS and RVa d is located in the RV apex)

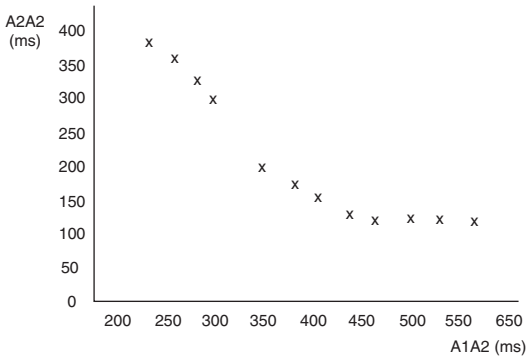

Fig. 2.28 Pacing is performed with a drive train (A1) followed by a gradually decmrental atrial extrastmulus (A2). As this interval shortens the interval from the atrial extrastimulus (A2) to the His (H2) prolongs. There is then a sudden increase in this interval by 50 ms which is generally suggestive of antegrade conduction shifting from the fast pathway to the slow pathway

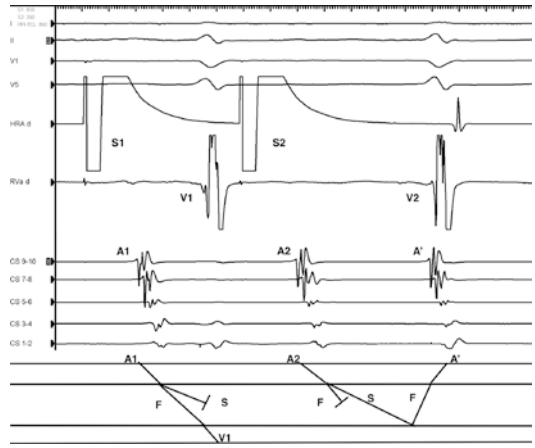

Fig. 2.29 Antegrade conduction occurs along the slow pathway with ventricular activation and retrograde activation up the fast pathway. This is an example of an atrial echo beat

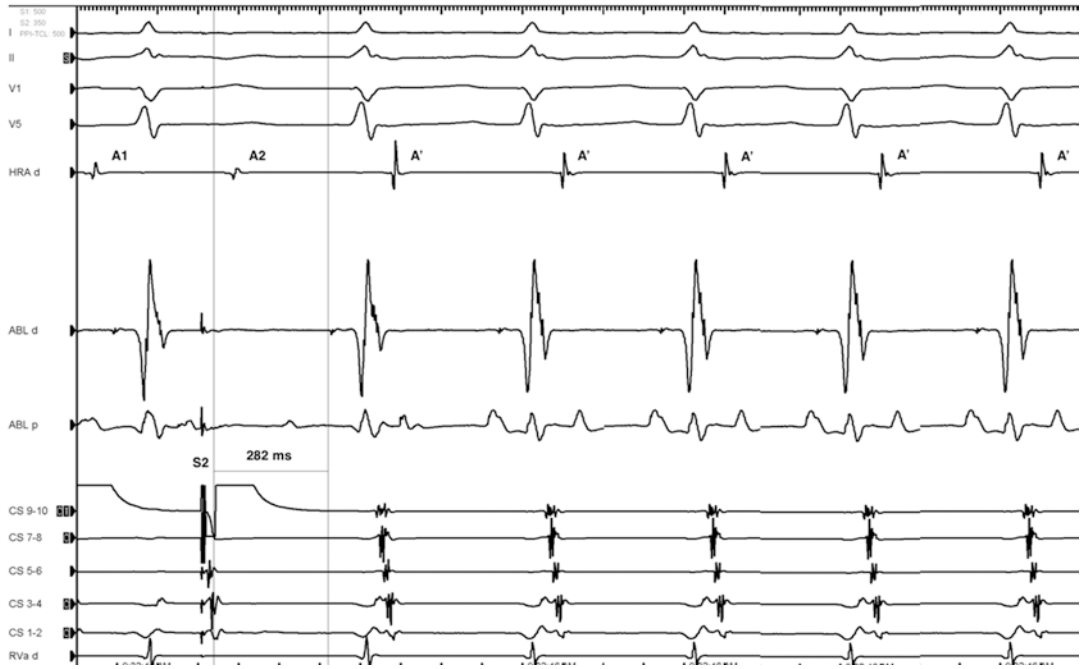

Fig. 2.30 Induction of typical AVNRT. Following a drive train at 500 ms (not shown) an extrastimulus is given after 350 ms from the proximal CS (S2). This results in an AH interval of 282 ms (200 ms on prior S2 indicating an AH jump of 82 ms). This is indicative of antegrade conduction shifting from the fast to the slow pathway followed by tachycardia. The ablation distal (ABL d) is positioned in the location of the His. Activation is earliest in the proximal CS with a short VA interval. Overall the inititiation and activation sequence is suggestive of a typical AVNRT (HRA d is positioned in the high right atrium, CS 9–10 is in the proximal CS while CS 1–2 is in the distal CS and RVa d is located in the RV apex)

context. Torsades de pointes in the setting of long QT syndrome is not inducible by ventricular pacing. On the contrary, a polymorphic VT in Brugada syndrome is highly significant.

VT induced during the study can often be terminated by pacing at a rate 20 ms faster than the VT. If this is unsuccessful or the patient is hemodynamically unstable, a DC cardioversion should be performed.

SVT Diagnostic Maneuvers

Although specific maneuvers will be discussed in each chapter, this section provides an overview of the topic. While the diagnosis can frequently be made during basic pacing, occasionally it may be difficult to differentiate between AVNRT, AVRT in particular utilizing paraseptal AP's and atrial tachycardia's. In order to differentiate between these, certain baseline observations may be made and followed by pacing maneuvers. In cases where tachycardia cannot be easily initiated, parahisian pacing can be performed. In other cases where tachycardia can be initiated, entrainment, His synchronous PVCs, and overdrive pacing can be performed. The choice of maneuver is therefore dependent on the individual case.

Baseline Observations

During baseline testing, any of the following can be used to establish the diagnosis: the presence of dual AV nodal physiology, the onset and termination of tachycardia, presence and effect of tachycardia variability, VA relationship and

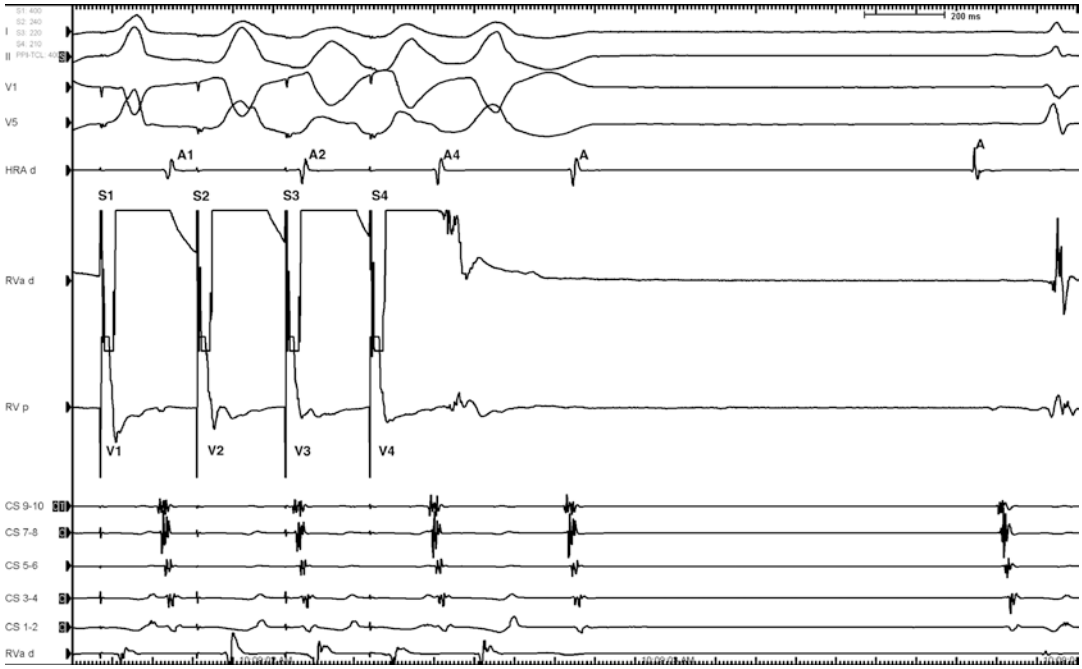

Fig. 2.31 VT stimulation protocol in which a drive train is performed at 400 ms with an S2 of 240, S3 220 and an S4 of 210 from the RV apex. Ventricular activation (V) and atrial activation (A) can be seen corresponding to each extrastimulus. (HRA d is positioned in the high right atrium, HIS d in the distal His, HIS p at the proximal component of the His, CS 9–10 is in the proximal CS while CS 1–2 is in the distal CS and RVa d is located in the RV apex)

atrial activation sequence, and effect of bundle branch block.

The presence of functional dual AV nodal physiology may increase the suspicion of AVNRT. This can be demonstrated as an **AH jump** of greater than or equal to **50 ms** in the case of a typical AVNRT or a HA jump of greater than or equal to 50 ms in the case of an atypical AVNRT. In a patient with tachycardia, the presence of dual AV nodal physiology is reasonably predictive of an underlying mechanism of AVNRT given that the patient has a prior documented SVT with no evidence of AP conduction.

Initiation and Termination

Both AVNRT and AVRT can be initiated by a premature atrial contraction (PAC). In the case of a typical AVNRT, there is a sudden prolongation of the duration between the PAC and the initial QRS complex as antegrade conduction occurs down along the slow pathway (AH jump) (Fig. 2.32).

In orthodromic AVRT, the time from the PAC to the initial QRS is shorter as antegrade conduction occurs along the fast pathway. As seen in Fig. 2.33, pacing is performed at a drive train (S1) of 400 ms with an extrastimulus (S2) at 280 ms. This atrial beat conducts antegradely along the fast pathway, demonstrating decrement without a jump. Conduction then occurs retrogradely with a VA interval of 94 ms. This may be in keeping with a paraseptal AP, atypical AVNRT or less likely, an AT. In this specific case, the diagnosis was a posteroseptal AP.

Atrial tachycardias tend to warm up and cool down with a gradual shortening of the tachycardia cycle length at the onset. Generally, the initial P wave in an atrial tachycardia has a different morphology to the preceding sinus beats; although occasionally, this may be subtle if the focus is close to the sinus node.

PVCs rarely initiate an AVNRT as the His is commonly refractory during the timing of retro-

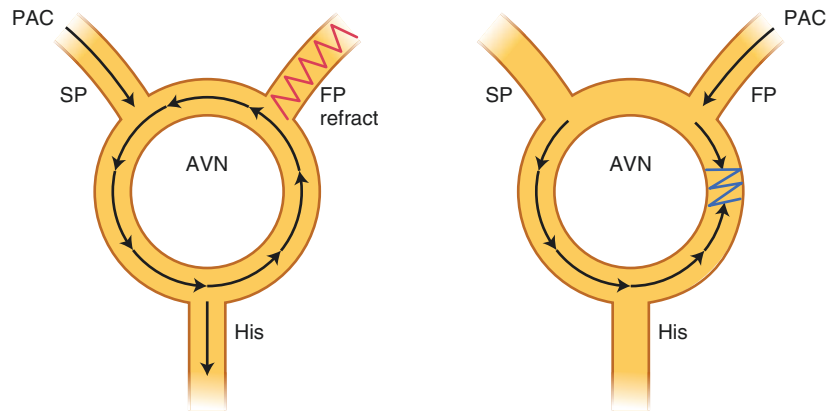

Fig. 2.32 Initiation of a Typical (Slow Fast) AVNRT with a PAC (1) and termination with another PAC (2)

grade activation. On the contrary, PVCs can commonly initiate an AVRT (Fig. 2.34).

Termination of tachycardia with AV block occurring either spontaneously, following a vagal maneuver, or following the administration of IV adenosine occurs in arrhythmias whereby the AV node plays a vital role in the circuit (i.e. AVNRT and AVRT) and does not occur in atrial tachycardia. ATs generally, but not exclusively, terminate with a ventricular complex (Fig. 2.35).

The continuation of tachycardia despite the presence of AV block, however, only rules out the possibility of AVRT. AVNRT and AT may continue to persist in the presence of AV block.

All SVTs can be terminated by varying degrees with either atrial or ventricular premature complexes. In the case of AVNRT, the number of atrial beats required depends on the location of the circuit. Generally, at least two premature ventricular complexes are required to terminate AVNRT, whereas, AVRT termination may occur with either premature atrial complexes or ventricular premature complexes. The number of beats required depends on the distance from the circuit as well as the rate of the tachycardia. In atrial tachycardia, the mechanism of the arrhythmia determines the ability for premature atrial complexes to terminate the tachycardia. In most cases, at least three PVCs are required for termination of an AT.

VA Relationship and Atrial Activation

The P wave should always be identified in the case of SVT in order to assist with ascertaining the diagnosis. The VA interval corresponds with the RP interval in the surface ECG and is useful in helping to discriminate between various SVT mechanisms. If the septal VA interval is less than 70 ms, it is highly predictive of a typical AVNRT. The VA time is generally longer than 70 ms in cases of orthodromic AVRT, atrial tachycardia and atypical AVNRT. Specifically, Coumel's tachycardia, also known as permanent junctional reciprocating tachycardia (PJRT), results in a long VA time with negative P waves in leads II, III and aVF during tachycardia. This is caused by an orthodromic reciprocating tachycardia using the AV node as the antegrade limb and a slowly conducting accessory pathway as the retrograde limb. The accessory pathway is generally a right sided posteroseptal pathway with an atrial insertion point close to the coronary sinus.

It is useful to compare the P wave morphology during tachycardia with sinus rhythm. This is particularly helpful in serving to localize the focus of an atrial tachycardia, in which narrower P waves are more indicative of septal origins.

The atrial activation sequence is very useful in discriminating between the potential causes of SVT. However, central atrial activation may

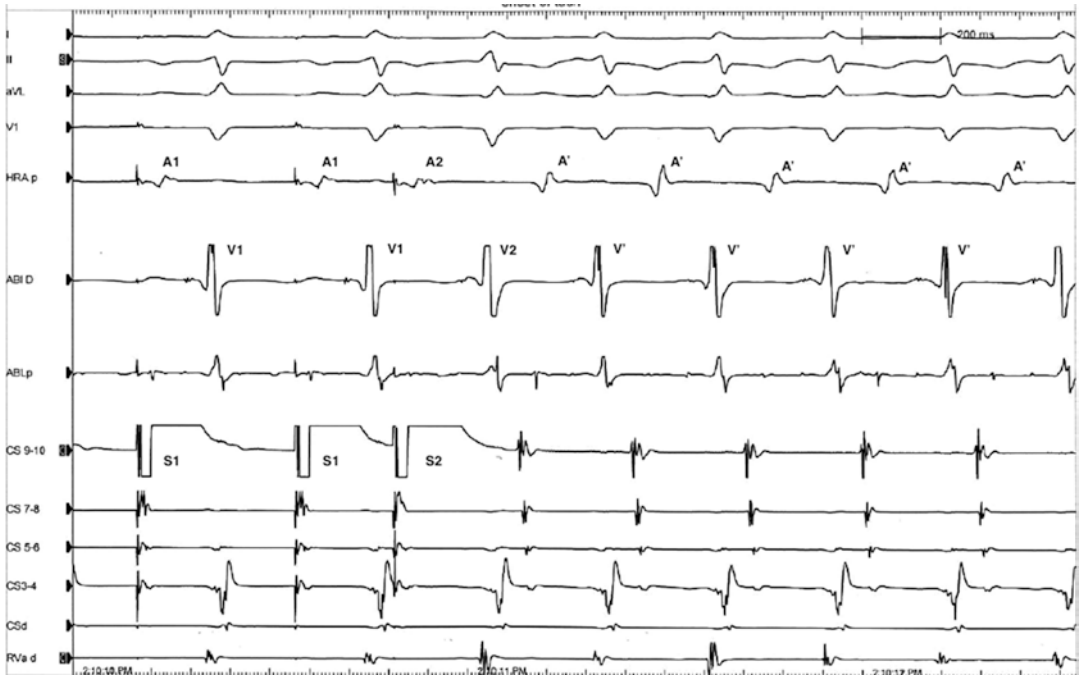

Fig. 2.33 Initiation of an ORT utilizing a retrograde posteroseptal AP. Following a drive train at 400 ms (S1) an atrial extrastimulus is given after 280 ms (S2). This conducts antegradely over the fast pathway and retrogradely over the AP with a VA interval of 94 ms. The corresponding atrial (A) and ventricular (V) activations are shown. (HRA p is positioned in the high right atrium, HIS d in the distal His, HIS p at the proximal component of the His, CS 9–10 is in the proximal CS while CS d is in the distal CS and RVa d is located in the RV apex)

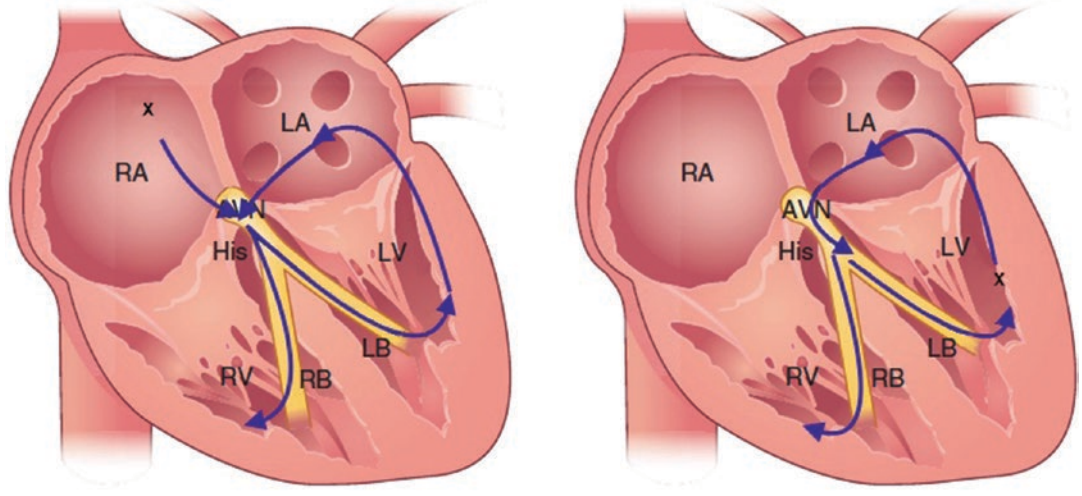

Fig. 2.34 Initiation of AV Re-entry Tachycardia with either a Premature Atrial Complex (PAC) (**a**) or Premature Ventricular Complex (PVC) (**b**)

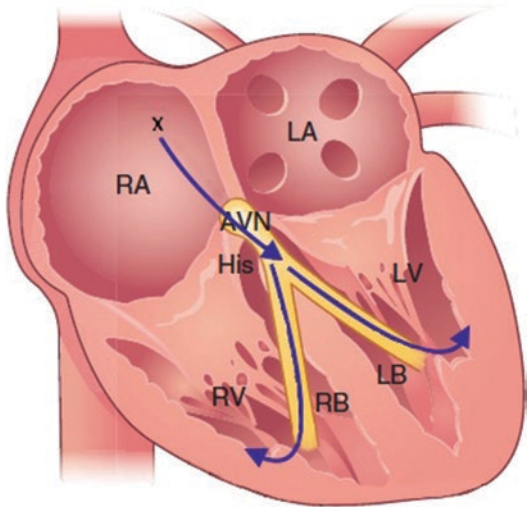

Fig. 2.35 Initiation and termination of Atrial Tachycardia with a long RP Interval

occur with any SVT while eccentric activation more commonly, but not exclusively, occurs with AVRT or an atrial tachycardia. Eccentric activation may also be seen with AVNRT depending on the atrial insertion point of the retrograde slow pathway. For this reason, pacing maneuvers are required to support further differentiation.

Effect of Bundle Branch Block

If the tachycardia cycle length (TCL) is prolonged with induction of BBB, it can be inferred that the arrhythmia is an AVRT with a VA connection on the same side as the BBB. This principle is known as **Coumel's sign** and is represented in Fig. 2.36 and on the electrogram in Fig. 2.37. As BBB does not affect the AV nodal common pathway, neither AVNRT or AT is affected. Due to the rapid ventricular conduction,

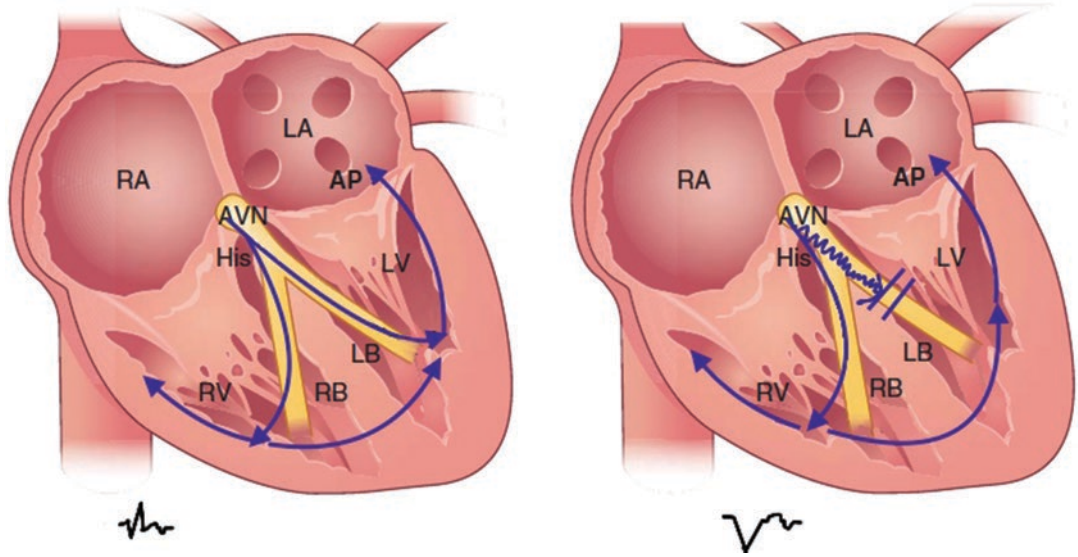

Fig. 2.36 Schematic demonstrating the effect of bundle branch block on the same side as a retrograde accessory pathway. In both images a orthodromic reciprocating tachycardia (ORT) using the AV node as the antegrade pathway is seen. Conduction then occurs through the His and bundle branches. The accessory pathway is located in the left lateral position. In image A conduction occurs through both the right and the left bundle. Given that this is a left lateral accessory pathway activation along the left bundle will activate the accessory pathway rapidly. In image B a LBBB occurs thus delaying activation which occurs through the right bundle and then across the interventricular septum. This results in an increase in the VA interval and prolongation of the tachycardia cycle length (TCL)

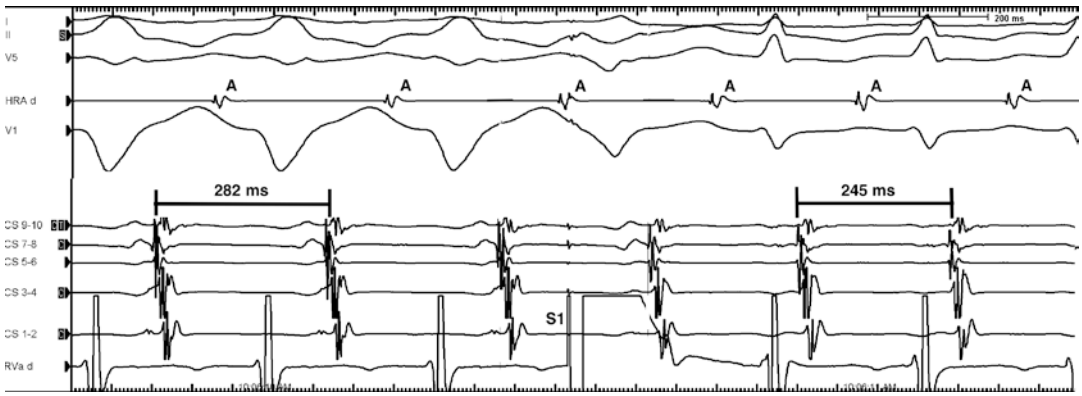

Fig. 2.37 Electrogram showing the effect of bundle branch block on the tachycardia cycle length in a orthodromic reciprocating tachycardia using a left sided accessory pathway as the retrograde limb. On the left of the electrogram the patient is in tachycardia with a wide complex left bundle pattern and a tachycardia cycle length of 282 ms. The atrial activation sequence is earliest in CS 7/8 which is located in the mid coronary sinus and indicates left sided activation. The introduction of a PVC during His refractoriness retrogradely penetrates the left bundle and retrogradely activates the accessory pathway with shortening of the tachycardia cycle length. Following resolution of the left bundle branch block the QRS is narrow and the tachycardia cycle length is shorter. This is indicative of a left sided AP playing a fundamental role in the tachycardia. This electrogram not only demonstrates the effect of a bundle branch block on the tachycardia cycle length but also the effect of a His refractory PVC advancing the next atrial activation. (HRA d is positioned in the high right atrium, CS 9–10 is in the proximal CS while CS 1–2 is in the distal CS and RVa d is located in the RV apex)

ventricular aberration is relatively common in the setting of SVT. Bundle branch block on the contralateral bundle has no impact on tachycardia cycle length.

RV Entrainment

Entrainment is the continual resetting of a reentry tachycardia by pacing at a site close to or within the circuit at a cycle length slightly shorter that the tachycardia cycle length. The pacing stimulus travels both orthodromically, in the same direction as the preceding tachycardia beat, and antidromically, resulting in a fused beat which is morphologically different to the tachycardia and the paced beats. This continues for all beats during entrainment apart from the final entrained beat, where there is no collision of an antidromic beat with the orthodromic waveform.

This concept is demonstrated in Fig. 2.38.

This pacing is performed at the RV apex cycle length 20–30 ms shorter than the TCL. This is then examined in order to ensure that capture during pacing has occurred.

If confirmed, the PPI—TCL is measured and the post pacing activation sequence is examined.

As shown in Fig. 2.39 in patients with **AVNRT (typical or atypical) the PPI—TCL is generally greater than 115 ms**. (Michaud et al. 2001) Fig. 2.39 demonstrates a short PPI-TCL of less than 115 ms, which is indicative of AVRT (Fig. 2.40).

It should be noted that rapid ventricular pacing may result in AH prolongation which could artificially prolong the PPI. Therefore, this may be corrected by subtracting the baseline AH interval from the PPI. The corrected PPI-TCL should be less than 110 ms for AVRT and greater than 110 ms for an AVNRT.

Examination of the post pacing activation sequence is also critical. If the final entrained ventricular beat is followed by an atrial, then ventricular beat, it is likely to be due to an underlying AVNRT or AVRT. Alternatively, if the post pacing sequence is AAV, this is more likely to represent an underlying atrial tachycardia.

An alternative maneuver is to pace from the RV apex and compare the PPI-TCL with pacing from the RV base. A difference of greater than

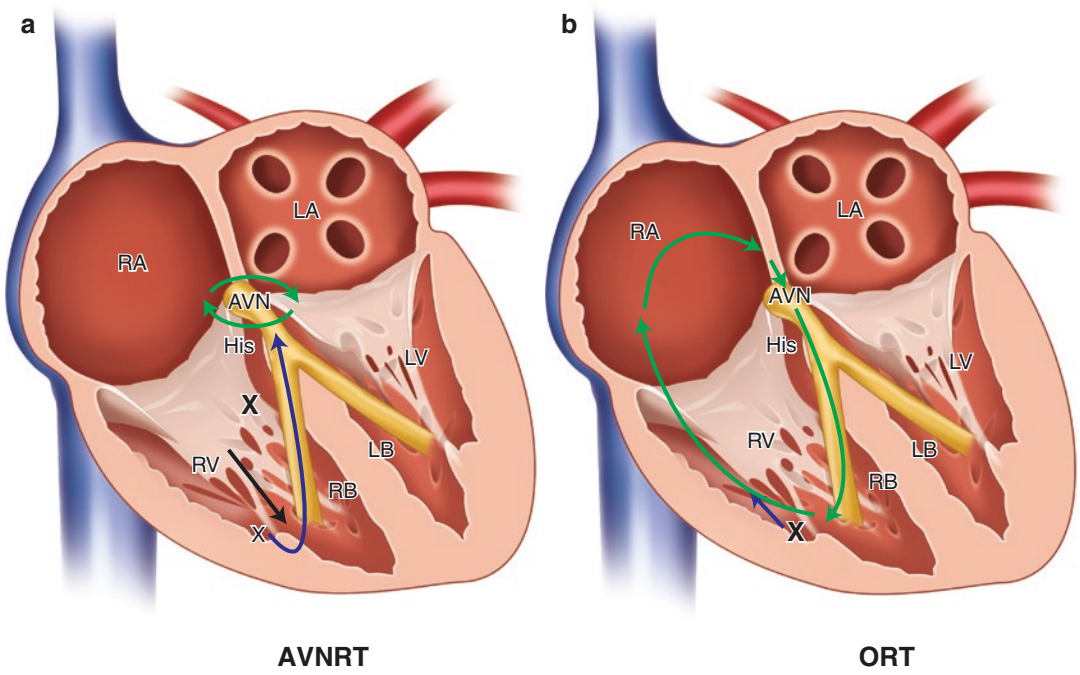

Fig. 2.38 Diagrammatic representation of entrainment from the RV apex. On the left image the AVNRT circuit is located in the slow and fast pathways in the AV node and pacing from the RV apex is anatomically and electrically distant from the critical circuit resulting in a long PPI—TCL. In the image on the right the ORT is utilizing the ventricle as part of the circuit and therefore pacing in the RV apex results in a PPI—TCL of less than 115 ms

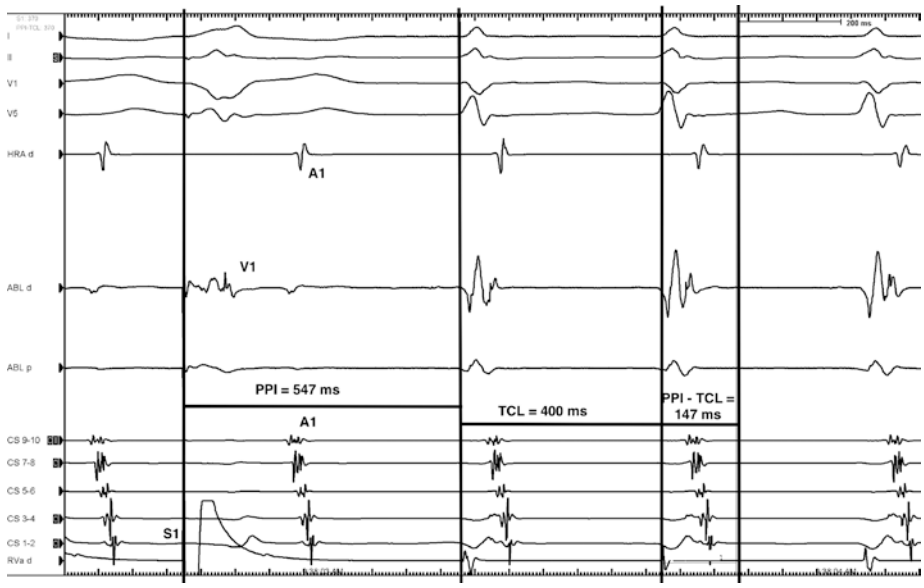

Fig. 2.39 Right ventricular entrainment during SVT. The tachycardia cycle length (TCL) of the tachycardia is 400 ms. Pacing is performed at a cycle length of 370 ms from the RV apex. Following confirmation of entrainment (not shown on this tracing) the post pacing interval (PPI) is calculated as 547 ms. The post pacing interval (PPI) minus the tachycardia cycle length (TCL) is 147 ms which is more indicative of an AVNRT (A refers to atrial activation while V is ventricular activation and S is stimulus. The ablation catheter (ABL d) is positioned close to the His, HRA d is positioned in the high right atrium, CS 9–10 is in the proximal CS while CS 1–2 is in the distal CS and RVa d is located in the RV apex)

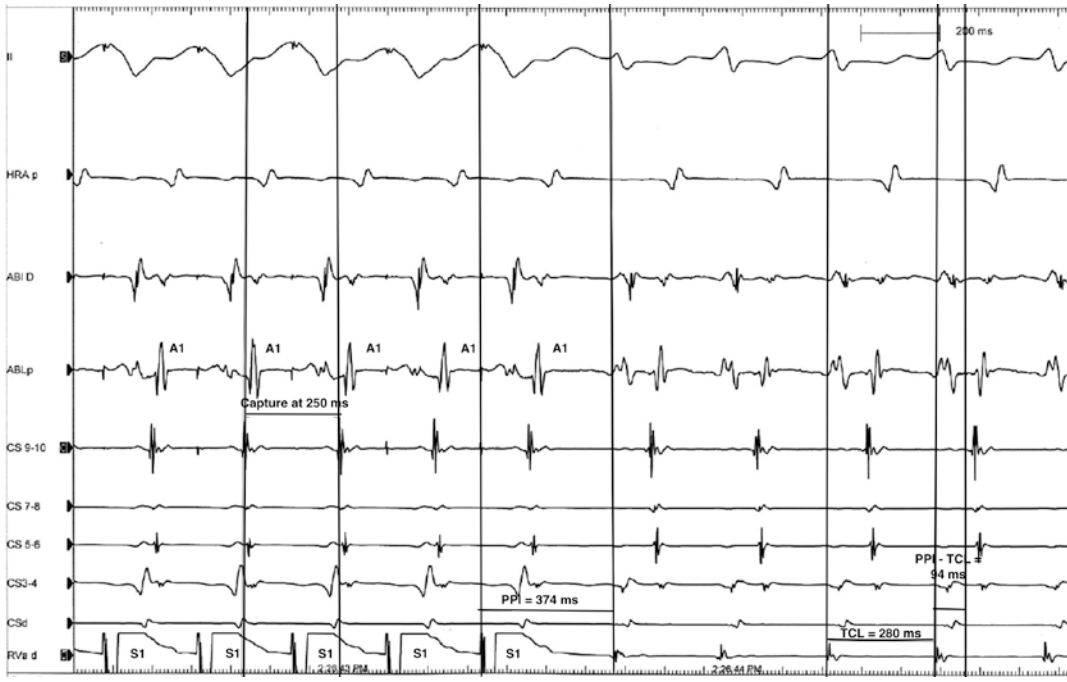

Fig. 2.40 RV entrainment during SVT. The tachycardia cycle length (TCL) is 280 ms. Pacing is performed at the RV apex at 250 ms with confirmation of atrial capture at that rate. The PPI—TCL is 94 ms which is suggestive of an ORT. The atrial activation sequence is suggestive of a left sided paraseptal pathway with the earliest retrograde atrial activation at CS 7/8. (The ablation catheter is positioned on the His, HRA d is positioned in the high right atrium, CS 9–10 is in the proximal CS while CS 1–2 is in the distal CS and RVa d is located in the RV apex)

30 ms between these two locations is suggestive of an AVNRT. This implies that there is a longer PPI-TCL moving further from the septum (Segal et al. 2009). In contrast, a difference less than 30 ms is indicative of an AP.

PVC During Tachycardia

This is performed in order to differentiate an SVT, in which the critical component of the circuit is not dependent on the His (i.e. AVNRT), from a mechanism which is dependent on the His (i.e. ORT).

In order to perform this maneuver, a PVC is delivered from the RV base sooner and sooner during tachycardia until the His is refractory. The subsequent atrial activation sequence and timing is then compared with that during the tachycardia. If there is no impact on the VA timing, either no accessory pathway is present or the accessory pathway was not penetrated by the PVC. This may occur if the pathway is anatomically distant from the site of pacing, such as a left lateral accessory pathway, or if it has decremental retrograde conduction properties in which the activation is blocked.

If the next atrial activation is advanced, it can be inferred that an accessory pathway conducting retrogradely is present. This, however, does not imply that the accessory pathway is part of the tachycardia circuit. If the atrial activation sequence for this beat is different to that during tachycardia, then this is referred to as a bystander. If the subsequent AH, AA and AV intervals are increased, it can be implied that the PVC has reset the tachycardia and therefore, the accessory pathway is part of the circuit.

If a PVC delivered during His refractoriness post excites the next atrial activation or terminates the tachycardia, the accessory pathway is part of the circuit. The concept of delivering a

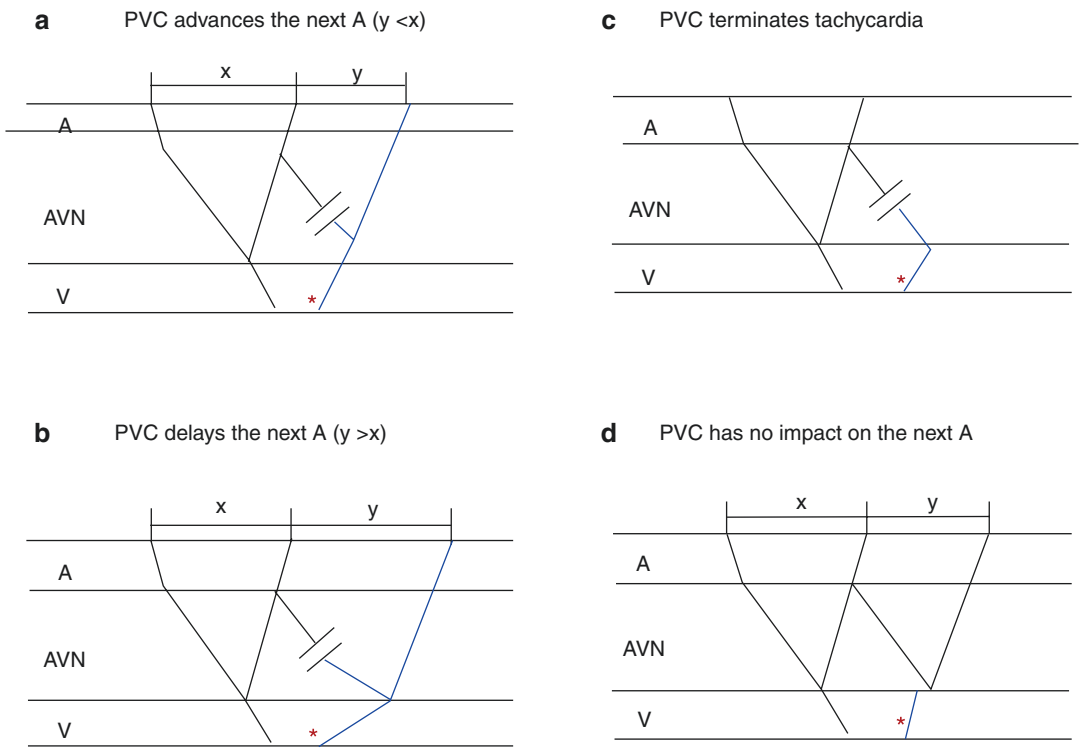

Fig. 2.41 Diagrammatic representation showing the effect of a PVC delivered during His refractoriness during tachycardia. The PVC (*) is delivered in the RV base. In A the PVC advances the next atrial activation. This indicates the presence of an accessory pathway however does not prove that this is a critical part of the circuit. In image B the PVC delays the next atrial signal. This indicates the presence of an accessory pathway which is a critical part of the circuit. In image C the PVC terminates the tachycardia. This also indicates the presence of an accessory pathway which is a critical component of the tachycardia circuit. In image D the PVC has no effect on the next atrial signal. This may indicate the absence of an accessory pathway. However, an accessory pathway may be present but may be anatomically distant from the site of the PVC or may be a decremental pathway which is refractory to the PVC

PVC during tachycardia is demonstrated in Fig. 2.41.

Para-Hisian Pacing

This can be performed if the tachycardia is unable to be induced or to differentiate retrograde conduction over the fast or slow pathway in the AV node from conduction over the accessory pathway. Although it is most commonly used for differentiating septal accessory pathways from AVNRT, it may also be used for left lateral (posterior) and right lateral (anterior) accessory pathways.

There are two methods to perform this maneuver. The first is to position the mapping catheter towards the RV outflow tract slightly superior to the His recording and pace at a 5 mA and 2 ms pulse duration (Nakagawa and Jackman 2005). The catheter is then slowly withdrawn with slight clockwise rotation along the RV anteroseptum until a His signal is recorded on the distal electrodes. The signal is then monitored for evidence of His capture and loss of capture with variability in respiration. With both capture of the His and the local anteroseptum, the QRS is less broad than with the loss of His capture.

Another method is to position the catheter along the RV basal anteroseptum so that a His signal is recorded on the distal electrodes and pacing is performed during normal sinus rhythm at a high output starting at 10 mA with a pulse

width of 2 ms. The output is then gradually reduced. At high pacing output, there is capture of both the His and the local ventricle. As the output is lowered, there is loss of His capture with widening of the QRS complex indicating activation of ventricular myocardium further away from the pacing site at the RV basal anteroseptum.

The following measurements are then compared between a single beat with His and local ventricular capture and a single beat with loss of direct His capture:

Stimulus—Atrial Interval (SA)
His—Atrial Interval (HA)
Atrial Activation Sequence (AAS)

The basic principle relies on anatomic position of the His, located in the subendocardial layer and encapsulated in annular tissue. Thus, the direct capture can only occur when a catheter is positioned along the RV anteroseptum at high pacing outputs. Lowering the output will result in local ventricular capture, which activates the RV apex with retrograde conduction up the right bundle to the His and causes a significant delay to His activation. Although any pacing catheter may be selected to perform this maneuver, the use of a deflectable catheter with 1 mm spaced electrodes allows easier visualization of the His signal by reducing the width of the recorded local ventricular signal. This principle is demonstrated in Fig. 2.42.

The usual responses to this are shown in Table 2.3. In VA conduction using only the AV node, loss of direct His capture results in a prolongation of stimulation to atrial activation interval. In general, there is no change in the HA interval although this may shorten in cases of dual AV nodal physiology. This is depicted on the electrogram in Fig. 2.43, in which the His and ventricle and the His are both captured at a higher pacing output resulting in a stimulus to atrial interval of 76 ms. When the pacing output is reduced, there is only ventricular capture with a prolongation of the stimulus to atrial activation of 136 ms. There is no change in the AAS and suggests AV nodal conduction only. Typically, in AV nodal conduction, the atrial activation sequence is unchanged, though this may change in certain cases. Indeed, the slow pathway may have a left atrial insertion point, the CS to atrial connections may be distal, or there may be functional block along the Eustachian ridge, causing activation in the left atrium preceding septal and right atrial activation. Given this, the retrograde AAS is not sufficient to rule out AV nodal conduction only.

In VA conduction using an accessory pathway, loss of direct His capture does not prolong the stimulation to atrial activation as the accessory pathway conduction is not dependent on conduction through the His. The HA interval often shortens concurrently. The AAS may or may not change depending on the atrial insertion point of the AP and occurs as a result of the fusion of retrograde VA nodal and AP conduction.

This maneuver cannot be performed in patients with retrogradely conducting fasciculoventricular accessory pathways as direct His capture will occur at the site of the accessory pathway insertion point during both high and low output pacing with no widening of the QRS at lower pacing output. In the reverse situation, proximal RBBB may imply that direct pacing of the His via the proximal right bundle is not possible, resulting in a wide QRS at both high and low pacing outputs.

High output pacing may result in capture of other closely related structures resulting in inaccurate interpretations. Direct atrial capture at high output may reveal an apparent short stimulus to atrial activation time. High output pacing may also result in capture of the left bundle branch, which may lead to shortening of VA conduction for left sided pathways with an apparent increase in VA conduction time as the pacing output is reduced.

Transseptal Access

Transseptal access is used in order to gain access to the left atrium and left ventricle for AP mapping and ablation, left sided ATs, AF ablation, VT ablation and left atrial appendage occlusion. This procedure is performed using a combination of fluoroscopic images, pressure monitoring, contrast and is often facilitated by the assistance of echocardiographic information.

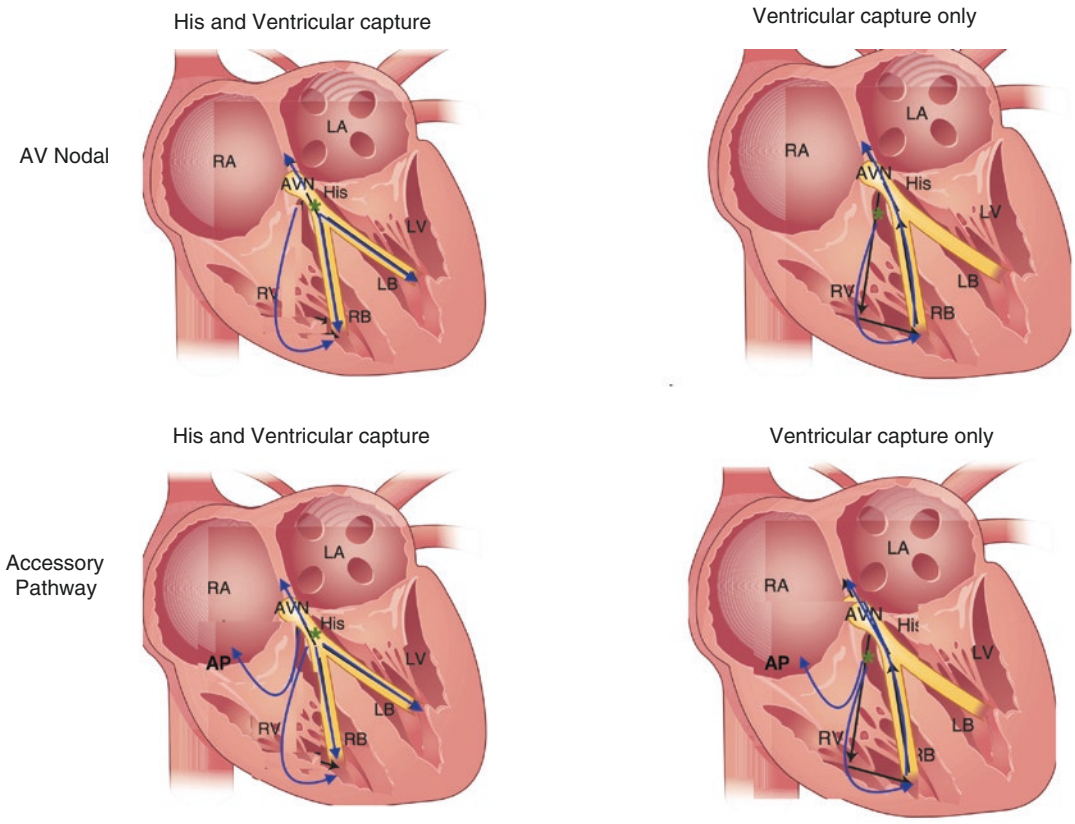

Fig. 2.42 Diagrammatic representation of Parahisian Pacing. In the top left image (**a**) there is capture of both the His and the Ventricle resulting in a relatively short VA time and stimulation to RV apical time. In the top right (**b**) image ventricular capture only conducts via the distal bundle branches via the His and to the atrium resulting in a prolonged VA time. This is indicative of AV nodal conduction. In the bottom left image (**c**) conduction through the His and ventricle results in the most rapid conduction through an accessory pathway (AP). Conduction through the ventricle only (bottom left; **d**) results in a similar short VA conduction time through the AP

Table 2.3 Responses to ParaHisian Pacing in AV Nodal and AP conduction. (VA Ventricular to Atrial Conduction, HA His to Atrial Conduction, AAS Atrial Activation Sequence)

VA conduction	SA	HA	AAS
AVN	Prolongs	Generally no change but may shorten with dual AVN physiology	Generally no change but may change with dual AVN physiology depending on the atrial insertion point of the slow pathway
AP Conduction only	Unchanged or shorter	Shorter	May or may not change

Equipment

Trans-septal Needles

A number of transseptal needles are available for use which vary both in length and angulation. The most commonly used is the Brockenbrough (BRK), an 18 Guage needle with an arrow at the proximal end which indicates the direction of the tip of the needle. The BRK needle has a shaft to needle tip angle of 19° while the BRK 1 needle, shown in Fig. 2.44, has a shaft to needle tip angle of 55°.

Additionally, BRK needles vary in length. For the majority of standard non deflectable sheaths,

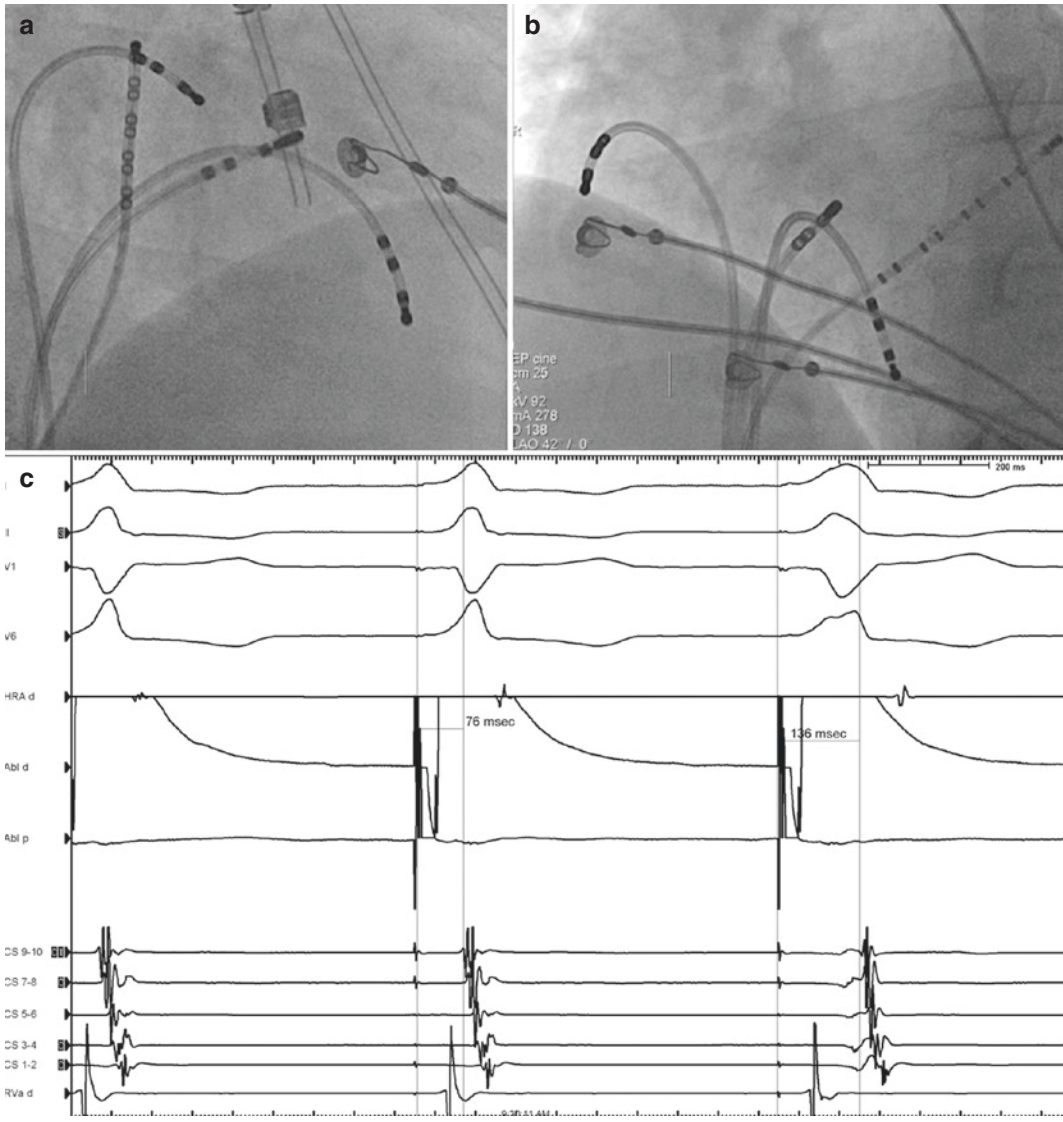

Fig. 2.43 Parahisian pacing in a patient with AV nodal conduction only. Pacing is performed from the ablation catheter which is positioned on the His. The narrower beat indicates capture of both the ventricle and the His with a stimulus to atrial time of 76 ms. When the pacing output is reduced there is only ventricular pacing with loss of His capture. The stimulus to atrial time is longer at 136 ms. This is indicative of AV nodal conduction. ((HRA d is positioned in the high right atrium, HIS d in the distal His, HIS p at the proximal component of the His, CS 9–10 is in the proximal CS while CS 1–2 is in the distal CS and RVa d is located in the RV apex)

the needle is 71 cm, while it is 98 cm for a long deflectable sheath.

An alternative to the standard transseptal needles is an RF wire with a sheath (Baylis Medical, Montreal, Canada). This is a modification of the RF needle (Hsu et al. 2013) and allows access to be performed in a single action as shown in Fig. 2.45.

Transseptal Sheaths

There are various sheaths available for transseptal access, which are either fixed or deflectable, but the Swartz Left (SL) range of sheaths (St. Jude Medical, St. Paul, MN, USA Medical) is most commonly used. These sheaths were

Fig. 2.44 Showing the main types of BRK Transseptal Needles (St. Jude Medical, St. Paul, MN, USA). The image on the top shows the 71 cm BRK needle at the top with a shaft to tip angle of 19°, below this is the 71 cm BRK1 needle which has a shaft to tip angle of 55°. Below this is the 56 sm BRK needle. On the bottom right image the tips of the three needles are shown in closer detail. The image on the bottom left shows the pointer arrow which in general should be directed at 4–5 o'clock.

principally designed to deflect towards the mitral annulus for accessory pathway mapping and ablation. All of these sheaths have a primary curve of 50° with a secondary curve of 0° in the SLO, 45° in the SL1, 90° in the SL2 and 135° in the SL3. The SL4 has a 35° primary curve and has an angulation of 180°. Other non-deflectable transseptal sheaths include the Channel FX (Boston Scientific Way Marlborough, MA, USA) and the Convoy Advanced (Boston Scientific Way Marlborough, MA, USA).

Several deflectable sheaths also exist. The Agilis sheath (St. Jude Medical, St. Paul, MN, USA Medical, St. Paul, MN, USA) is 91 cm long and requires the 98 cm transeptal needle. This sheath is available in medium and long reach options. Other deflectable sheaths include the Channel steerable (Boston Scientific Way Marlborough, MA, USA), the Direx (Boston Scientific Way Marlborough, MA, USA) and the Mobicath (© Biosense Webster, Inc).

Guidewires

These are generally 0.032 inches in diameter with a J shaped distal end of approximately 3 mm in length at the tip. These wires are placed into the superior vena cava and are used to advance the sheath and dilator over. They may also be advanced through the sheath and dilator into the left superior pulmonary vein in order to confirm position and allow dilatation of the transseptal access point, all while minimizing the potential risk of the dilator advancing through the lateral left atrial wall. If uncertainties over whether the transseptal needle is in the left atrium arise, an angioplasty wire can also be advanced through the needle prior to advancement of the sheath and dilator.

Fluoroscopic Approach

In order to help with fluoroscopic access, a catheter can be positioned in the coronary sinus and the His. The His catheter is located at the same level but anterior to the fossa ovalis. The electrode recording the proximal His acts as a surrogate for the aortic root. The coronary sinus catheter shows the direction in which the transseptal needle should pass in a LAO projection. This is parallel and inferior to the direction of the transseptal needle. Septal anatomy from the right atrium is demonstrated in Fig. 2.46. As shown in Fig. 2.47 the distal end of the coronary sinus also marks the lateral wall of the left atrium.

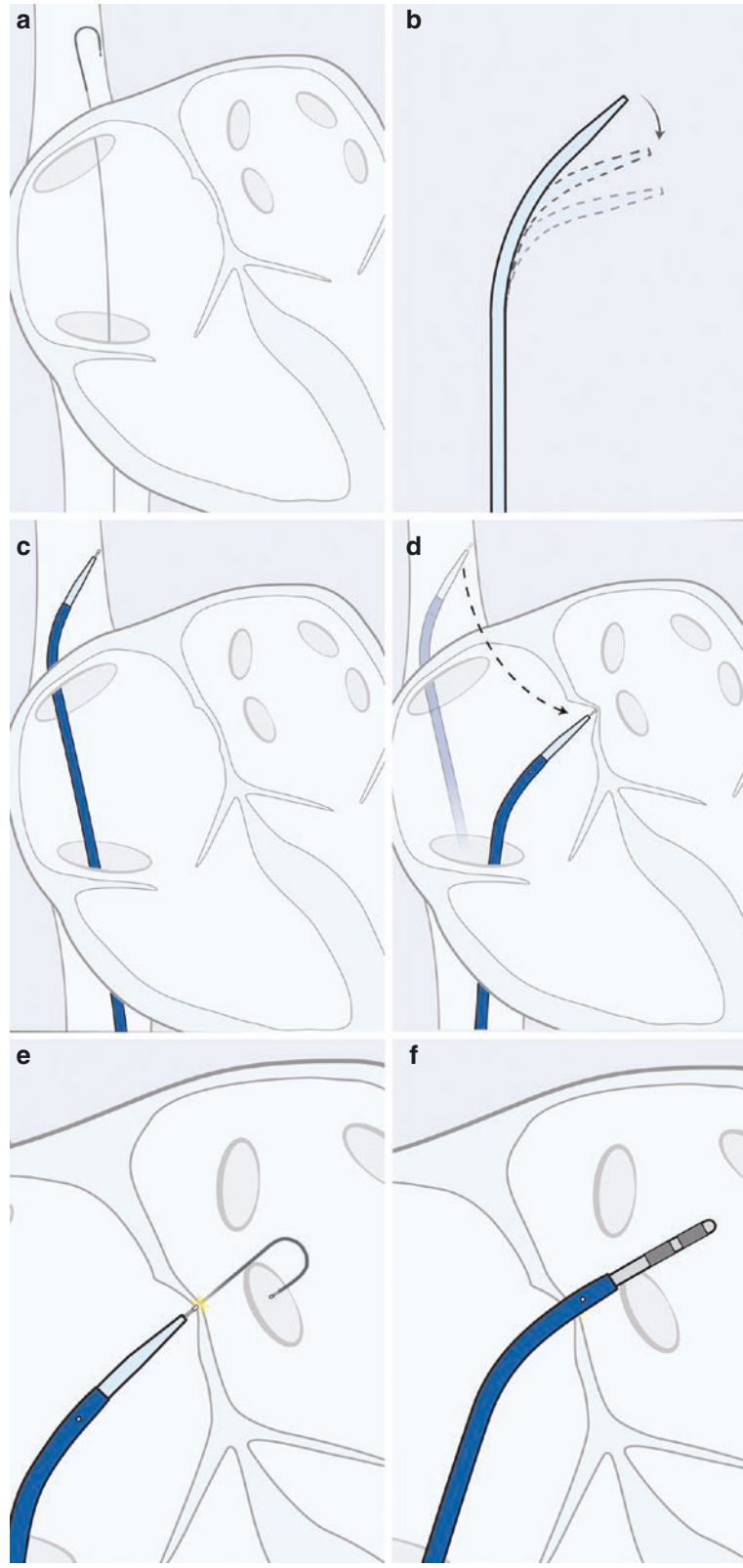

Fig. 2.45 RF wire with sheath (Baylis, Montreal, Canada). As shown in panel **a** the wire is positioned from the femoral vein to the superior vena cava. The dilator of the sheath is shaped according to the angle required for transseptal access (panel **b**) and positioned over the wire into the superior vena cava (panel **c**). With the tip of the wire outside of the sheath and dilator the apparatus is withdrawn into the right atrium (panel **d**) where there is engagement of the fossa ovalis. RF energy is transmitted to the tip of the RF wire and the wire is advanced into the left atrium (panel e). The sheath and dilator are advanced over the wire and the wire and dilator are removed. Following this an ablation or mapping catheter is advanced through the sheath into the left atrium (panel **f**)

Although various fluroscopic views may be utilized, the most useful are the LAO 30, RAO 30 (Fig. 2.48) and the left lateral. The sheath and dilator are flushed with heparinized saline in order to eliminate all air. The trans-septal needle is flushed and in the case of a BRK, the stylet is placed back inside the needle and locked in place. The needle can be placed inside the sheath and dilator in order to ensure that these are compatible in terms of length. The needle is then removed, and the sheath and dilator are introduced over a 0.032 J shaped wire into the superior vena cava. Following this, the wire is removed and the dilator is aspirated and flushed with heparinized saline. The transseptal needle is then introduced into the dilator and sheath with the tip of the needle kept inside the dilator. In the case of a BRK needle, it is important that the stylet is kept inside the needle while introducing this into the dilator in order to prevent sheering of plastic from the dilator. However, this is not required for the NRG RF, in which the tip is not as sharp. Once the needle is close to and still inside the dilator tip, the stylet is removed and the needle is aspirated and flushed with heparinized saline. This can then be connected to a three way tap and connected to pressure monitoring and contrast if required. Finally, systemic heparin is administered to the patient prior to transseptal access being achieved.

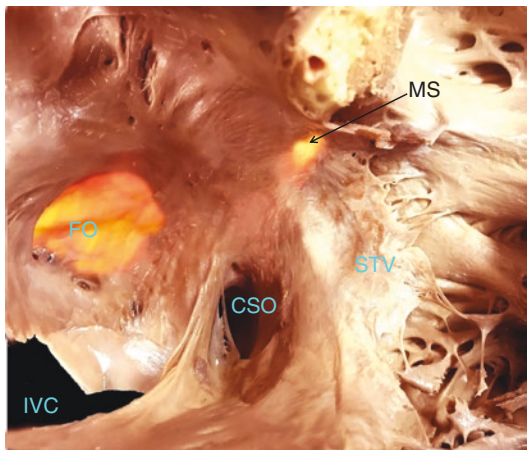

Fig. 2.46 Relevant anatomy in a trans septal approach from the right atrium. The fossa ovalis (FO) is superior and posterior to the coronary sinus os (CSO) Anterior to the fossa ovalis is the muscular septum (MS). Also seen in this image is the inferior vena cava (IVC) and the septal leaflet of the tricuspid valve (STV)

The sheath, with dilator and needle, are positioned between 4 and 6 o'clock and withdrawn from the superior vena into the right atrium using a LAO 30 projection. As the apparatus is withdrawn along the superior vena cava, the sheath and dilator jump to the left as it deflects from the descending aorta into the right atrium. Further

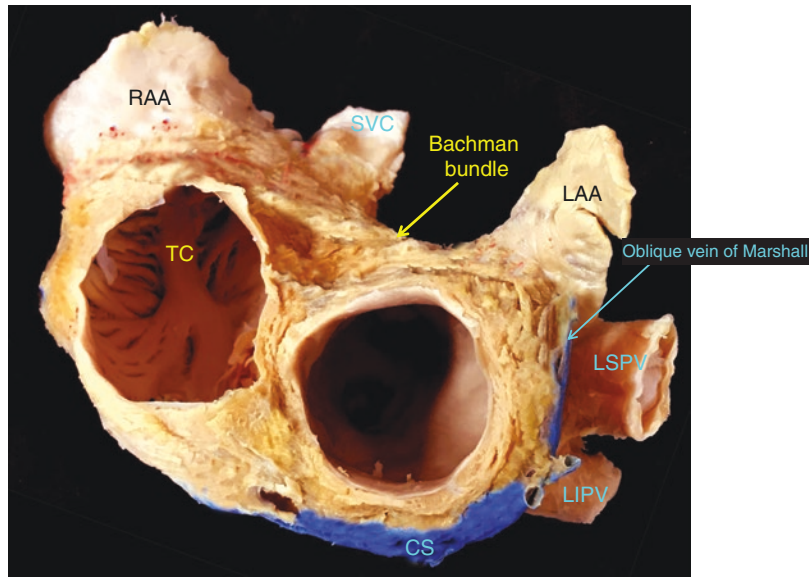

Fig. 2.47 Relationship of the coronary sinus and the oblique vein of Marshall with the lateral wall of the left atrium acting as a marker of the boundaries of the left atrium

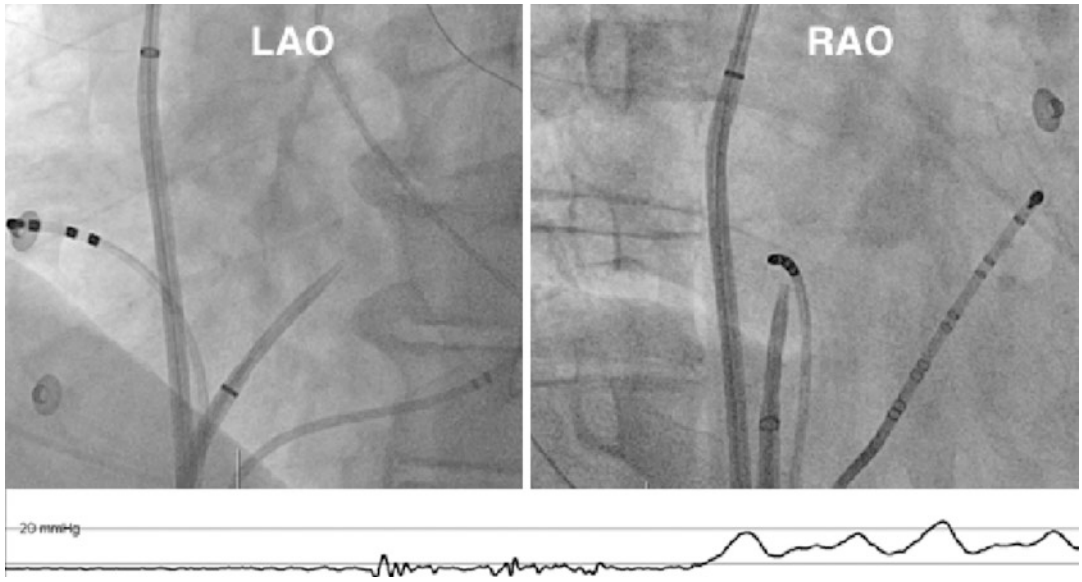

Fig. 2.48 Fluoroscopic guidance of trans-septal access in the LAO view (top left) and RAO view (top right). In the LAO projection the tip of the dilator should be superior to and parallel to the coronary sinus which demonstrates the AV groove parallel and posterior to the mitral annulus. The proximal poles of the quadripolar catheter are positioned along the His which acts as an approximate marker of the aortic root. In the RAO image on the top right the needle and sheath is clearly posterior to the His catheter. The pressure tracing on the bottom is recorded through the trans septal needle and shows a damped pressure tracing as it is against the septum followed by a left atrial pressure as access is achieved

withdrawal results in a second jump as the apparatus engages the fossa ovalis. In the LAO projection, the tip of the dilator should be superior and parallel to the coronary sinus which demonstrates that the AV groove is parallel and posterior to the mitral annulus, thus helping to demonstrate the widest portion of the LA. In the RAO projection, the anterior and posterior projections can be confirmed relative to the His catheter. This can also be demonstrated in the left lateral position with the His catheter pointing anteriorly and the CS posteriorly. In this view, the needle is pointed at 1 o'clock for engagement of the fossa ovalis. The proximal His recording identifies the central fibrous body at the most inferior aspect of the noncoronary aortic cusp. Prior to transseptal access, a bolus of heparin should be administered.

The apparatus is then withdrawn very slightly and then advanced with the needle outside of the sheath and dilator with pressure measured from the tip of the needle. There is usually a jump as the needle crosses the septum. Confirmation should be attained by checking the pressure and injecting contrast. Immediately when this is confirmed, the dilator and sheath can be advanced over the needle, with the needle and dilator removed so that a long J wire can be gently advanced into the left superior pulmonary vein. Care must be taken at all times to ensure that the sheath and dilator are not advanced too far, resulting in a perforation, or that the wire is not advanced into the left atrial appendage. As shown in Fig. 2.49 the ablation catheter should be rotated in a posterior direction in order to direct this towards the pulmonary veins.

For the second transseptal sheath, some operators may prefer to withdraw the sheath and leave the J wire in place and then advance the ablation catheter through the puncture site, while others perform a second transseptal puncture using the same puncture.

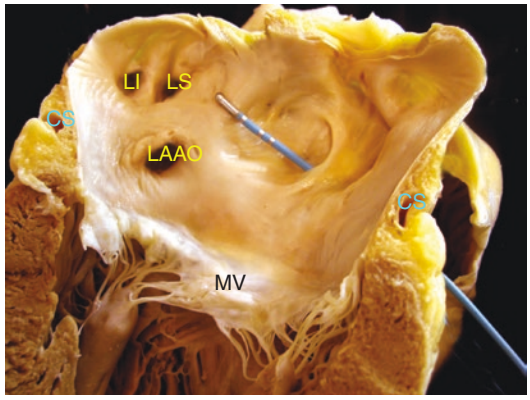

Fig. 2.49 As the ablation catheter is advanced it should be rotated in a posterior orientation in order to direct this towards the pulmonary veins

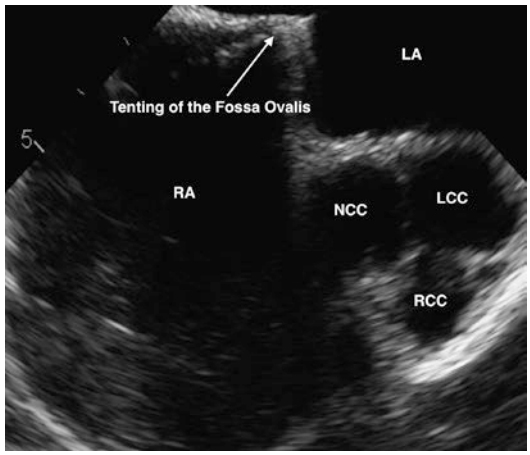

Fig. 2.50 Transesophageal imaging showing tenting of the Fossa Ovalis during trans-septal access. The right atrium (RA) and left atrium (LA) are seen as well as the non coronary cusp (NCC), left coronary cusp (LCC) and right coronary cusp (RCC) of the aortic valve

Echocardiographic Visualization

Although fluoroscopic guidance is fundamental in achieving transseptal access, variations in anatomy may result in difficulties crossing the foramen ovale. These include: an aneurysmal atrial septum defined as a deviation during the cardiorespiratory cycle of at least 10 mm, prior cardiac surgery, congenital heart disease, dilated atria, multiple prior trans-septal procedures and a dilated aortic root. The interatrial septum cannot be reliably differentiated from the aortic root on transthoracic echocardiogram and therefore, either ICE or TEE may be used. Both of these imaging modalities possess the advantage of being able to directly visualize the fossa, while the disadvantage of ICE is that it often requires additional vascular access and is generally quite expensive. TEE is extremely useful, but requires the patient to be under general anesthesia and carries the potential for esophageal injury. Tenting of the fossa ovalis can be seen on TEE in Fig. 2.50.

Important Points

1. Unipolar electrograms are amplified signals recorded between the distal pole of the catheter (+) and Wilsons Central Terminal (−).
2. Bipolar signals are amplified signals recorded from two closely spaced unipoles. In general, the distal pole is negative while the proximal pole is positive.
3. All signals are amplified and filtered. The amplified signal first passes through a high pass filter which allows higher frequency signals to pass through while removing signals below a designated frequency. This then passes through an isolation amplifier which isolates the current from the patient and is subsequently transmitted through a low pass filter. This allows lower frequency signals to be transmitted while filtering out higher frequencies.
4. SNRT is measured using the principle of overdrive suppression in which pacing is performed close to the sinus node at a rate faster than the sinus rate. Subsequently, the time taken from the last paced beat to the first intrinsic sinus beat is measured. A sinus node recovery time, defined as the longest interval after pacing at any cycle

length, is generally considered abnormal if it exceeds 1500 ms.

5. SACT is the conduction time from the SN to the RA tissue. A normal SACT is considered to be to be 50–125 ms.
6. The AH interval is measured from the onset of the local atrial electrogram recorded in the His catheter to the onset of the His signal and represents conduction through the AV node. The normal range is anywhere from 50 to 120 ms. A prolonged AH interval may occur as a result of intrinsic AV nodal dysfunction or from antiarrhythmic drugs. A short AH interval generally occurs in the presence of catecholamines.
7. The HV interval is measured from the onset of the local His signal to the local ventricular signal on the His catheter (Fig. 2.24). This generally reflects the conduction time through the proximal His, bundle branches and the Purkinje system. The normal range is considered to be between 30 and 55 ms. Intrinsic His dysfunction or antiarrhythmic drugs may prolong the HV interval. A short HV interval may be seen with accessory pathway conduction which may even be negative. Care must be taken not to mistaken the right bundle electrogram as the His electrogram may artificially lead to a seemingly short HV interval.
8. The effective refractory period (ERP) is the longest coupling interval in which the stimulus fails to stimulate the myocardium at twice the diastolic threshold.
9. The AV Wenckebach point is defined as the longest cycle length which results in 2:1 AV block.
10. If the tachycardia cycle length is prolonged with induction of BBB, this implies that the arrhythmia is AVRT with a VA connection on the same side as the BBB otherwise known as Coumel's sign.
11. Entrainment is the continual resetting of a re-entry tachycardia by pacing at a site close to or within the circuit at a cycle length slightly shorter than the tachycardia cycle length. During an SVT, entrainment from the RV results in a shorter PPI-TCL for AVRT versus AVNRT.
12. If a PVC delivered at the same time as the antegrade His signal results in an advancement of the next atrial activation with no change in the AAS, this is suggestive of the presence of an accessory pathway participating in the circuit. A change in the AAS implies that the accessory pathway is not participating in the tachycardia. If a His refractory PVC does not affect the following atrial beat, then there is either no AP or the PVC has not conducted retrogradely up the AP. This may occur if the AP has decremental retrograde conduction or is anatomically far from the location of delivery of the PVC.
13. If a tachycardia cannot be easily induced, parahisian pacing may be helpful to study retrograde conduction properties. In the presence of VA conduction using only the AV node, loss of direct His capture results in a prolongation of stimulus to atrial activation interval. In genera, there is no change in the HA interval although this may shorten in cases of dual AV nodal physiology. In VA conduction using an AP, loss of direct His capture does not prolong the stimulation to atrial activation as the AP conduction is not dependent on conduction through the His. The HA interval often shortens. The AAS may or may not change depending on the atrial insertion point of the AP and occurs as a result of the fusion

of retrograde VA nodal and AP conduction.

14. Trans-septal access may be obtained using a fluoroscopic approach or with the addition of echocardiographic guidance. In the fluoroscopic image, the coronary sinus catheter reveals the direction in which the transseptal needle should pass in a LAO projection. This is parallel and inferior to the direction of the trans-septal needle. The distal end of the coronary sinus also marks the lateral wall of the left atrium.

    This can also be demonstrated in the left lateral position with the His catheter pointing anteriorly and the CS posteriorly. As shown in Fig. 2.49, pointing the needle at 1 o'clock is reasonable for engagement of the fossa ovalis in this view. The proximal His recording identifies the central fibrous body at the most inferior aspect of the noncoronary aortic cusp.

References

Aliot EM, Stevenson WG, Almendral-Garrote JM, et al. European Heart Rhythm Association (EHRA); Registered Branch of the European Society of Cardiology (ESC); Heart Rhythm Society (HRS); American College of Cardiology (ACC); American Heart Association (AHA/EHRA/HRS). Expert Consensus on Catheter Ablation of Ventricular Arrhythmias: developed in a partnership with the European Heart Rhythm Association (EHRA), a Registered Branch of the European Society of Cardiology (ESC), and the Heart Rhythm Society (HRS); in collaboration with the American College of Cardiology (ACC) and the American Heart Association (AHA). Heart Rhythm. 2009;6:886–933.

Andrade JG, Khairy P, Guerra PG, Deyell MW, Rivard L, Macle L, et al. Efficacy and safety of cryoballoon ablation for atrial fibrillation: a systematic review of published studies. Heart Rhythm. 2011;8:1444–51.

ANSI/AAMI. Medical electrical equipment, part 1: general requirements for basic safety and essential performance. ES 60601-1. 2005.

Arbelo E, Brugada J, Hindricks G, et al. ESC-EURObservational Research Programme: the Atrial Fibrillation Ablation Pilot Study, conducted by the European Heart Rhythm Association. Europace. 2012;14(8):1094–103.

Bohnen M, Stevenson WG, Tedrow UB, et al. Incidence and predictors of major complications from contemporary catheter ablation to treat cardiac arrhythmias. Heart Rhythm J. 2011;8:1661–6.

Brugada J, Katritsis DG, Arbelo E, et al. 2019 ESC Guidelines for the management of patients with supraventricular tachycardia: The Task Force for the management of patients with supraventricular tachycardia of the European Society of Cardiology (ESC). Eur Heart J. 2020;41(5):655–720.

Calkins H, Yong P, Miller J, Olshansky B, Carlson M. Catheter ablation of accessory pathways, atrioventricular nodal reentrant tachycardia, and the atrioventricular junction: final results of a prospective, multicenter clinical trial. Circulation. 1999;99:262–70.

Calkins H, Epstein A, Packer D, et al. Catheter ablation of ventricular tachycardia in patients with structural heart disease using cooled radiofrequency energy: results of a prospective multicenter study. Cooled RF Multi Center Investigators Group. J Am Coll Cardiol. 2000;35(7):1905–14.

Chugh A, Makkar A, Yen Ho S, et al. Manifestations of coronary arterial injury during catheter ablation of atrial fibrillation and related arrhythmias. Heart Rhythm. 2013;10(11):1638–45.

Dagres N, Hindricks G, Kottkamp H, et al. Complications of atrial fibrillation ablation in a high-volume center in 1,000 procedures: still cause for concern? J Cardiovasc Electrophysiol. 2009;20:1014–9.

DiBiase L, Bunkhardt JD, Mohanty P, et al. Periprocedural stroke and management of major bleeding complications in patients undergoing catheter ablation of atrial fibrillation: the impact of periprocedural therapeutic international normalized ratio. Circulation. 2010;121:2550–6.

Ghia KK, Chugh A, Good E, et al. A nationwide survey on the prevalence of atrioesophageal fistula after left atrial catheter ablation. Circulation. 2005;112:II-392–3.

Haines DE, Beheiry S, Akar JG, et al. Heart Rhythm Society expert consensus statement on electrophysiology laboratory standards: process, protocols, equipment, personnel, and safety. Heart Rhythm. 2014;11(8):9–51.

Hsu JC, Badhwar N, Gerstenfeld EP, et al. Randomized trial of conventional transseptal needle versus radiofrequency energy needle puncture for left atrial access (the TRAVERSE-LA study). J Am Heart Assoc. 2013;2:5.

January CT, Wann LS, Alpert JS, et al. 2014 AHA/ACC/HRS guideline for the management of patients with atrial fibrillation: executive summary: a report of the American College of Cardiology/American Heart Association Task Force on practice guidelines and the Heart Rhythm Society. Circulation. 2014;130:2071–104.

Josephson's Clinical Cardiac Electrophysiology. David Callans Wolters Kluwer 2020.

Mallidi J, Nadkarni GN, Berger RD, et al. Meta-analysis of catheter ablation as an adjunct to medical therapy for treatment of ventricular tachycardia in patients with structural heart disease. Heart Rhythm. 2011;8(4):503–10.

Martinek M, Lemes C, Sigmund E, et al. Clinical impact of an open-irrigated radiofrequency catheter with direct force measurement on atrial fibrillation ablation. Pacing Clin Electrophysiol. 2012;35:1312–8.

Michaud GF, Tada H, Chough S, Baker R, Wasmer K, Sticherling C, Oral H, Pelosi F Jr, Knight BP, Strickberger SA, Morady F. Differentiation of atypical atrioventricular node re-entrant tachycardia from orthodromic reciprocating tachycardia using a septal accessory pathway by the response to ventricular pacing. J Am Coll Cardiol. 2001;38:1163.

Nakagawa H, Jackman WM. Para-Hisian pacing: useful clinical technique to differentiate retrograde conduction between accessory atrioventricular pathways and atrioventricular nodal pathways. Heart Rhythm J. 2005;2:667–72.

Nanthakumar K, Kay GN, Plumb VJ. Decrease in fluoroscopic cardiac silhouette excursion precedes hemodynamic compromise in intraprocedural tamponade. Heart Rhythm. 2005;2:1224–30.

Neuzil P, Reddy V, Kautzner J, et al. Electrical reconnection after pulmonary vein isolation is contingent on contact force during initial treatment: Results from the EFFICAS I study. Circ Arrhythm Electrophysiol. 2013;6(2):327–33.

Otomo K, Yamanashi WS, Tondo C. Why a large tip electrode makes a deeper radiofrequency lesion: effects of increase in electrode cooling and electrode-tissue interface area. J Cardiovasc Electrophysiol. 1998;9(1):47–54.

Peichl P, Wichterle D, Pavlu L, et al. Complications of catheter ablation of ventricular tachycardia: a single-center experience. Circ Arrhythm Electrophysiol. 2014;7:684–90.

Pison L, La Meir M, van Opstal J, et al. Hybrid thoracoscopic surgical and transvenous catheter ablation of atrial fibrillation. J Am Coll Cardiol. 2012;60:54–61.

Pons M, Beck L, Leclercq F, et al. Chronic left main coronary artery occlusion: a complication of radiofrequency ablation of idiopathic left ventricular tachycardia. Pacing Clin Electrophysiol. 1997;20(7):1874–6.

Reddy V, Shah D, Kautzner J, et al. The relationship between contact force and clinical outcome during radiofrequency catheter ablation of atrial fibrillation in the TOCCATA study. Heart Rhythm. 2012;9(11):1789–95.

Roberts-Thomson KC, Steven D, Seiler J, et al. Coronary artery injury due to catheter ablation in adults: presentations and outcomes. Circulation. 2009;120(15):1465–73.

Rodriguez LM, Nabar A, Timmermans C, et al. Comparison of results of an 8-mm split-tip versus a 4-mm tip ablation catheter to perform radiofrequency ablation of type I atrial flutter. Am J Cardiol. 2000;85(1):109–12, A9

Sacher F, Roberts-Thomson K, Maury P, et al. Epicardial ventricular tachycardia ablation: a multicenter safety study. J Am Coll Cardiol. 2010;55(21):2366–72.

Sánchez-Quintana D, Cabrera JA, Climent V, Farré J, et al. Anatomic relations between the esophagus and left atrium and relevance for ablation of atrial fibrillation. Circulation. 2005;112(10):1400–5.

Scheinman MM, Huang S. The 1998 NASPE prospective catheter ablation registry. Pacing Clin Electrophysiol. 2000;23:1020–8.

Schmidt M, Nolker G, Marschang H, et al. Incidence of oesophageal wall injury post-pulmonary vein antrum isolation for treatment of patients with atrial fibrillation. Europace. 2008;10:205–9.

Segal OR, Gula LJ, Skanes AC, Krahn AD, Yee R, Klein GJ. Differential ventricular entrainment: a maneuver to differentiate AV node reentrant tachycardia from orthodromic reciprocating tachycardia. Heart Rhythm. 2009;6:493.

Shah RU, Freeman JV, Shilane, et al. Procedural complications, rehospitalizations, and repeat procedures after catheter ablation for atrial fibrillation. J Am Coll Cardiol. 2012;59:143–9.

Simmers TA, Hauer RN, Wever EF, et al. Unipolar electrogram models for the prediction of outcome in radiofrequency ablation of accessory pathways. Pacing Clin Electrophysiol. 1994;17:186–98.

Spector P, Reynolds MR, Calkins H, et al. Meta-analysis of ablation of atrial flutter and supraventricular tachycardia. Am J Cardiol. 2009;104(5):671–7.

Tokuda M, Kojodjojo P, Epstein M, et al. Outcomes of cardiac perforation complicating catheter ablation of ventricular arrhythmias. Circ Arrhythm Electrophysiol. 2011;4(5):660–6.

Yamada T, McElderry HT, Doppalapudi H, et al. Idiopathic ventricular arrhythmias originating from the aortic root prevalence, electrocardiographic and electrophysiologic characteristics, and results of radiofrequency catheter ablation. J Am Coll Cardiol. 2008;52:139–47.

Electroanatomic Mapping

3

Benedict M. Glover and Pedro Brugada

Abstract

Electroanatomic mapping (EAM) involves the rapid acquisition of multiple electrical and anatomical points in order to create a three-dimensional map encompassing this data. These systems use magnetic, impedance or a combination of the two for the non-fluoroscopic location of the catheters. Data can be displayed on a recreated anatomic structure. This data includes activation times, voltage recordings and entrainment mapping. One of the original mapping systems the Localisa (© Medtronic plc 2015) has been replaced by three systems which are used most commonly in clinical practice which include CARTO (© Biosense Webster, Inc), NavX Precision (St Jude Medical, St Paul, MN, USA) and Rhythmia (Boston Scientific Way Marlborough, MA, USA). Despite advances in the automation of these systems it is important to examine electrogram quality and annotation otherwise the map may not make any sense.

B. M. Glover (✉)
Division of Cardiology, Department of Medicine, University of Toronto, Toronto, Ontario, Canada

P. Brugada
University Hospital of Brussel, Brussels, Belgium
e-mail: pedro@brugada.org

General Principles of EAM Mapping

Although the current mapping systems differ in the specific technology employed for catheter localization and electrogram acquisition and processing, there are several important general principles across all aspects of mapping systems. It is important that useful data are processed. In the electrophysiology laboratory the most common mapping includes activation (isochronal), voltage (isopotential) and entrainment mapping. If respiratory gating is used all points in all systems are generally recorded during the same phase of respiration which is generally end expiration.

Reference Point

A stable reference point is required for activation mapping so that all points can be measured relative to the same electrogram. An ideal reference electrogram should be stable with an obvious positive or negative peak for measurement. The trigger is then set on either the most positive or negative change in voltage over time (dV/dT). In the ventricle a surface QRS can be used for this or the electrogram from the RV apical catheter. In the atrium the surface P wave is not satisfactory and therefore the coronary sinus catheter is generally used given its relative stability. It is important that this is positioned in a stable position with a clear atrial signal.

B. M. Glover, P. Brugada (eds.), *Clinical Handbook of Cardiac Electrophysiology*,
https://doi.org/10.1007/978-3-030-74319-2_3

Window of Interest

It is important to ensure that every point taken for an arrhythmia is related to the same beat. For a **focal arrhythmia** such as PVC's, focal VT and many AT's the window of interest is set relative to the onset of the P wave or QRS. **The earliest component may be set at 80 ms ahead of the surface signal and 30 ms after the offset**.

For a **re-entry tachycardia** such as atrial flutter (both typical cavotricuspid isthmus dependent and atypical), some atrial tachycardia's and scar related VT the window of interest is chosen as **90% of the tachycardia cycle length** (TCL) to allow for a degree of cycle length variability. The earliest component in the window is half of the value prior to the onset of the P wave or QRS and the latest component is half of the value after the onset of the P wave or QRS. The early and late signals in this method are arbitrary and only used to have an understanding of the mechanism and anatomical regions involved in the circuit. The best location for ablation may therefore not be the earliest recording on this map but a critical isthmus within it.

In order to perform an activation map which helps to locate the isthmus in an atrial re-entry circuit a slightly different technique is used while setting the window of interest. The **earliest component** of the window is set for **mid diastole of the beat of interest and the late component of the window is set for mid diastole for the following beat** (De Ponti et al. 2007). This means that the region where early meets late is the **mid-diastolic region**.

The P wave duration is measured from the surface ECG at 100 mm/s with or without the administration of intravenous adenosine. The early component of the window is calculated by subtracting the P wave duration from the tachycardia cycle length and dividing by two. As the window is being set from the reference signal the distance from the reference to the onset of the P wave is subtracted if the reference occurs before the p wave or added if it occurs after the P wave. This should correspond with mid-diastole. In order to calculate the late component to the window the duration of the early window is subtracted from the tachycardia cycle length and multiplied by 90% (Fig. 3.1).

Activation Mapping (Isochronal)

One of the many advantages of electroanatomic mapping is the ability to acquire multiple electrogram signals during a tachycardia and color code these so that an activation map can be acquired. Following selection of an appropriate reference signal and window of interest points

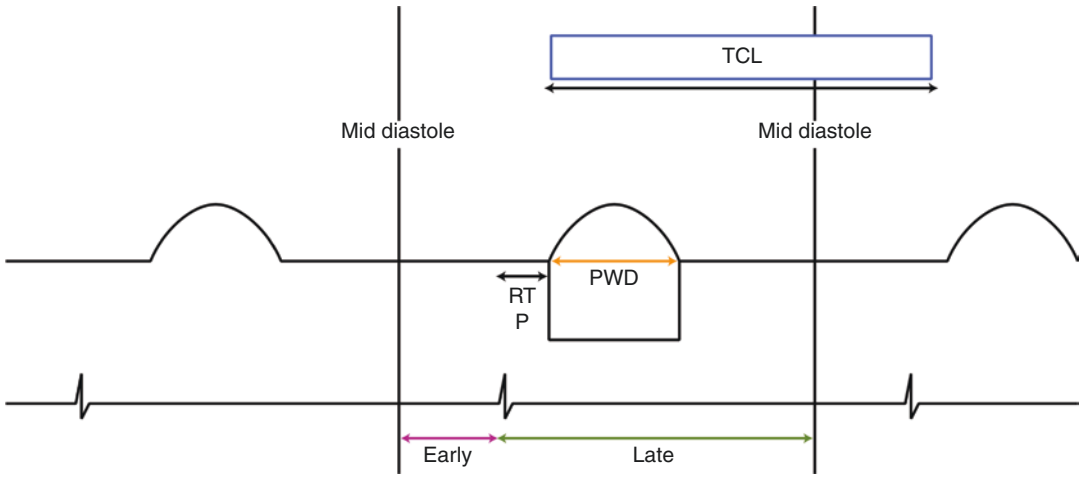

Fig. 3.1 Calculation of window of interest in a re-entry tachycardia. *TCL* tachycardia cycle length, *PWD* P wave duration, *RTP* reference to onset of P wave

are acquired and selected relative to the reference signal. Electrograms can be individually viewed and a marker is used to designate the onset of the signal which can then be moved if required. These signals are then color coded so that early is designated as red followed by yellow, green blue, and purple which indicates later activation. In focal arrhythmias regions which are coded red tend to be reasonable areas to explore and consider ablation particularly for the very earliest signal with a QS and no R wave on the unipolar electrogram. In unipolar electrograms the distal pole of the catheter (anode) is connected to a remote electrode known as the indifferent electrode (cathode). Depolarization towards the distal electrode results in a positive deflection while depolarization away from the electrode results in a negative deflection. A QR therefore implies that the wave of depolarization is moving away from the electrode. In cases of poor electrode contact a slurred S wave may also be present which implies that better catheter manipulation is required.

In macro re-entry circuits the earliest site as designated by red is not generally targeted with ablation. Rather the activation sequence should be examined in order to understand the basis of the arrhythmia and further mapping with the catheter should be performed in order to help localize the critical isthmus with mid diastolic signals. As shown in the activation map in Fig. 3.2 a re-entry circuit is seen rotating around a right atrial lateral wall atriotomy scar. Ablation (light and dark red dots) is performed along the lateral wall from the superior vena cava to the inferior vena cava after pacing for phrenic nerve stimulation is performed and marked as a white line. This resulted in termination of the tachycardia.

Prior to delivery of ablation in this region entrainment can be performed to ensure that the location is within the circuit. If the tachycardia terminates pace mapping may be performed and compared with the clinical arrhythmia. In order to perform pace mapping the minimum output is used from the distal electrodes of the ablation catheter and the paced beats are compared with the clinical arrhythmia. It is possible to have multiple different pace maps by pacing from the same site as the same isthmus may have multiple exit sites. In VT a long stimulation to onset of QRS with an excellent pace map generally indicates close proximity to the isthmus which then conducts to the exit site. Data acquired from an activation map can be used to create a propagation map. This demonstrates a wavefront of activation color coded red with a background blue image. This demonstrates conduction velocity and the overall direction of depolarization for both focal and re-entry circuits.

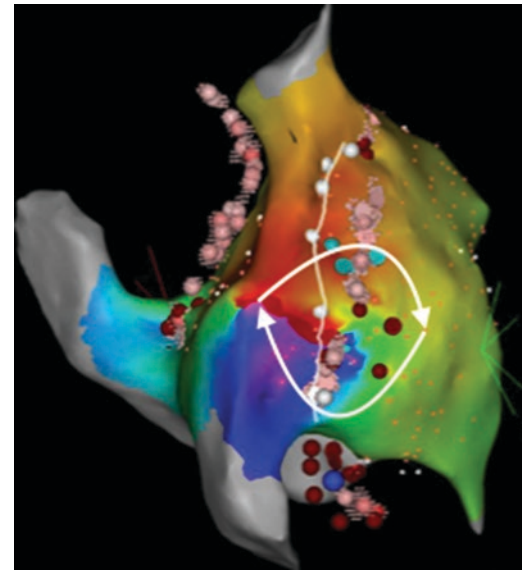

Fig. 3.2 Activation map showing a macro re-entry circuit around an atriotomy scar in a patient who previously underwent mitral valve surgery. The earliest activation is seen as red followed by yellow, green, blue and then purple. The white arrow shows the overall direction of conduction. Prior to ablation high output pacing was performed and the approximate location of the right phrenic nerve was mapped out (shown as a white line). Ablation was performed (light and dark red dots) from the superior vena cava to the inferior vena cava with termination of the tachycardia. The light blue dots indicate fractionated potentials. Also seen on the left side of the image in the background is an ablation line along the left interatrial septum which resulted in termination of a second tachycardia and at the inferior aspect of the image a cavotricuspid ablation line which terminated a third tachycardia

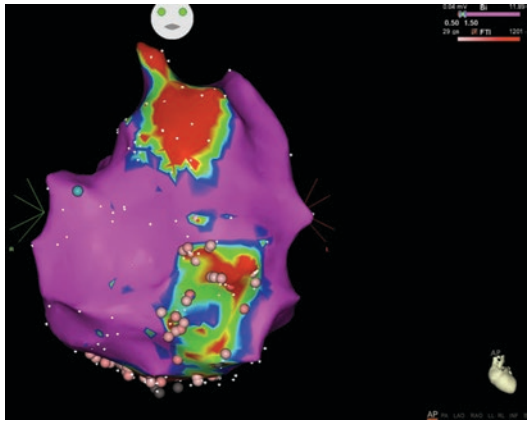

Fig. 3.3 Voltage map of the right ventricle in a patient with a history of tetralogy of fallot. Two regions of dense scar are seen, one in the anterosuperior tricuspid annulus and the other in the anteroapical region. Both of these are surrounded by heterogenous tissue. The inducible VT was found to circulate around the anteroapical scar which terminated with ablation

Voltage Map (Isopotential)

Is used to map local potentials during either sinus rhythm, tachycardia or pacing. The concept is that low amplitude endocardial signals are more indicative of regions of scar while higher amplitudes imply relatively healthy myocytes. As well as the amplitude of the signal the degree of fractionation and duration of the signal are very important as this may imply regions of slow conduction, which are often targeted for ablation.

The amplitude of each signal can be color calibrated so that red implies scar with orange, yellow, green, blue and purple indicating progressively higher amplitudes.

In the right ventricle normal bipolar electrograms have an amplitude of 3.7 ± 1.7 mV and in the left ventricle 4.8 ± 3.1 mV with **1.5 mV or less defined as scar and 0.5 mV or less** (Fig. 3.3).

Entrainment Mapping

Entrainment mapping can be performed by pacing from the ablation catheter in various locations where the tachycardia circuit location is suspected. By overdrive pacing at a cycle length shorter than the tachycardia cycle length the tachycardia is continuously reset without terminating to the same cycle length with manifest and concealed entrainment. In general the pacing cycle length is 20–30 ms shorter than the tachycardia cycle length although in certain circumstances such as an orthodromic reciprocating tachycardia a rate just slightly less than the tachycardia cycle length is chosen from the RV apex as faster rates may penetrate the AV node and result in termination of the tachycardia.

A short PPI—TCL generally indicated closer proximity to the circuit. This difference can then entered onto the mapping system as a color coded time where red is less than 30 ms followed by yellow, green, blue and finally purple where the difference is greater than 100 ms. This is an effective strategy to help map out the regions of the chamber involved in the re-entry circuit. It does not provide data on where exactly to ablate and this decision must be made based on the location of the isthmus or by joining various anatomic structures. In a diseased atrium where multiple ablations have been performed it may be difficult to capture all areas as well as the potential to terminate the arrhythmia as well as initiation of a different tachycardia.

Specific Mapping Systems

Ensite Precision (Abbott Technologies, Minnesota, USA)

This system uses a hybrid impedance and magnetic system for localization of catheters. This system emits a 8.136 kHz current between eight surface electrodes in three different planes; cranial to caudal, right to left and posterior to anterior. There are also two patient reference sensors which help with map stability.

One of the major advantages of Ensite over CARTO is the ability to acquire data from any catheter rather than a catheter designated by the system. Another attractive feature is the ability of the system to review data while still acquiring further data. An example of an Ensite Precision velocity map is shown on Fig. 3.4.

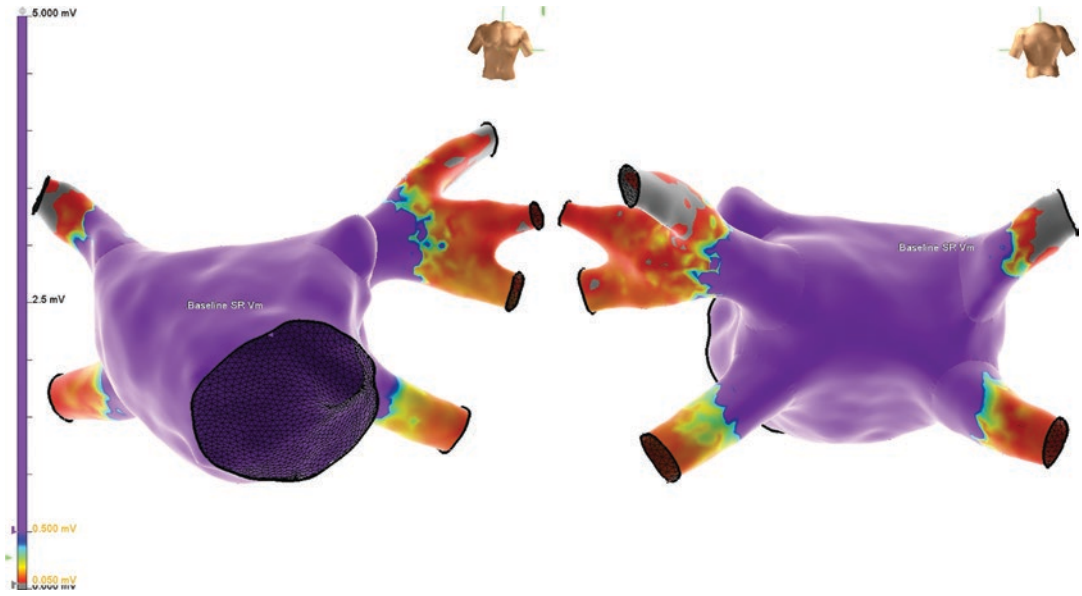

Fig. 3.4 Ensite Precision Map system (Abbott Technologies, Minnesota 55,442, USA) showing a voltage map of the left atrium with an anterior view on the left and posterior view on the right

CARTO Mapping System (© Biosense Webster, Inc.)

This system uses a combination of magnetic and impedance based technology for catheter localization and data acquisition. A locator pad composed of three coils is positioned under the table and emits very low intensity magnetic fields between 5×10^{-6} to 10^{-5} Tesla. Each coil emits a slightly different field strength which is then detected by a sensor in the proximal tip of the ablation catheter. The relative magnetic field from each coil is then fed back to the system with a three dimensional location in the x, y and z axis and catheter orientation in three planes termed roll, pitch and yaw. The ablation and diagnostic catheters also emit a low level current which is detected by six reference patches. Although the locations of diagnostic catheters can be visualized the electrogram's can unfortunately only be seen in specific catheters designed by the company such as the Lasso, the Pentarray and the Decanav.

The Lasso is a 10 or 20 pole circular deflectable catheter which is predominantly used for left atrial mapping and in particular pulmonary vein isolation. The circular component is flexible with a 4.5 Fr diameter and a shaft which fits through an 8 Fr sheath (Fig. 3.5).

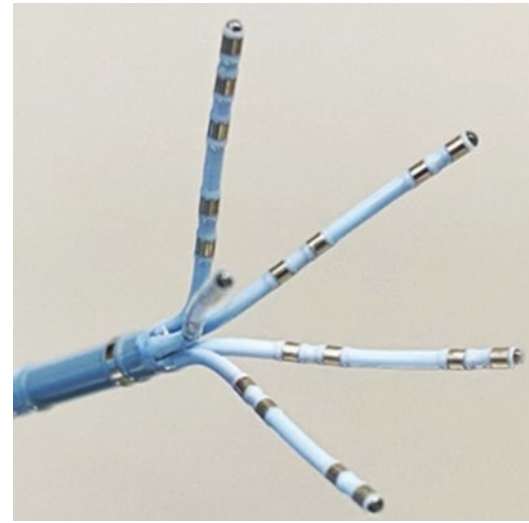

Fig. 3.5 Image of Pentarray showing 20 electrodes on five splines. Each spline has a 3 Fr diameter with 1 mm electrodes spaced at either 4 mm or 2-6-2 mm spacing

The Pentarray catheter consists of 20 electrodes on five arms (Fig. 3.6). Each arm is soft with a 3 Fr diameter and a shaft, which can be positioned through a 7 Fr sheath and comes in

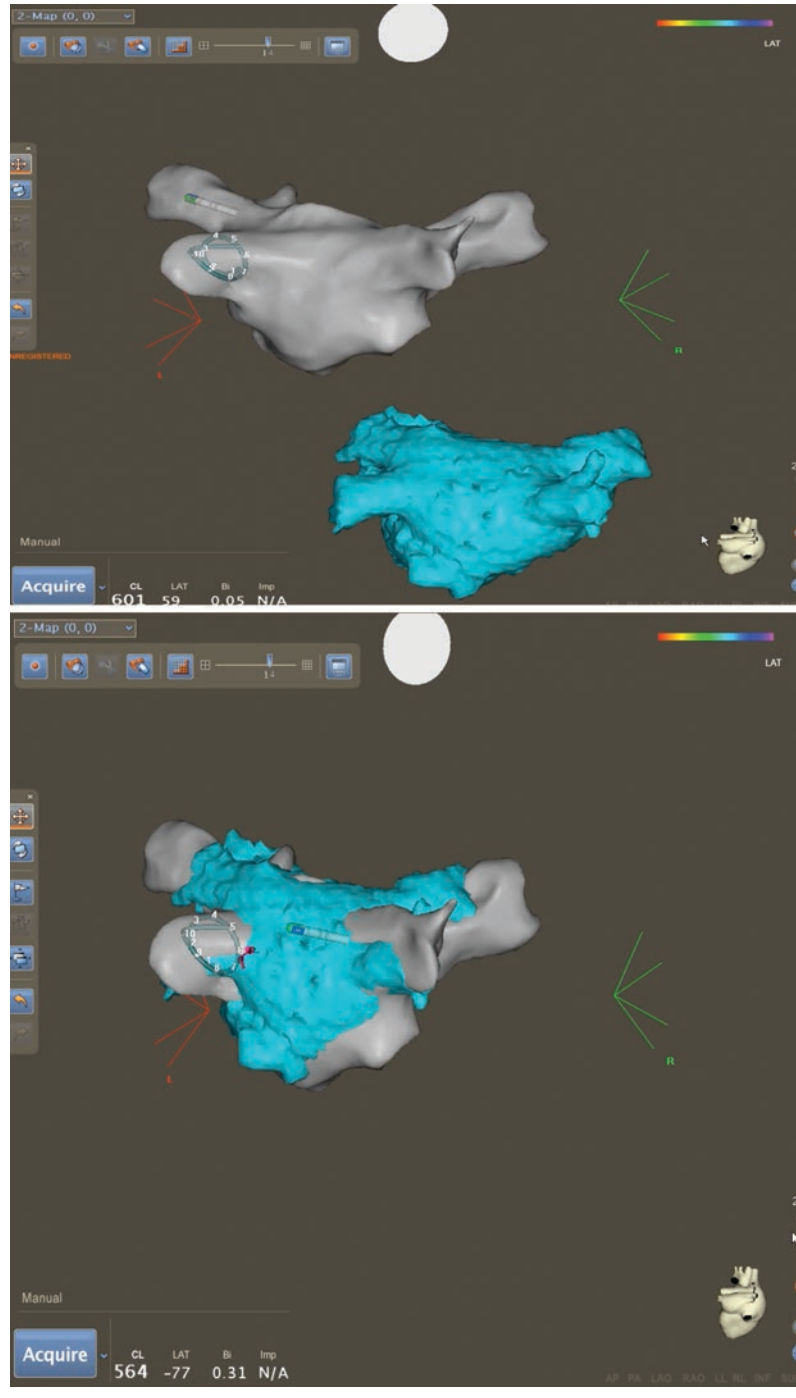

Fig. 3.6 Fast Anatomic Map created using the Lasso Catheter with a CT LA in the top image. Landmarks are selected on both the map and the CT and the images are merged as shown in the bottom image

different curves. Each individual electrode is 1 mm in length with varying electrode spacing; either 4 mm spacing or 2-6-2 mm spacing.

The Decanav catheter is a ten pole catheter in which each electrode is 2 mm in length and with electrode spacing of 2-8-2 mm. This allows the rapid acquisition of multiple points during mapping and can be useful for both atrial tachycardia and ventricular tachycardia including outflow tract tachycardia. Like the Pentarray it can be advanced through a 7 Fr sheath and is available in both a D and an F curve.

The location patches also transmit low level current to each other, which helps to record chest impedance allowing for respiratory gating. This is calibrated at the start of the procedure so that points are taken during end expiration and is particularly useful for accurate fast anatomic mapping. In order to gate the circular mapping catheter should be in contact with the wall of the left atrium. This can easily be achieved by positioning the catheter along the mitral annulus or in one of the pulmonary veins. A threshold for respiratory gating can be set with lower values resulting in more accurate but slightly slower data acquisition.

Merging the Baseline CT/MRI onto the Anatomic Map

Often baseline imaging is useful in order to assess pulmonary vein anatomy and assess for aberrant pulmonary veins. The baseline CT or MRI of the left atrium can also be superimposed on the left atrial shell obtained during fast anatomic mapping in order to create a merge. In order to perform this the baseline CT has to be imported onto the mapping system. This is then segmented so that the chamber of interest is enhanced. Following creation of the map the CT or MRI can be integrated by using a combination of both landmark and surface registration. As shown in Fig. 3.8 select points are chosen on the map and the same points on the CT which are used during the merge process. Inaccuracies may exist between the CT and the map due to changes in time with alterations in either the rhythm or hydration affecting the LA geometry.

Additional Features of Carto

This system has several software features which may be considered to be clinically useful.

Visitag (© Biosense Webster, Inc.) uses automation in order to create 4 mm^2 points on the map which fulfill specific pre-programmed parameters. These parameters consist of the minimum time at a particular point, the maximum range of movement of the catheter tip, the minimum force applied as well as the percentage time that the force was obtained for. Impedance and temperature changes can also be tracked. Additionally a grid feature marks 2 mm^2 points along the entire ablation lesion.

Paso (© Biosense Webster, Inc) software has been introduced into the Carto 3 platform in order to help to perform accurate pace mapping. This provides a numerical value for each lead and provides an overall assessment of the accuracy between the clinical arrhythmia and the paced beat. Although the overall efficacy has yet to be studied it appears to have a useful clinical role in particular for focal PVC's as shown in Fig. 3.7 and VT.

CartoUnivu (© Biosense Webster, Inc) allows real time catheter movement to be tracked on a pre-recorded cine angiogram. This is particularly useful for AF ablations where a three dimensional rotational angiogram of the left atrium is performed at the start of the procedure following the administration of intravenous adenosine or with rapid ventricular pacing. This image can then be integrated onto the map and viewed in any angle. Coronary angiograms can also be integrated for epicardial ablation as well as LVOT ablations. This may have an overall effect in lowering the total radiation exposure for the entire case, however, data proving this statement are still missing.

Rhythmia Mapping System (Rhythmia Mapping, Rhythmia Medical, Boston Scientific Inc., Marlborough, MA, USA).

Fig. 3.7 Paso Software (© Biosense Webster, Inc.) Used to compare a paced ventricular beat (yellow) with intrinsic ectopic beat (green) in the anterior mitral valve annulus

This system uses a combination of magnetic and impedance degradation in order to localize catheters. A magnetic sensor in the tip of the Orion mapping catheter is the predominant guide to location with impedance used for additional clarification of location on each of the electrodes. As any diagnostic or ablation catheter can be used catheter localization for all other catheters is based on impedance. The Orion catheter requires irrigation at a rate of 1 mL/min.

One of the major advantages to this system appears to be the ability to rapidly acquire a high spatial resolution map using the Orion mapping catheter. This is a 64 electrode small basket catheter mounted on eight splines in which each electrode is separated by 2 mm. Signals as small as

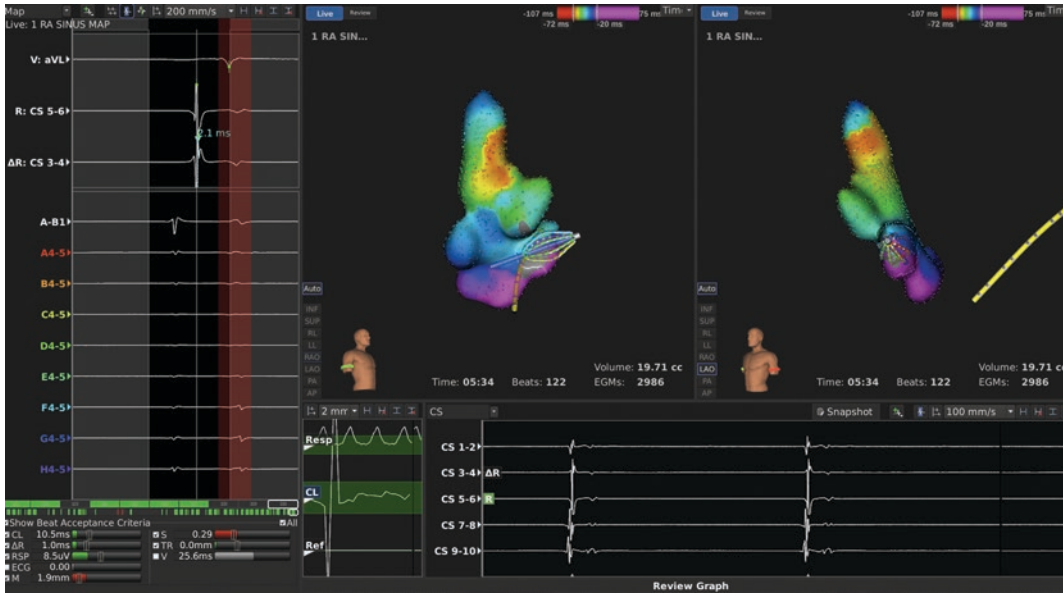

Fig. 3.8 Rhythmia (Rhythmia Mapping, Rhythmia Medical, Boston Scientific Inc., Marlborough, MA, USA) screen setup. A surface lead is chosen on the top left image. Below this is the CS which is used as a reference electrode. As well as using the electrode timing a change in activation is also recorded in order to minimize the chance of a change in the activation sequence. Both the RAO image on the left and LAO in the right show the RA during normal sinus rhythm

0.01 mV can be collected. The catheter is deflectable and can be advanced through an 8.5 Fr sheath. Mapping can be performed with the catheter either fully closed (3 mm diameter), fully opened (22 mm diameter) or any range between these two extremes. Anatomic data is only acquired if the electrode is deemed to be within 2 mm of the endocardial surface. Each electrode has a surface area of 0.4 mm^2 with an interelectrode separation of 2.5 mm. This catheter is irrigated and it is recommended that heparin is administered for all procedures where this catheter is used with an ACT of 300 s.

The setup of Rhythmia is shown in Fig. 3.8. The surface ECG is seen on the top left with reference signals from the CS below this and a combination of electrograms from the Orion catheter below this. Each electrode is code by letter and number. An RAO image of the RA and LAO of the RA are shown during normal sinus rhythm.

Given that multiple signals are acquired simultaneously this system must have the ability to rapidly self annotate signals and in particular activation times. This is achieved by recording the maximum deflection on the bipolar signal or the most negative dV/dT on the unipolar electrogram. There is continuous and automatic electrogram acquisition based on beat acceptance criteria.

In order to set up the system at the start of the case the chamber of interest and type of map is programmed as well as the rhythm (sinus, paced, tachycardia) and the reference. Although the mechanism of the arrhythmia should be programmed at the start i.e. either focal or re-entry this can be changed during or after completion of the map. The system makes recommenda-

tions based on analysis of the last 10 s of the intracardiac signals and calculates the tachycardia cycle length and therefore calculates the mapping window as well as suggesting the reference electrograms. An example of mapping across a previous CTI ablation by pacing from the proximal CS during sinus rhythm is seen in Fig. 3.9.

Important Points

1. A stable reference point is required for activation mapping so that all points can be measured relative to the same electrogram. An ideal reference electrogram should be stable with an obvious positive or negative peak for measurement. The trigger is then set off either the most positive or negative change in voltage over time (dV/dT).
2. The window of interest is set according to whether the arrhythmia mechanism is focal or re-entry. For a focal tachycardia the earliest component may be set at 80 ms ahead of the surface signal and 30 ms after the offset. For a re-entry tachycardia the window of interest is chosen as 90% of the tachycardia cycle length to allow for a degree of cycle length variability.
3. In activation mapping electrical signals are color coded according to how early or late they are in the window of interest. The earliest is coded as red followed by yellow, green blue, and purple which indicates later activation. In focal arrhythmias early signals are generally targeted. In re-entry ablation is often performed where early meets late.
4. In voltage mapping bipolar signals of 1.5 mV or less defined as scar and 0.5 mV or less dense scar in the ventricle.
5. CFAE's are defined as low amplitude fractionated atrial electrograms with a cycle length of less than 120 ms.

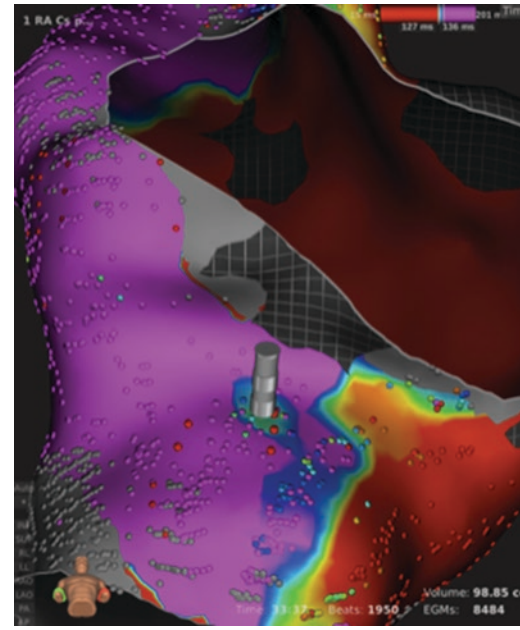

Fig. 3.9 Activation mapping using Rhythmia (Rhythmia Mapping, Rhythmia Medical, Boston Scientific Inc., Marlborough, MA, USA) with pacing from the proximal coronary sinus and mapping the right atrium in a patient with a recurrence of atrial flutter following a previous CTI ablation. The image is taken from an inferior angle with the tricuspid annulus at the top of the image and the inferior vena cava at the bottom. Although conventional pacing maneouvres suggested clockwise block there is a region of slow conduction in the mid CTI which required further ablation

Reference

De Ponti R, Verlato RR, Emanuele Bertaglia E, et al. Treatment of macro-re-entrant atrial tachycardia based on electroanatomic mapping: identification and ablation of the mid-diastolic isthmus. Europace. 2007;9:449–57.

AV Nodal Re-Entry Tachycardia (AVNRT)

4

Duc H. Do, Noel G. Boyle, Benedict M. Glover, and Pedro Brugada

Abstract

AVNRT is the most common paroxysmal supraventricular tachycardia seen in adults. It occurs as a result of reentry within dual AV pathways (two connections between the atrium and the compact AV node). In typical AVNRT reentry occurs with antegrade conduction down a 'slow' pathway and retrograde conduction up a 'fast' pathway resulting in a short RP tachycardia. In atypical AVNRT, conduction occurs antegrade along the fast pathway and retrograde along the slow pathway resulting a long RP tachycardia. It is important to carefully map during tachycardia and perform the relevant maneuvers in order to establish the diagnosis. AVNRT is treatable with catheter ablation and this is highly successful with a low recurrence rate. AV block is a major potential complication in ablation of AVNRT.

D. H. Do · N. G. Boyle (✉)
University of California, Los Angeles, CA, USA
e-mail: boyle@mednet.ucla.edu

B. M. Glover
Division of Cardiology, Department of Medicine, University of Toronto, Toronto, Ontario, Canada

P. Brugada
University Hospital of Brussel, Brussels, Belgium
e-mail: pedro@brugada.org

Introduction

AVNRT is the most common paroxysmal supraventricular arrhythmia in adults, accounting for approximately 60% of all SVTs (Katritsis and Camm 2006). AVNRT most commonly presents in young patients under the age 40 years (median age 28), though it can still affect patients over the age of 65 generally with slower tachycardia rates; it is also more common in females than males (Chen et al. 1994; Jackman et al. 1992; Haissaguerre et al. 1992; Lee et al. 1991). Presentation tends to occur with intermittent palpitations of acute onset which may terminate with vagal maneuvers. The baseline ECG is usually normal. During tachycardia the RP interval for typical AVNRT is short and atrial activation occurs in or at the terminal region of the QRS complex. The P wave is generally negative in the inferior ECG leads (II, II, aVF) and narrow, indicating an inferior to superior atrial activation from the retrograde fast pathway location.

Anatomy

The anatomy relevant for AVNRT is contained within the triangle of Koch (Fig. 4.1), bounded anteriorly by the septal leaflet of the tricuspid valve, posteriorly by the tendon of Todaro and inferiorly by an imaginary line connecting the

B. M. Glover, P. Brugada (eds.), *Clinical Handbook of Cardiac Electrophysiology*,
https://doi.org/10.1007/978-3-030-74319-2_4

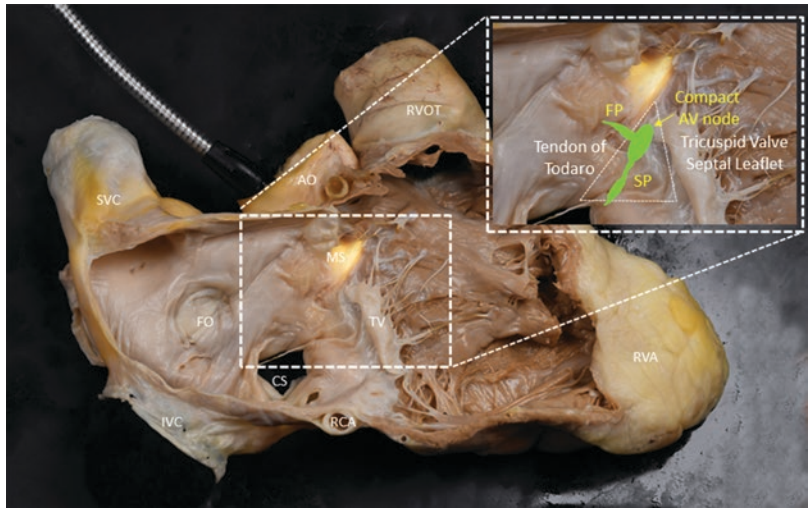

Fig. 4.1 Triangle of Koch. A pathological specimen of the right atrium and right ventricle is displayed in the right anterior oblique (RAO) projection. A light source is passed through the aorta (AO) to illuminate the membranous septum (MS). The inset shows a zoomed up image of the Triangle of Koch, which is formed by the Tendon of Todaro, the septal leaflet of the tricuspid valve (TV), and a line connecting the TV to the coronary sinus ostium. The compact AV node is located at the apex of the triangle. The fast pathway extends posteriorly and superiorly across the Tendon of Todaro. The slow pathway (SP, i.e., right inferior extension) extends inferiorly. Abbreviations: *SVC* superior vena cava, *IVC* inferior vena cava, *RVOT* right ventricular outflow tract, *RVA* right ventricular apex, *RCA* right coronary artery, *FO* fossa ovalis. (Images courtesy of Dr. Shumpei Mori, MD PhD)

superior aspect of the coronary sinus ostium to the tricuspid valve. The compact AV node is located in the interatrial septum at the apex of the triangle of Koch. Surrounding the compact AV node, there is a zone of transitional cells which connect the compact node to the atrial myocytes. This transitional zone is composed of cells which share similar features to both nodal and atrial myocytes. There are three atrial extensions from the compact AV node to the atria as well as a single common pathway which connects to the ventricular aspect (Fig. 4.2).

The fast pathway generally extends superiorly from the compact AV node and crosses the Tendon of Todaro. The slow pathway(s) are formed by the rightward inferior extension, located anterior to the coronary sinus ostium, and the leftward inferior extension, which is directed towards the mitral annulus. The rightward inferior extension is the most common slow pathway involved in AVNRT (~95%) (Nakagawa and Jackman 2007).

Mechanism

Mechanistically AVNRT is generated by reentry between two connections linking the atria and the compact AV node (i.e., AV nodal pathways). The presence of two AV nodal pathways is referred to as dual AV nodal physiology. While dual AV nodal physiology is required for AVNRT, most patients with dual AV nodal physiology do not have AVNRT; 10–20% of patients without AVNRT undergoing electrophysiologic assessment demonstrate dual AV nodal physiology (Zardini et al. 1990). These AV nodal pathways are classified according to the velocity through the tissue. The 'slow' pathway has slower conduction velocity but a shorter refractory period. The 'fast' pathway has a faster conduction velocity, but longer refractory period. The presence of dual AV nodal pathways is demonstrated by the presence of a sudden prolongation of the AH interval ('AH jump') during electrophysiologic

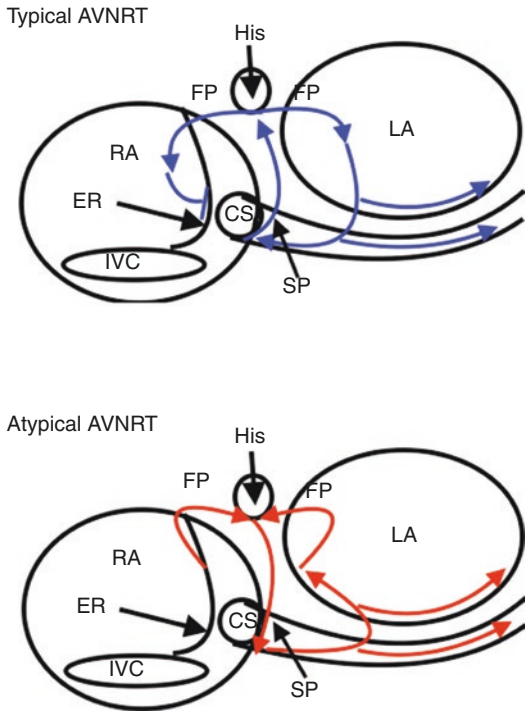

Fig. 4.2 Schematic of the AVNRT circuit. The top image shows an LAO view showing a typical slow/fast AVNRT utilizing an antegrade right inferior extension slow pathway (SP) and retrograde fast pathway (FP). Both the left and right atrium are simultaneously activated by retrograde FP conduction. The left atrial activation front propagates inferiorly and then across the coronary sinus musculature to activate the SP in the anterograde direction, completing the reentrant circuit. The bottom image shows an atypical fast/slow AVNRT utilizing the FP antegrade and the SP retrograde. (Abbreviations: *CS* coronary sinus, *ER* Eustachian ridge, *LA* left arium, *RA* right atrium, *IVC* inferior vena cava)

testing. An increase of ≥50 ms in the AH interval with a decrement in the A1A2 interval of 10 ms, is defined by convention as a change in antegrade conduction from the 'fast' to the 'slow' pathway.

Classification

Slow/Fast AVNRT (Typical AVNRT)

This occurs when a premature atrial complex (PAC) travels antegrade down a slow pathway followed by retrograde conduction up the fast pathway. The most commonly involved slow pathway is the right inferior extension (~95% of cases). Less commonly, (~5%) antegrade conduction may occur along the left inferior extension slow pathway. These are generally associated with an AH interval greater than 200 ms. As shown in Fig. 4.3 there is generally a short septal VA interval of <70 ms.

The earliest atrial activation generally occurs along the superior septum posterior to the Tendon of Todaro (via retrograde fast pathway conduction), though recent data from high-density mapping studies have shown significant variability in the anatomic location of this retrograde limb (Chua et al. 2018). Activation on the left side of the septum continues laterally and inferiorly activating the coronary sinus musculature and subsequently the slow pathway, propagating the tachycardia. Activation on the right side of the septum is blocked by the Eustachian ridge.

Fast/Slow AVNRT (Atypical AVNRT)

Atypical AVNRT occurs in about 5–10% of AVNRT cases (Katritsis and Camm 2006). As demonstrated in Fig. 4.4 antegrade conduction occurs down the fast pathway and retrograde conduction occurs up the slow pathway (right inferior extension) with earliest atrial activation at the inferior septum (CS 9–10). Occasionally retrograde conduction occurs up the left inferior extension (leftward slow pathway). The AH interval is shorter than the HA interval. As the RP interval is long it is easier to identify the P wave which is negative in II, III, aVF and V6 and positive in V1. This should be differentiated from an atrial tachycardia originating close to the CS ostium or an AV reentrant tachycardia using a septal AP.

Slow/Slow AVNRT

Antegrade down the rightward inferior extension and retrogradely up the leftward inferior extension of the AV node can result in the uncommon 'Slow-Slow' form of AVNRT. The earliest retrograde atrial activation is therefore often the roof

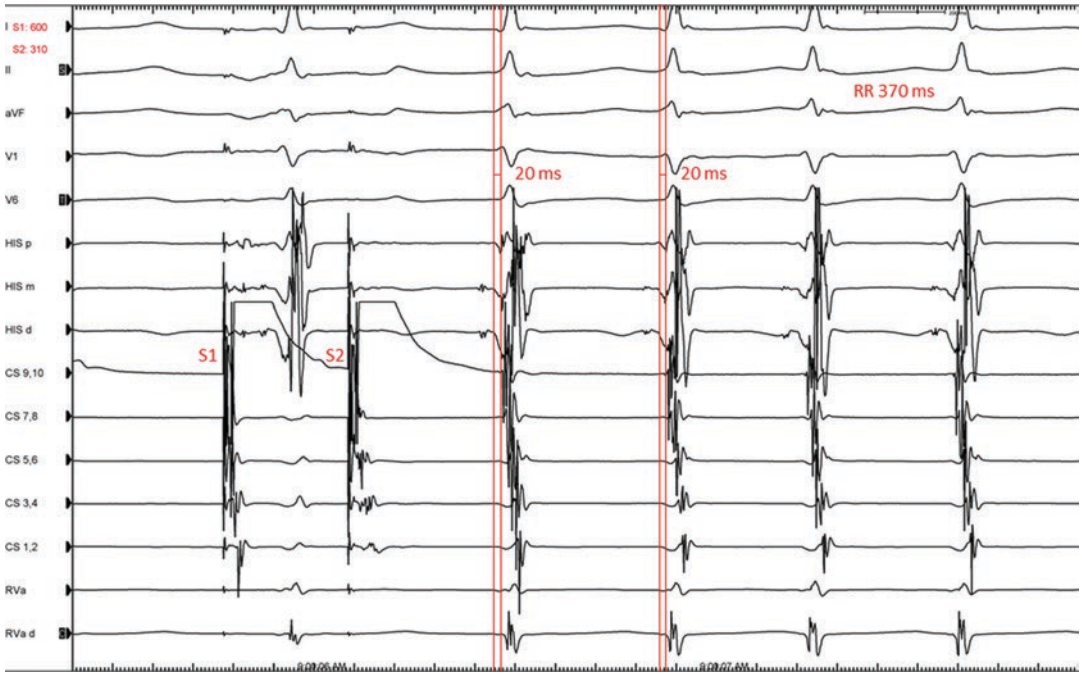

Fig. 4.3 Typical AVNRT initiation. Following a single extrastimulus (S2), note the markedly prolonged AH interval representing anterograde conduction down the slow pathway, followed by retrograde conduction up the fast pathway with a very short VA time of 20 ms. Despite wobble in the cycle length, the VA time remains 20 ms showing the presence of VA linking, excluding atrial tachycardia (AT). Earliest atrial activation is along the distal His catheter, consistent with fast pathway retrograde activation. In addition, the very short VA time excludes retrograde conduction over a septal pathway, and thus AV reentrant tachycardia (AVRT). (HIS p, m, d electrodes are positioned at the superior tricuspid annulus; CS 9,10 electrodes are positioned in the proximal CS with CS 1,2 in the distal CS; RVA d are positioned in the RV apex; *p* proximal, *m* mid, *d* distal)

of the coronary sinus although it may also be between the coronary sinus and the tricuspid annulus if retrograde conduction occurs along the rightward inferior extension. There are often multiple AH 'jumps' reflecting multiple slow pathways. The AH interval is generally greater than 200 ms and is longer than the HA interval.

Electrophysiological Evaluation

Baseline Data

The ECG in AVNRT generally shows a narrow QRS tachycardia, duration less than 120 ms, with a short RP interval in the case of a typical AVNRT and a long RP interval in the case of an atypical AVNRT. If aberrancy is present, this is more frequently a RBBB morphology. A P wave hidden within the QRS complex, or located at the end of the QRS is highly suggestive of a typical AVNRT as shown in Fig. 4.5. RR alternans may be seen in AVNRT though the mechanism is unclear.

Procedure

The diagnostic EP evaluation is generally performed with minimal sedation in order to maintain as close to normal physiological parameters of the pathways involved as possible, and therefore maximize the chance of arrhythmia induction. Mapping catheters are positioned in the right ventricle (RV), coronary sinus (CS), high right atrium (HRA) and at the HIS region across the superior tricuspid annulus.

Decremental pacing is first performed from the RV in order to assess the presence of retro-

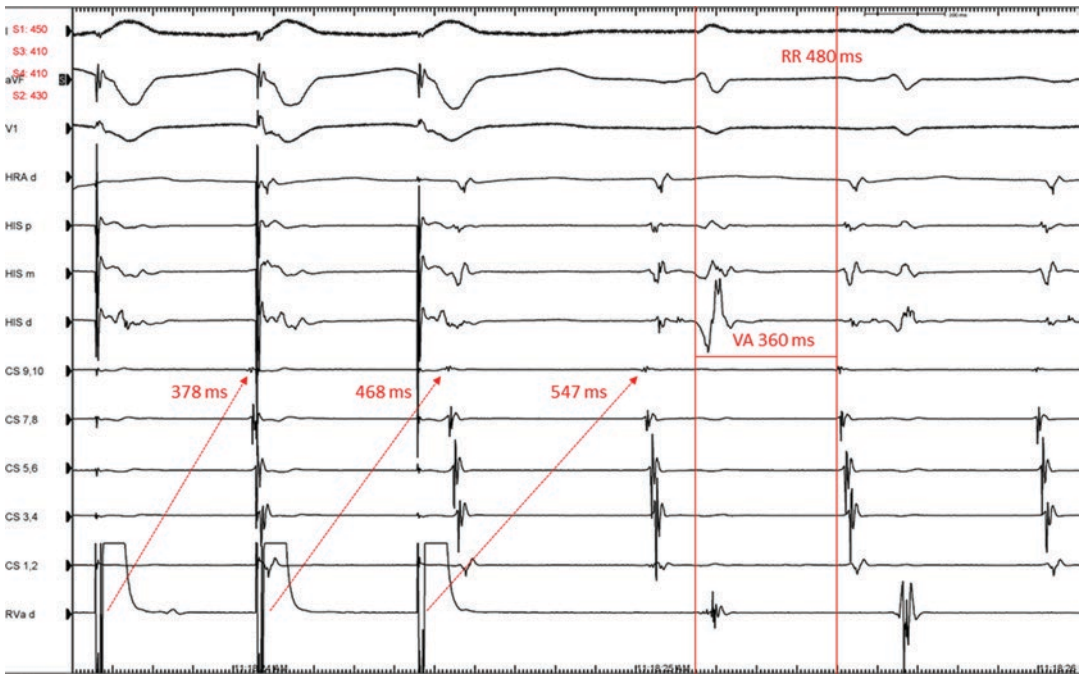

Fig. 4.4 Initiation of atypical AVNRT. Pacing from the RV apex results in decremental retrograde conduction along the slow pathway for the first three beats as evidenced by the earliest activation recorded along the proximal CS (CS 9,10). Upon cessation of RV pacing, atypical AVNRT initiates with a prolonged VA interval of 360 ms and earliest atrial activation in the proximal coronary sinus. This subsequently conducts antegrade down the fast pathway and back down the slow pathway. (HRA d is positioned in the high right atrium, CS 9,10 is in the proximal CS with CS 1,2 in the distal CS, RVa d is in the distal RV apex)

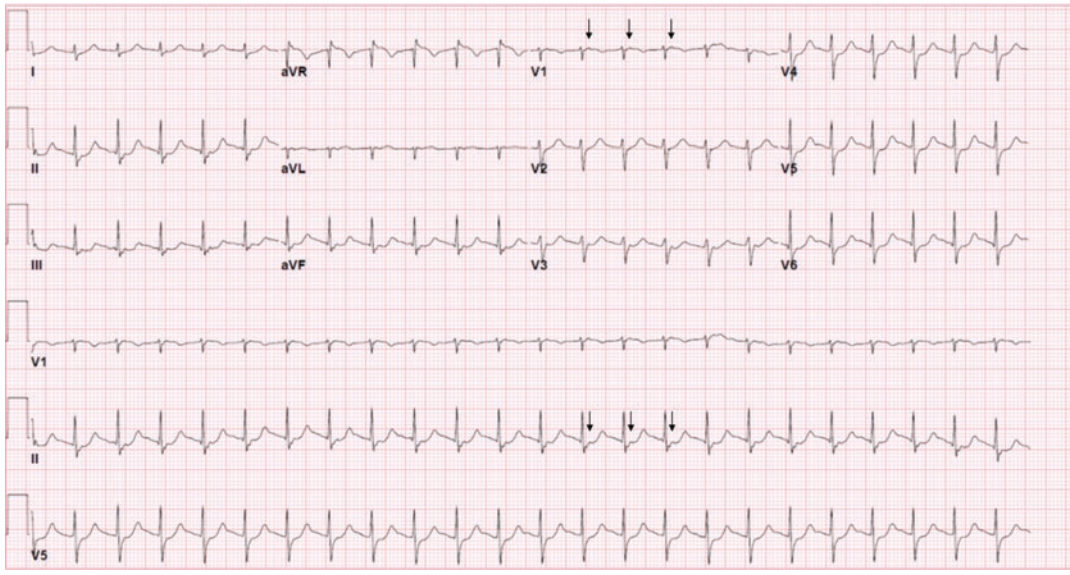

Fig. 4.5 Electrocardiogram of typical AVNRT. This 12 lead ECG shows typical AVNRT with a retrograde P wave inscribed at the end of the QRS complex (black arrows). This is sometimes referred to as a pseudo-R' in lead V1. The ventricular rate is approximately 150/min

grade conduction, the retrograde atrial activation sequence, and to evaluate for evidence of dual AV nodal conduction. Following this, decremental extrastimulus atrial pacing (S1S2) is performed in order to assess for the presence of dual or multiple AV nodal pathways and to try to induce AV nodal re-entry tachycardia. Atrial pacing can be performed from either the HRA or the CS. It is uncommon for a ventricular paced beat to initiate typical AVNRT. This is in contrast with atypical AVNRT and AV reentrant tachycardia (AVRT), where induction of the re-entry arrhythmia by ventricular pacing is common.

Dual AV nodal physiology is demonstrated by the presence of an AH or HA jump as defined above. This is the result of a change in conduction from the fast pathway to the slow AV nodal pathway. Similar findings may be seen during incremental atrial pacing (i.e., evaluating the Wenckebach cycle length) as seen in Fig. 4.6. This phenomenon may be more easily demonstrated using a recently described method of ventricular-triggered atrial pacing (Duchateau et al. 2020).

During ventricular pacing a HA jump of greater than or equal to 50 ms generally represents a retrograde switch from the fast to the slow pathway conduction. In the absence of a clear retrograde His, an increase in the VA interval ≥50 ms may either represent a retrograde switch from fast to slow pathway or retrograde right bundle branch block requiring transseptal activation and retrograde left bundle activation.

The administration of intravenous sedation may depress fast pathway conduction thus increasing the incidence of a jump to the slow pathway. Additionally, the administration of isoproterenol may increase fast pathway conduction which may mask the appearance of an AH jump with single atrial extrastimuli, requiring more atrial extrastimuli to elicit an AH jump.

If tachycardia cannot be induced with multiple atrial extrastimuli or decremental atrial pacing then isoproterenol should be administered in

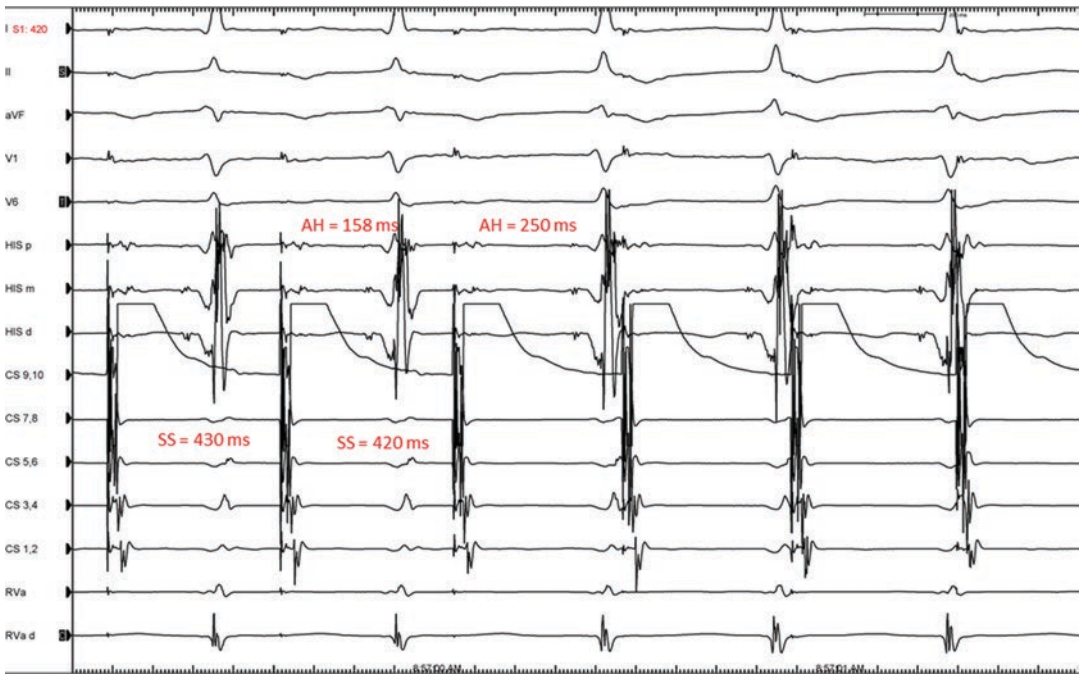

Fig. 4.6 Demonstration of dual AV nodal physiology during incremental atrial pacing. With shortening of the atrial extrastimulus interval (S1S2) from 430 to 420 ms, the AH interval prolongs from 158 to 250 ms (>50 ms) demonstrating change in anterograde conduction from the fast pathway to the slow pathway

boluses or drip at a dose of 1–4 μg/min. Induction should be attempted from multiple right atrial and coronary sinus sites, both during isoproterenol effect and washout. Isoproterenol should be stopped prior to ablation because it causes hypercontractility of the heart leading to catheter instability.

Differentiation Between AVNRT and AVRT

The fact that AV reentrant tachycardia (AVRT) involves the ventricle as a component of the reentry circuit can be used to differentiate these arrhythmias from AV nodal reentrant tachycardia (AVNRT) with simple observations as well as pacing maneuvers, that may be performed for differential diagnosis confirmation.

A VA conduction time of less than 70 ms in typical Slow/Fast AVNRT excludes AVRT (Knight et al. 2000).

The delivery of ventricular extrastimuli from a pacing catheter in the basal RV during His-bundle refractoriness in order to assess the effect on atrial activation is the most straightforward method to help differentiate between the two arrhythmias.

In order to perform this maneuver a ventricular extrastimulus is delivered within 50 ms after the onset of the His electrogram during tachycardia, and advanced in 10 ms increments. Any advancement in the atrial activation with no advancement in the His electrogram or QRS fusion (i.e., proving His-bundle refractoriness) implies the presence of an accessory pathway. If the atrial activation sequence of the advanced beat is identical to the tachycardia sequence and the next His electrogram is advanced (i.e., tachycardia is reset) then this proves that the accessory pathway is part of the arrhythmia mechanism (i.e., the tachycardia is AVRT). Delay in the next atrial activation or termination without reaching the atrium also proves that the accessory pathway participates in the arrhythmia mechanism. It should be noted, however, that a His-refractory ventricular extrastimlus may not always advance the atrial activation in an AVRT using a left lateral pathway.

RV entrainment (pacing the ventricle 10–20 ms faster than the tachycardia to ensure acceleration of the tachycardia to the paced rate with terminating tachycardia) can also be used to distinguish AVRT and AVNRT. Upon termination of RV entrainment pacing, both will exhibit a 'VA(H)V' response (Knight et al. 1999). However, given that the ventricle is part of the AVRT circuit while it is remote to the reentrant circuit in AVNRT, the post-pacing interval (PPI) will be closer to the tachycardia cycle length (TCL) in AVRT. A difference between PPI and TCL (PPI-TCL) < 115 ms supports a diagnosis of AVRT. A PPI-TCL corrected for the difference in AH during RV entrainment and tachycardia (cPPI-TCL) < 110 ms is a strong predictor for AVRT (González-Torrecilla et al. 2006). Similarly, the difference in the Stim-A (SA) interval and the VA interval of less than 85 ms is also highly suggestive of AVRT (Michaud et al. 2001). AVRT can also be more quickly entrained than AVNRT from the ventricles; in AVNRT, it will take more than one fully captured beat to advance the atrium while it will take 1 or fewer fully captured beats to advance the atrium in AVRT (Dandamudi et al. 2010).

Differentiation of AVNRT from Atrial Tachycardia (AT)

In general, typical AVNRT can be distinguished from a septal atrial tachycardia by the short duration of the VA interval. It may be more difficult to distinguish an atypical AVNRT as the VA interval is generally longer and there is frequently wobble in the VA interval. Entrainment from the RV apex is useful to differentiate these tachycardias.

As shown in Fig. 4.7 following entrainment of AVNRT from the RV apex the following sequence is a V followed by an A followed by V pattern (VAV). In the case of an atrial tachycardia, a V-A-A-V response is usually seen following ventricular entrainment pacing. However, care must be made to exclude a pseudo V-A-A-V response

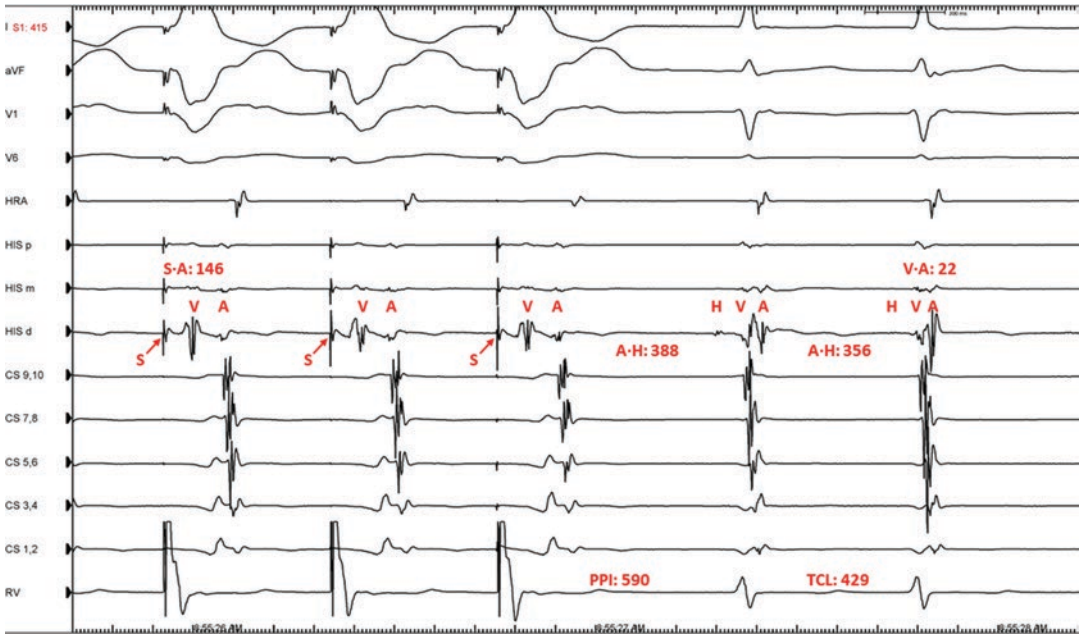

Fig. 4.7 VAV Response to Right Ventricular Entrainment during tachycardia. RV apical overdrive pacing is performed at cycle length of 415 ms; a V-A-(H)-V response is noted following cessation of ventricular overdrive pacing. The PPI-TCL is 590 – 429 = 171 ms, corrected PPI-TCL is 171-(388 – 356) = 139 ms, Stim-A (SA) – VA = 124 ms all of which are suggestive of AVNRT

which is common in atypical AVNRT (Knight et al. 1999). If the tachycardia is terminated during ventricular pacing and if the ventricular beat resulting in termination did not conduct to the atrium then atrial tachycardia can be excluded as the critical circuit is outside of both atria.

Several other useful pacing techniques may also be used. The AH interval can be recorded during tachycardia and compared with the AH interval during pacing from the high right atrium at the same cycle length (performed around the same time point, in order to ensure similar autonomic tone). In cases of atypical AVNRT the AH interval during atrial pacing is longer by more than 40 ms compared to tachycardia since the atrium is not part of the AVNRT circuit and atrial activation in the retrograde direction occurs in parallel with His bundle activation in the anterograde direction (Man et al. 1995; Hadid et al. 2018). In both atrial tachycardia and AVRT there is very minimal different in the AH during high right atrial pacing compared with tachycardia since the atrium and His bundle are activated in series during both atrial pacing and tachycardia.

Additionally pacing from the high right atrium at different rates during tachycardia can be performed and the VA interval recorded. If the VA interval at different rates is unchanged (i.e., VA linking is present) then atrial tachycardia can be excluded (Maruyama et al. 2007). Wobble in the tachycardia cycle length can also be used; in atrial tachycardia changes in AA precede changes in HH or VV whereas in AVNRT, changes in HH precede changes in the AA.

Ablation Techniques

Ablation is most commonly performed using a 3.5 or 4 mm non-irrigated RF ablation catheter, though recently, contact force sensing catheters with low-flow irrigation have also been used effectively and safely.

The ablation catheter is first positioned in the right ventricle and slowly withdrawn with clockwise torque on the catheter in order to maintain a posterior septal position at the level of the coronary sinus. This is demonstrated on the fluoro-

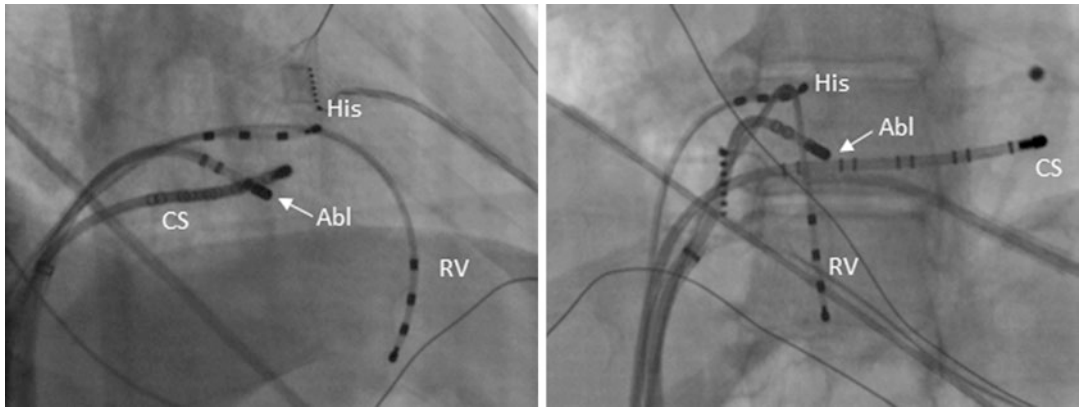

Fig. 4.8 Fluoroscopic location of ablation catheter when mapping the slow pathway. The image on the left is an RAO view and the image on the right is an LAO view. In both views the ablation catheter (Abl) is seen anterior to the coronary sinus os, and inferior and septal compared to the location of the His bundle. Also seen in the image is a quadripolar catheter in the right ventricle (RV), His bundle, and a decapolar catheter in the coronary sinus (CS)

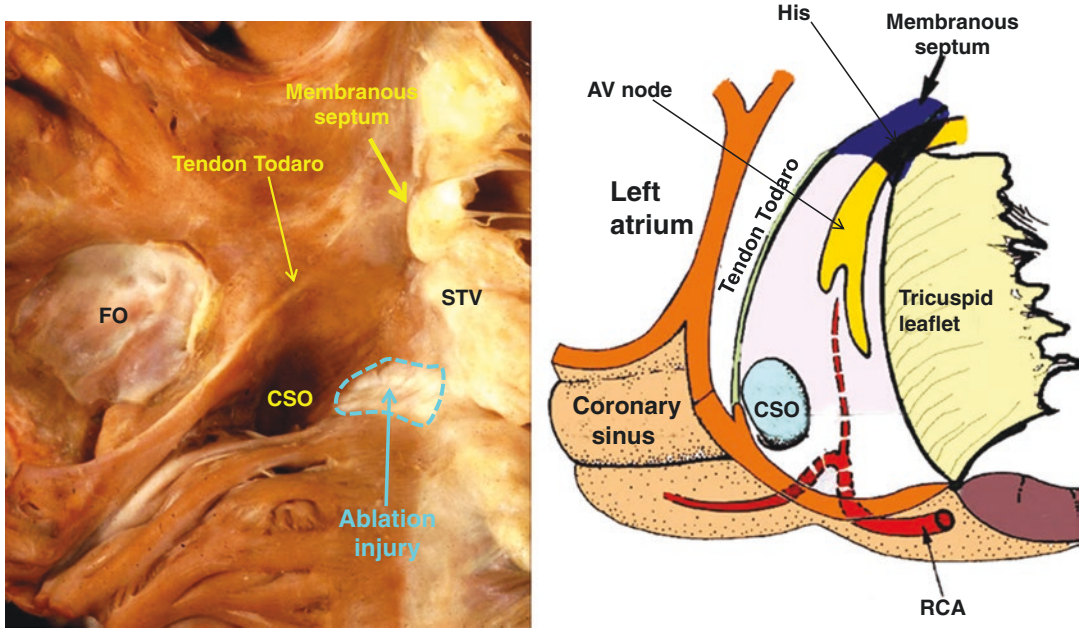

Fig. 4.9 Anatomical (left) and schematic (right) of the location of the slow pathway. A region of ablation is seen anterior to the coronary sinus ostium (CSO) and within the Triangle of Koch bounded by the Septal leaflet of the tricuspid valve (STV), tendon of Todaro and the coronary sinus ostium. The location of the AN node and the right coronary artery (RCA) are seen on the image relative to the location of the slow pathway

scopic images on Fig. 4.8 which shows the ablation catheter position in an RAO and LAO view. The location of a slow pathway ablation relative to the surrounding anatomical structures is shown in Fig. 4.9.

Mapping is then performed between the coronary sinus ostium and the tricuspid annulus. An A:V ratio of 1:2 to 1:10 should be recorded in which the atrial signal is approximately 20 ms later than the A on the His. As shown in Fig. 4.10 a small discrete slow pathway potential may sometimes be recorded on the ablation catheter. If this is seen the latest and highest frequency slow pathway potential should be targeted. Often a

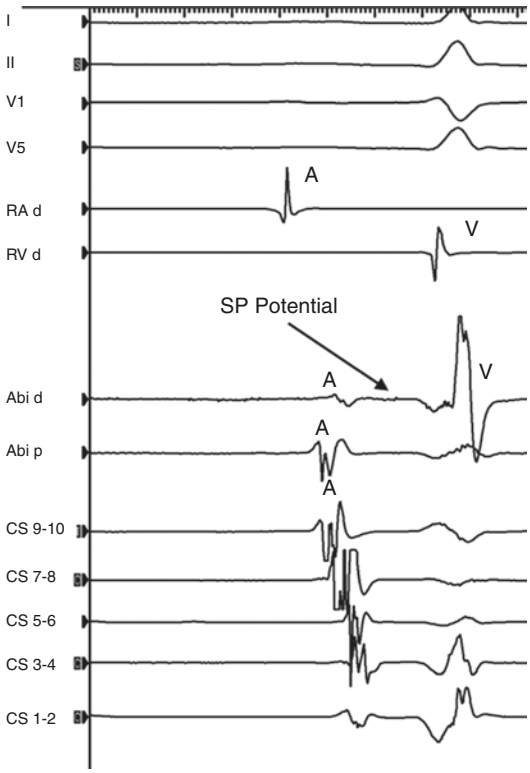

Fig. 4.10 Mapping of the Slow Pathway. The ablation catheter is positioned anterior to the coronary sinus with an A:V ratio of 1:6. There is a small discrete potential recorded on the distal ablation catheter corresponding with a slow pathway potential. Ablation at this location was successful in slow pathway modification with no further inducible AVNRT. Shown are recordings from ECG leads I, II, V1 and V5, distal right atrium (RA d), distal right ventricle (RV d), Ablation distal (Abl d), Ablation proximal (Abl p), Coronary sinus proximal (CS 9-10), Coronary sinus (CS 7-8, CD 5-6, CS 3-4) and Coronary Sinus distal (CS 1-2). Abbreviations: A: Atrial, V: Ventricular, SP: Slow Pathway

degree of clockwise rotation is required while trying to avoid falling into the coronary sinus. This is required to counteract the counterclockwise force of the Eustachian ridge which tends to rotate the catheter away from the septum during systole. A long sheath (e.g., SR-0 or deflectable sheath) may be helpful to maintain septal contact.

RF is generally started at 40–50 W with a maximum temperature set at 55–60 °C.

Junctional beats during ablation are generally considered an indicator of slow pathway modification. These are shown in Fig. 4.11. These beats are likely due to conduction of current injury from the slow pathway to the AV junctional area enhancing diastolic depolarization of the cells in this region (John et al. 1996; Estner et al. 2005). Other potential explanations for junctional beats include an increase in AV junctional automaticity (Boyle et al. 1997) as a result of post ganglionic noradrenaline release exceeding the increase in vagal tone associated with RF application in this region therefore increasing the rate of diastolic depolarization (Chen and Guo 1999) as well as a possible heat sensitive region close to the AV node which may lead to increased junctional activation (Thibault et al. 1998).

Accelerated junctional beats occurring at a cycle length of less than 500 ms or with transient loss of VA conduction is an indicator of potential AV block (Li et al. 1993). It is also important to monitor the AH interval during ablation. Ablation should be stopped immediately in the event of any prologation of the AH interval, any loss of retrograde atrial conduction during junctional beats, junctional tachycardia or if there is a sudden increase or reduction in impedance.

If there are no junctional beats during ablation alternative sites should be chosen. This generally involves moving the ablation catheter to a more superior position although this increases the risk of AV block and a high level of caution should be exercised superior to the level of the coronary sinus roof.

Other potential locations for the slow pathway are the leftward inferior extension which can often be successfully ablated along the roof of the proximal coronary sinus.

If AVNRT develops, ablation should be stopped due to catheter instability as well as a difficulty in establishing early signs of AV block. Overdrive atrial pacing can help avoid development of AVNRT during ablation and allow for monitoring of anterograde AV conduction. However, junctional beats will not be seen during overdrive atrial pacing.

AV block may be due to ablation injury of the compact AV node or may reflect underlying poor fast pathway conduction. AV block occurring at a more inferior position, including within the coronary sinus ostium may occur due to a posterior fast pathway variant or as a result of the effects of ablation on the AV nodal artery.

Ablation Endpoints

Following application of RF with good target temperatures (over 50 °C) and junctional beats a

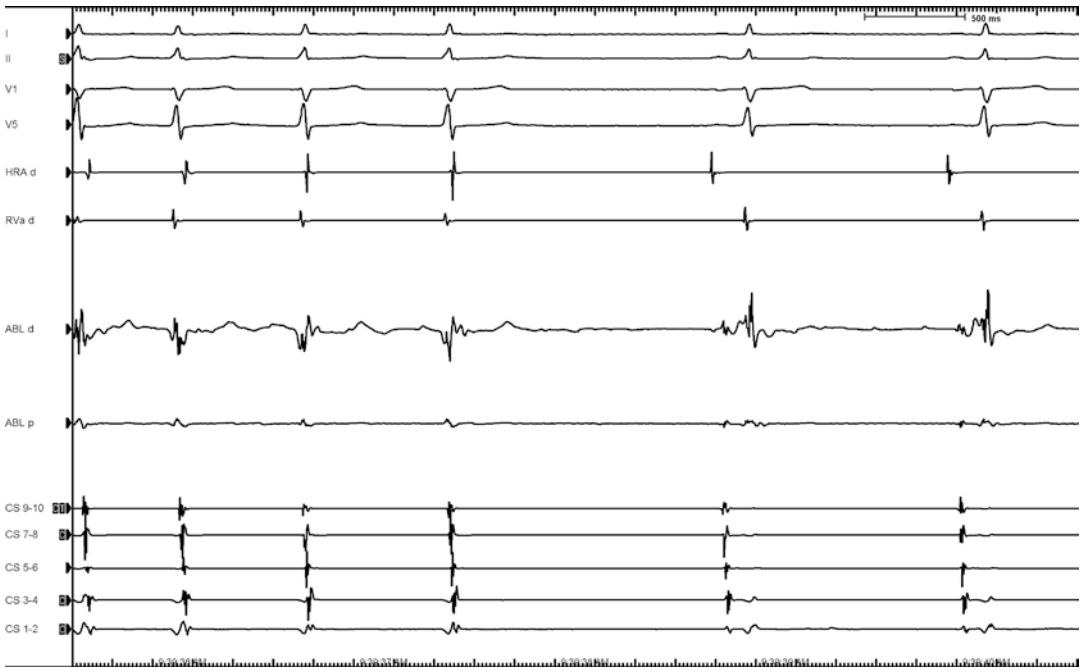

Fig. 4.11 Junctional beats seen during RF ablation at the site of a slow pathway ablation. Following the first 4 beats of junctional rhythm normal sinus rhythm resumes with 1:1 AV conduction. This is generally considered a sign of a successful slow pathway ablation. (HRA-d is positioned at the high right atrium, RVa-d is positioned at the RV apex, CS 9–10 is positioned at the proximal CS while CS 1–2 is positioned at the distal CS; d-distal)

repeat atrial or ventricular stimulation should be performed to try to re-induce the tachycardia using the same induction protocol as pre-ablation. Isoproterenol should be considered even if it was not required for induction pre-ablation. An AH jump is still frequently seen due to the presence of other slow pathways (e.g. Left inferior extension). A single atrial echo beat despite multiple attempts at tachycardia induction is an acceptable endpoint, associated with a low tachycardia recurrence rate.

Troubleshooting the Difficult Cases

The main anatomical difficulties which may arise are often related to a large coronary sinus ostium, difficult to reach slow pathways, close proximity between the slow and fast pathways and variability in the location of the slow pathway.

In general a slight clockwise rotation of the ablation catheter is required when applying RF to the slow pathway. In cases where the CS ostium is large it can be difficult to maintain a stable position. A coronary sinus venogram to fluoroscopically define the coronary sinus ostium may be helpful. A long sheath is helpful in order to maintain catheter stability in most cases (SR0); a long deflectable sheath can also be considered in very difficult cases. Contact-sensing catheters such as the Tacticath (Abbott, St Paul, MN) or Smarttouch (Biosense Webster, Irvine, CA) may also be helpful.

Occasionally ablation at the conventional slow pathway location results in junctional beats but AVNRT continues to be inducible. In these cases a more superior approach is often required. This most likely targets the junction of the right and left inferior extensions rather than just the right inferior extension. If a higher position is unsuccessful the roof of the proximal coronary sinus (1–3 cm from the coronary sinus ostium) targeting the left inferior extension may result in a successful ablation.

In rare cases the slow pathway has a left sided insertion point and therefore cannot be successfully ablated from any sites on the right side of the interatrial septum. For these cases either

transseptal or trans aortic access if required with mapping of the earliest atrial activation during AVNRT along the mitral annulus. This may range from septal to inferolateral mitral annulus. A case of successful ablation of the slow pathway from the inferoseptal process of the left ventricle has also been reported (Green et al. 2016).

Delivering premature atrial beats at different potential slow pathway locations, and evaluating for the site with the latest premature beat that can reset tachycardia, can help identify the responsible slow pathway in a systematic manner (Stavrakis et al. 2018).

Risks of EP Study and RF Ablation of AVNRT

Vascular access injuries include bleeding with hematoma, arterio-venous fistula, aneurysm or pseudo-aneurysm. The risks of catheter manipulation in the heart include cardiac perforation and tamponade and thromboembolism. AV block (requiring a permanent pacemaker) is generally considered to be the most significant complication and has an incidence of approximately 0.5% with radiofrequency (RF) ablation in the slow pathway region (Kesek et al. 2019). AV block is more common if the distance between the slow pathway and fast pathway is small, if a more superior approach (ie at the level of the superior coronary sinus ostium) is required for successful ablation, if more ablation lesions are required and in patients with retrograde block in association with a junctional rhythm. It is therefore important to monitor AV conduction during application of RF and stop if any evidence of AV block. It is generally good practice if the risk of AV block is considered high to stop and reassess risk of the ablation. Cryoablation may be associated with a slightly lower risk of AV block, but has a higher risk of AVNRT recurrence (De Sisti and Tonet 2012). The acute success of a slow pathway RF ablation is approximately 97% with a tachycardia recurrence rate of 0.7–5.2%.

Important Points

1. The triangle of Koch is bounded anteriorly by the septal leaflet of the tricuspid valve, posteriorly by the tendon of Todaro and inferiorly by the superior aspect of the coronary sinus os.
2. The common AV node is located at the apex of the triangle of Koch. The fast pathway is located in the superior portion of the triangle of Koch. The slow pathway is generally located anteriorly to the CS although may have a variable course including within the CS.
3. An AH jump is defined as an increase in the AH interval of greater than or equal to 50 ms in association with a reduction in an atrial extrastimulus interval of 10 ms during decremental atrial pacing. An AH jump indicates the presence of dual AV nodal physiology.
4. An AH jump may not be elicited in all patients with clinical AVNRT.
5. Dual AV nodal physiology is often present in patients without AVNRT.
6. In Slow/Fast AVNRT (typical AVNRT) a PAC travels antegrade down the slow pathway (SP) with retrograde conduction up the fast pathway (FP). This generally results in a short VA tachycardia with the earliest atrial activation along the superior septum posterior to the Tendon of Todaro
7. In Fast/Slow AVNRT (atypical AVNRT) antegrade conduction occurs down the FP and retrograde conduction occurs up the SP with a long VA time during tachycardia.
8. SP ablation is generally performed using a 4 mm non-irrigated ablation catheter positioned between the CS ostium and the tricuspid annulus with an A:V ratio of 1:2 to 1:10. RF is gen-

erally started at 50 W with a maximum temperature set at 55–60 °C.

9. Junctional beats during ablation are most likely due to conduction of current injury from the SP to the AV junctional area enhancing diastolic depolarization of the cells in this region and are generally considered an indicator of SP modification.
10. Junctional tachycardia occurring at a cycle length of less than 500 ms or VA block are an indicator of potential AV block. Ablation should be immediately stopped if these findings are observed, or if there is AH prolongation.
11. The most useful endpoint following SP ablation is lack of inducibility of the tachycardia. The presence of an AH jump and a single atrial echo beat is an acceptable endpoint as these may often be due to other slow pathways which may be clinically insignificant such as a left inferior extension.

References

Boyle NG, Anselme F, Monahan K, et al. Origin of junctional rhythm during radiofrequency ablation of atrioventricular nodal reentrant tachycardia in patients without structural heart disease. Am J Cardiol. 1997;80:575–80.

Chen M-C, Guo GB-F. Junctional tachycardia during radiofrequency a blation of the slow pathway in patients with AV nodal reentrant tachycardia: effects of autonomic blockade. J Cardiovasc Electrophysiol. 1999;10:56–60.

Chen S-A, Chiang C-E, Yang C-J, et al. Accessory pathway and atrioventricular node reentrant tachycardia in elderly patients: clinical features, electrophysiologic characteristics and results of radiofrequency ablation. J Am Coll Cardiol. 1994;23:702–8.

Chua K, Upadhyay GA, Lee E, et al. High-resolution mapping of the triangle of Koch: spatial heterogeneity of fast pathway atrionodal connections. Heart Rhythm. 2018;15:421–9.

Dandamudi G, Mokabberi R, Assal C, et al. A novel approach to differentiating orthodromic reciprocating tachycardia from atrioventricular nodal reentrant tachycardia. Heart Rhythm. 2010;7:1326–9.

De Sisti A, Tonet J. Cryoablation of atrioventricular nodal reentrant tachycardia: a clinical review. Pacing Clin Electrophysiol. 2012;35:233–40.

Duchateau J, Tixier R, Vlachos K, et al. Ventricular-triggered atrial pacing: a new maneuver for slow-fast atrioventricular nodal reentrant tachycardia. Heart Rhythm. 2020;17:955–64.

Estner HL, Ndrepepa G, Dong J, et al. Acute and long-term results of slow pathway ablation in patients with atrioventricular nodal reentrant tachycardia—an analysis of the predictive factors for arrhythmia recurrence. Pacing Clin Electrophysiol. 2005;28:102–10.

González-Torrecilla E, Arenal A, Atienza F, et al. First postpacing interval after tachycardia entrainment with correction for atrioventricular node delay: a simple maneuver for differential diagnosis of atrioventricular nodal reentrant tachycardias versus orthodromic reciprocating tachycardias. Heart Rhythm. 2006;3:674–9.

Green J, Aziz Z, Nayak HM, Upadhyay GA, Moss JD, Tung R, Left ventricular AV. nodal reentrant tachycardia: case report and review of the literature. Heart Rhythm Case Rep. 2016;2:367–71.

Hadid C, Gonzalez S, Almendral J. Atrioventricular nodal reentrant tachycardia: evidence of an upper common pathway in some patients. Heart Rhythm Case Rep. 2018;4:227–31.

Haissaguerre M, Gaita F, Fischer B, et al. Elimination of atrioventricular nodal reentrant tachycardia using discrete slow potentials to guide application of radiofrequency energy. Circulation. 1992;85:2162–75.

Jackman WM, Beckman KJ, McClelland JH, et al. Treatment of supraventricular tachycardia due to atrioventricular nodal reentry by radiofrequency catheter ablation of slow-pathway conduction. N Engl J Med. 1992;327:313–8.

John C, Lauer MR, Young C, Liem LB, Hou C, Sung RJ. Localization of the origin of the atrioventricular junctional rhythm induced during selective ablation of slow-pathway conduction in patients with atrioventricular node reentrant tachycardia. Am Heart J. 1996;131:937–46.

Katritsis DG, Camm AJ. Classification and differential diagnosis of atrioventricular nodal re-entrant tachycardia. Europace. 2006;8:29–36.

Kesek M, Lindmark D, Rashid A, Jensen SM. Increased risk of late pacemaker implantation after ablation for atrioventricular nodal reentry tachycardia: a 10-year follow-up of a nationwide cohort. Heart Rhythm. 2019;16:1182–8.

Knight BP, Zivin A, Souza J, et al. A technique for the rapid diagnosis of atrial tachycardia in the electrophysiology laboratory. J Am Coll Cardiol. 1999;33:775–81.

Knight BP, Ebinger M, Oral H, et al. Diagnostic value of tachycardia features and pacing maneuvers during paroxysmal supraventricular tachycardia. J Am Coll Cardiol. 2000;36:574–82.

Lee M, Morady F, Kadish A, et al. Catheter modification of the atrioventricular junction with radiofrequency energy for control of atrioventricular nodal reentry tachycardia. Circulation. 1991;83:827–35.

Li HG, Klein GJ, Stites HW, et al. Elimination of slow pathway conduction: an accurate indicator of clinical success after radiofrequency atrioventricular node modification. J Am Coll Cardiol. 1993;22: 1849–53.

Man KC, Niebauer M, Daoud E, et al. Comparison of atrial-His intervals during tachycardia and atrial pacing in patients with long RP tachycardia. J Cardiovasc Electrophysiol. 1995;6:700–10.

Maruyama M, Kobayashi Y, Miyauchi Y, et al. The VA relationship after differential atrial overdrive pacing: a novel tool for the diagnosis of atrial tachycardia in the electrophysiologic laboratory. J Cardiovasc Electrophysiol. 2007;18:1127–33.

Michaud GF, Tada H, Chough S, et al. Differentiation of atypical atrioventricular node re-entrant tachycardia from orthodromic reciprocating tachycardia using a septal accessory pathway by the response to ventricular pacing. J Am Coll Cardiol. 2001;38:1163–7.

Nakagawa H, Jackman WM. Catheter ablation of paroxysmal supraventricular tachycardia. Circulation. 2007;116:2465–78.

Stavrakis S, Jackman WM, Lockwood D, et al. Slow/fast atrioventricular nodal reentrant tachycardia using the inferolateral left atrial slow pathway. Circulation. 2018;11:e006631.

Thibault B, de Bakker JM, Hocini M, Loh P, Wittkampf FH, Janse MJ. Origin of heat-induced accelerated junctional rhythm. J Cardiovasc Electrophysiol. 1998;9:631–41.

Zardini M, Leitch JW, Guiraudon GM, Klein GJ, Yee R. Atrioventricular nodal reentry and dual atrioventricular node physiology in patients undergoing accessory pathway ablation. Am J Cardiol. 1990;66:1388–9.

5 Accessory Pathway (AP) Conduction

Jacob Larsen, Jason Andrade, Benedict M. Glover, and Pedro Brugada

Abstract

Ventricular pre-excitation occurs as a result of an extranodal accessory pathway connecting the atrium with the ventricle along the AV groove. Although the baseline ECG may be normal, the common features seen are a slurring of the initial portion of the QRS complex resulting in a delta wave, a short PR interval during normal sinus rhythm, a wide QRS duration, and secondary ST and T wave changes, all of which result from a combination of eccentric accessory pathway and midline AV nodal conduction. Ventricular pre-excitation in association with a history of palpitations is named the Wolff–Parkinson–White (WPW) syndrome.

J. Larsen
Department of Cardiology, Aalborg University Hospital, Aalborg, Denmark
e-mail: jacl@regionsjaelland.dk

J. Andrade (✉)
Division of Cardiology, University of British Columbia, Vancouver, BC, Canada

B. M. Glover
Division of Cardiology, Department of Medicine, University of Toronto, Toronto, Ontario, Canada

P. Brugada
University Hospital of Brussel, Brussels, Belgium
e-mail: pedro@brugada.org

Anatomy

Accessory pathways are muscle fibers which connect the atrium to the ventricle through the fibrofatty and fibrous parietal AV junctional regions. They are generally up to 3 mm in diameter and up to 1 cm in length (Becker et al. 1978).

They are generally not found in the aortomitral continuity due to the distance between the atrial and ventricular tissues in this region (Ho 2008). It has been shown that the majority of accessory pathways contain ventricular myocytes which function in a similar fashion (Peters et al. 1994).

Thin extensions of atrial myocardium overlie thicker ventricular myocardium at the right anterior, mid, and posterior septum. The left anterior and left mid septal regions tend to have fibrotic tissue and therefore it is unusual to find AP's in this location.

The majority of accessory pathways are located within the endocardial atrioventricular fat pad close to the atrioventricular junctions. The anatomy of the tricuspid and the mitral annuli is shown in Fig. 5.1 with the superimposed traditional locations of AP's.

The traditional description of accessory pathway locations has been dependent on a combination of anterior to posterior and left to right in which the coronary sinus is the most posterior landmark and the aortic valve the most anterior. In the LAO view posterior is therefore seen as

B. M. Glover, P. Brugada (eds.), *Clinical Handbook of Cardiac Electrophysiology*,
https://doi.org/10.1007/978-3-030-74319-2_5

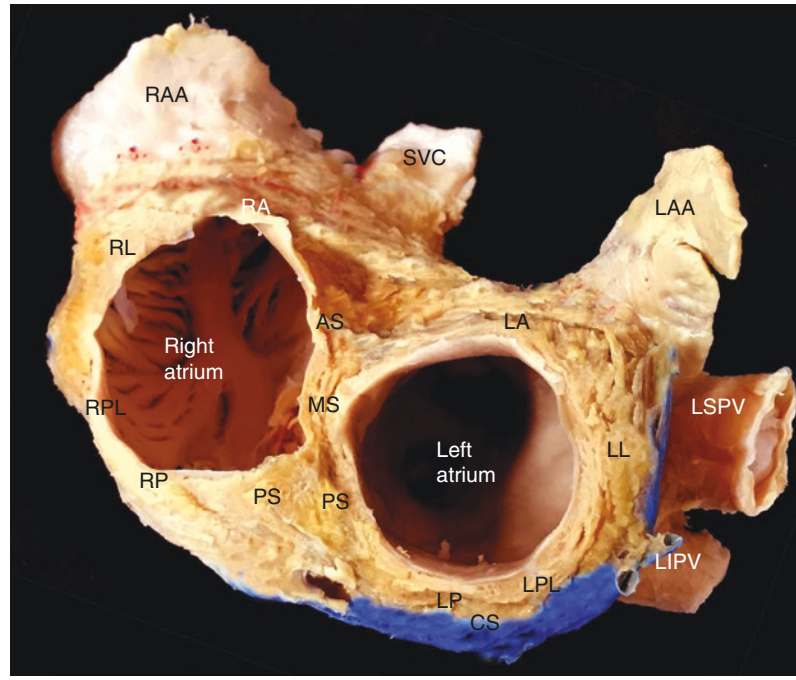

Fig. 5.1 Anatomical locations of the majority of accessory pathways around the annulus of the right atrium and left atrium (*PS* posteroseptal, *MS* midseptal, *AS* anteroseptal, *RA* right anterior, *RL* right lateral, *RPL* right posterolateral, *RP* right posterior, *LP* left posterior, *LPL* left posterolateral, *LL* left lateral, *LA* left anterior, *RAA* right atrial appendage, *LAA* left atrial appendage, *SVC* superior vena cava, *CS* coronary sinus, *LSPV* left superior pulmonary vein, *LIPV* left inferior pulmonary vein)

being at the most inferior location along both the mitral and tricuspid annulus while anterior is located at the most superior aspect. In this view the septum is in the centre of the image with lateral being located at the peripheries. In reality what is described as anterior is actually superior. As the left atrium lies posterior to the right atrium what is described as right lateral should be described as right anterior and left lateral should be described as left posterior. This is shown in Fig. 5.2.

Less common accessory pathway locations are shown in Fig. 5.3.

Mechanisms

During normal sinus rhythm, conduction may occur antegrade down the AP as well as through the AV node, resulting in **manifest pre-excitation** on the ECG. Occasionally, this may not be evident if the ventricle has depolarized through the AV node prior to the conclusion of conduction through the accessory pathway, such as in a slowly conducting left lateral accessory pathway. This is called **latent pre-excitation** as the 12-lead ECG during normal sinus rhythm may appear normal. If the AP exclusively conducts retrogradely during normal sinus rhythm the ECG will also appear normal and this is called a **concealed accessory pathway.** Concealed accessory pathways are generally considered to be lower risk of sudden death as they are not capable of conducting rapid AF. The majority of accessory pathways have antegrade and retrograde properties. Diagrammatic representation of the predominant direction of conduction of accessory pathways is shown in Fig. 5.4.

Orthodromic AVRT occurs when the antegrade accessory pathway is refractory and conduction occurs *antegradely* through the AV node activating the His and ventricle and *retrogradely* along the accessory pathway. This is shown in Fig. 5.5. The VA time required for this to occur is generally greater than 70 ms. Despite slight changes in antegrade conduction via the AV node the VA time which represents the time taken to conduction along the accessory pathway is generally stable and does not change.

In antidromic AVRT conduction occurs when the AV node is refractory, facilitating *antegrade conduction* via the accessory pathway and *retrograde* atrial activation via the His and AV node. This is generally associated with a pre-excitated

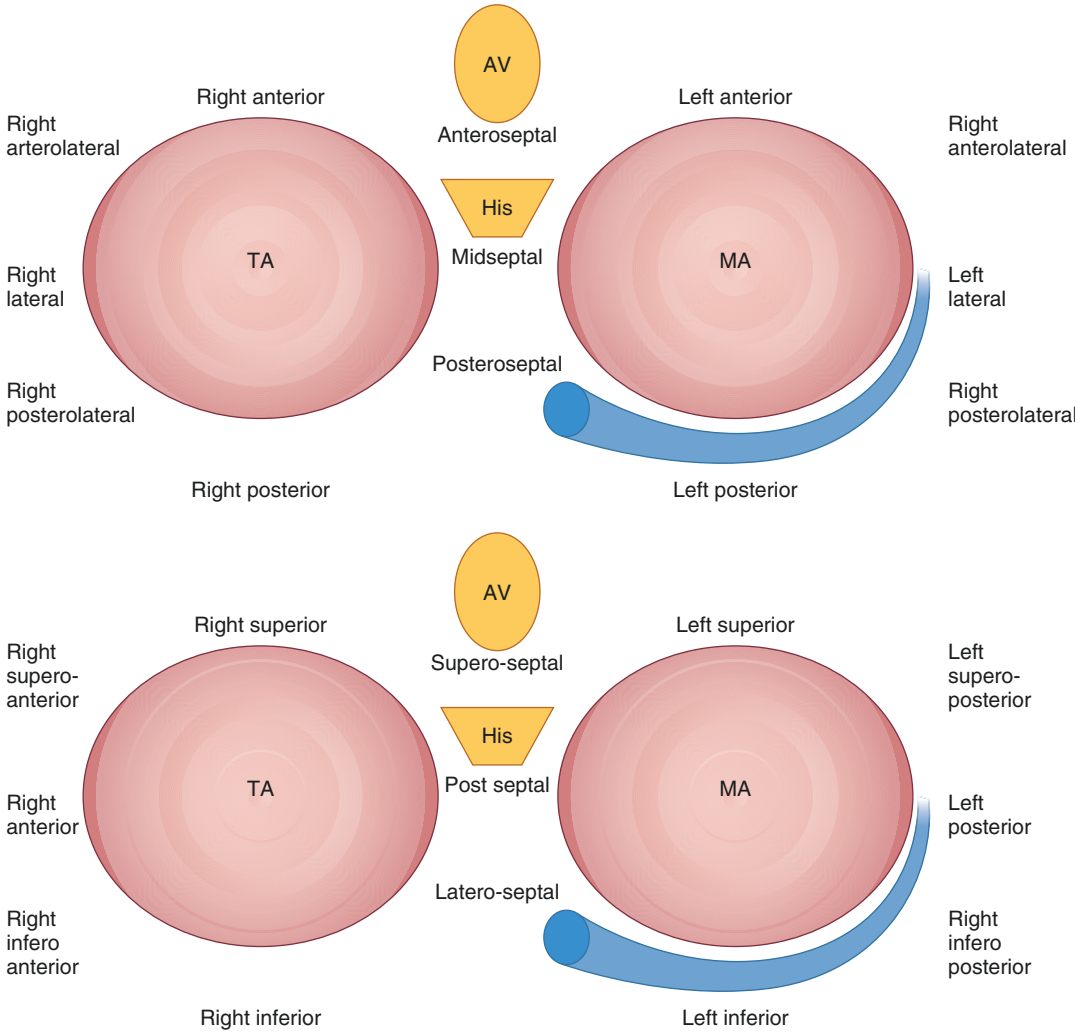

Fig. 5.2 Schematic in LAO view showing the historic (top) and attitudinally correct (bottom) locations of Accessory Pathways along the Tricuspid and Mitral Annulus (*TA* tricuspid annulus, *MA* mitral annulus, *AV* atrioventricular)

QRS as ventricular activation only occurs via the accessory pathway. HA times are generally greater than 70 ms as conduction is via the VA node. This is more commonly seen in left lateral accessory pathways as the longer conduction is required to allow the AV node to recover.

Classification

Accessory pathways are classified according to their anatomical location, direction of conduction, conduction properties and mechanism of action during tachycardia.

Anatomically these are divided into septal, left-sided, and right-sided pathways. The septal pathways can be sub-classified as posteroseptal, midseptal and anteroseptal; and the left-/right-sided pathways can be sub-classified as posterior, posterolateral, lateral, anterolateral, and anterior.

Some accessory pathways may be located in unusual anatomical locations, involving epicardial connections between the coronary sinus and the left ventricle, the non-coronary cusp of the aortic valve to the left ventricle, the right atrial appendage to right ventricle, or left atrial appendage to left ventricle. Additionally, some accessory pathways may be directly connected into the

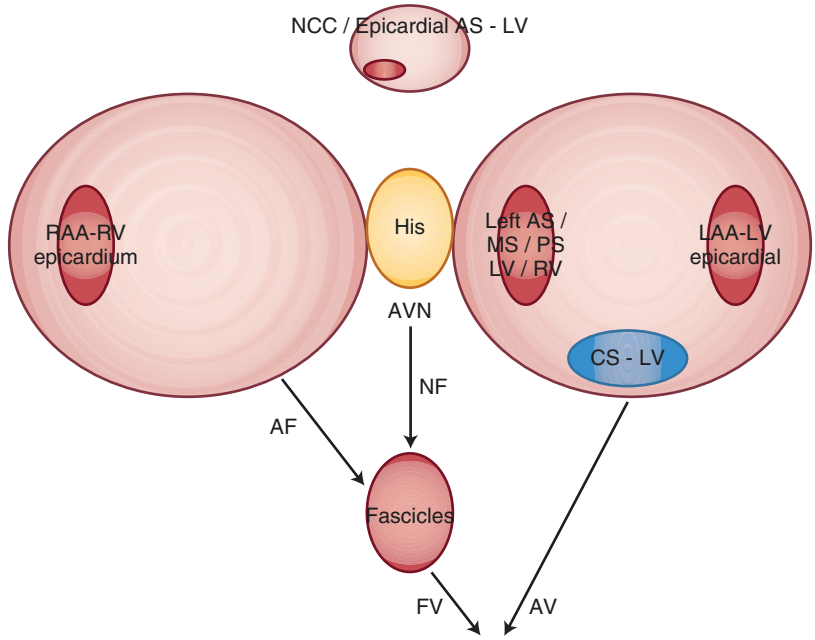

Fig. 5.3 Unusual Locations of Accessory Pathway connections including right atrial appendage (RAA) to right ventricular (RV) epicardium, the non coronary cusp (NCC)/epicardial anteroseptal to left ventricle (LV), left sided anteroseptal, midseptal and posteroseptal to left ventricle or right ventricle, left atrial appendage (LAA) to left ventricular (LV) epicardium, coronary sinus (CS) to left ventricle (LV) as well as atriofascicular (AF), nodofascicular (NF), atrioventricular (AV) and fasciculoventricular (FV) pathways

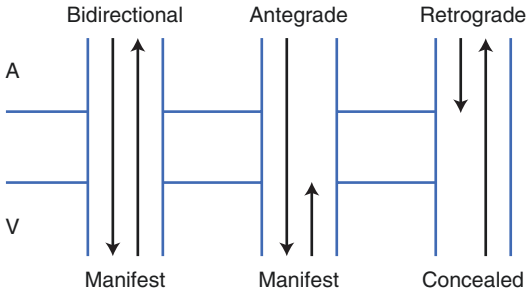

Fig. 5.4 Direction of Conduction in Accessory Pathways. Bidirectional (antegrade and retrograde) resulting in manifest pre-excitation, antegrade only resulting in manifest pre-excitation and retrograde only resulting in concealed conduction

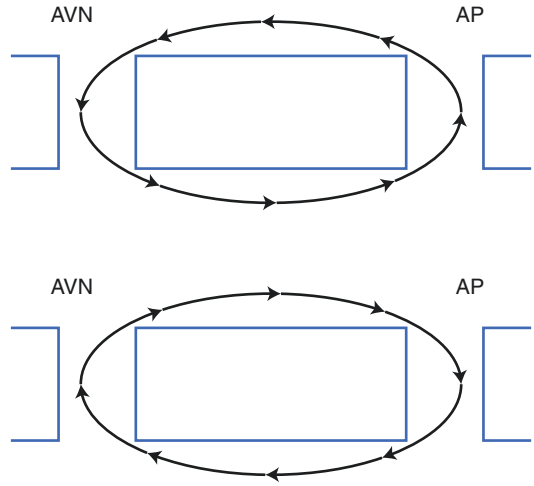

Fig. 5.5 Mode of conduction of circuit in AVRT. Orthodromic Reciprocating Tachycardia (Top image) in which antegrade conduction occurs through the AV node and retrograde through the accessory pathway and Antidromic Reciprocating Tachycardia (Bottom image) in which antegrade conduction occurs down the accessory pathway and retrograde through the AV node

specialized conduction system such as atriofascicular, nodofascicular, and fasciculoventricular pathways.

Accessory pathways can also be described according to the direction of conduction (e.g. anterograde, retrograde, or bidirectional—see

above), or their conduction properties. With respect to the latter, almost all accessory pathways exhibit rapid non-decremental conduction, however a few paraseptal pathways may exhibit slow or decremental conduction properties similar to the AV node.

Electrophysiological Evaluation

Baseline ECG

The location of the accessory pathway can be estimated from the ECG based on the polarity of the delta wave. Localization of the accessory pathway on the 12 lead ECG is useful in order to risk stratify patients, and can help plan the EP study and ablation.

Algorithms

Several algorithms have been developed to help predict the location of the accessory pathway based on the 12 lead ECG during normal sinus rhythm. These generally use the axis of the delta wave, the R wave transition, and the QRS morphology. These features are dependent on the ventricular insertion point of the accessory pathway and may be altered by the degree of fusion between the accessory pathway conduction and the AV node conduction.

Unfortunately, no algorithm is 100% accurate given anatomical variability, as well as differences in underlying ECG patterns, the possibility of more than one accessory pathway, and variability in the conduction properties of the AV node.

An example of a useful and practical algorithm for accessory pathway localization is shown in Fig. 5.6.

The polarity of the delta wave is best measured 20 ms after the initial onset and is described as either positive, negative or isoelectric.

In general, a negative or isoelectric delta wave in certain ECG leads implies that the ventricular activation is originating from that location.

Assess the polarity of the delta wave on the surface QRS. Initially look at V1 if positive then more likely left sided than right sided. If this is the case then look at leads I and aVL. If the delta wave is positive in these leads then the AP is either septal or left posterior. To differentiate assess lead III. If the delta wave is positive in lead III then this is likely to be septal. If the delta wave os negative in lead III then the AP is more likely to be left posterior. If the delta wave is negative in V1 then the AP is more likely to be right sided. To assess the location within the septum the inferior leads (II, III and aVF) can be assessed. If the delta wave is positive in these leads the AP is more likely to be anteroseptal or midseptal. If this is negative then the AP is more likely to be posteroseptal (AS anteroseptal, MS midseptal, PS posteroseptal).

ECG Features of Posteroseptal Accessory Pathways

The delta wave in posteroseptal accessory pathways is generally negative in III, with a smaller R than S wave in lead II and an R:S ratio in V2 greater than 1 (Fig. 5.7). The majority of posteroseptal accessory pathways have negative P waves in the inferior leads during tachycardia.

The majority of posteroseptal pathways can be ablated from the right side. It is important to try to differentiate right sided and left sided posteroseptal accessory pathways. Although this is difficult to conclude from an ECG it has been suggested that a negative delta wave in V1 may favor a right sided AP while a positive delta wave in V1 maybe more suggestive of a left sided AP (Haissaguerre et al. 1994). An R wave greater than S wave in V1 is suggestive of a left sided accessory pathway as is a narrower QRS in V1. A positive delta wave in II with a negative delta wave in III is also more suggestive of a right sided posteroseptal accessory pathway (Fig. 5.8).

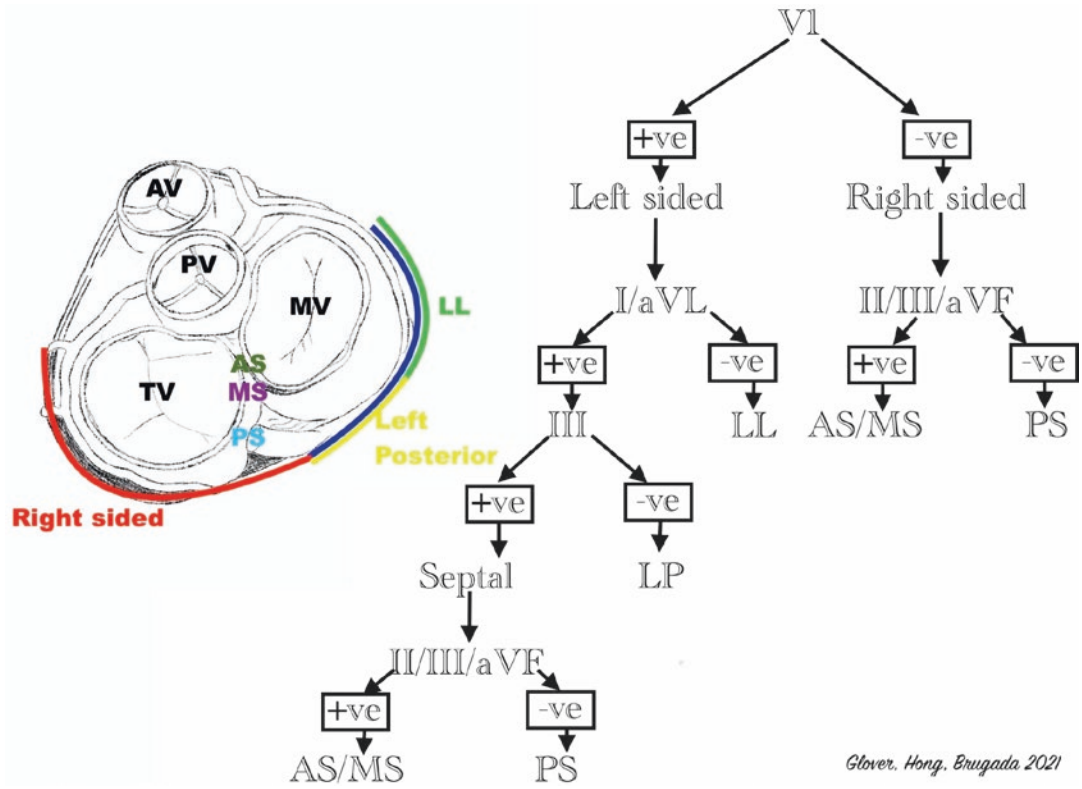

Fig. 5.6 Algorithm to determine the location of an accessory pathway (Glover, Hong, Brugada 2021). Assess the polarity of the delta wave on the surface QRS. Initially look at V1 if positive then more likely left sided than right sided. If this is the case then look at leads I and aVL. If the delta wave is positive in these leads then the AP is either septal or left posterior. To differentiate assess lead III. If the delta wave is positive in lead III then this is likely to be septal. If the delta wave os negative in lead III then the AP is more likely to be left posterior. If the delta wave is negative in V1 then the AP is more likely to be right sided. To assess the location within the septum the inferior leads (II, III and aVF) can be assessed. If the delta wave is positive in these leads the AP is more likely to be anteroseptal or midseptal. If this is negative then the AP is more likely to be posteroseptal (AS anteroseptal, MS midseptal, PS posteroseptal)

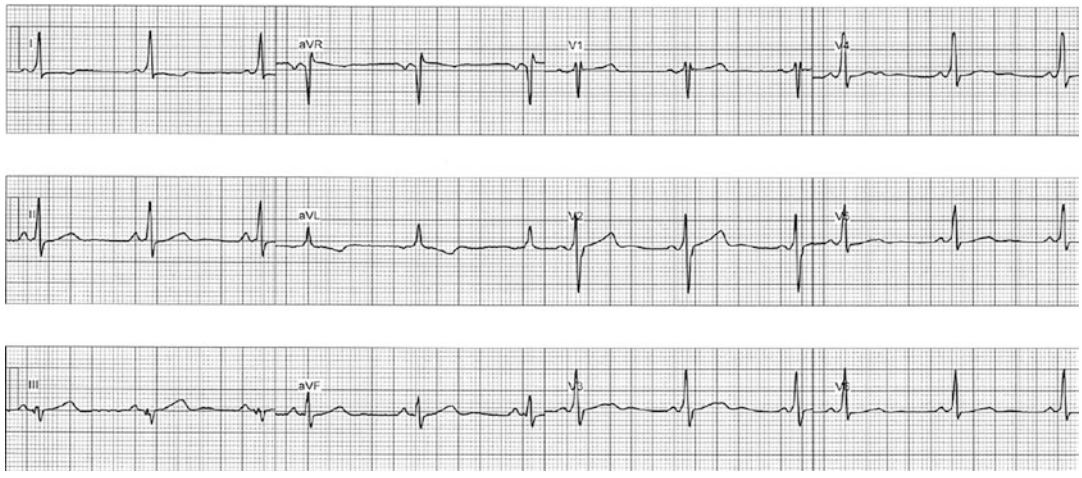

Fig. 5.7 ECG of Posteroseptal Accessory Pathway. There is a negative delta wave in lead III. Although the positive delta in V1 is suggestive of a left sided location the fact that the R wave in V1 is less than the S wave and the positive delta wave in lead II with a negative delta in lead III are more suggestive of a right sided posteroseptal pathway

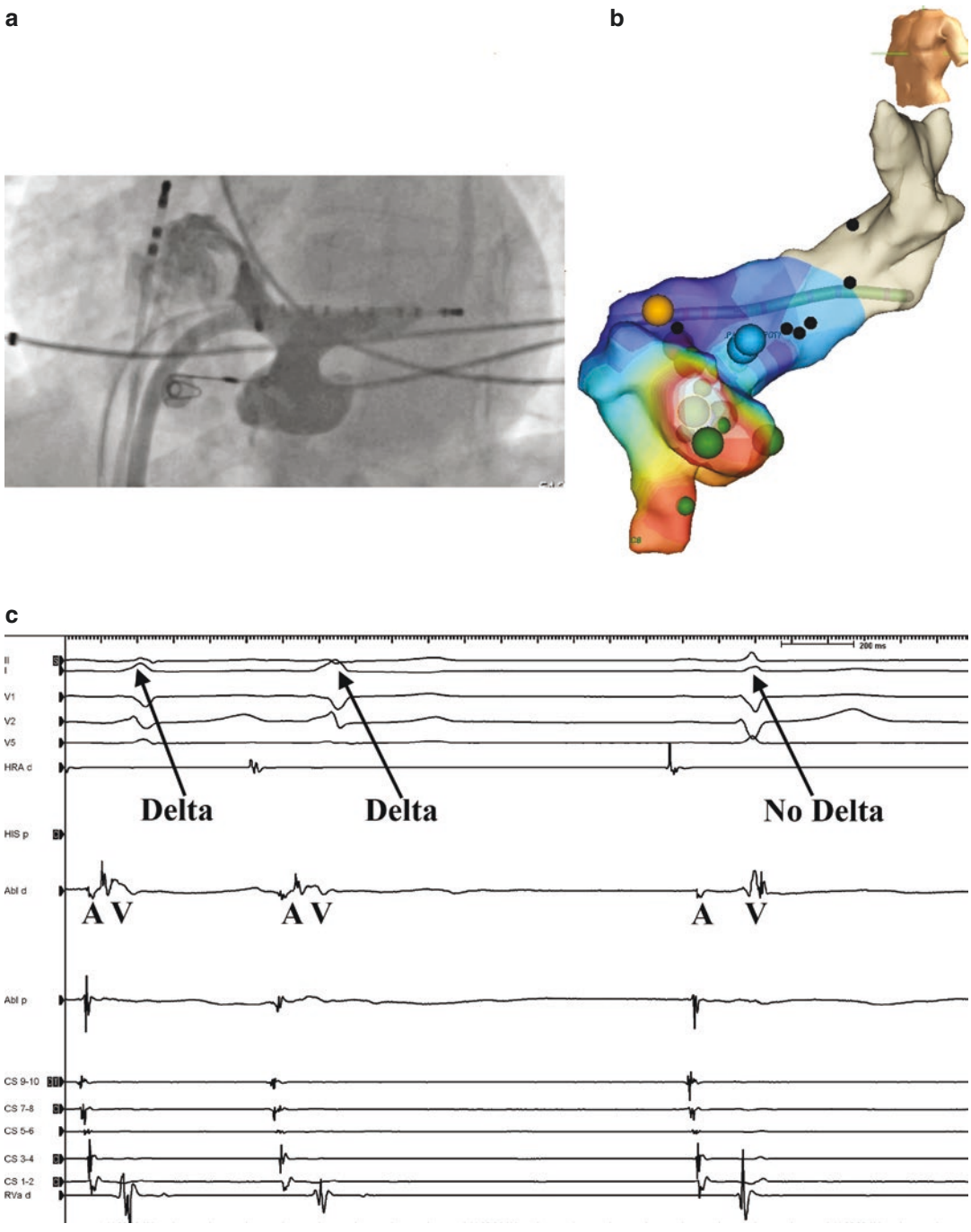

Fig. 5.8 Venogram and map of an accesory pathway in a coronary sinus diverticulum

ECG Features of Anteroseptal Accessory Pathways

Given that anteroseptal accessory pathways connect from the RA to the RV paraseptal region the delta waves are positive in the inferior leads II, III and aVF as well as the lateral leads I, aVL and V3–V6. An example of an ECG in a patient with an anteroseptal accessory pathway is shown in Fig. 5.9.

ECG Features of Mid-Septal Accessory Pathways

There is a greater degree of variability in the ECG patterns of mid-septal accessory pathways reflecting the variability in the atrial and ventricular insertion points and course within this region. In general, there are positive delta waves in lead II as well as in the lateral leads with an earlier precordial transition from V2 to V6. Unlike anteroseptal accessory pathways the delta wave is negative in lead III.

ECG Features of Left Lateral Accessory Pathways

The most important ECG feature of a left lateral accessory pathway is a negative delta wave in leads I, aVL and V6. Additionally, the delta wave in V1 is positive with an R wave greater than S wave in V1. More posterior left lateral accessory pathways are negative in the inferior leads. Anterior accessory pathways are positive in the inferior leads. A negative P wave in lead I during tachycardia is a feature of an ORT involving a left lateral accessory pathway (Fig. 5.10).

ECG Features of Right Free Wall Accessory Pathways

It can be difficult to differentiate right free wall accessory pathways from other accessory pathways. This is because a positive delta wave in V1 may also occur in left lateral accessory pathways. In order to differentiate these, the R wave in V1 should be less than the S wave with a late precordial transition. The delta wave is usually positive in the lateral leads I and aVL. The presence of a positive p wave in lead I during tachycardia is suggestive of a right free wall accessory pathway. An example of pre-excitation in a patient with a right free wall accessory pathway is seen in Fig. 5.11.

Risk Stratification of Accessory Pathways

Accessory pathways are associated with 0.05–0.1% annual risk of sudden death. This risk is

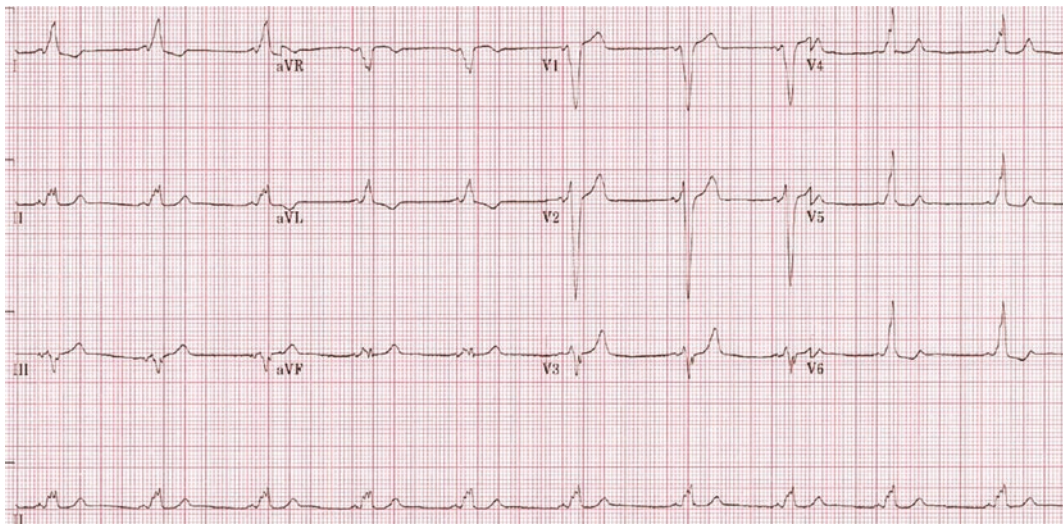

Fig. 5.9 ECG of Anteroseptal Accessory Pathway. There is a LBBB type pattern. The delta wave is positive in lead I and the lateral precordial leads as well as leads II and aVF

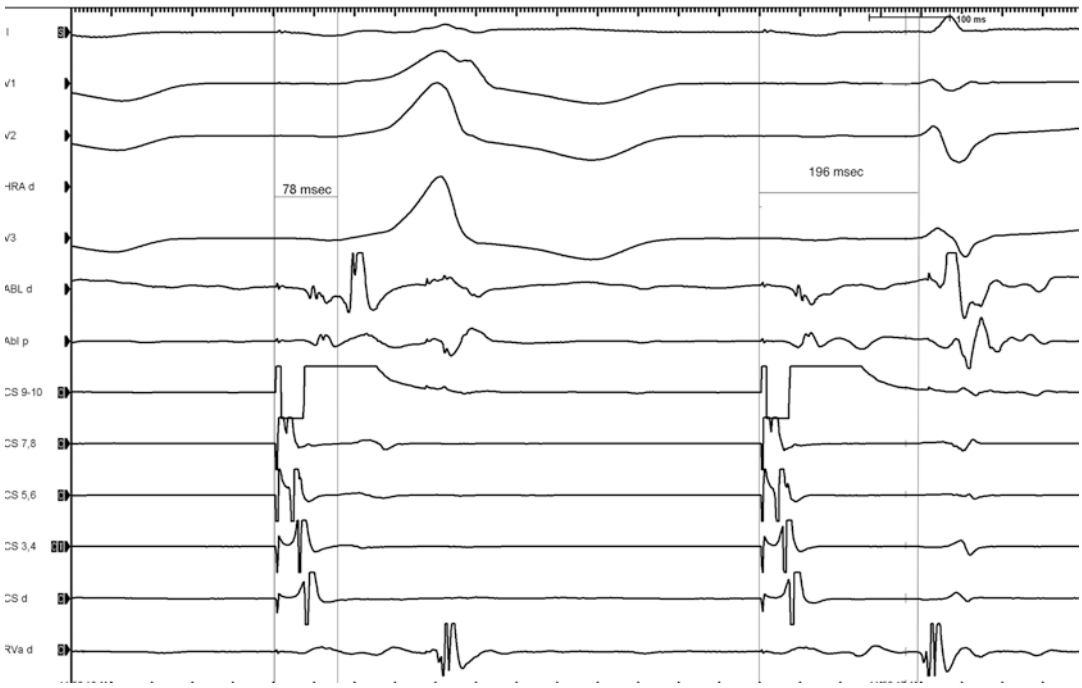

Fig. 5.10 ECG and intracardiac electrograms of ablation being performed for a left anterolateral accessory pathway. The first beat is pre-excited with a positive delta and R wave in lead V1 and a positive delta wave in lead II. Coronary sinus activation is from proximal to distal as a result of atrial pacing with ventricular activation earliest in the distal coronary sinus. There is a short AV interval at the site of the ablation catheter. The second beat shows loss of pre-excitation with RF ablation. The surface ECG normalizes with AV prolongation and although the atrial activation in the CS is the same, the ventricular activation is proximal to distal implying activation through the AV node. The atrial stimulation to surface QRS is measured and is prolonged from the pre-excited beat at 78–196 ms during normal AV conduction. (CS 9–10 is positioned in the proximal CS while CS 1–2 is located in the distal CS, RVa d is located in the RV apex)

Fig. 5.11 ECG of right lateral accessory pathway. There is a large S wave in lead V1 with a small R wave. Precordial transition occurs in lead V3. There is a positive delta wave in leads I, aVL and the lateral precordial leads

inversely proportional to the anterograde refractory period of the accessory pathway. The risk is due to the incidence of rapid antegrade conduction during AF with subsequent risk of ventricular fibrillation. This risk is independent of whether the pathway is manifest or latent.

Risk stratification can be performed using an exercise stress test and Holter monitoring. The presence of intermittent pre-excitation on Holter monitor, or a*brupt loss of preexcitation* on stress testing, suggests that rapid antegrade conduction of atrial fibrillation through the AP is less likely to occur.

High risk features include: (1) An anterograde Accessory Pathway Effective Refractory Period (APERP) of ≤250 ms, (2) Shortest pre-excited RR Interval during AF (SPERRI) ≤250 ms, (3) History of symptomatic AVRT (or inducible AVRT at EP study, (4) The presence of multiple accessory pathways, (5) A mid-septal or right-sided pathway location, (6) WPW associated with Ebstein's anomaly, and (6) Male sex.

Risks of EP Study and Ablation

The most common complication is that of groin haematoma and vascular injury in approximately 1.4% (PACES/HRS 2012), particularly if a transaortic retrograde approach is used. The risk of thrombo-embolism is 0.6–0.8% (Epstein et al. 1996), which could result in a cardio-embolic stroke or TIA if the systemic circulation is accessed transaortic or transseptal.

The risk of AV block is highest for septal pathways and virtually zero for left lateral accessory pathways.

Ablation within the coronary sinus may result in coronary stenosis or spasm. The incidence of coronary artery injury is 0.06–0.1% in adults. This generally occurs acutely or shortly after an ablation. Delayed coronary injury may present weeks later as coronary thrombosis secondary to intimal hyperplasia.

The overall success rate for ablation is approximately 85–95%. The success is highest for a left lateral AP (>95% success) and lowest for a posteroseptal accessory pathway (85–95%).

Diagnostic EP Study

A quadripolar catheter is positioned in the HRA, a quadripolar catheter is positioned in the His bundle region, a quadripolar catheter is positioned in the RV apex, and a decapolar catheter in the coronary sinus. In cases of manifest pre-excitation baseline measurements show a **HV interval that is less than 35 ms,** which may even be negative. In order to calculate the accessory pathway ERP an atrial extrastimulus testing is performed. As the S2 is reduced the AH interval prolongs however the HV interval shortens so that the AV interval is unchanged provided that there is still antegrade accessory pathway conduction. The **antegrade accessory pathway ERP** is defined as the maximum atrial cycle length which results in lack of conduction along the accessory pathway. In the presence of residual conduction along the AVN the loss of pre-excitation will demonstrate normalization of the AH and HV intervals. Figure 5.12 demonstrates loss of pre-excitation with decremental atrial pacing and prolongation of the AV interval as antegrade conduction moves from a combination of AV node and accessory pathway to AV node only. If AV conduction is lost with no normalization of the QRS then the AVNRP is noted to be less than or equal to the APERP.

Atrial pacing should be performed from both the catheter in the right atrial appendage and the distal coronary sinus as pre-excitation may be more evident depending on the relative timing of AP and AVN activation. Additionally, there will be a change in the morphology of the QRS or direction of ventricular activation if more than one accessory pathway is present.

Ventricular pacing will reveal the predominant retrograde atrial activation sequence. This may help to localize the accessory pathway. Retrograde accessory pathway ERP should be noted with incremental ventricular pacing.

Following assessment of AP properties, attempts should be made to induce AVRT. During decremental atrial pacing antegrade block of the accessory pathway may occur. Antegrade conduction through the AV node activates the ventricle, which may conduct retrogradely up the

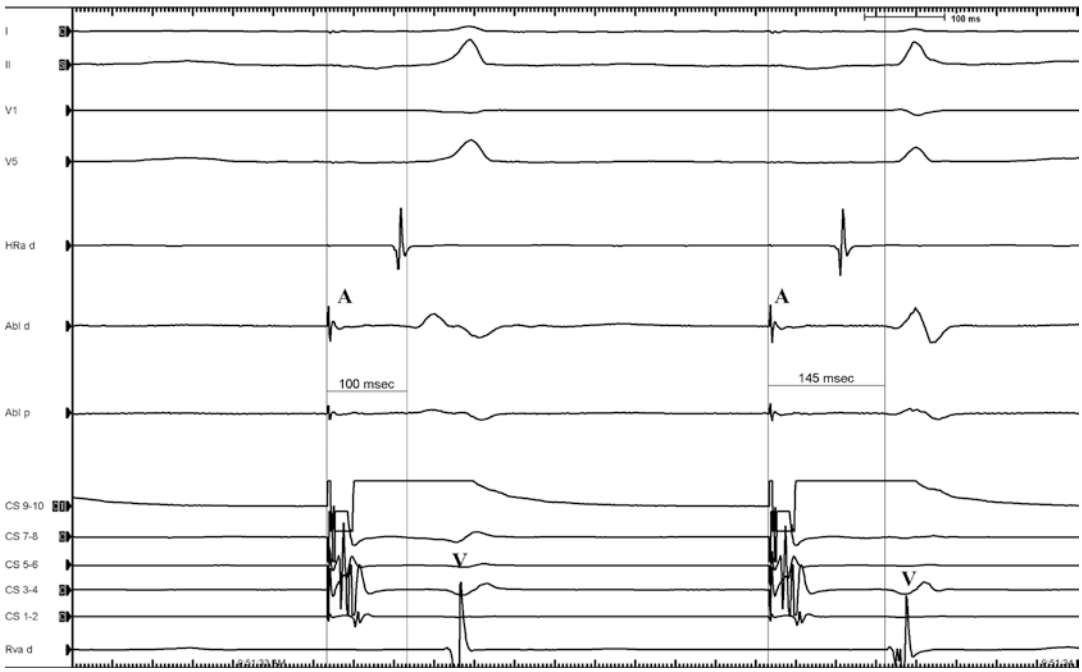

Fig. 5.12 Effective refractory period of the accessory pathway. Decremental pacing from the proximal coronary sinus shows that the first beat is pre-excited with an AV interval of 100 ms. The following beat shows a normal narrow QRS complex with a longer AV interval of 145. At this point antegrade conduction is through the AV node and the accessory pathway is refractory at a cycle length of 480 ms

accessory pathway if it is no longer refractory. This may conduct antegrade through the AV node if it is no longer refractory, resulting in orthrodromic AVRT. Less commonly, the AV node may become refractory, facilitating antegrade conduction down the accessory pathway with retrograde conduction through the AV node. This would result in an antidromic AVRT.

Differentiation Between AVRT, AVNRT and AT

Ventricular pacing during sinus rhythm may be useful in order to assess for decrement versus conduction. However, this is not foolproof as some accessory pathways have decremental conduction properties. Para-Hisian pacing may be performed during normal sinus rhythm in order to differentiate between retrograde nodal conduction and retrograde septal accessory pathway conduction.

If a tachycardia can be induced, a His refractory PVC may be introduced in order to assess if this has any effect on the atrial activation or the tachycardia cycle. A His refractory PVC which advances or delays the next atrial depolarization without changing the activation sequence is suggestive of AVRT. A His refractory PVC which terminates the tachycardia without atrial activation is indicative of AVRT. A very premature PVC that advances the next atrial depolarization only by advancing the local His suggests the mechanism is AVNRT.

RV entrainment can be used to differentiate AVRT from atypical AVNRT and AT. With AT, ventricular overdrive pacing will suppress the AT, thus the last paced beat is conducted to the atria (A EGM) followed by resumption of the first beat of tachycardia (A EGM) which then conducts back to the ventricle via the AV node (V-A-A-V Response). With AVNRT the last entrained ventricular beat is conducted back to the atria (A EGM) by the fast pathway of the AV

Fig. 5.13 Atrial activation is earliest on the proximal coronary sinus followed by the distal ablation (positioned on the His). The tachycardia cycle length is 279 ms. Entrainment is performed from the RV apex at 250 ms. The post pacing interval is 323 ms. The PPI—TCl is therefore 44 ms which is indicative of an AVRT rather than an AVNRT (HRA p is positioned in the high right atrium, the ablation catheter is positioned in the location of the His, CS 9–10 is located at the proximal CS while CS 1–2 is located in the distal CS and RVa d is located in the RV apex)

node, and then back down to the ventricle via the slow pathway (V-A-V Response). However, the time from the last pacing stimulus to the next ventricular electrogram on the RV catheter (PPI—TCL) is more than 115 ms (Fig. 5.13). With AVRT the last entrained ventricular beat (V EGM) is conducted back to the atria (A EGM) by the accessory pathway and then back down to the ventricle via the AV node (V EGM; V-A-V Response). In this case the PPI—TCL is short (>115 ms) but can be longer with decremental conducting AP or when pacing the V far from the AP e.g. left lateral AP.

Mapping the Accessory Pathway

If an accessory pathway is perpendicular to the AV groove then mapping can be performed by localizing the earliest atrial signal during ventricular pacing or mapping the earliest ventricular signal during sinus rhythm or atrial pacing.

When mapping along the annulus an atrial and ventricular signal are evident. When the catheter is positioned at the location of the accessory pathway then the atrial and the ventricular signals are close together and often merged.

Of note, the shortest AV or VA interval is not always the perfect location for ablation. This is due to the observation that a significant percentage of accessory pathways have an oblique course. In this case the ideal electrogram may also contain an accessory pathway potential between the A and V electrograms.

Ventricular and atrial extrastimuli can be delivered to check whether the potential is an accessory pathway potential. During mapping of an accessory pathway during antegrade conduction a late ventricular extrastimuli will advance the ventricular electrogram with no effect on the

accessory pathway potential. An early ventricular extrastimuli will advance the accessory pathway potential with no effect on the local atrial electrogram. For mapping of the accessory pathway with retrograde conduction a late atrial extrastimuli will advance the atrial electrogram with no effect on the accessory pathway potential while an early atrial extrastimuli will advance the accessory pathway potential with no effect on the atrial electrogram.

An accessory pathway potential may be mapped in 89% of all cases provided appropriate pacing maneuvers are performed in order to separate out the signals (Otomo et al. 2001). In order to separate out the local atrial and ventricular signals and expose the accessory pathway potential, pacing can be performed from two different locations in either the atrium or the ventricle. A difference in the local AV interval of greater than or equal to 15 ms without moving the mapping catheter when pacing from two different sites implies an oblique accessory pathway. In order to perform this from the atrium, pacing can be performed from the right atrial appendage and the distal coronary sinus. The locations of pacing from the ventricular aspect depends on the location of the accessory pathway.

For left lateral, anterolateral, posteroseptal and RV free wall accessory pathways, a counterclockwise activation is achieved from pacing from the inferobasal RV while in anteroseptal and right anterior septal accessory pathways counterclockwise activation is achieved by pacing from the parahisian location.

As shown in Fig. 5.14 pacing from lateral to medial in a concurrent direction to the direction of the accessory pathway prolongs the local VA time and therefore exposes the accessory pathway potential. Targeting this region where a potential can be recorded results in a successful ablation of the accessory pathway.

Clockwise activation for left lateral and anterolateral accessory pathways is achieved by pacing from the RVOT. For posteroseptal accessory pathways, clockwise activation is achieved by pacing from a lateral coronary vein with ventricular capture. For right free wall accessory pathways clockwise activation is achieved by pacing from the base of the RV septum while for anteroseptal and right anterior septal accessory pathways clockwise activation is achieved by pacing from the basal anterolateral RV free wall. The optimal ablation location is around the middle of this oblique pathway. In order to separate these potentials pacing can be performed in the opposite direction to course of the accessory pathway (Nakagawa and Jackman 2007).

Occasionally mapping has to be performed during tachycardia. This is frequently the case during mapping of an ORT with unreliable VA conduction during RV pacing. Ablation can be performed during tachycardia looking for the shortest VA interval (Fig. 5.15). If ablation is performed during tachycardia the catheter often falls off the annulus on termination of tachycardia. In order to maintain catheter stability on termination of tachycardia either ventricular pacing can be performed at a faster rate to avoid an abrupt change in the rate and loss of catheter position or further ablation can be performed in the anatomic region during sinus rhythm.

Accessory pathway potentials may be recorded on a unipolar or bipolar electrogram. Both of these can be recorded at the same time, but the sharp unipolar signal is more accurate as it reflects the distal pole of the ablation catheter where RF is delivered.

Ablation of Accessory Pathways

Posteroseptal Accessory Pathways

These are located between the inferior wall of the right atrium and the superoposterior aspect of the left ventricle (Jazayeri et al. 1995). The left border of this region is the left posterior paraseptal region, the right border the right posterior paraseptal region and the anterior and superior border the midseptum.

Local electrograms in this region tend to show a small atrial signal with a large ventricular signal. This occurs as the thin atrial myocardium in this region overlies the thicker ventricular myocardium.

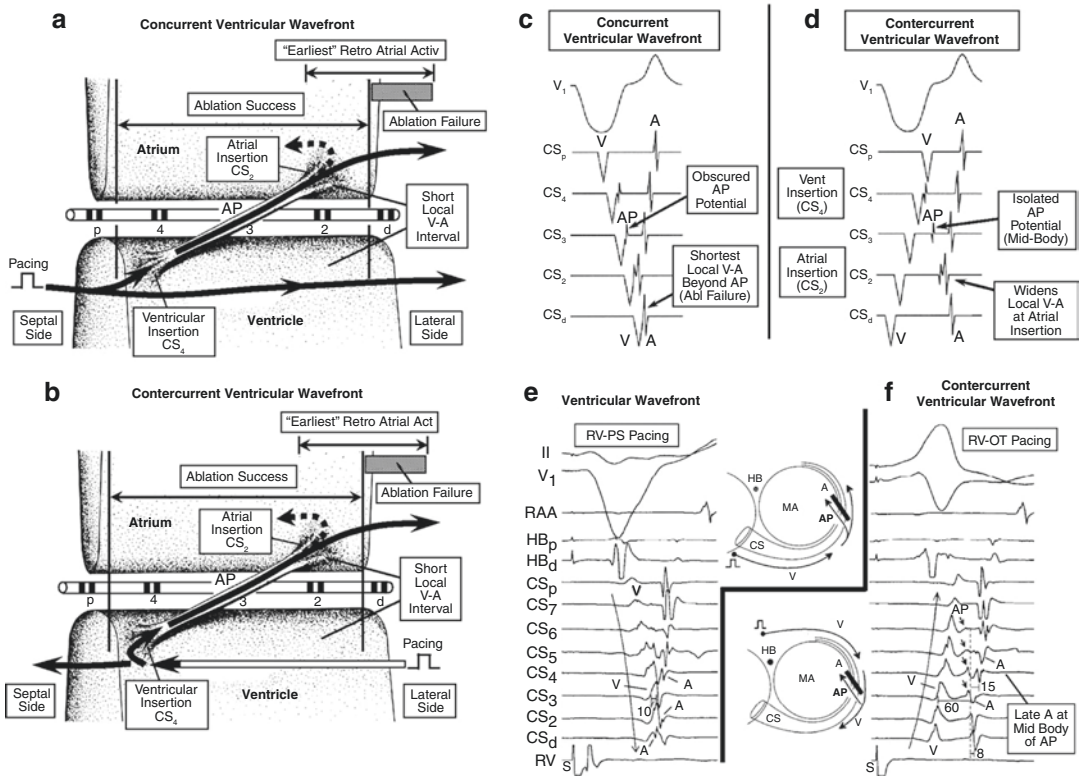

Fig. 5.14 Effects of the oblique course in a left free-wall accessory pathway on the timing of ventricular (V), atrial (A), and accessory pathway potentials by reversing the direction of the ventricular wave front. (**a**–**d**) Schematic representations. (**e**, **f**) Recordings from a patient with a left lateral accessory pathway. Reversing the ventricular wave front from the concurrent direction (**e**; posteroseptal basal RV pacing [RV-PS]) to the countercurrent direction (**f**; distal RV outflow tract pacing [RV-OT]) increased the local VA interval at the site in the coronary sinus of earliest atrial activation (electrogram CS3) from 10 to 60 ms and exposed the accessory pathway potential. The ventricular insertion (left) was located 15 mm septal to the atrial insertion (right). RAA indicates right atrial appendage. (Reproduced with permission from Hiroshi Nakagawa, and Warren M. Jackman Circulation. 2007;116:2465–2478, Wolters Kluwer Health, Inc.)

An accessory pathway in this region is posterior to the coronary sinus os and may be either on the tricuspid annular or mitral annular side of the septum. Pacing from the RV catheter and mapping the earliest atrial signal is often unreliable in posteroseptal accessory pathways. Near simultaneous atrial and ventricular activation in this region results in an AV interval which appears ideal but is not. The optimal approach is targeting of an accessory pathway potential.

As shown in Fig. 5.16 mapping is first performed on the right side of the septum posterior to the coronary sinus and only moved to the left if the accessory pathway cannot be mapped or successfully ablated. Pacing the atrium from either side of the atrial insertion point while mapping for an accessory pathway potential is generally the most accurate method of mapping.

Ablation can be performed with 30 W with a target temperature of 60 °C and the power can be titrated up if necessary, for a minimum period of 60 s. In general, ablation should not be performed in AVRT as the catheter tip can move with sinus rhythm restoration, resulting in an increased risk of AV nodal damage.

The patient can be monitored for a period of 30 min with atrial and ventricular pacing to ensure that accessory pathway conduction has not recovered.

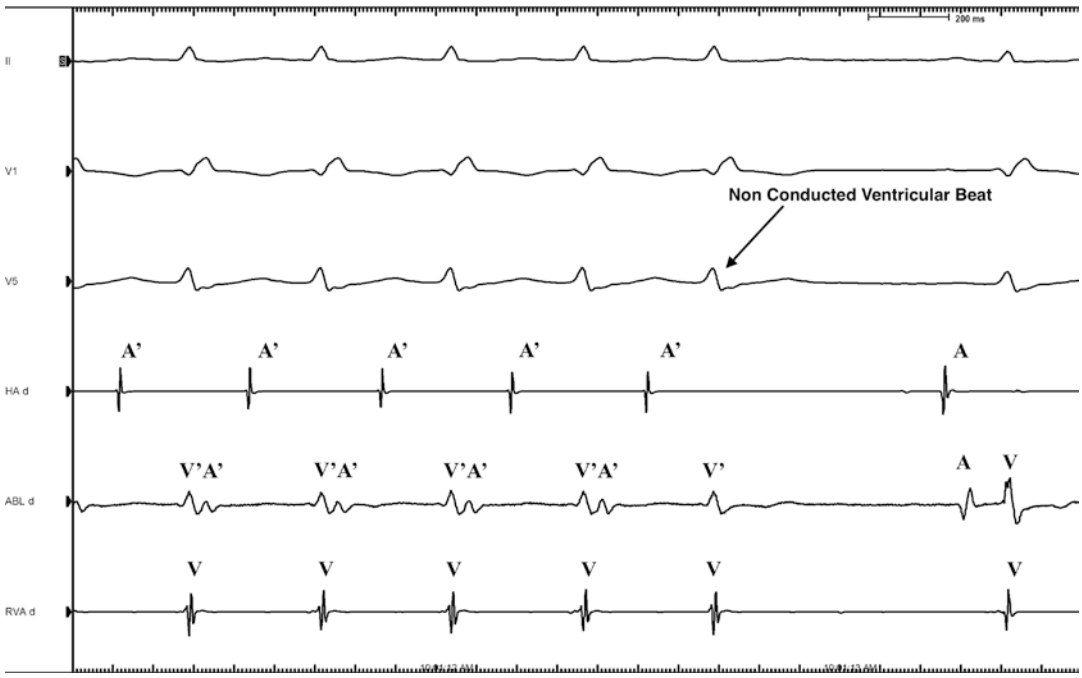

Fig. 5.15 Ablation during orthodromic reciprocating tachycardia in a concealed retrograde left lateral accessory pathway. Mapping is performed during tachycardia looking for the shortest VA interval. Ablation results in block with a non conducted ventricular beat. Thereafter there is sinus rhythm with a normal AV interval is observed. (HRA d is positioned in the high right atrium, ABL d is positioned along the left lateral accessory pathway location and RVa d is located in the RV apex)

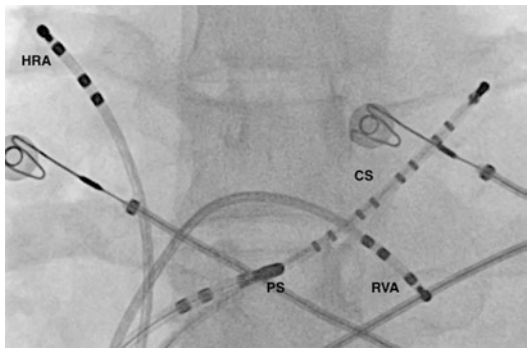

Fig. 5.16 LAO projection of a successful site for a right sided posteroseptal accessory pathway. The ablation catheter (PS) is posterior to the coronary sinus (CS) catheter. A catheter is also positioned in the HRA and the RV Apex

Posteroseptal Accessory Pathway: Difficult Case

Some posteroseptal accessory pathways are within the coronary sinus. These subepicardial pathways may involve myocardial connections between the coronary sinus os or within the middle cardiac vein, and the epicardium of the left ventricle. In these cases, endocardial mapping does not reveal any sites of early activation and the mapping catheter should be advanced into the coronary sinus looking for early ventricular activation during atrial pacing as well as an accessory pathway potential. It is useful to perform a coronary sinus venogram in order to assess for diverticula where accessory pathways may be located. Although the majority of accessory pathways involving coronary sinus connections do not occur in the presence of a coronary sinus diverticulum it is worth checking for this anomaly (Fig. 5.17. These diverticula contain fibres which connect to the coronary sinus myocardial coat and the ventricle. The coronary sinus myocardial coat is generally connected to both atria unless previously disconnected by ablation. There are certain ECG features which may help

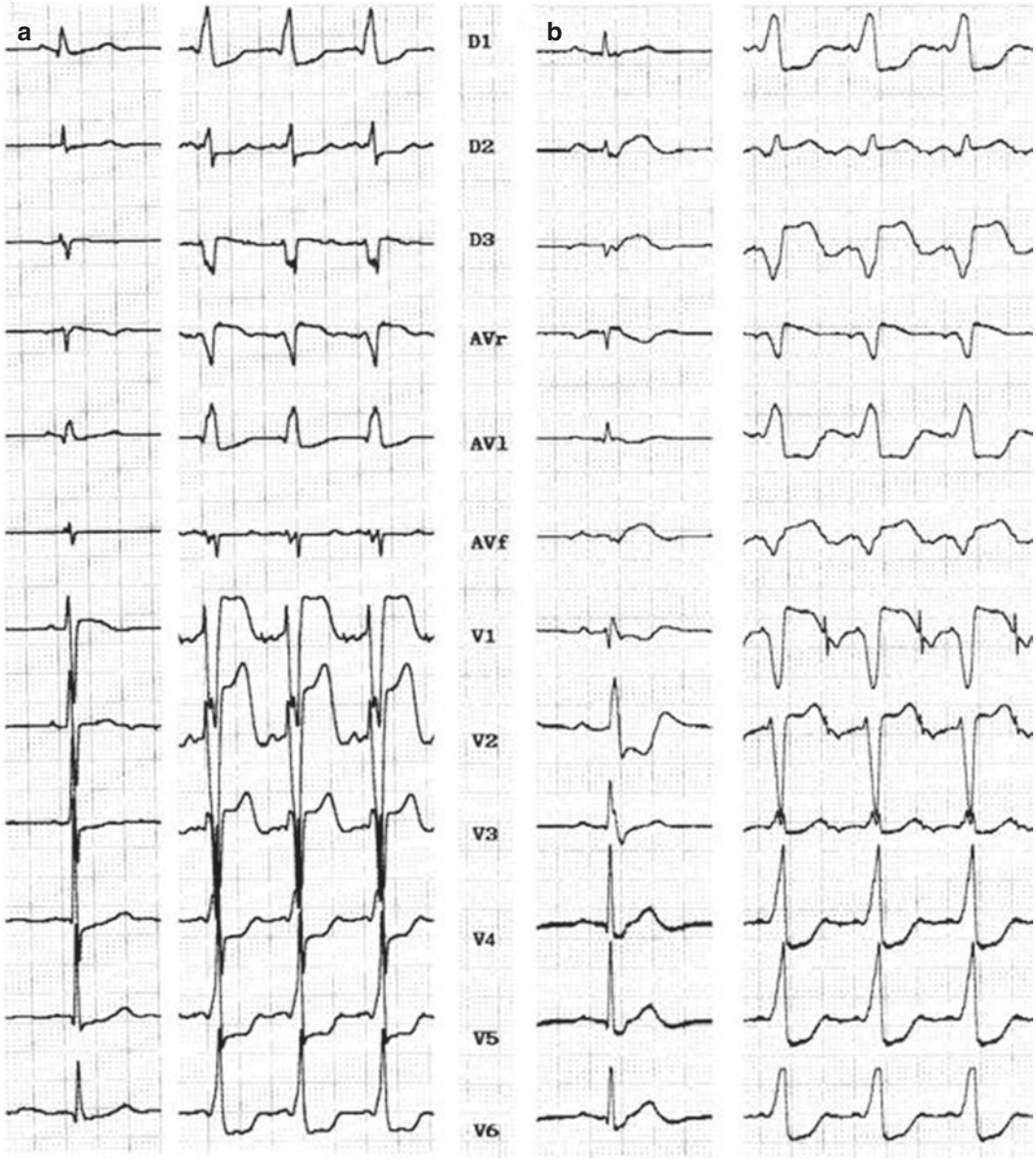

Fig. 5.17 Pre-excitation involving an accessory pathway located on the epicardial surface of a CS diverticulum. Panel **a** shows a venogram of the diverticulum in a PA view which is also shown in the electroanatomic map (Panel **b**). The ECG (Panel **c**) shows clear pre-excitation with a positive delta wave in lead II followed by a slight negative deflection. There is loss of pre-excitation during the third beat with an increase in the AV interval

suggest that a CS connection is involved. The most reliable of them is the presence of a negative delta wave in lead II. Other features include a steep positive delta wave in lead aVR as well as a deep S wave in V6.

When considering ablation within the coronary sinus, the operator should consider performing a coronary angiogram. Ablation should not be attempted if the coronary artery is within 5 mm of the site of ablation. If ablation has to be per-

formed within the coronary sinus, use a lower power of 10 W up to a maximum of 25 W irrigated and ablation should be stopped immediately in the event of a rise in the impedance.

Anteroseptal Accessory Pathway

These accessory pathways are located anteriorly along the central fibrous body close to the His bundle. They are manifest in 80% of cases in concealed in 20% and are less common than posteroseptal accessory pathways.

The difficulty with anteroseptal accessory pathways is the ability to separately map the accessory pathway and AV nodal conduction, as well as the proximity of the accessory pathway to the AV node (i.e. risk of AV block).

Ablation of an anteroseptal accessory pathway should target a relatively ventricular position. This is best accomplished by placement of the ablation catheter under the tricuspid valve leaflet. This provides a more stable catheter position during ablation of anteroseptal and midseptal accessory pathway. This can be performed by positioning the ablation catheter in the RV and then retroflexing the catheter back on the tricuspid annulus. Mapping can be performed looking for the earliest ventricular signal during sinus rhythm or atrial pacing. The ventricular electrogram should precede the surface delta wave by up to 40 ms.

Midseptal Accessory Pathway

Midseptal Accessory pathways occur between the His and the CS. They are in close proximity to the compact node and therefore carry the highest risk of AV block. In order to minimize this risk, the ablation catheter should be positioned with a more dominant ventricular signal. If ablation is unsuccessful despite good contact and a stable position the left side may be mapped. The ideal site is typically found along the mitral annulus in a position posterior to the His and anterior to the CS. At the ideal site a large, sharp AP potential may be recorded. Ablation in this location should eliminate AP conduction without AV block.

Right Atriofascicular Accessory Pathways

Atriofascicular accessory pathways can be considered a duplication of the normal conduction system, whereby an accessory AV node located along the anterolateral to posterolateral TV annulus connects to an isolated bundle of Purkinje fibers that extend to the apical RV free wall.

ECG Features

The baseline ECG generally has minimal or no pre-excitation owing to slow, decremental, antegrade conduction. Subtle ECG findings may include a LBBB-like morphology with absent q waves in the lateral leads (I, aVL, V5, and V6).

Tachycardia occurs via antidromic AVRT, as these pathways do not conduct retrogradely. The QRS morphology is typically LBBB-like with a QRS duration <150 ms, leftward axis, and a QRS transition later than V4.

EP Study and Mapping of a Right Atriofascicular Accessory Pathway

As pre-excitation is often minimal at baseline. Incremental pacing results in increasing pre-excitation with long AH intervals, with shortening of the HV interval. Pacing from the right atrium tends to result in a greater degree of pre-excitation than left atrial pacing. Decremental pacing from close to the atrial insertion point tends to result in increasing pre-excitation as antegrade conduction favours the accessory pathway. If tachycardia is induced the morphology is a LBBB with a superior directed axis.

Tachycardia is always an antidromic AVRT as these accessory pathways only conduct antegrade. The activation sequence is through the pathway into the fascicle followed by retrograde conduction up the right bundle and His followed

by the AV node. This activation sequence is useful in order to establish the diagnosis. If an atrial extrastimulus is introduced along the lateral tricuspid annulus whenever the atrial septum is refractory and the extrastimulus advances the tachycardia, then there is likely to be an atriofascicular accessory pathway. In order to prove that this accessory pathway participates in the tachycardia a late atrial extrastimulus can be delivered from close to the atrial insertion point of the accessory pathway. If this advances the ventricular activation and in particular does not advance the His signal during tachycardia, then this accessory pathway is participating in the circuit.

Mapping of an atriofascicular accessory pathway may be difficult. Although the right atrium can be paced and the ventricular insertion point can be mapped, this does not always prove successful and may cause injury to the right bundle branch with an incessant tachycardia and a longer cycle length conducting retrogradely up the left bundle.

Additionally, given that these pathways do not conduct retrogradely, mapping the earliest atrial activation during ventricular pacing cannot be performed.

The preferred method is to use a 20 pole catheter along the tricuspid annulus in order to map for a Mahaim potential. A Mahaim potential is seen as a sharp deflection between the A and the V which are both widely separated due to the distance between the atrial and ventricular insertion points and the relatively slow antegrade AP conduction. Examples of these are shown in Fig. 5.18. The interval between this potential and the ventricular potential is constant with decremental atrial pacing. Care must be taken when positioning this catheter to ensure that the accessory pathway is not bumped. If the Mahaim potential disappears while bumped with the ablation catheter, it is reasonable to apply RF to this location. During ablation there is often a slow accelerated rhythm for several seconds known as Mahaim automaticity (Back Sternick 2005). This is generally similar in morphology to the tachycardia. Typically, this is considered a good prognostic sign during the application of RF.

Left Lateral Accessory Pathway

These are the most common accessory pathways and ablation success rates are highest for these APs (~95%) (Calkins et al. 1999). They may have minimal pre-excitation given the distance of the ventricular insertion point from the AV nodal conduction. They also have the highest rate of concealed retrograde conduction of all accessory pathways.

Mapping of the accessory pathway is guided by the coronary sinus catheter which is slightly superior to the mitral annulus but runs along the same direction as the annulus and therefore gives an approximate idea of where the accessory pathway may be located. Further mapping can be performed with an ablation catheter either via a transseptal or retrograde approach. The electrodes are parallel to the CS electrodes and the catheter is moved along the catheter with ventricular pacing in order to assess the earliest atrial signal and an A:V ratio of 1:1.

Transseptal access is generally relatively straightforward through the fossa ovalis as the atrial anatomy is normal and can be achieved with a Brockenbrough needle and a long non-deflectable sheath. For a retrograde approach, femoral arterial access is gained, and the ablation catheter is prolapsed across the aortic valve in an RAO view with the curve pointing in an anterior direction to the right of the image. After crossing the aortic valve, the catheter is then rotated counterclockwise while maintaining the curve, bringing it in a posterior alignment toward the coronary sinus in the plane of the posterior mitral annulus. The curvature is then slowly released in order to move along the annulus. In order to achieve a greater atrial signal, the catheter is withdrawn slightly with an A:V ratio of approximately 1:10 and an atrial electrogram amplitude of 0.4–1.0 mV. Although a retrograde approach may be associated with greater catheter stability, it is generally more straightforward to maneuver the catheter via transseptal access.

As soon as either transseptal access has been obtained or the aortic valve has been crossed heparin should be administered at an initial dose of

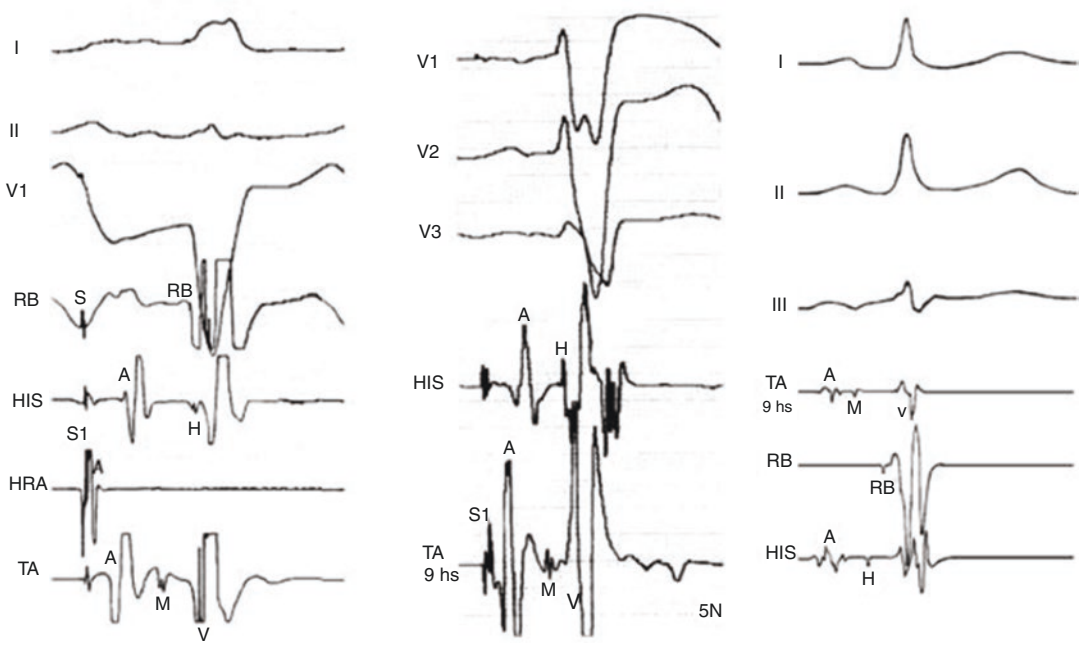

Fig. 5.18 Mahaim (M) potentials from left to right: first two cases with His-like potentials and the third with narrow and low amplitude potential. Ablation was successful in each of those sites. (TA- tricuspid annulus electrograms). (Courtesy of Back Sternick, E. Mahaim Fibre Tachycardia: Recognition and Management. IPEJ 2003: 3:47–59)

100 units/kg aiming for an ACT greater than 300 s. A continual infusion of heparinized saline should be infused through the side arm of the long sheath. Provided there is retrograde conduction along the accessory pathway the most straightforward method of mapping is to pace the ventricle and map for the earliest atrial activation. Pacing from different locations can be used in order to separate out the A and the V so as to record an accessory pathway potential. The ablation catheter can be moved along the mitral annulus. An example of the optimal position for an ablation catheter in a concealed retrograde posterolateral accessory pathway is shown in Fig. 5.19.

Mapping for the earliest ventricular electrogram can also be performed during atrial pacing. For a left lateral accessory pathway, the local ventricular electrogram should precede the surface delta by up to 10 ms. A negative QS in a unipolar electrogram is also a sign of a good position.

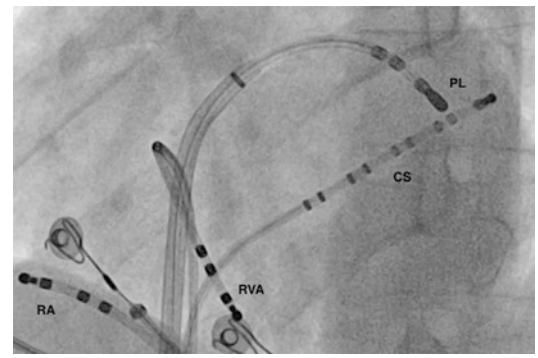

Fig. 5.19 Ablation catheter position on the posterolateral concealed retrograde accessory pathway

It is not ideal to ablate during tachycardia as the catheter can move considerably following termination of the tachycardia. However, in some cases of incessant tachycardia there is no other option.

Catheter stability may not be as good as a retrograde approach, but this method is associated

with a lower incidence of vascular complications. Additionally, the transseptal approach is better for accessing extreme lateral and anterolateral accessory pathways.

For a retrograde approach femoral arterial access is achieved with a 7 Fr sheath. The ablation catheter is directed up the descending aorta and a curve is placed in the catheter as it is advanced around the aortic arch.

Right Free Wall Accessory Pathway

These are considered to be the most difficult accessory pathways to map and successfully ablate. This is due to a combination of catheter instability, the presence of other structural abnormalities such as Ebstein's anomaly, and the lack of support structure which may assist mapping of the annulus. A 20 pole catheter can be positioned in the RA in order to help map the tricuspid annulus. A deflectable sheath may also be helpful for catheter stability. The catheter is moved looking for an early atrial or ventricular signal with an A:V ratio of 1:1 as well as an accessory pathway potential. The local ventricular signal should be compared with the surface delta wave and should be earlier by up to 20 ms (Haissaguerre et al. 1994). An example of mapping of the tricuspid annulus using an ablation catheter in a right sided accessory pathway is shown in Fig. 5.20.

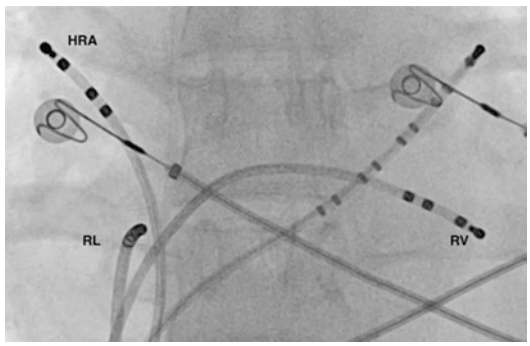

Fig. 5.20 Mapping of an accessory pathway along the tricuspid annulus. The ablation catheter is positioned in the right posterolateral annulus where ablation was successful. Also shown in this image is a catheter in the HRA, RV and CS

Accessory Pathway General: Difficult Case

The most common cause for failure to successfully ablate an accessory pathway is the inability to manipulate the ablation catheter to the atrial or ventricular insertion point. For left lateral accessory pathways, this may be overcome by switching from retrograde to a transseptal access or vice versa. Changing the curve on the ablation catheter and occasionally the use of a long sheath may also help to maneuver the catheter and provide stability.

The inability to deliver a successful lesion limited by power or temperature may be overcome by repositioning the catheter or changing the angulation of the catheter. If this does not work, then switching to an irrigated catheter may help.

If a septal or left-sided accessory pathway potential cannot be mapped or is small, then the coronary sinus should be mapped. If this is the case, then ablation can be performed at lower power from within the coronary sinus.

If the patient is in incessant AVRT, ablation can be performed during tachycardia. It is important that ablation is continued after termination of the tachycardia as often the catheter moves during reversion to sinus rhythm.

Important Points

1. Accessory pathways are muscle fibers which connect the atrium to the ventricle through the fibrofatty and fibrous parietal AV junctional regions. The majority are located within the epicardial atrioventricular fat pad close to the atrioventricular junctions.
2. Anatomically these are divided into septal (paraseptal) which include posteroseptal, midseptal and anteroseptal, left lateral (left posterior), left posterolateral (left infero-posterior), left posterior (left inferior), left anterolateral (left superoposterior) and left anterior (left superior).

The equivalent locations are also possible on the right side using similar nomenclature. Additionally, some accessory pathways may be directly connected into the specialized conduction system such as atriofascicular, atrioventricular, nodoventricular and fasciculoventricular pathways. Accessory pathways may also be located in unusual anatomical locations involving epicardial connections between the coronary sinus and the left ventricle, the non-coronary cusp of the aortic valve to the left ventricle, the right atrial appendage to right ventricle or left atrial appendage to left ventricle.

3. Orthodromic AVRT occurs when the antegrade accessory pathway is refractory and conduction occurs antegradely through the AV node activating the His and ventricle and retrogradely along the accessory pathway if it is no longer refractory. The VA time required for this to occur is generally greater than 70 ms.
4. Antidromic AVRT conduction occurs antegradely via the accessory pathway as the AV node is refractory. This is generally associated with a pre-excited QRS as conduction is only via the AP. VA times are generally greater than 70 ms as conduction is via the VA node.
5. The Shortest Pre-Excited R-R Interval (SPERRI) $\leq$250 ms may be associated with a higher risk of antegrade conduction during AF and may be an indication for catheter ablation.
6. In order to help maximize pre-excitation during an EP study pacing may be performed from different locations on different catheters. This may also help to reveal an accessory pathway potential which should be targeted for ablation.

References

Sternick B. Automaticity in a Mahaim fiber. Heart Rhythm. 2005;2(4):453.

Becker AE, Anderson RH, Durrer D, Wellens HJ. The anatomical substrates of Wolff-Parkinson-White syndrome: a clinicopathologic correlation in seven patients. Circulation. 1978;57:870.

Calkins H, Yong P, Miller JM, et al. Catheter ablation of accessory pathways, atrioventricular nodal reentrant tachycardia, and the atrioventricular junction: final results of a prospective, multicenter clinical trial. The Atakr Multicenter Investigators Group. Circulation. 1999;99:262–70.

Epstein MR, Knapp LD, Martindill M, et al. Embolic complications associated with radiofrequency catheter ablation. Atakr Investigator Group. Am J Cardiol. 1996;77:655–8.

Haissaguerre M, Gaita F, Marcus FI, Clementy J. Radiofrequency catheter ablation of accessory pathways. a contemporary review. J Cardiovasc Electrophysiol. 1994;5:532–52.

Ho SY. Accessory atrioventricular pathways: getting to the origins. Circulation. 2008;117:1502–4.

Jazayeri MR, Dhala A, Deshpande S, et al. Posteroseptal accessory pathways: an overview of anatomical characteristics, electrocardiographic patterns, electrophysiological features, and ablative therapy. J Interv Cardiol. 1995;8:89–101.

Nakagawa H, Jackman WM. Catheter ablation of paroxysmal supraventricular tachycardia. Circulation. 2007;116:2465–78.

Otomo K, Gonzakez MD, Beckman KJ, et al. Reversing the direction of paced ventricular and atrial wavefronts reveals an oblique course in accessory AV pathways and improves localization for catheter ablation. Circulation. 2001;104:550.

PACES/HRS. PACES/HRS expert consensus statement on the management of the asymptomatic young patient with a Wolff-Parkinson-White (WPW, ventricular preexcitation) electrocardiographic pattern: developed in partnership between the Pediatric and Congenital Electrophysiology Society (PACES) and the Heart Rhythm Society (HRS). Endorsed by the governing bodies of PACES, HRS, the American College of Cardiology Foundation (ACCF), the American Heart Association (AHA), the American Academy of Pediatrics (AAP), and the Canadian Heart Rhythm Society (CHRS). Heart Rhythm. 2012;9:1006–24.

Peters NS, Rowland E, Bennett JG, et al. The Wolff-Parkinson-White syndrome: the cellular substrate for conduction in the accessory atrioventricular pathway. Eur Heart J. 1994;15:981.

Atrial Tachycardias

6

Adam Lee, Henry H. Hsia, Haris M. Haqqani, Benedict M. Glover, Pedro Brugada, and Melvin M. Scheinman

Abstract

Atrial tachycardia is a focal or macro re-entry supraventricular arrhythmia which does not directly involve the AV node. Overall it accounts for approximately 7% of all SVT's (Wellens HJ, Circulation. 90(3): 1576–1577, 1994).

Focal atrial tachycardia occurs as a result of either micro re-entry, increased automaticity or triggered activity while macro re-entry occurs over a region of tissue surrounding a region of conduction block. Focal atrial tachycardia due to increased automaticity can usually be initiated with isoprenaline while decremental atrial pacing tends to initiate and terminate micro and macro re-entry.

Although atrial tachycardia's may occur anywhere within the right atrium or left atrium there are more common locations and in particular where anisotropic conduction occurs in which there is rapid linear conduction and slowed transverse conduction. The most common locations are the crista terminalis, coronary sinus os, the pulmonary veins and antral regions, the tricuspid and mitral annuli, the right and left atrial appendages and the interatrial septum. The location is to an extent dependent on the patient's age, history of structural heart disease, prior ablations or surgery and the presence of other arrhythmias.

Introduction

Atrial tachycardia (AT) refers to an arrhythmia which is entirely confirmed to the atria**.** Overall it accounts for approximately 7% of all SVTs (Wellens 1994). Mechanistically, these can be focal or macro-reentrant.

The nomenclature of different mechanisms of AT can be confusing. From a practical standpoint, it is useful to classify ATs into one of three categories (Fig. 6.1):

1. Focal AT
2. Localized or small circuit re-entrant AT
3. Large circuit macro-reentrant AT

A. Lee · H. H. Hsia · M. M. Scheinman (✉)
University of California San Francisco, San Francisco, CA, USA
e-mail: adam.lee@ucsf.edu; henry.hsia@ucsf.edu; melvin.scheinmam@ucsf.edu

H. M. Haqqani
Faculty of Medicine, University of Queensland, Brisbane, QLD, Australia
e-mail: h.haqqani@uq.edu.au

B. M. Glover
Division of Cardiology, Department of Medicine, University of Toronto, Toronto, Ontario, Canada

P. Brugada
University Hospital of Brussel, Brussels, Belgium
e-mail: pedro@brugada.org

B. M. Glover, P. Brugada (eds.), *Clinical Handbook of Cardiac Electrophysiology*,
https://doi.org/10.1007/978-3-030-74319-2_6

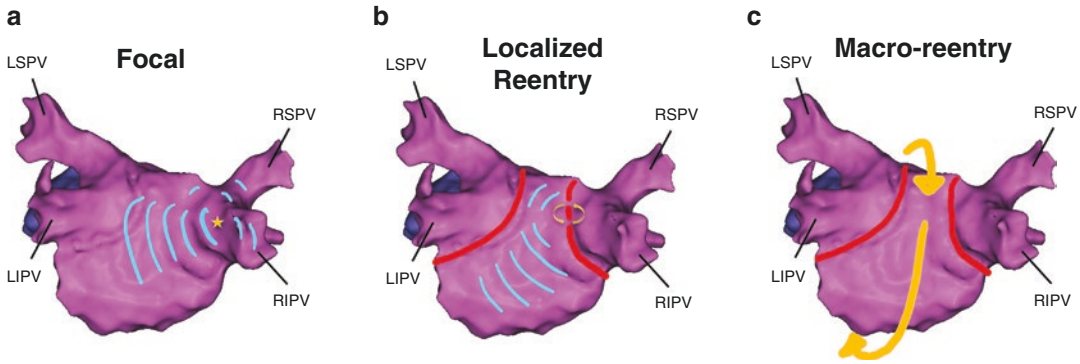

Fig. 6.1 Examples of the three mechanisms of AT. (**a**) Focal AT arising from the right inferior pulmonary vein; (**b**) small circuit or localized re-entrant AT utilizing two gaps on the roof of a previously performed wide antral circumferential ablation (WACA) lesion set; (**c**) left atrial roof dependent large circuit macro-reentrant AT arising in the setting of previously performed bilateral WACA lesion sets resulting in a narrow isthmus across the LA roof

Focal atrial tachycardia (FAT) arise from a discrete focus and are characterized by centrifugal passive activation of the remainder of the atria from this site. The underlying mechanism may be automatic, triggered or micro-reentrant (Liu et al. 2016), though in the latter case, the re-entry circuit is beyond the resolution of current recording systems. Though the underlying mechanism may be inferred from the clinical context and the response to certain drugs and pacing/resetting (Liu et al. 2016), this distinction is somewhat academic as invasive treatment of a FAT involves seeking out the earliest site of atrial activation during the arrhythmia.

The other mechanism of atrial tachycardia is macro-reentry. Here activation occurs across an intra- (and/or inter-) atrial circuit, which can be macroscopically defined with electroanatomic mapping. Arrhythmias related to macro-reentry associated with no diastolic interval are termed "atrial flutter".

Further dividing macro-reentrant ATs into "localized or small circuit re-entry" and "large circuit macro-reentry" has utility in relation to the approach to ablation. Atrial flutter is most commonly due to a large macro-reentrant circuit with the prototypical example being counterclockwise cavotricuspid isthmus (CTI) dependent (or "typical") atrial flutter. Other examples including non-CTI dependent (or "atypical") flutters, such as those involving the left atrium (mitral annular or roof dependent flutter). As the tachycardia rate is driven by the circuit, electroanatomic mapping of the involved atrium (or atria) will account for the entire tachycardia cycle length. The ablation strategy generally involves identifying an isthmus critical to the circuit that can be transected between two electrically inert structures (e.g., the tricuspid annulus and the inferior vena cava for CTI-dependent flutters).

"Localized or small circuit re-entrant" ATs, involve smaller macro-reentrant circuits, that superficially, on an EA map may appear "focal". However, with detailed mapping (using current high resolution mapping tools) the re-entrant circuit becomes evident. These have historically been arbitrarily defined as a circuit with a diameter <2 cm (by entrainment mapping) (Luther et al. 2017), though such a cut-off does not have much practical utility. As the relatively large recording bipole of current ablation catheters can often span a sizeable portion of these small reentrant circuits, prolonged fractionated signals accounting for a large proportion of the tachycardia cycle length may be recorded across a single bipole and the arrhythmia may terminate with limited ablation at these sites (Fig. 6.2).

From a practical standpoint, focal ATs should be distinguished from macro-reentrant ATs (both small and large circuit). FATs are considered in the differential diagnosis of paroxysmal SVTs and often occur in patients with "normal" atria.

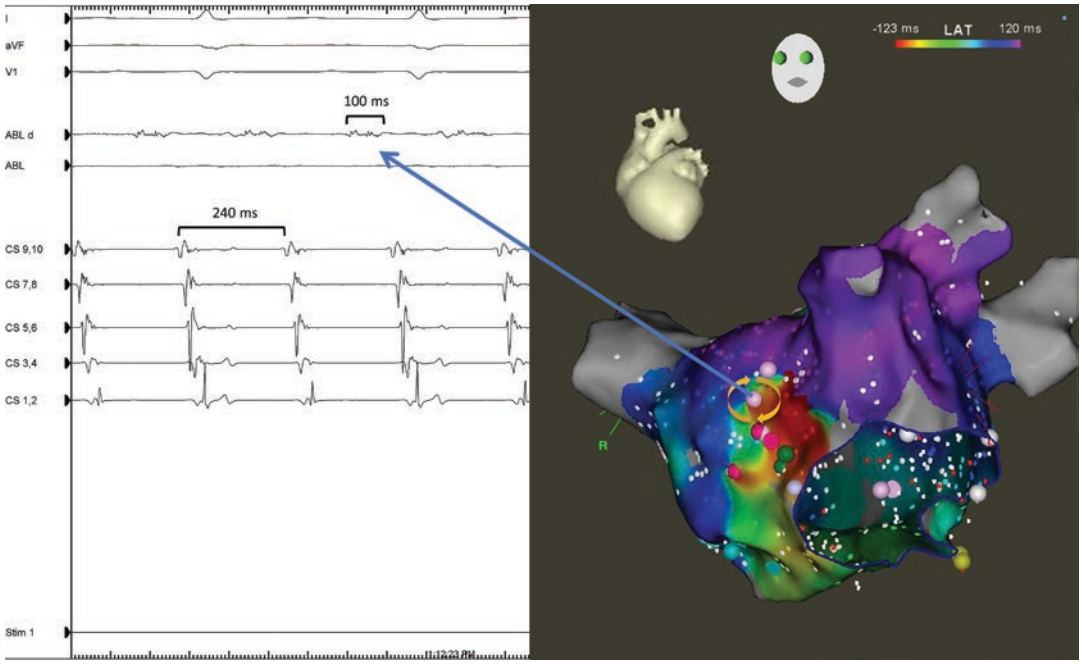

Fig. 6.2 An example of localized re-entry in a patient with prior left atrial ablation for atrial fibrillation flutter. Superficially, the activation map (AP view of the left atrium) resembles focal activation arising from the superior mitral annulus. High density mapping, however, confirms a small re-entrant circuit in this previously scarred region. The ablation catheter bipole is over a critical site within this small circuit and records a fractionated electrogram that accounts for >40% of the tachycardia cycle length. The arrhythmia terminated during ablation at this site

Macro-reentrant ATs/atrial flutters, on the other hand, can often be recognized by a continuous flutter-wave on the ECG and can occur in diseased (or post-ablation) atria or in patients without structural heart disease. The medical management of atrial flutter mirrors that of atrial fibrillation more than paroxysmal SVT. As Chap. 7 focuses on Atrial Flutter, this chapter will predominantly address focal AT.

Procedural Planning

Consideration for commencing EP studies with local anesthesia alone, with appropriate patient counselling, is worthwhile in cases of suspected AT. Although most SVTs are minimally affected by sedation, FAT can be exquisitely sensitive to sedation and may be rendered non-inducible (Lai et al. 1999).

Intracardiac Mapping and Ablation

Catheter ablation of FAT involves delivery of radiofrequency energy (or less commonly cryoablation) to the site of origin of these arrhythmias. Use of 3-dimensional (3D) electroanatomic mapping is helpful but not essential during these procedures. 3D mapping has additional advantages including (a) allowing rapid tachycardia mapping with multipolar catheters, (b) recording all sites where ablation has already been performed and/or sites of bump termination and (c) allowing for a minimal or zero-fluoroscopy procedure.

If the mechanism of arrhythmia is unclear, 3D mapping with activation and entrainment mapping can be useful. Local activation times can be acquired relative to a fixed reference (e.g., a stable coronary sinus atrial EGM). In general, FAT or localized re-entry, the activation map should

demonstrate focal activation with centrifugal spread of the subsequent wavefront throughout the atrium (Fig. 6.3). In macro-reentry (atrial flutter), with sufficient point acquisition, the potential re-entrant circuit should be evident. Note, the presence of "early meets late" on an activation map is merely an indicator that the arrhythmia mechanism is possibly macro-reentry, but the site of this phenomenon is in itself meaningless and arbitrarily dependent on the chosen fiducial reference.

Overdrive pacing (at 10–20 ms faster than the tachycardia cycle length [TCL] to minimize overdrive suppression or decrement) will further clarify the arrhythmia mechanism. In FAT or localized re-entry, the post-pacing interval (PPI) will shorten and approach the TCL as you pace closer to the focal point of origin or the localized re-entry circuit. Whilst for macro-reentry, the PPI can be closer to the TCL over a wide area that is within the re-entrant circuit.

The principal of mapping a FAT involves searching for the earliest site of electrical onset as seen on the distal bipole of the mapping/ablation catheter. The atrial EGM at this site tends to be approximately 30 ms pre-P wave, as this is the time it takes for a critical mass of atrial tissue to be depolarized and generate a P-wave on the surface ECG. Unlike focal PVC ablation, however, the P-wave (and specifically the P-wave onset) can be difficult to see on the surface ECG, as it is often buried within the preceding T-wave. It is therefore critical to establish a reliable fiducial reference which is most often a stable atrial EGM (usually a coronary sinus [CS] bipole). Brief ventricular burst pacing at approximately 250–400 ms, will often conceal retrogradely into the AV node and unmask a clean surface P-wave (Figs. 6.5, 6.7, and 6.12). The chosen fiducial reference can then be measured to the P-wave onset and used in place of the P-wave onset when assessing appropriate precocity at potential sites of ablation (Fig. 6.4).

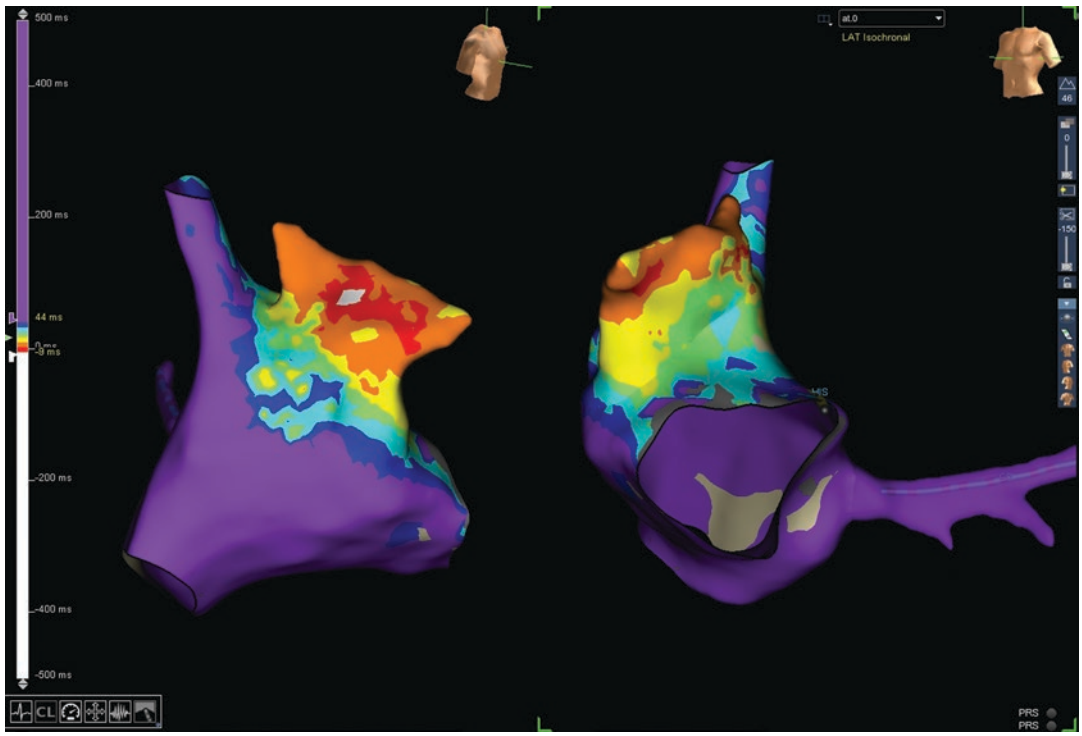

Fig. 6.3 An activation map of a FAT arising from the right atrial appendage with earliest activation at this site and centrifugal wavefront propagation to the remainder of the right atrium (white—earliest site of activation, purple—latest site of activation)

Fig. 6.4 RV burst pacing unmasks the onset of the AT P-wave, which can then be referenced against a stable intracardiac electrogram (in this case prox CS). The prox CS is 46 ms pre-P wave onset. Therefore, one should expect a near field EGM approximately 66–76 ms pre-prox CS (i.e., 20–30 ms pre-P wave) at the FAT site of origin

The unipolar EGM from the distal electrode on the mapping/ablation catheter can also be useful. If the catheter is at the true AT site of origin, electrical activity should always be propagating away from the distal tip electrode, therefore manifesting a QS pattern on the unipolar EGM. Whilst this may be a sensitive finding at the appropriate ablation site, specificity may be lacking due to a QS pattern being seen over a relatively large area.

Focal Atrial Tachycardia

Although atrial tachycardias may occur anywhere within the right atrium or left atrium, certain sites demonstrate predilection to AT, in particular where anisotropic conduction occurs in which there is rapid linear conduction and slowed transverse conduction. In patients with structurally normal hearts, common right atrial locations include the the crista terminalis, tricuspid annulus and the coronary sinus os, whilst common left atrial locations include the pulmonary veins and mitral annulus (Kistler et al. 2006) (Fig. 6.5).

Tachycardiomyopathy and Incessant Atrial Tachycardia

Approximately 10% of patients with FAT will develop a cardiomyopathy (LV ejection fraction <50%). Many of these patients present with incessant AT in which the tachycardia continues

without interruption or paroxysms occur, but only with brief intervening periods of sinus rhythm (≤2 beats). Focal AT arising from the atrial appendages and pulmonary veins are commonly incessant and are more likely to lead to the development of LV dysfunction (Medi et al. 2009). Successful eradication of the incessant AT will often lead to improvement, if not normalization of LV function.

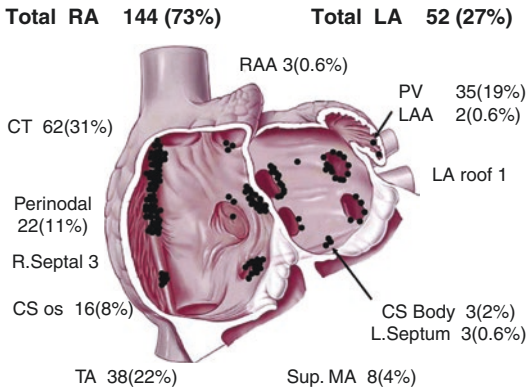

Fig. 6.5 Distribution of common sites of origin of focal AT in structurally normal hearts in a series of 196 foci. (*Borrowed with permission from Kistler PM. P-wave morphology in focal atrial tachycardia: development of an algorithm to predict the anatomic site of origin. J Am Coll Cardiol. 2006;48(5):1010–7*)

Locations of Atrial Tachycardias

It is useful to use the ECG to predict whether the atrial tachycardia is left- or right-sided prior to performing an ablation in order to adequately inform the patient about procedural risk and particularly the likely need for transseptal puncture. The P-wave morphology on the surface ECG is surprisingly accurate at predicting the site of origin of focal ATs. Kistler et al. developed a simple algorithm that allowed prediction of the most common sites of both right and left sided ATs (Fig. 6.6) (Kistler et al. 2006). The most useful leads to examine are V1 and the inferior leads (II/III/aVF). As the left atrium is the most posterior structure in the heart, left sided ATs tend to have a positive P wave in V1 (Fig. 6.7). Any other V1 P-wave morphology (pos-neg, neg-pos, isoelectric or entirely neg) usually suggests origin from the RA, though septal or annular structures (including the CS) remain on the differential.

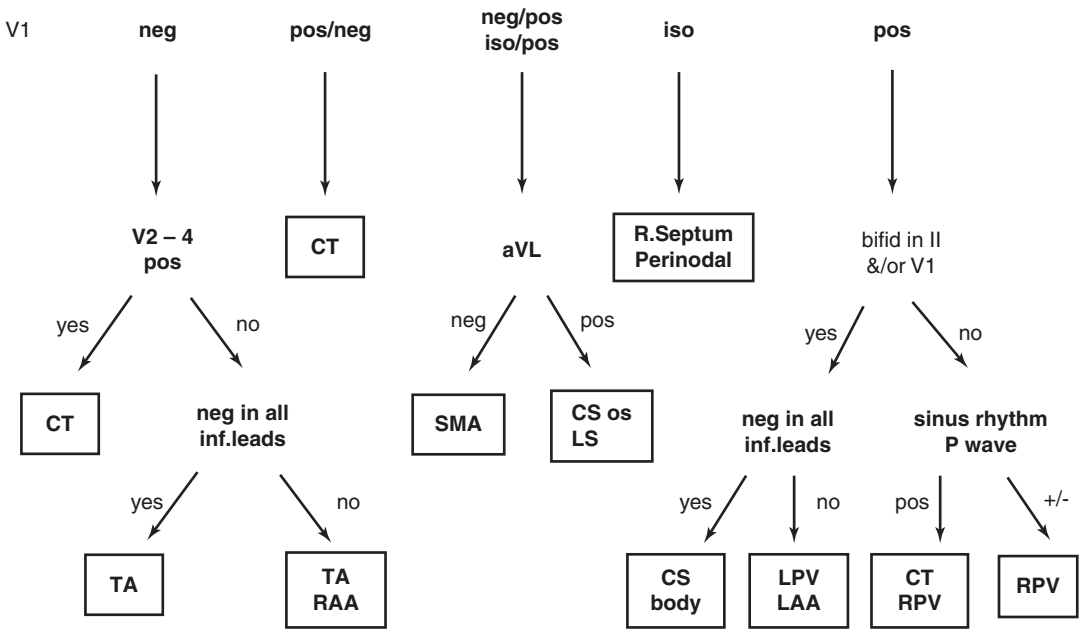

Fig. 6.6 Algorithm predicting focal atrial tachycardia site of origin in patients with structurally normal hearts. (*Borrowed with permission from Kistler PM. P-wave morphology in focal atrial tachycardia: development of an algorithm to predict the anatomic site of origin. J Am Coll Cardiol. 2006;48(5):1010–7*)

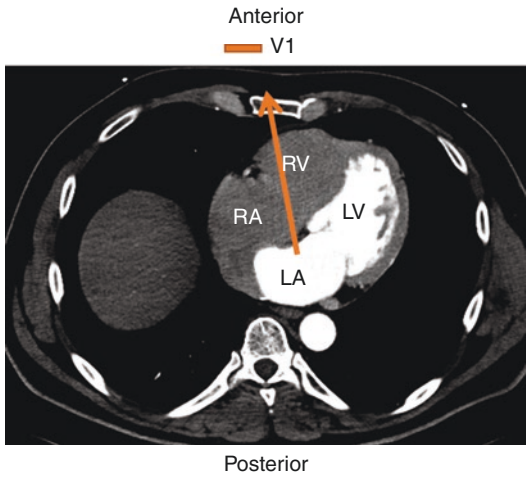

Fig. 6.7 CT scan demonstrating the posterior location of the LA and its relationship to lead V1 on the surface ECG. The presence of a positive P-wave in lead V1 usually indicates a left atrial FAT origin

The Kistler algorithm (and all others) are validated only in the setting of structurally normal hearts. Significant structural heart disease and/or scarring from prior surgeries or ablation can altered the relative position of atrial structures in the thorax and/or distort electrical wavefront propagation such that the surface P-wave may no longer represent an accurate predictor of AT site of origin (Kistler et al. 2006; Medi et al. 2009).

Crista Terminalis

The crista terminalis (CT) runs from the anteromedial high right atrium inferiorly along the lateral RA wall where it ends at the posteroinferior right atrium at the eustachian valve. The CT is the most common site of origin for all FAT and accounts for approximately 50% of FAT in the RA (Morris et al. 2019). Anisotropic conduction in this region predisposes to micro-reentry manifesting as FAT (Saffitz et al. 1994).

The CT is a linear structure along the posterolateral RA wall that separates the trabeculated RA (including the appendage) from the smooth walled RA (derived from the embryological sinus venosus). Accordingly, the V1 P-wave morphology of FAT originating from this region often have a P wave morphology similar to sinus rhythm (pos-neg in V1) as the sinus node is a subepicardial structure located in the nearby posterolateral SVC/RA junction. The P-wave morphology in the inferior leads (II/III/aVF) is determined by the specific AT vertical site of origin within the CT. Inferiorly directed and superiorly directed P-waves are seen with AT arising from the high and low crista respectively (Fig. 6.8). FAT arising from the high CT may have indistinguishable or very subtly different P-wave morphologies compared to sinus rhythm. Paroxysmal characteristics of the tachycardia (abrupt onset and offset) can distinguish this from inappropriate sinus tachycardia in which onset/offset should be gradual.

In patients with posteriorly rotated hearts, FAT arising from the CT may demonstrate purely positive P-waves in V1. This is the common exception to the rule where positive V1 P-waves identify AT origin from the LA, though such patients will also demonstrate positive V1 P-waves during sinus rhythm.

Ablation of FAT arising from the CT is relatively straightforward with standard activation mapping, but care should be taken to exclude phrenic capture with high output pacing prior to delivery of ablative energy at this site.

Tricuspid Annulus

The tricuspid annulus (TA) represents the second most common site of FAT arising from the RA. As the TA is an anterior structure of the RA, the P-wave morphology in V1 is entirely negative with negative concordance throughout the precordial leads. The P-wave morphology in the inferior leads determines the vertical site of origin along the TA with the inferior TA (superiorly directed P-waves) being a more common site for focal ATs than the superior TA (inferiorly directed P-waves) (Morton et al. 2001). The right atrial appendage, also being an anterior RA structure, shares a similar P-wave morphology to that of the superior TA. Whilst the RAA is a relatively rare site of origin for FAT, this site should be mapped if no suitably early electrograms (EGMs) are found at the superior TA. Catheter stability can be challenging

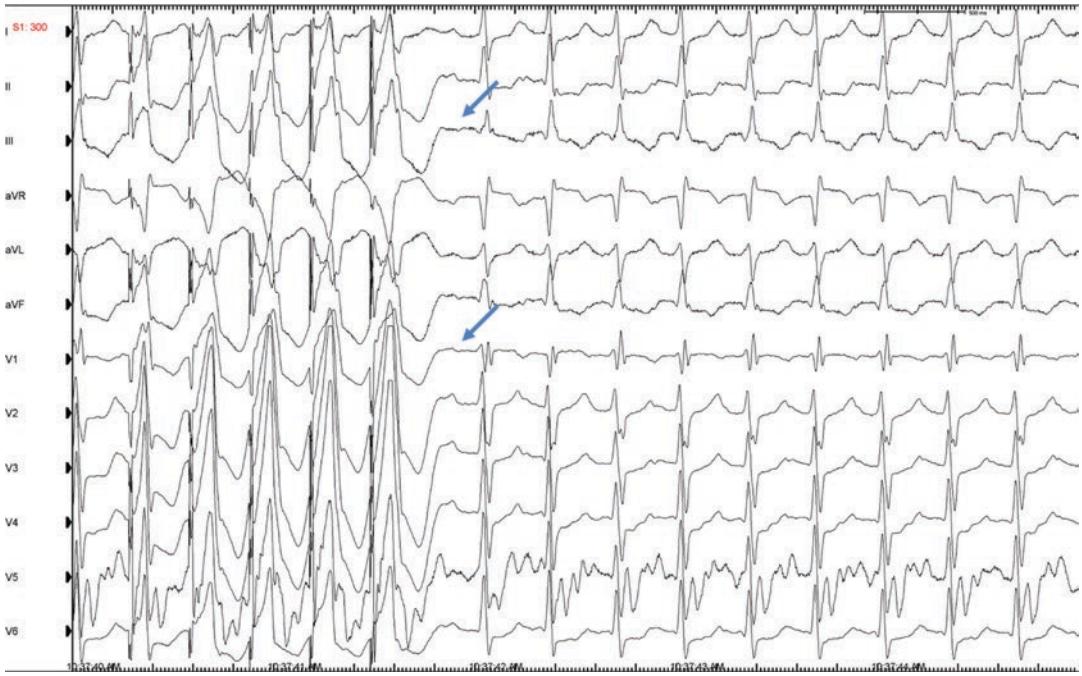

Fig. 6.8 RV burst pacing to reveal P-wave morphology during AT (pos-neg in V1, pos in II/aVF and slightly negative in III—blue arrows). This AT was ablated from the mid crista terminalis

on the TA and deflectable sheaths may be helpful when ablating focal ATs from this region (Fig. 6.9).

Perinodal/Parahisian Region

FATs from the perinodal or parahisian region are characterized by the presence of a His EGM at the site of earliest atrial activation. This site is in proximity to the atrial insertion of the AV nodal fast pathway and hence shares a similar narrow P-wave morphology to that of typical (slow-fast) AV nodal re-entrant tachycardia (AVNRT). An isoelectric P-wave in V1 is specific but only modestly sensitive for perinodal ATs due to significant variation in P-wave morphology at this site (Fig. 6.10).

Ablation at this site entails a higher risk of AV block, although published series indicate these AT can be treated effectively and safely. The purported "reversibility" of cryoablation may represent an option in high risk cases (Bastani et al. 2009), though radiofrequency ablation at the adjacent non-coronary cusp via the retrograde aortic approach (Fig. 6.11) appears safe and to be the approach of choice in such circumstances (Beukema et al. 2014; Lyan et al. 2017).

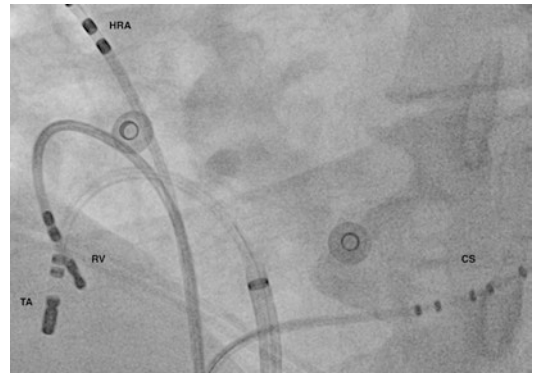

Fig. 6.9 LAO 30° view demonstrating the ablation catheter at the successful ablation site of a lateral tricuspid annular AT with a long sheath used for support

Coronary Sinus Os

Anisotropic conduction at the site of insertion of the coronary sinus fibers to the RA are predisposed to micro-reentry and triggered activity;

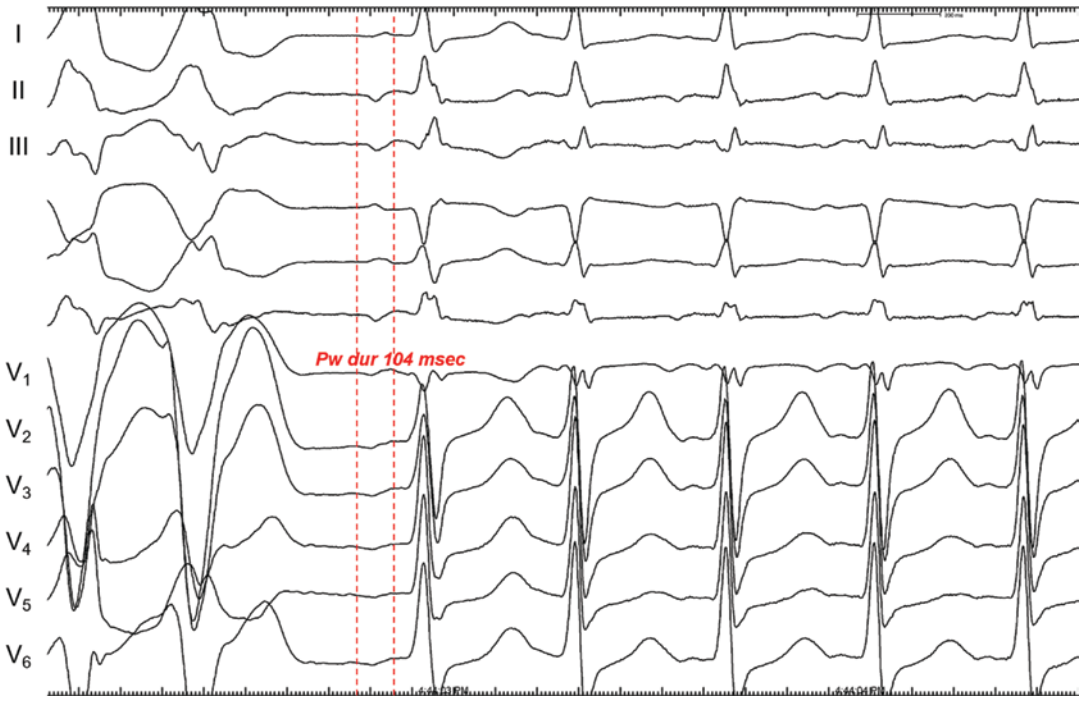

Fig. 6.10 The P-wave morphology of a focal AT mapped to the parahisian region, demonstrating a relatively isoelectric V1 and narrow P-wave as this site is central to both atria resulting in parallel activation of both atria

hence the CS os is frequent site of RA FAT (McGuire et al. 1994; Johnson et al. 1986).

FAT from the CS Os demonstrate the same "posteroseptal P-wave" as other arrhythmias that result in earliest atrial activation in this region (e.g., counter-clockwise CTI isthmus dependent flutter, permanent reciprocating junctional tachycardia [PJRT], atypical AVNRT). The P-wave in V1 has a late positive (either neg-pos or iso-pos) morphology. Lead aVL tends to be positive (Fig. 6.12). This P-wave can be is similar to that of focal ATs arising from the left septum, though the latter is relatively uncommon.

For narrow complex SVTs with 1:1 AV relationships and a P-wave consistent with CS Os origin, a detailed electrophysiology study utilizing ventricular-based pacing maneuvers and atrial overdrive pacing should be performed to distinguish between the diagnosis of atypical AVNRT, atrioventricular re-entrant tachycardia (AVRT) utilizing a posteroseptal accessory pathway or CS Os FAT. Once a diagnosis of FAT is established, ablation within the proximal CS especially if in close proximity to a CS potential is effective, safe and entails a low risk of AV block (Badhwar et al. 2005).

Pulmonary Vein Atrial Tachycardia

The pulmonary veins (PVs) are well established as sites of AF triggers. This forms the basis for pulmonary vein isolation (PVI) as the cornerstone of catheter-based therapies in these patients (Haissaguerre et al. 1998). PV foci represent the most common site of AT in the LA and whilst the anatomical distribution of these foci are similar to that of PV AF triggers (more common from the superior versus inferior veins), AT foci are usually unifocal and both recurrences and AF are uncommon following successful ablation (Kistler et al. 2003a). Accordingly, focal radiofrequency ablation can be utilized as opposed to pulmonary vein isolation as the vast majority of these foci are ostial rather than deep within the PV anatomy. Finally, PV AT have a propensity to be

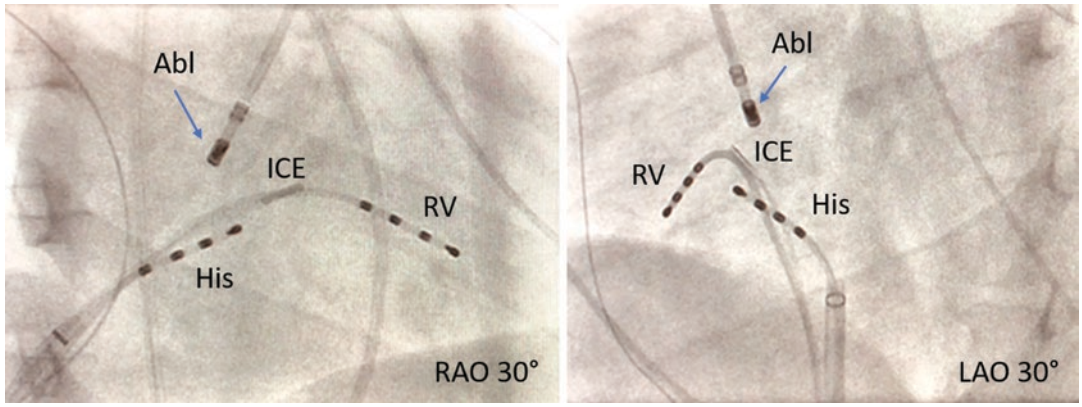

Fig. 6.11 RAO 30° and LAO 30° fluoroscopic images of the ablation catheter (Abl) targeting a parahisian AT from the non-coronary cusp, located posteriorly in RAO and right ward in LAO

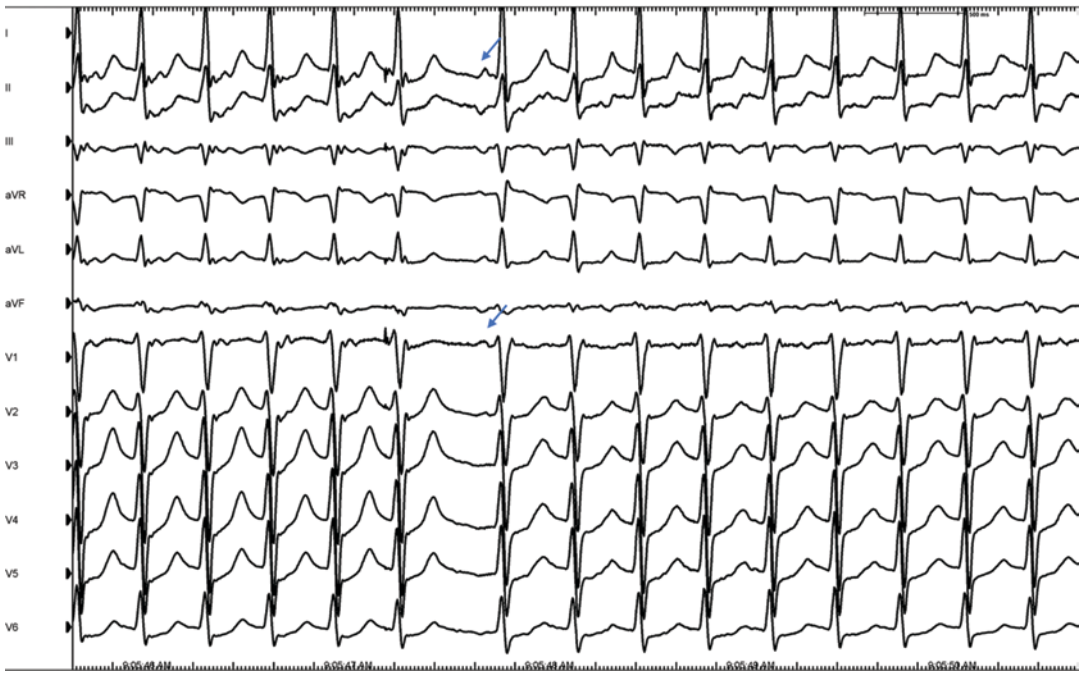

Fig. 6.12 A focal AT mapped to the CS ostium with a P-wave demonstrating an iso-pos morphology in V1 and pos morphology in lead I (blue arrows)

incessant and/or lead to tachy-cardiomyopathy (Medi et al. 2009).

The P-wave morphology of FAT originating from the PVs are positive in V1 and tend to remain positive across all precordial leads due to the posterior location. Distinction of left from right PVs relies on the knowledge that the right PVs are central structures resulting in simultaneous activation of both atria, whilst foci from the peripheral left PVs result in sequential activation of the LA followed by the RA. Accordingly, the P-waves in V1 and/or II tend to be narrow when originating from the right PVs and broader and bifid when originating from the left PVs. The superior veins have a strong inferior axis (positive P-wave in II/III/aVF), whilst the inferior

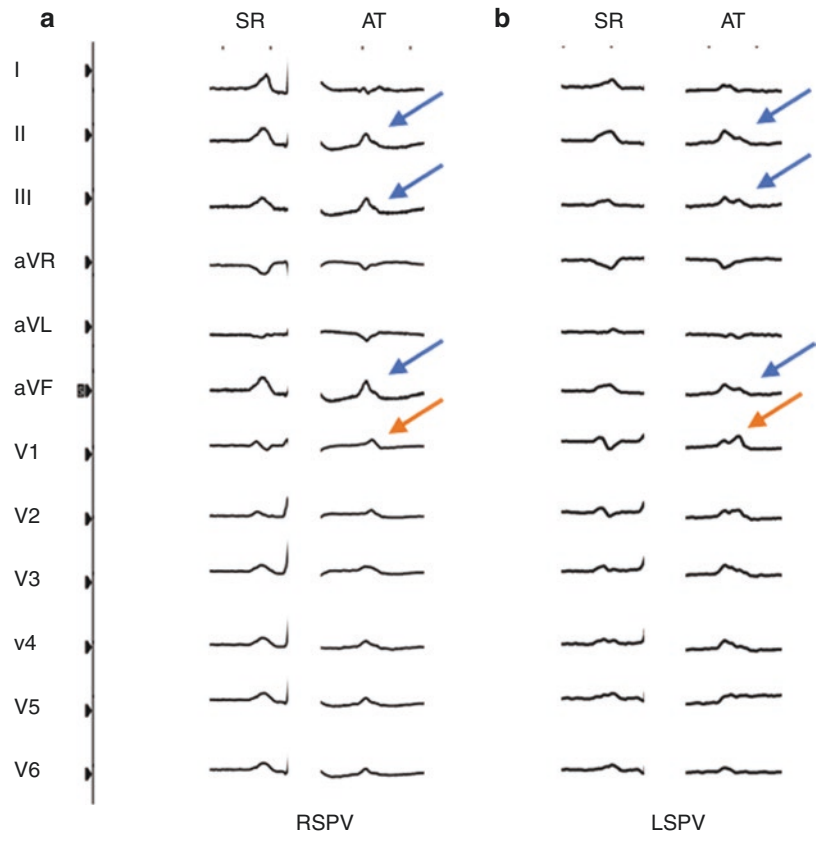

Fig. 6.13 (**a**) Example of a FAT arising from the RSPV with a positive P-wave morphology in V1 (orange arrow) and a relatively narrow (compared to sinus rhythm) and positive P-wave in the inferior leads (blue arrows). (**b**) Example of a FAT arising from the LSPV which also has positive P-waves in V1 and the inferior leads (orange and blue arrows respectively), but the P-wave is much wider and bifid due to sequential atrial (left then right) activation

veins are lower (but still relatively superior compared to other atrial structures such as the CS) and will have slightly positive or isoelectric P-waves in II/III/aVF (Fig. 6.13). As described previously, one must be cautious if the V1 P-wave during SR is positive (instead of pos-neg). In this circumstance, it is difficult to distinguish between a high crista or RSPV origin based on P-wave morphology alone.

Mitral Annular Atrial Tachycardia

The mitral annulus (MA) is a relatively uncommon site of origin for FAT. Those that have a propensity to arise do so from the superior and medial MA near the left fibrous trigone or aorto-mitral continuity (Kistler et al. 2003b). Like AT arising from the CS Os, the V1 P-waves tends to be neg-pos or iso-pos, but a negative P-wave in leads aVL/I distinguishes this site from the former.

Atrial Appendage Tachycardias

Right and left atrial appendage tachycardias are rare overall, however like PV ATs, are over-represented in patients presenting with incessant AT with or without tachy-cardiomyopathy (Medi et al. 2009).

The right atrial appendage is an anterior structure that overlies the superior TA and the basal right ventricle. As such, it has a very similar P-wave morphology to the superior TA (neg V1, transitioning to pos in V2–V4, pos II/III/aVF). The surface P-wave lacks the sensitivity to accurately distinguish between these two sites (Fig. 6.14).

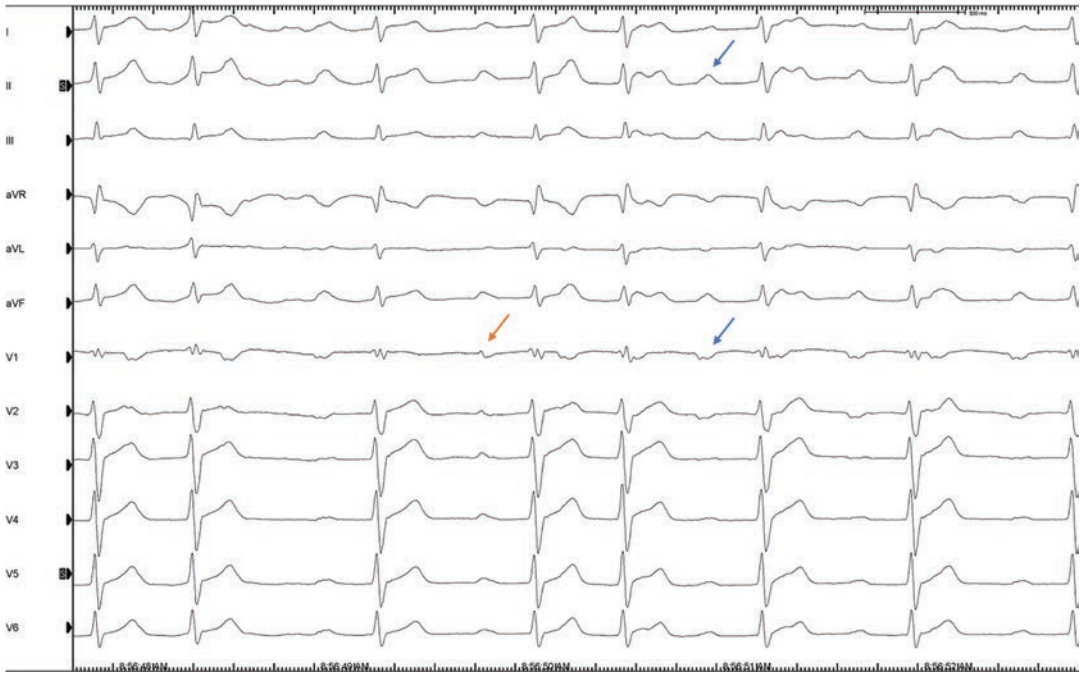

Fig. 6.14 An example of FAT mapped to the right atrial appendage in a patient with incessant arrhythmia. The P-wave is negative in V1 (orange) and positive in the inferior leads (blue arrows). Note compared to the sinus rhythm P-wave, the RAA AT P-wave is broader and notched as the RAA is further lateral than the sinus node

Left atrial appendage (LAA) FAT have a similar P-wave morphology to those originating from the LSPV (pos V1, broad bifid V1 and/or II). Again, distinction between these two structures can be challenging and both sites should be mapped. However, by virtue of being very lateral, LAA FAT tend to have deeply negative P-waves in lead I. Given the more anterior position of the LAA, the p-waves transition becomes isoelectric in V2 (Wang et al. 2007).

Endocardial ablation can be successful at both appendage sites, though irrigated catheters may be required due to limited power delivery within the corrugated appendages (Wang et al. 2007; Roberts-Thomson et al. 2007). Prior to ablation high output pacing should be performed in order to ensure that there is no capture of the respective phrenic nerves. When ablating in the atrial appendages, care must be taken to avoid perforation in these thin-walled structures.

Important Points

1. The three mechanisms of atrial tachycardia include (a) focal atrial tachycardia, (b) localized or small circuit re-entrant atrial tachycardia and (c) macro-reentrant atrial tachycardia.
2. Common sites of FAT in the right atrium include the crista terminalis and the tricuspid annulus.
3. Common sites of FAT in the left atrium include the pulmonary veins.
4. Incessant AT often arises from the pulmonary veins or the atrial appendages and can lead to tachy-cardiomyopathy.
5. In order to help decide whether an atrial tachycardia is right-sided or left-sided the most useful leads to examine are V1 and the inferior leads (II/III/aVF). A pos-

itive P-wave in V1 is very specific for left atrial sites of origin, whilst most other V1 morphologies suggest right atrial origin.
6. Excessive sedation can render FAT non-inducible and impossible to map.
7. If the P-wave morphology is not evident during sustained SVT, ventricular burst pacing should be performed to unmask the P-wave to discern morphology and onset.
8. A fiducial reference (usually a coronary sinus bipolar electrogram) should be established relative to the p-wave onset to allow for accurate activation mapping of FAT.

References

Badhwar N, Kalman JM, Sparks PB, Kistler PM, Attari M, Berger M, et al. Atrial tachycardia arising from the coronary sinus musculature: electrophysiological characteristics and long-term outcomes of radiofrequency ablation. J Am Coll Cardiol. 2005;46(10):1921–30.

Bastani H, Insulander P, Schwieler J, Tabrizi F, Braunschweig F, Kennebäck G, et al. Safety and efficacy of cryoablation of atrial tachycardia with high risk of ablation-related injuries. EP Europace. 2009;11(5):625–9.

Beukema RJ, Smit JJJ, Adiyaman A, Van Casteren L, Delnoy PPHM, Ramdat Misier AR, et al. Ablation of focal atrial tachycardia from the non-coronary aortic cusp: case series and review of the literature. EP Europace. 2014;17(6):953–61.

Haissaguerre M, Jais P, Shah DC, Takahashi A, Hocini M, Quiniou G, et al. Spontaneous initiation of atrial fibrillation by ectopic beats originating in the pulmonary veins. N Engl J Med. 1998;339(10):659–66.

Johnson N, Danilo P Jr, Wit AL, Rosen MR. Characteristics of initiation and termination of catecholamine-induced triggered activity in atrial fibers of the coronary sinus. Circulation. 1986;74(5):1168–79.

Kistler PM, Sanders P, Fynn SP, Stevenson IH, Hussin A, Vohra JK, et al. Electrophysiological and electrocardiographic characteristics of focal atrial tachycardia originating from the pulmonary veins: acute and long-term outcomes of radiofrequency ablation. Circulation. 2003a;108(16):1968–75.

Kistler PM, Sanders P, Hussin A, Morton JB, Vohra JK, Sparks PB, et al. Focal atrial tachycardia arising from the mitral annulus. Electrocardiograph Electrophysiol Charact. 2003b;41(12):2212–9.

Kistler PM, Roberts-Thomson KC, Haqqani HM, Fynn SP, Singarayar S, Vohra JK, et al. P-wave morphology in focal atrial tachycardia: development of an algorithm to predict the anatomic site of origin. J Am Coll Cardiol. 2006;48(5):1010–7.

Lai LP, Lin JL, Wu MH, Wang MJ, Huang CH, Yeh HM, et al. Usefulness of intravenous propofol anesthesia for radiofrequency catheter ablation in patients with tachyarrhythmias: infeasibility for pediatric patients with ectopic atrial tachycardia. Pacing Clin Electrophysiol. 1999;22(9):1358–64.

Liu CF, Cheung JW, Ip JE, Thomas G, Yang H, Sharma S, et al. Unifying algorithm for mechanistic diagnosis of atrial tachycardia. Circ Arrhythm Electrophysiol. 2016;9(8):e004028.

Luther V, Sikkel M, Bennett N, Guerrero F, Leong K, Qureshi N, et al. Visualizing localized reentry with ultra–high density mapping in iatrogenic atrial tachycardia. Circulation. 2017;10(4):e004724.

Lyan E, Toniolo M, Tsyganov A, Rebellato L, Proclemer A, Manfrin M, et al. Comparison of strategies for catheter ablation of focal atrial tachycardia originating near the His bundle region. Heart Rhythm. 2017;14(7):998–1005.

McGuire MA, de Bakker JM, Vermeulen JT, Opthof T, Becker AE, Janse MJ. Origin and significance of double potentials near the atrioventricular node Correlation of extracellular potentials, intracellular potentials, and histology. Circulation. 1994;89(5):2351–60.

Medi C, Kalman JM, Haqqani H, Vohra JK, Morton JB, Sparks PB, et al. Tachycardia-mediated cardiomyopathy secondary to focal atrial tachycardia: long-term outcome after catheter ablation. J Am Coll Cardiol. 2009;53(19):1791–7.

Morris GM, Segan L, Wong G, Wynn G, Watts T, Heck P, et al. Atrial tachycardia arising from the crista terminalis, detailed electrophysiological features and long-term ablation outcomes. JACC: Clin Electrophysiol. 2019;5(4):448–58.

Morton JB, Sanders P, Das A, Vohra JK, Sparks PB, Kalman JM. Focal atrial tachycardia arising from the tricuspid annulus: electrophysiologic and electrocardiographic characteristics. J Cardiovasc Electrophysiol. 2001;12(6):653–9.

Roberts-Thomson KC, Kistler PM, Haqqani HM, McGavigan AD, Hillock RJ, Stevenson IH, et al. Focal atrial tachycardias arising from the right atrial appendage: electrocardiographic and electrophysiologic characteristics and radiofrequency ablation. J Cardiovasc Electrophysiol. 2007;18(4):367–72.

Saffitz JE, Kanter HL, Green KG, Tolley TK, Beyer EC. Tissue-specific determinants of anisotropic conduction velocity in canine atrial and ventricular myocardium. Circ Res. 1994;74(6):1065–70.

Wang YL, Li XB, Quan X, Ma JX, Zhang P, Xu Y, et al. Focal atrial tachycardia originating from the left atrial appendage: electrocardiographic and electrophysiologic characterization and long-term outcomes of radiofrequency ablation. J Cardiovasc Electrophysiol. 2007;18(5):459–64.

Wellens HJ. Atrial tachycardia. How important is the mechanism? Circulation. 1994;90(3):1576–7.

Atrial Flutter

7

Kathryn L. Hong, Benedict M. Glover, and Pedro Brugada

Abstract

Atrial flutter is caused by either macro or micro re-entry circuits within either the right atrium or left atrium. It is broadly divided into either typical or atypical forms. Typical atrial flutter involves the cavotricuspid isthmus as part of the circuit with either a counterclockwise or clockwise activation. The cavotricuspid isthmus extends from the tricuspid valve to the inferior vena cava, which supports slow conduction.

Atypical atrial flutter involves non-cavotricuspid isthmus dependent circuits in the right atrium, septum or left atrium. Right atrial flutters which are not dependent on the cavotricuspid isthmus include upper loop re-entry, lower loop re-entry, right lateral wall incisional type atrial flutter and circuits around the fossa ovalis. Upper loop re-entry tends to occur around the superior vena cava with slow conduction through the upper component of the crista terminalis. Lower loop re-entry occurs around the inferior vena cava with slow conduction through the lower portion of the crista terminalis.

Left atrial flutters tend to occur around the mitral valve annulus, the ostia of the pulmonary veins or the fossa ovalis on the left side. Mitral annular flutter may propagate either in a clockwise or counterclockwise direction.

ECG analysis of the flutter wave is important in order to help localize the circuit and plan an appropriate ablation strategy for the patient as well as helping to predict the potential success of the procedure.

ECG interpretation does have its own limitations particularly in patients who have undergone prior atrial ablations or in patients with structural heart disease. The most important differentiation is between cavotricuspid isthmus dependent flutter and atypical atrial flutter as well as predict whether the circuit is in the right or left atrium (Fig. 7.1).

Cavotricuspid Isthmus Dependent Atrial Flutter

Overall this is the most common flutter circuit and should always be suspected even in cases of congenital heart disease and post atrial fibrilla-

K. L. Hong · B. M. Glover (✉)
Division of Cardiology, Department of Medicine, University of Toronto, Toronto, Ontario, Canada

P. Brugada
University Hospital of Brussel, Brussels, Belgium
e-mail: pedro@brugada.org

B. M. Glover, P. Brugada (eds.), *Clinical Handbook of Cardiac Electrophysiology*,
https://doi.org/10.1007/978-3-030-74319-2_7

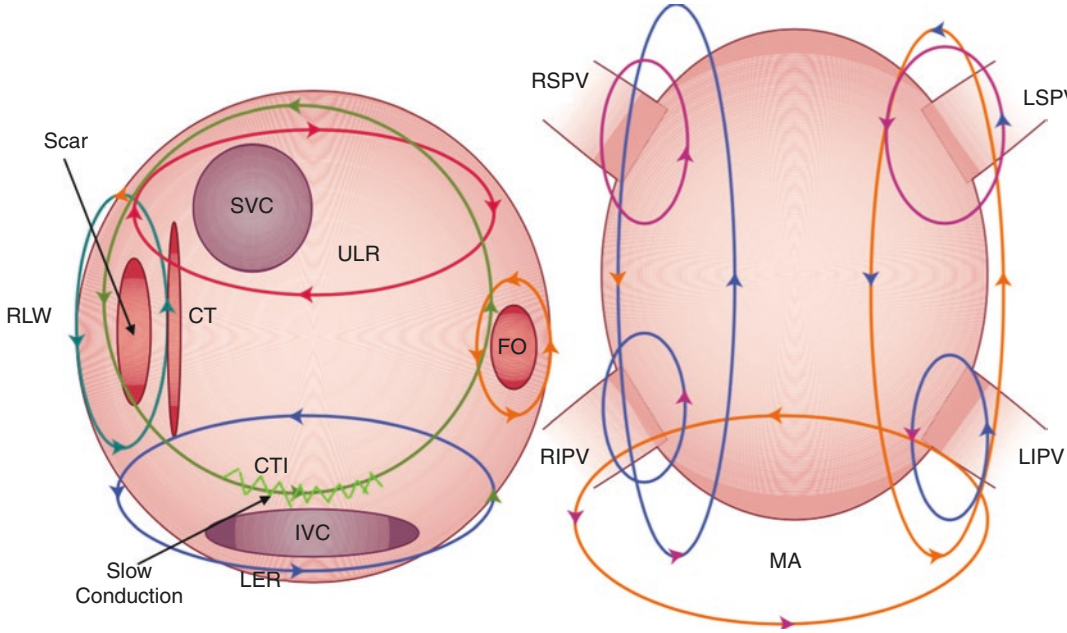

Fig. 7.1 Location of Atrial Flutters in the Right and Left Atrium. Cavotricuspid Isthmus (CTI) dependent circulates around the right atrium commonly with counterclockwise propagation (green arrows). Upper loop re-entry (ULR) rotates around the superior vena cava (SVC) with slow conduction through the crista terminalis (CT). Lower loop re-entry rotates around the inferior vena cava (IVC) also involving the crista terminalis (CT). Re-entry may also occur around the right lateral wall (RLW) often in post surgical cases where this is related to an incision as well as around the fossa ovalis (FO). In the left atrium atrial flutter may occur around the mitral annulus (MA) in either a clockwise or counterclockwise direction as well as around the pulmonary veins (*LSPV* left superior pulmonary vein, *LIPV* left inferior pulmonary vein, *RSPV* right superior pulmonary vein, *RIPV* right inferior pulmonary vein)

tion ablation, even if the ECG does not look typical.

Anatomy

The cavotricuspid isthmus is an important anatomical structure which acts as an area of slow conduction. As seen in the anatomic image in Fig. 7.2 it is located posteriorly to the tricuspid annulus and anteriorly to the Eustachian valve at the junction of the right atrium and the inferior vena cava. The coronary sinus is superior and medial to the cavotricuspid isthmus. During mapping and ablation of the cavotricuspid isthmus the catheter is generally positioned at 6 o'clock in an LAO projection (Fig. 7.3) which is the mid segment and is considered the thinnest portion where ablation can generally be performed. Moving towards the septum this region is shorter in distance but thicker where the fibers merge with the coronary sinus. Inferolaterally it is broader and thicker. The anterior aspect at the tricuspid annulus is muscular while the posterior component at the junction with the inferior vena cava has minimal muscle and is generally fibrofatty tissue. The cavotricuspid isthmus elevates into the eustachian ridge and this divides it into two components: the sub-eustachian isthmus (between the eustachian ridge and the tricuspid valve) and the crest of the eustachian ridge to the inferior vena cava, separated from the compact AV node by the coronary sinus.

Although the mid cavotricuspid isthmus is the thinnest component and therefore the best target for ablation the anatomy is variable: muscular fibers in this region result in irregularities which extend inferiorly and laterally from the coronary sinus wall or medially and superiorly from the crista terminalis. Between the muscular structures

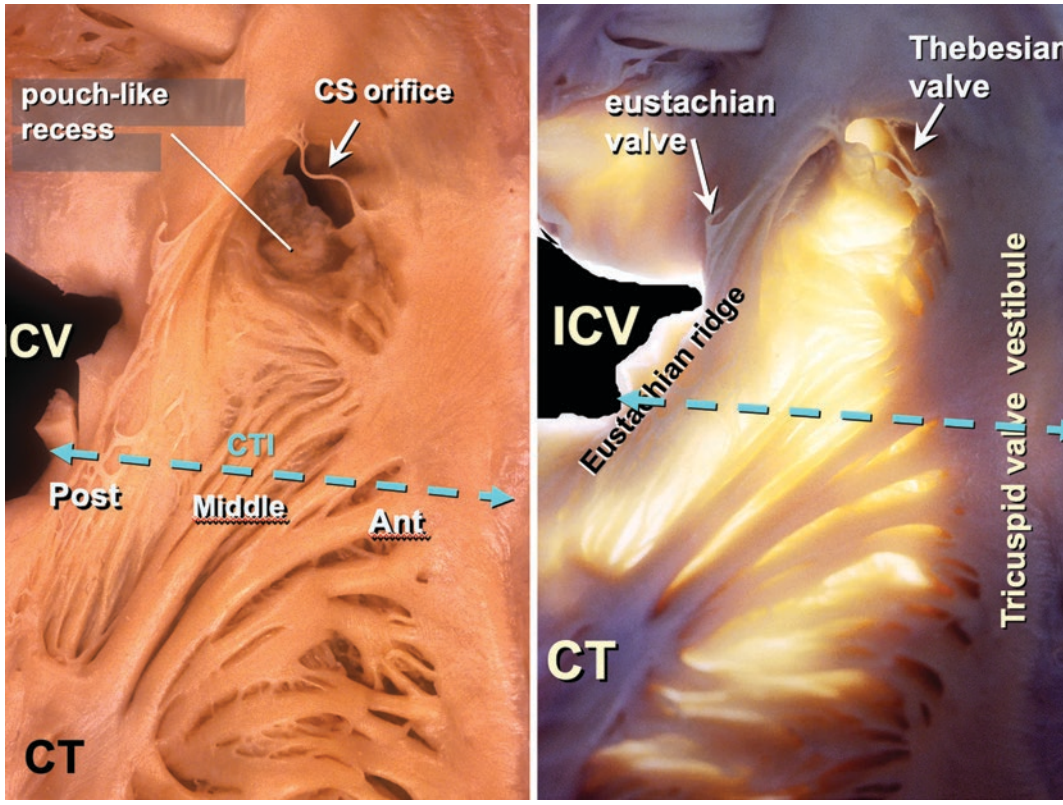

Fig. 7.2 Anatomical location of the cavotricuspid isthmus (CTI) showing the anterior, middle and posterior portions on the left as well as the coronary sinus (CS) orifice and a pouch like recess. This is also shown with transillumination showing the demarcation of the pectinate muscles. Also shown is the crista terminalis (CT), eustachian ride, eustachian valve and thebesian valve

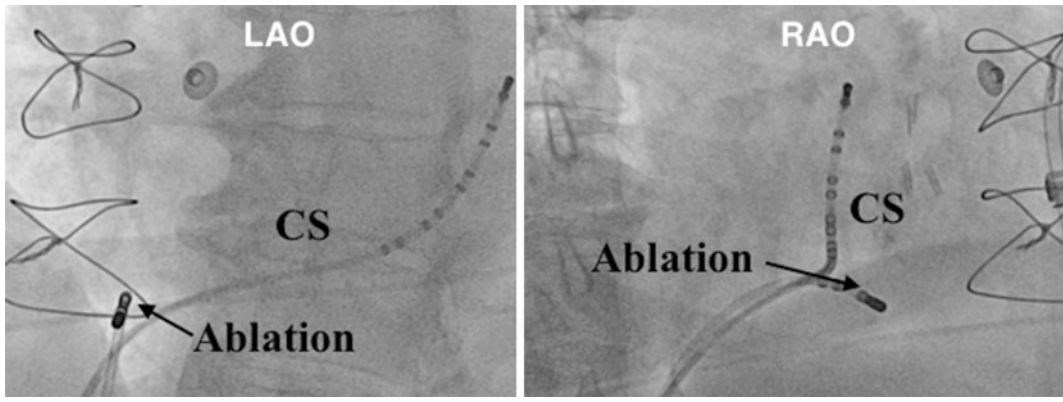

Fig. 7.3 Fluoroscopic image of the catheter location in the mid CTI in an LAO (left) and RAO (right) projection. The ablation catheter is positioned along the mid CTI. There is a 10 pole catheter positioned in the coronary sinus (CS)

are thin membranes. Often these muscular fibres overlap at their superomedial and inferolateral origins and therefore in theory the most parallel segment is the medial cavotricuspid isthmus. The muscular fibers which pass through the cavotricuspid isthmus are of different sizes and therefore have different conduction properties. Narrower fibers in the mid isthmus tend to conduct more slowly than broader fibers in the septal and lateral positions.

ECG Features

Cavotricuspid isthmus dependent atrial flutter tends to have a saw tooth type appearance observed in the inferior leads and V1. The most common direction of conduction is counterclockwise which accounts for approximately 90% of cases. As shown in Fig. 7.4 this result's in negative flutter waves in the inferior leads with an initial gradual and then steep downslope followed by a steep upslope and then a gradual downslope to baseline. The flutter wave is positive in V1 in counterclockwise activation with a gradual transition from V1 to V6 from positive to isoelectric to negative.

Clockwise (reversed) cavotricuspid isthmus dependent atrial flutter accounts for approximately 10% of cases of typical atrial flutter. The activation sequence is the reverse of typical counterclockwise atrial flutter. The inferior leads therefore demonstrate a broad positive with a negative flutter wave in V1. There is a transition from V1 to V6 from negative to isoelectric to positive.

Ablation of the CTI for Typical Atrial Flutter

In general this can be performed with two catheters. A quadripolar or decapolar catheter is positioned in the coronary sinus while an ablation catheter can be used for ablation and mapping. Some operators use a multipolar catheter in the right atrium in order to help assess the activation sequence during the atrial flutter as well as to assess for isthmus block at the end of the procedure. This catheter may be positioned in order to map the septum with the proximal electrodes and the lateral wall of the right atrium with the distal electrodes and the mid electrodes spanning across the right atrial roof. The distal electrodes can also

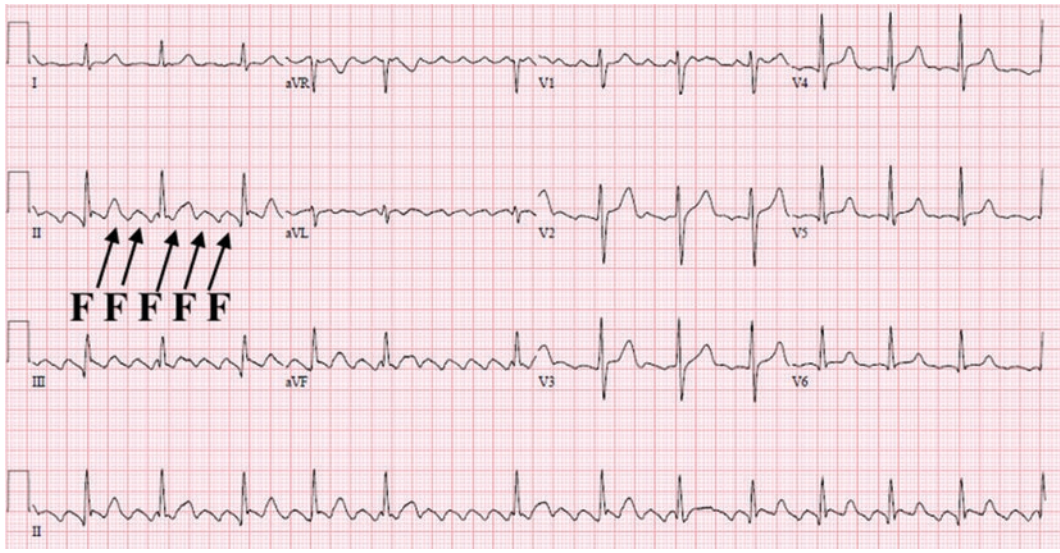

Fig. 7.4 ECG of counterclockwise cavotricuspid isthmus depedent atrial flutter. The flutter waves are negative in the inferior leads II. III and aVF implying activation from inferior to superior in the right atrium

be positioned in the proximal coronary sinus with the mid poles spanning the cavotricuspid isthmus and the proximal poles spanning from the high to low right atrium along the crista terminalis in order to assess for bidirectional block at the end of the ablation. This is generally not required and can often lead to diagnostic errors if the catheter is not positioned exactly as described above.

A range of ablation catheters may be considered for ablation of the cavotricuspid isthmus ranging in size from 4 to 10 mm as well as the possibility of irrigation versus non-irrigation of the tip. The choice is operator dependent and generally a large curve is used in order to ensure adequate reach of the ventricular side of the isthmus.

It is our practice to use a decapolar catheter in the coronary sinus and a 4 mm irrigated catheter for ablation. A quadripolar catheter may be considered for back up right ventricular pacing in certain cases where the patient is in atrial flutter and there is a suspicion that the patient may develop bradycardia following termination of the arrhythmia.

The ablation catheter is normally positioned at the tricuspid annulus so that the atrial and ventricular electrograms are of equal amplitude. In the LAO projection the ablation catheter is at the 6 o' clock position where the cavotricuspid isthmus is at its narrowest. A more medial position increases the risk of AV block and potential ablation within the middle cardiac vein. A more lateral position generally requires a longer ablation line.

If the patient is in atrial flutter entrainment should be performed from this location at a rate 20 ms faster than the tachycardia cycle length looking for a PPI—TCL of less than 30 ms. An example of this is shown in Fig. 7.5. This patient presented with an atrial flutter following a prior PVI for AF. The tachycardia cycle length was 348 ms. Pacing from the ablation catheter which was positioned along the cavotricuspid isthmus was performed at 320 ms. The PPI was 348 ms which was exactly the same as the tachycardia cycle length indicating that the cavotricuspid isthmus was a part of the circuit.

While pacing from the cavotricuspid isthmus the stimulation to onset of atrial activation is generally quite long due to the slow conduction in the isthmus. This is obviously much shorter on the septal side of the isthmus.

Power settings for a 4 mm irrigated catheter are usually 30–40 W. The temperature limit is generally set at 60 ° C for non-irrigated catheters. Larger 8-mm tip catheters require a higher power often up to 70 W with a maximum temperature of 60 °C. Following a period of 60–90 s and with significant diminution of the local signal the catheter is moved to a more proximal location. Ablation can be performed either as a point by point technique or a continuous dragging technique from the tricuspid annulus to the junction with the inferior vena cava spending 60–90 s at each position looking for a reduction in local electrogram voltage. Some operators use lack of unipolar pacing to assess whether a lesion has

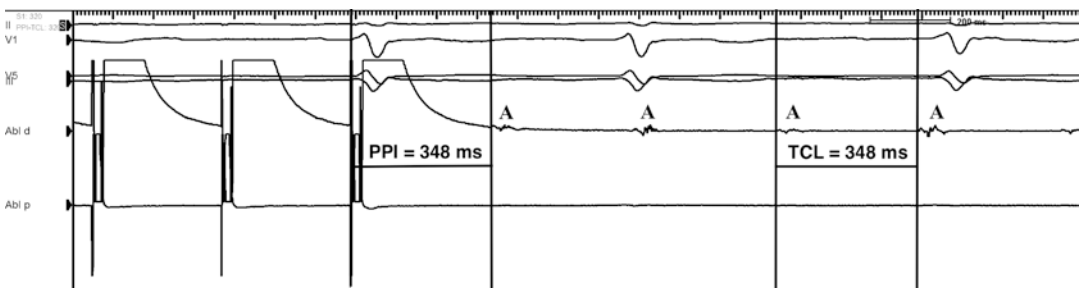

Fig. 7.5 PPI—TCL in Atrial Flutter during and after entrainment from the CTI. This patient presented with atrial flutter following a prior ablation for atrial fibrillation. The tachycardia cycle length was 348 ms. Pacing was performed from the ablation catheter which was positioned along the CTI at 320 ms. The post pacing interval was 348 ms. This was exactly the same as the tachycardia cycle length implying that the CTI was a critical component to the circuit

been created prior to moving onto a more proximal location where capture occurs and further ablation is performed in this location. Often atrial flutter terminates prior to the development of bidirectional block across the CTI. If bidirectional block does not occur the same line can be repeated on a more medial or lateral position.

If the patient is in sinus rhythm at the start of the procedure ablation can be performed during proximal coronary sinus pacing assessing for double potentials along the ablation line (Shah et al. 1997, 1999). The proximal coronary sinus is generally paced at a cycle length of 600 ms and the ablation catheter is moved along the ablation line from the ventricular aspect to the junction with the inferior vena cava. The first potential is recorded from the medial aspect of the line while the second component is lateral to the line. As shown in Fig. 7.6 an interval of greater than 110 ms with minimal variability is generally associated with conduction block across the ablation line (Tada et al. 2001). As shown in Fig. 7.7 this can be reversed so that pacing is performed lateral to the ablation line and the interval between this and the proximal coronary sinus can be measured. This is recorded and the ablation catheter is moved further away from the cavotricuspid ablation line and pacing performed. If moving further from the ablation line results in a shorter stimulation to proximal coronary sinus activation then this likely represents counterclockwise block.

When pacing from the proximal CS an interval of less than 90 ms indicates intact conduction across the line.

As shown in Fig. 7.8 the delay from the onset of the first to the second potential is 40 ms. The line between the two potentials is also not isoelectric. This represents intact conduction across the CTI.

If the interval between the two potentials is between 90–110 ms then the electrograms should be examined further. Features indicative of block include an isoelectric line between the first and

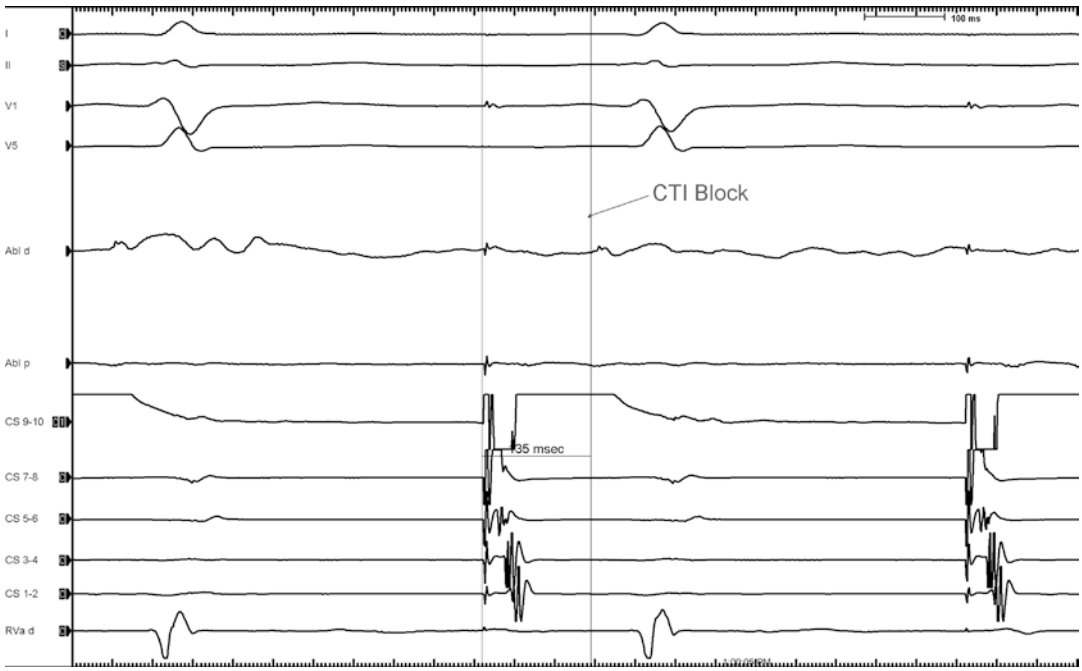

Fig. 7.6 Pacing is performed from the proximal CS (CS 9–10) at a rate of 600 ms. The ablation catheter is positioned along the CTI so that it is recording activation medial to the CTI line seen as the first deflection followed by an isoelectric line and then another atrial activation lateral to the CTI 135 ms later. This represents clockwise block across the CTI. CS 1–2 is located in the distal coronary sinus, RVa d is located in the RV apex

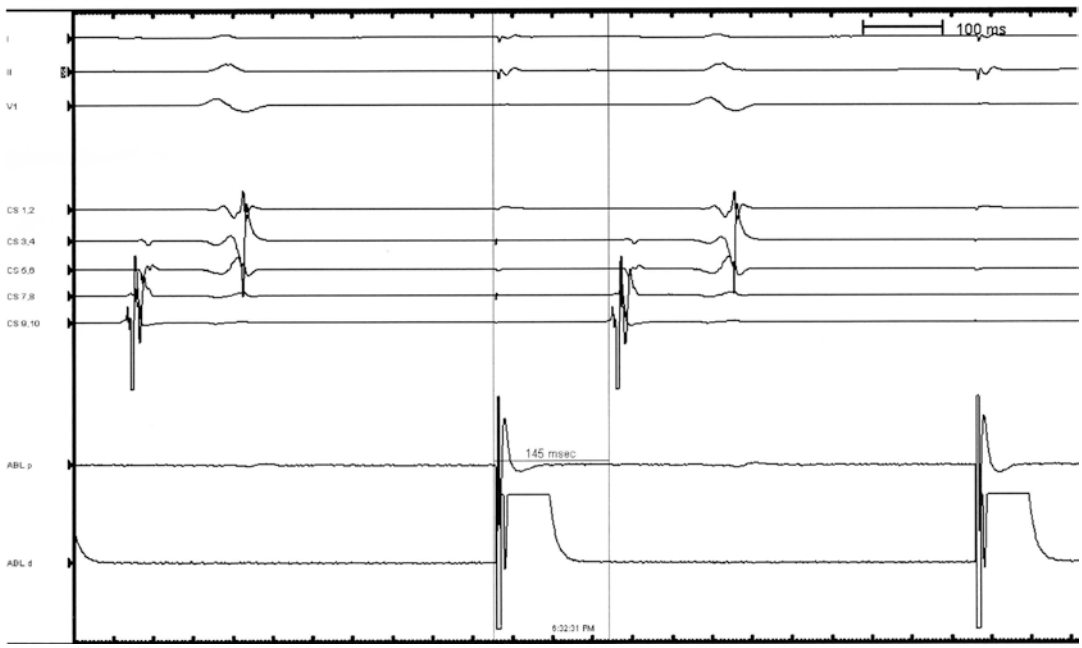

Fig. 7.7 Pacing is performed lateral to the ablation line and the stimulation to proximal CS (CS 9–10) is recorded as 145 ms representing a significant delay. The ablation catheter is moved more superior and lateral to this point and pacing is performed with a delay from stimulation to proximal CS activation of 128 ms (not shown in this image). This is suggestive of counterclockwise block across the CTI. CS 1–2 is positioned in the distal coronary sinus

the second component of the double potential with a negative second potential. The interval between the first and second components of the potentials is generally isoelectric in the presence of block. If this has a fractionated aspect or low amplitude signals there is generally slow conduction across the line.

In the presence of block the second component of the double potential is negative as a result of a change in the polarity of the activation wavefront. The change from positive to negative should be noted on completion of the gap.

The closer to a gap the shorter the distance between the two components. Wider splitting of the double potentials implies a distance further from the gap.

As shown in Fig. 7.9 where the ablation catheter is positioned on the cavotricuspid isthmus while pacing from the proximal CS. The duration from the pacing spike on the proximal CS to the onset of the second potential is 182 ms. The delay from the onset of the first potential to the onset of the second potential is 94 ms. There is a clear isoelectric line between the potentials and the second component is negative. This represents clockwise block across the CTI.

Decremental Pacing

This technique is useful in cases where it is difficult to make a conclusion based on intermediate double potentials (Bazan et al. 2010). Ablation is performed along the cavotricuspid isthmus until double potentials are noted. Pacing is then performed from the proximal coronary sinus at 600 down to 250 ms while the ablation catheter is used to record double potentials along the ablation line. If the second component of the double potential does not increase by more than 20 ms with decremental pacing then this demonstrates clockwise block. This is then repeated from the lateral right atrial wall in order to prove counterclockwise block. A change in the second compo-

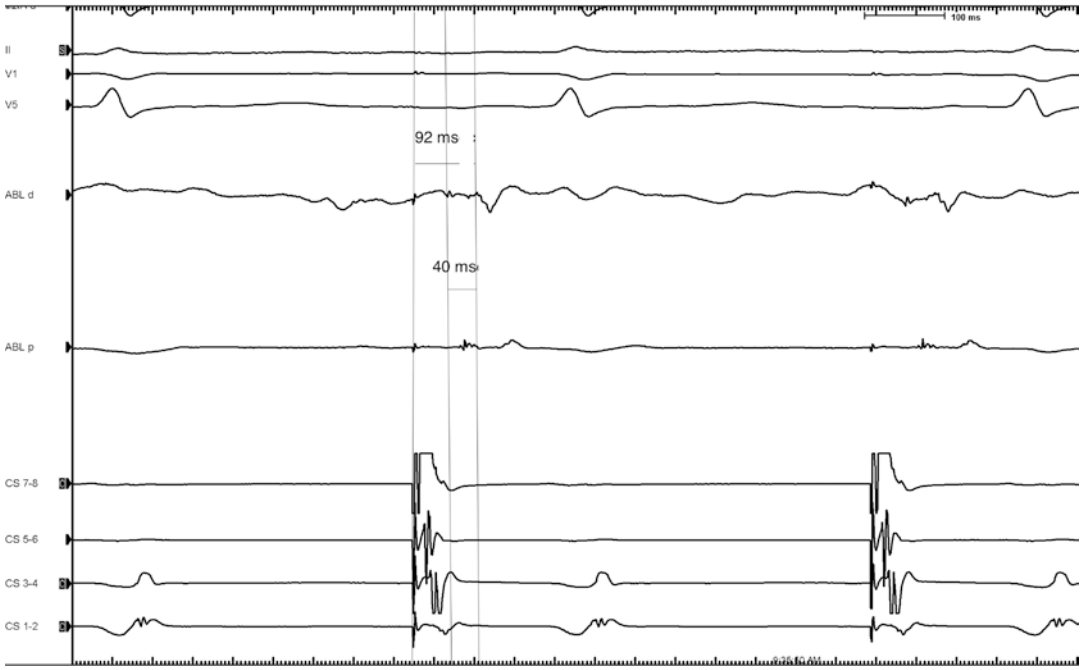

Fig. 7.8 Pacing is performed from the proximal CS (CS 7–8) with the ablation catheter positioned on the CTI. Double potentials are recorded on the ablation catheter. The first potential represents atrial activation medial to the CTI ablation line. The second component represents activation lateral to the CTI ablation line. The time from the proximal CS stimulation to the lateral atrial activation is recorded as 92 ms. The delay from the onset of the first potential to the onset of the second potential is 40 ms. The interval between the two potentials is not isoelectric. This represents intact conduction across the ablation line. CS 1–2 is positioned in the distal coronary sinus

nent by more than 20 ms with incremental pacing implies conduction through the CTI. A diagrammatic representation of this is shown in Fig. 7.10.

Decremental His to Coronary Sinus Pacing

This is a modification of differential pacing in which pacing is performed from lateral to the CTI ablation line and activation of the atrial electrogram in the His region is compared with activation of the atrial electrogram in the proximal coronary sinus electrogram (Valles et al. 2013).

When pacing from the lateral lower right atrium when conduction across the CTI is intact activation occurs in a counterclockwise fashion across the isthmus, via the posteroseptal region followed by activation of the coronary sinus. Activation anterior to the tricuspid annulus results in atrial activation of the His region. Following CTI ablation anterior activation still occurs and the His is still activated which then spreads to coronary sinus which results in an increase in the His—CS timing of >40 ms from baseline. In the presence of CTI block the His to CS timing does not change significantly as activation occurs on the same rather than two pathways.

The advantage of this is that it does not rely on the accurate identification of double potentials which may be difficult to identify. This appears to be an effective strategy in helping to prove block across the CTI.

An Alternative Ablation Technique: Maximum Voltage Guided Ablation

Given that different fibers of muscular have different orientations, dimensions and conduction properties there may be discrete regions with

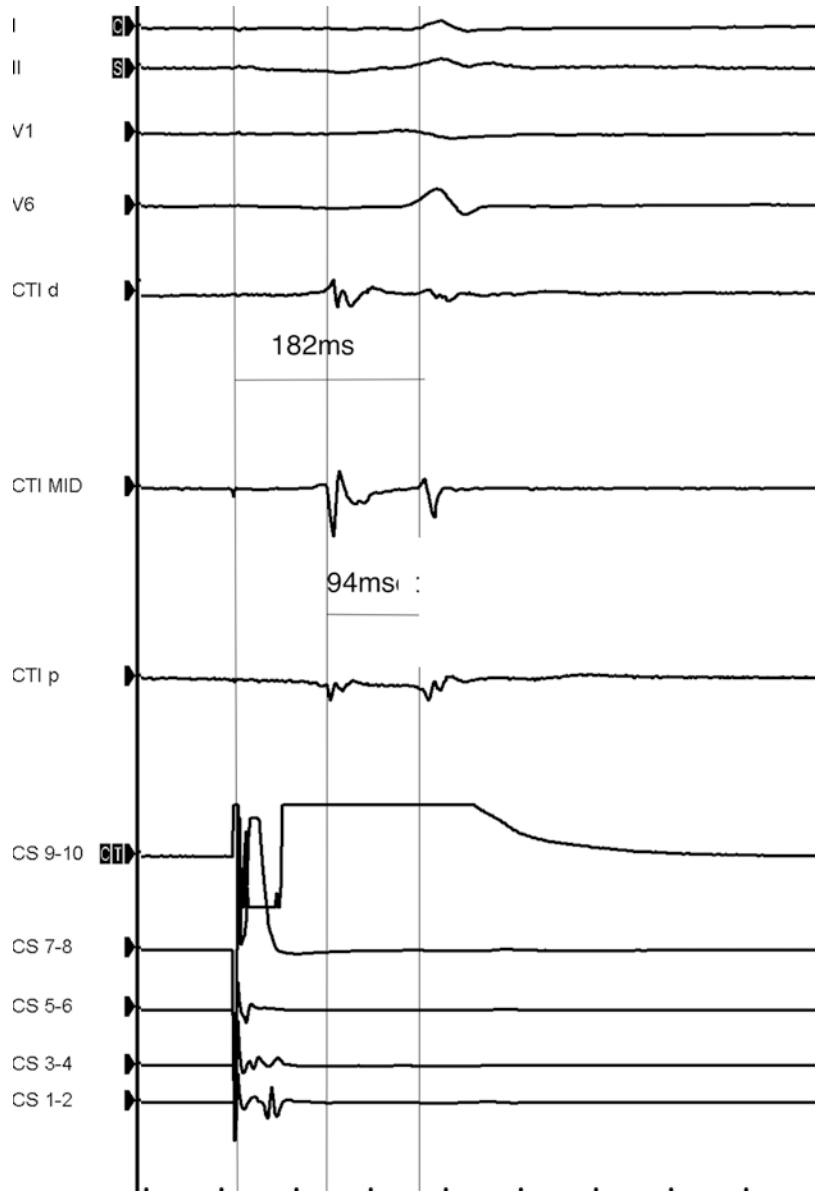

Fig. 7.9 Clockwise block across the CTI. Pacing is performed from the proximal CS (CS 9–10) while the ablation catheter is positioned along the CTI. The duration from the pacing spike to the onset of the second potential is 182 ms. The time from the onset of the first to the onset of the second potential is 94 ms. The line between both potentials recorded on ablation distal (CTId), middle (CTImid) and proximal (CTIp) is isoelectric. The second component of the double potential is negative on the ablation catheter. These features are suggestive of clockwise block across the CTI. CS 1–2 is positioned in the distal coronary sinus

high voltage electrograms which can be selectively targeted for ablation.

As shown in Fig. 7.11 pacing is performed at 600 ms from the proximal coronary sinus while the ablation catheter is moved from the ventricular of the CTI to the inferior vena cava. The region of highest bipolar voltage is noted and RF delivered in this region for 60 s or shorter if the local potential reduces by more than 50% from baseline (Ozaydin et al. 2003).

Following this the CTI is remapped looking for the maximum signal and ablated in a similar fashion. This is repeated until bidirectional block is obtained.

This technique appears to be as successful as a conventional line with reduced procedural and fluoroscopy time (Gula et al. 2009).

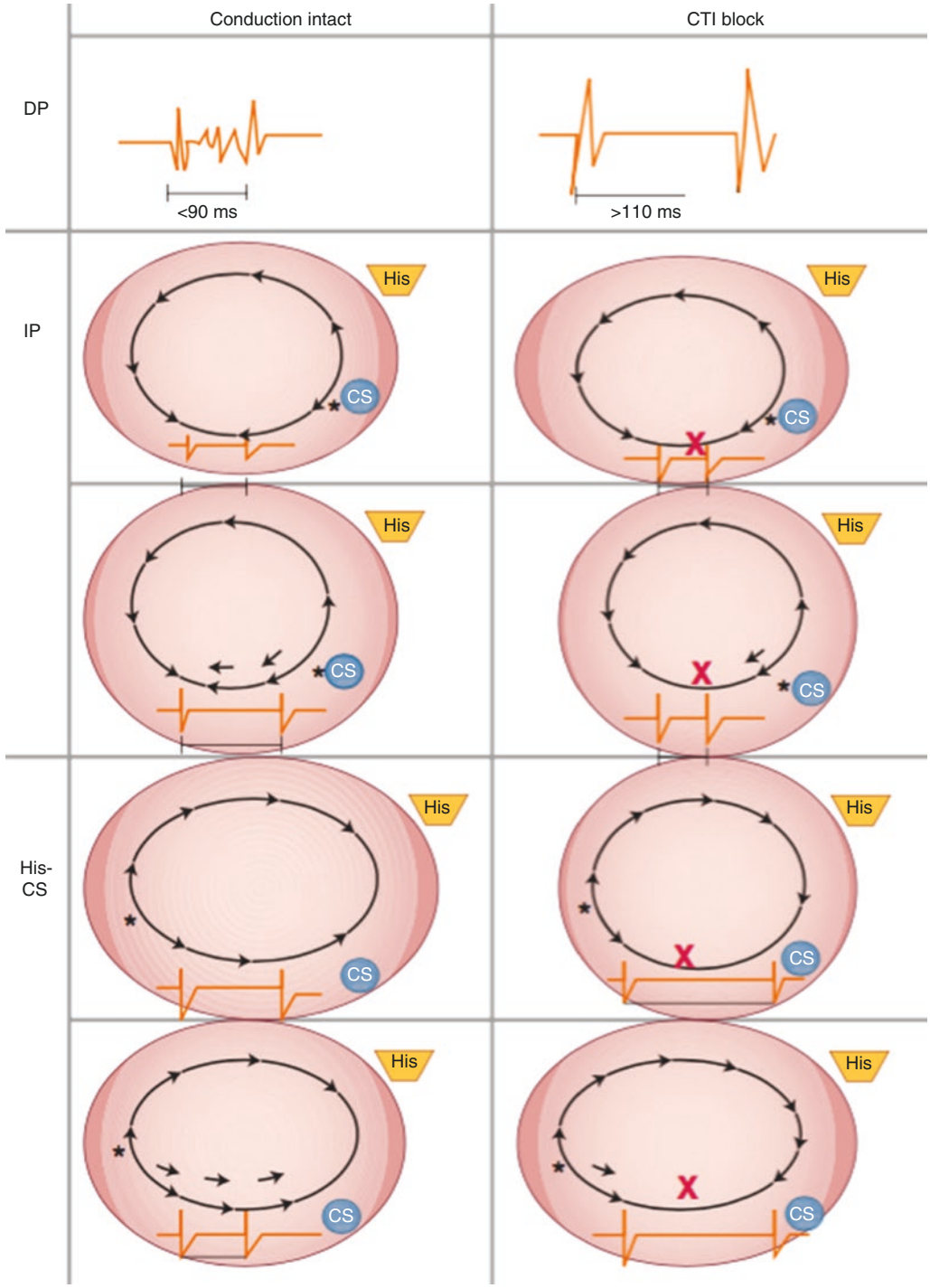

Fig. 7.10 Maneuvers used to prove CTI block. The presence of double potentials with an isoelectric line between potentials of greater than 110 ms is indicative of block across the CTI. Incremental pacing from the CS results in an increase in the separation of the double potentials by greater then 20 ms if CTI conduction is intact. If the CTI line is blocked then there is no significant change with incremental pacing from the CS (middle images). Alternatively the atrial signal can be recorded on the His and CS with pacing from the low lateral right atrial wall. If CTI conduction is intact the double potentials narrow with incremental pacing while if the CTI is blocked the potentials separate further but do not decrement with incremental pacing

Fig. 7.11 Maximum voltage guided ablation of the CTI. Pacing is performed at 600 ms from proximal CS. A 20 pole catheter (labeled Spi) is positioned in the RA showing earliest activation in the proximal and distal poles and subsequent activation across the RA with no evidence of block across the CTI. The ablation catheter is positioned along the CTI and is recording the region of maximum voltage which in this cases is recorded as 1.81 mV. CS 9–10 is positioned in the proximal coronary sinus with CS 1–2 in the distal CS

Potential Complications of Cavotricuspid Isthmus Ablation

There is a risk of AV block if the ablation performed is septal. This is close to zero if a lateral line is performed. Although the risk of thromboembolism is very low, the patient should be anticoagulated if they are in atrial flutter at the start of the procedure, either with heparin or with continuation of full anticoagulation. Like all catheter ablations there is always a risk of groin hematoma and cardiac perforation.

The risk of coronary artery damage, and in particular the PDA, is very unlikely.

Difficult CTI Ablation

Although the majority of cavotricuspid isthmus ablations are relatively straightforward variability in anatomy may result in technical difficulties. The most common of these are difficulty in reaching the ventricular end of the isthmus which is overcome with a long sheath or persistent conduction at the junction between the right atrium and the inferior vena cava which generally requires catheter manipulation.

Additional issues which may not be obvious include prominent pectinate muscles, a prominent Pouch of Keith or prominent Eustachian ridge.

Prominent pectinate muscles in the region of the isthmus may impair the ability to create a line of block. It may be seen on the ablation catheter as large amplitude electrograms. In order to deal with this issue, either a more medial line of ablation can be performed or an irrigated catheter can be considered in order to achieve a deeper lesion.

The Pouch of Keith is located along the isthmus and lateral to the Thebesian valve at the CS orifice. Although this is generally a slight ridge in most patients, occasionally it may be a deep outpouching with poor blood flow, meaning that either the catheter does not make sufficient con-

tact or, if it does, power delivery is not sufficient to result in a satisfactory ablation line. A prominent Thebesian valve may be a clue to the Pouch of Keith. In order to deal with this problem the isthmus line can be made more laterally.

The Eustachian ridge is a fibrous structure which generally has no impact in an isthmus ablation but if very prominent may actually affect the rotation of the ablation catheter. This means that if the catheter is rotated in a clockwise manner towards the septum, the Eustachian ridge may cause a counter-clockwise rotation away from the septum. In order to counteract this issue a long sheath can be used.

Success of Cavotricuspid Isthmus Ablation

The overall success for an isthmus dependent atrial flutter is approximately 90%, provided bidirectional block has been demonstrated at the end of the ablation. The bigger issue is the occurance of atrial fibrillation where the reported rate is as high as 82% after 39 months in patients with isolated atrial flutter and no other arrhythmias (Ellis et al. 2007).

Upper and Lower Loop Re-Entry

Upper loop re-entry occurs around the superior vena cava with a breakthrough in a gap in the crista terminalis. It often has a similar ECG appearance to clockwise cavotricuspid isthmus dependent flutter with positive flutter waves in the inferior leads. In order to help distinguish upper loop re-entry from clockwise cavotricuspid isthmus dependent flutter lead I can be examined. If the flutter wave in lead I is negative or isoelectric then it is more likely to be upper loop re-entry. If the flutter wave in lead I is positive it may be either. If the flutter wave is less than or equal to 0.07 mV in amplitude then it is more likely to be a result of upper loop re-entry (Yuniadi et al. 2005). As the circuit is shorter the tachycardia cycle length is often shorter than typical atrial flutter. It may occur as a result of typical atrial flutter or atrial fibrillation. If entrainment in this region is suggestive for an upper loop re-entry then ablation can be performed at the upper gap along the superior crista terminalis as this may be the narrowest part of the circuit.

Lower loop re-entry uses the cavotricuspid isthmus as part of its circuit but breaks through a gap in the lower portion of the crista terminalis. It is generally counterclockwise and therefore could be confused with typical counterclockwise atrial flutter. As it breaks through at a lower level along the lateral right atrial wall the flutter waves in the inferior leads tend to be less positive and the tachycardia cycle length in general is shorter. Ablation along the cavotricuspid isthmus should result in termination of this tachycardia.

Right Atrial Lateral and Postero-Lateral Wall Flutter

This may occur around areas of scar or low voltage areas such as in patients who have had prior cardiac surgery. It has a variable appearance on ECG depending on the conduction properties in this region, the direction of the circuit and subsequent activation of the right atrium. Right atrial flutter originating from the lateral wall may often resemble cavotricuspid isthmus dependent flutter. The flutter wave is generally negative in V1. Right atrial flutter involving the septum tends to have an isoelectric or biphasic flutter wave in V1. In general these flutters require detailed mapping looking for regions of scar as well as the activation sequence. Entrainment should help to determine whether the region being mapped is part of the circuit although it may often be difficult to capture due to the presence of scar and low amplitude signals. Certain ablation lines can be performed. For lateral circuits on the lateral wall a line can be made from the region of scar to either the superior or inferior vena cava. If this is performed mapping of the right phrenic nerve should be performed prior to delivery of ablation energy.

Left Atrial Flutter

In order to differentiate a right from a left sided atrial flutter on ECG the most useful lead to examine is V1. If the **initial segment of the flutter wave is negative or isoelectric followed by a positive deflection or the entire flutter wave is negative it is more likely to be right sided while a positive flutter wave is more likely to be left sided**. If the entire flutter wave in V1 is isoelectric it is difficult to localize the flutter to either right or left sided. In left sided atrial flutters as well as these changes noted in V1 the flutter waves in the inferior leads tend to be positive but of low amplitude, generally a reflection of the underlying substrate.

The most simplistic way to distinguish left atrial flutter from atrial tachycardia is to assess the onset and termination of the tachycardia. Re-entry atrial flutter tends to be of acute onset and termination while focal atrial tachycardia tends to accelerate at the onset of the tachycardia and decelerate at the termination of the tachycardia.

Most left atrial flutter circuits either revolve around the mitral annulus in either a clockwise or counterclockwise direction or around the pulmonary veins.

Mitral Isthmus Dependent Atrial Flutter

This circulates around the mitral annulus in either a clockwise or counterclockwise direction and traverses the mitral isthmus. The relevant anatomy is demonstrated in Fig. 7.12. The mitral isthmus is posterior to the mitral annulus and anterior to the left atrial posterior wall. Mitral isthmus dependent flutter may occur following pulmonary vein isolation and in particular as a result of ablation lesions inferior and slightly anterior to the left inferior pulmonary vein.

In order to perform a mitral isthmus line a catheter is positioned in the coronary sinus so that the distal electrodes are slightly posterior to the line. An ablation catheter is then positioned along the lateral mitral annulus with an A:V ratio of 1:2 at 4 o'clock in the LAO 30 view. In general a 4 mm irrigated catheter may be used with a power setting of 40 W at the annulus which can then be reduced to 30 W at the inferior pulmonary vein side. In order to move the catheter from the annulus which is anterior to the left inferior pulmonary vein which is posterior, clockwise rotation is applied to the ablation catheter. Following completion of the line pacing can be performed from either the distal coronary sinus or the left atrial appendage to confirm conduction.

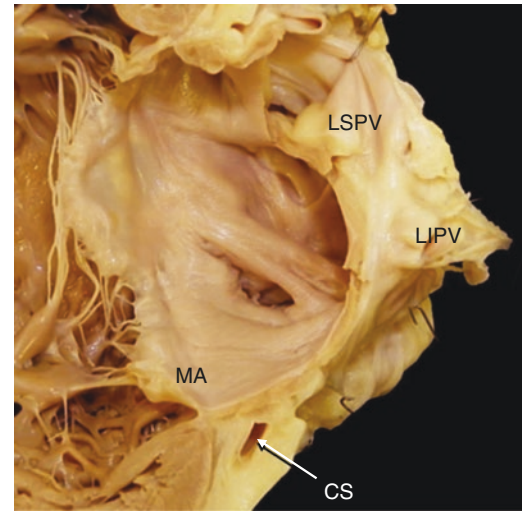

Fig. 7.12 Anatomical image showing the location of the mitral isthmus between the mitral annulus (MA) and the left inferior pulmonary vein (LIPV). The coronary sinus (CS) is also shown in close proximity to the MA

If conduction persists then further mapping can be performed looking for early atrial signals during pacing from the left atrial appendage. If conduction persists despite this then ablation can be performed in the coronary sinus in the same location as the endocardial lesions with flexion towards the endocardial mitral isthmus lesions at 25 W.

In order to prove block across the mitral isthmus line pacing can be performed from the left atrial appendage which is anterior to the line and the activation sequence examined in the coronary sinus catheter. Clockwise block is demonstrated by an activation from the proximal to the distal coronary sinus indicating counterclockwise acti-

vation around the mitral annulus. It is possible to electrically isolate the coronary sinus with resultant proximal to distal activation which may mimic isthmus block. Counterclockwise block is demonstrated by pacing from the distal coronary sinus which is posterior to the mitral isthmus line. Activation therefore occurs from the distal coronary sinus electrodes to proximal prior to activation of the left atrial appendage.

Additionally the ablation catheter can be moved along the mitral line during pacing from either the left atrial appendage or the distal coronary sinus looking for the presence of double potentials.

References

Bazan V, Marti-Almor J, Perez-Rodon J, et al. Incremental pacing for the diagnosis of complete cavotricuspid isthmus block during radiofrequency ablation of atrial flutter. J Cardiovasc Electrophysiol. 2010;21:33–9.

Ellis K, Wazni O, Marrouche N, et al. Incidence of atrial fibrillation post-cavotricuspid isthmus ablation in patients with typical atrial flutter: left-atrial size as an independent predictor of atrial fibrillation recurrence. J Cardiovasc Electrophysiol. 2007;18:799–802.

Gula LJ, Redfearn DP, Veenhuyzen GD. Reduction in atrial flutter ablation time by targeting maximum voltage: results of a prospective randomized clinical trial. J Cardiovasc Electrophysiol. 2009;20:1108–12.

Ozaydin M, Tada H, Chugh A, et al. Atrial electrogram amplitude and efficacy of cavotricuspid isthmus ablation for atrial flutter. Pacing Clin Electrophysiol. 2003;26:1859–63.

Shah DC, Haissaguerre M, Jais P, et al. Simplified electrophysiologically directed catheter ablation of recurrent common atrial flutter. Circulation. 1997;96:2505–8.

Shah DC, Takahashi A, Jais P, et al. Local electrogram-based criteria of cavo-tricuspid isthmus block. J Cardiovasc Electrophysiol. 1999;10:662–9.

Tada H, Oral H, Sticherling C, et al. Double potentials along the ablation line as a guide to radiofrequency ablation of typical atrial flutter. J Am Coll Cardiol. 2001;38:750–5.

Valles E, Bazan V, Benito B, et al. Incremental His-to-coronary sinus maneuver: a nonlocal electrogram-based technique to assess complete cavotricuspid isthmus block during typical flutter ablation. Circ Arrhythm Electrophysiol. 2013;6:784–9.

Yuniadi Y, Tai CT, Lee KT, et al. A new electrocardiographic algorithm to differentiate upper loop re-entry from reverse typical atrial flutter. J Am Coll Cardiol. 2005;46:524–8.

Atrial Fibrillation

8

Michel Haissaguerre, Benedict M. Glover, and Pedro Brugada

Abstract

AF is the most common sustained arrhythmia seen in clinical practice with an overall prevalence of 700–750 per 100,000 of the population in North America (Chugh et al., Circulation 129:837–847, 2014). In addition to causing considerable adverse sequelae and an increase in hospitalizations, there is a five-fold increase in the risk of stroke associated with non-valvular AF (Wolf et al., Stroke 22:983–988, 1991) which increases by a factor of 17 in the presence of significant valvular heart disease (Fuster et al., Circulation 123:e269–e367, 2011). The risk of AF increases markedly with older age affecting approximately 5% of people over 65 years and 10% of people age over 80 years (Miyasaka et al., Circulation 2006; 12: 114–119, 2006).

Classification of AF

AF is classified as paroxysmal, persistent, long-standing persistent or permanent. Paroxysmal AF is defined as two or more episodes of AF, each of which terminate within 7 days and commonly within 24 h. Persistent AF is generally sustained for greater than 7 days (or less if a cardioversion was performed in this time) and requires chemical or electrical cardioversion for termination of the arrhythmia. Longstanding persistent AF refers to cases in which the arrhythmia has been present for more than 1 year and previously may have been designated as being permanent; however, an electrical cardioversion or ablation strategy is being pursued and therefore sinus rhythm may be achieved. Permanent AF also persists for more than 7 days and can no longer be terminated; thus, a rhythm control strategy has been unsuccessful or not appropriate.

Etiology

The incidence of AF is increased by other cardiovascular and metabolic conditions as well as several lifestyle factors. It may also be secondary to either acute reversible insults or to other arrhythmias.

The main cardiovascular causes of AF are shown on Fig. 8.1 and include hypertension, coronary artery disease and valvular heart dis-

M. Haissaguerre (✉)
Cardiac Electrophysiology and Cardiac Pacing Department, CHU de Bordeaux, University of Bordeaux, Bordeaux, France

B. M. Glover
Division of Cardiology, Department of Medicine, University of Toronto, Toronto, Ontario, Canada

P. Brugada
University Hospital of Brussel, Brussels, Belgium
e-mail: pedro@brugada.org

B. M. Glover, P. Brugada (eds.), *Clinical Handbook of Cardiac Electrophysiology*,
https://doi.org/10.1007/978-3-030-74319-2_8

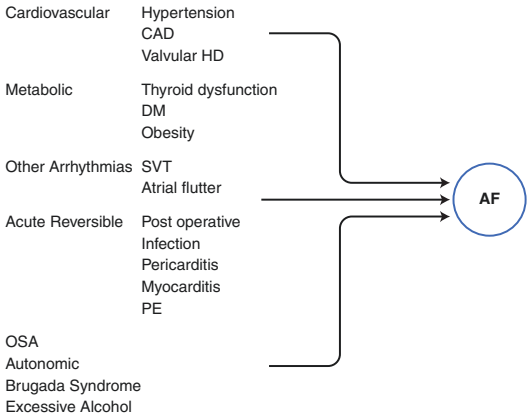

Fig. 8.1 Causes of Atrial Fibrillation. These can be divided into cardiovascular such as hypertension, coronary artery disease (CAD) and valvular heart disease (HD), metabolic, such as thyroid dysfunction, diabetes mellitus (DM) and obesity other arrhythmias such as SVT and atrial flutter and acute reversible causes such as post operative, infections, pericarditis, myocarditis and pulmonary embolism (PE). Other causes include OSA, autonomic, Brugada and excess alcohol

ease. Metabolic causes of AF include thyroid dysfunction and diabetes mellitus while lifestyle risk factors include obesity, excessive alcohol and obstructive sleep apnea. AF is frequently seen in the acute setting in post-operative patients as well as those who have infection, or in association with pulmonary embolism, pericarditis and myocarditis. AF may also occur in association with other supraventricular arrhythmias, such as AV nodal re-entry tachycardia, AV re-entry tachycardia and atrial flutter. It is important to perform an EP study in patients who are being considered for an AF ablation and in particular young patients to ensure that there is no underlying SVT. In patients who have undergone a successful ablation for typical atrial flutter the incidence of AF with 2.5 years post ablation is 50% (Chinitz et al. 2007). There has been some recent evidence to suggest that triggers from the pulmonary veins may also play a role in the initiation of typical atrial flutter (Schneider et al. 2015). Other less common causes of AF may be associated with autonomic activity, familial forms (particularly Brugada syndrome), and inflammatory mediators.

Hypertension

The odds ratio for developing AF in association with hypertension is 1.5 for men and 1.4 for women (Benjamin et al. 1994). Although this is not the highest risk for AF in an individual it is the most common cause of AF due to the high incidence of hypertension. Hypertension is often accompanied by left atrial remodeling due to pressure and volume overload as a result of a degree of left ventricular diastolic dysfunction. These changes may alter the electrical properties of the myocytes in the pulmonary veins, increasing their potential to act as triggers.

Effective treatment of hypertension in patients with AF has been shown to reduce all cause mortality (7.8%), cardiovascular mortality (4.3%), nonfatal myocardial infarction (5.3%) and stroke (2.2%), independent of blood pressure lowering effects (Dagenais et al. 2006). Additionally effective treatment of hypertension has been shown to reduce the overall risk of developing AF by 28% (Healey et al. 2005). Data supporting this has been inconsistent however, which may be a reflection of difficulties in optimal blood pressure control.

Coronary Artery Disease

AF is relatively common following an acute myocardial infarction (MI) occurring in approximately 15% of patients. Early reperfusion as well as the use of beta blockers appears to have an impact on lowering the incidence of AF post-MI. AF may result from occlusion to or proximal to the sinus node artery as well as the hemodynamic changes associated with left ventricular dysfunction. It may also occur as a result of changes in autonomic tone, particularly with an increase in adrenergic stimulation or as a result of pericarditis.

Of additional note, some patients with AF present with chest pain, an elevated cardiac troponin and no evidence of significant obstructive coronary artery disease. It has been suggested that this may be a result of AT1 receptor-mediated oxidative stress accompanied by a reduction in microvascular blood flow (Goette et al. 2009).

Valvular Heart Disease

The incidence of AF in patients with significant valvular heart disease is approximately 30% and in patients with mitral stenosis, approximately 50%. AF tends to be an early manifestation of mitral valve disease and tends to present later in aortic valve disease. Patients with significant mitral and aortic valve disease tend to have elevated left atrial pressure with left atrial dilatation and left atrial fibrosis which increases the possibility of re-entry circuits. The overall reduction in the incidence of rheumatic heart disease in the Western World has led to a significant reduction in valvular heart disease as an overall contributor to AF.

Diabetes Mellitus

Diabetes mellitus (DM) has been shown to be associated with an increased incidence of AF, whereby increasing risk is associated with diabetes duration and poor glycemic control (Dublin et al. 2010; Tesfaye et al. 2005). DM may result in a disturbance of cardiac autonomic function, in particular an increase in sympathetic tone, which may result in the initiation of AF (Dimmer et al. 1998). The cardiac autonomic dysfunction in patients with DM may also result in coronary microvascular dysfunction and diastolic dysfunction in diabetic subjects (Di Carli et al. 1999; Sacre et al. 2010; Pop-Busui et al. 2004) which may increase the potential for AF. There may also be inflammatory changes responsible for both conditions. CRP and interleukin 6 (IL-6) have been shown to be elevated in atrial biopsies in patients with lone AF which may also be elevated in DM (Chung et al. 2001; Frustaci et al. 1997).

Obesity and Obstructive Sleep Apnea (OSA)

Obesity is a significant public health concern with increasing prevalence. There is a 2.4-fold increased risk of AF in obese individuals versus those with a normal body mass index (BMI) (Frost et al. 2005). Furthermore this risk appears to increase with higher BMI values, as seen by a 1.2-fold increased risk in those with a BMI of 25–30 kg/m^2 and a 2.3-fold increase in those with a BMI greater than 40 kg/m^2 (Zacharias et al. 2005).

There are several potential explanations for an increased AF risk in patients who are overweight or obese. Indeed, AF may occur as a direct result of obesity or in association with other risk factors, which are more commonly associated with an elevated BMI.

There is a direct association between left atrial dilatation and obesity with a 2.4-fold 10-year risk of left atrial enlargement on echocardiogram (Stritzke et al. 2009).

In the settings of obesity and in particular, hypertension, left atrial pressure may also increase as a result of left ventricular hypertrophy and diastolic dysfunction. It has also been shown that obese patients have slower left atrial conduction times and shorter effective refractory periods in the left atrium and pulmonary veins even when adjusting for confounding variables including hypertension, DM and OSA (Munger et al. 2012). Overall these changes may result in atrial remodeling and atrial arrhythmias.

Atrial remodeling can be summarized as a heterogeneous process characterized by the disruption of atrial electrical integrity. Delayed interatrial conduction reflected as a broad and biphasic P wave in the inferior leads has been shown to increase with BMI and waist circumference (Magnani et al. 2012).

Increased pericardial fat occurs frequently with obesity, which may lead to a disturbance in atrial conduction. Variable expression of this adipose tissue may result in heterogeneity of atrial conduction. This has been shown to result in an increased risk of developing AF (Magnani et al. 2011).

OSA may be found in up to 90% of individuals with obesity (Frey and Pilcher 2003). If untreated, this is characterized by significant negative drops in intrathoracic pressure, intermittent hypercapnic hypoxia, and transient repeated wakening at the end of each episode. These drops in intrathoracic pressure may subsequently result in alterations of the left atrial chamber dimen-

sions which may, in itself, increase the risk of developing AF. Additionally, both hypercapnic hypoxia and frequent changes in sleep patterns may result in an increase in sympathetic tone. Overall, these changes may lead to an increase in the left atrial volume (Otto et al. 2007).

Effective treatment with CPAP in patients with OSA and no history of AF has been shown to reduce right and left atrial dimensions (Colish et al. 2012). OSA has been shown to be independently associated with failure of catheter ablation for AF (Patel et al. 2010). Ablation success rates are higher in patients with OSA who are treated with CPAP versus those not treated (Patel et al. 2010; Fein et al. 2013).

Obesity and its associated conditions are potentially modifiable risk factors for AF. In general, it is currently recommended that individuals with a BMI > 25 kg/m^2 with 1 associated comorbidity (diabetes, prediabetes, hypertension, dyslipidemia, elevated waist circumference) should be offered advice on dietary and lifestyle modification (Fein et al. 2013).

Aggressive risk factor modification in patients with a BMI > 27 kg/m^2 and at least one other risk factor (hypertension, DM, OSA, smoking and excessive alcohol consumption) in patients awaiting catheter ablation has been shown to result in an improvement in patient's symptoms, with 30% of patients avoiding the need for ablation (Abed et al. 2013). In patients undergoing catheter ablation for symptomatic AF, a significant improvement in symptoms was observed post-ablation as measured by the AF severity score (Pathak et al. 2014). AF-free survival after a single ablation procedure was 62% for patients with risk-factor-modification and only 26% for the control arm. After multiple ablations, AF-free survival increased to 87% in the risk-factor-modification group versus 48% in the control arm. Structural changes of the heart were also significantly better with left atrial volume and LV diastolic volume reduction.

Autonomic AF

An alteration in sympathetic activity may result in an increase in the potential for the initiation or maintenance of AF. This can occur either by direct effects on the action potential duration and refractory period of the cells in the pulmonary veins or left atrium or by structural changes.

An increase in adrenergic stimulation may result in an enhancement of focal automaticity which may act as a potential trigger for AF. Increased parasympathetic activation increases the action potential duration. However, its contribution to AF may result from its ability to shorten the atrial effective refractory period by varying degrees throughout the left atrium, which may contribute to a heterogeneity of conduction properties (Liu and Nattel 1997).

Both vagally induced and adrenergic AF tend to occur in younger patients with no other obvious risk factors. Vagally-induced AF is much more common than adrenergic AF and tends to occur after a preceding sinus pause or sinus bradycardia. Vagally induced AF may be partially responsive to flecainide and disopyramide and frequently worsens with beta blockers. Adrenergic AF is often provoked by exercise or increased emotional stress and tends to be preceded by an increase in sinus rate. This type of AF responds well to beta-adrenoceptor blockade.

It has been suggested that ganglionic plexi denervation may have a role in the treatment of AF. Indeed, left atrial ablation may have some impact by its effects on the autonomic innervation of the heart. One of the main restrictions in ganglionic plexus denervation using an ablation catheter is the difficulty in optimal access to the nerves which are not easily ablated from the endocardium.

Familial AF

Approximately 5% of cases of AF may have a genetic component (Darbar et al. 2003). This may be even higher in patients who develop AF at a younger age and those with no other obvious risk factors for AF. The risk of developing AF in an individual who has a parent with a history of AF is increased by a factor of 1.85 times that of the population (Fox et al. 2004). Additionally an

increased incidence of AF has been noted in long QT4, short QT and Brugada syndrome.

Several genetic mutations have been implicated in AF. A missense mutation in the KCNQ1 gene has been shown to result in an alteration of the activity of the voltage gated delayed potassium current (IKS) (Chen et al. 2003). In addition to other mutations in the KCNQ1 gene, SHOX2, TBX3 and PITX2 gene mutations have been linked to enhanced susceptibility to familial AF.

Mutations have also been detected in the KCNN3 gene, which encodes calcium activated potassium channels within in the atria (Ellinor et al. 2010).

Oral Anticoagulation

The issue of oral anticoagulation is one of the more complex issues in clinical cardiology. Most risk stratifying scores have been designed to be simple and easy to remember. Currently the most widely used risk scoring system is the CHA2DS2VASc, which is shown in Fig. 8.2. This was based on the CHADS2 score with a greater emphasis on age as well as the addition of vascular disease (prior MI or peripheral vascular disease), female gender and diabetes mellitus. It is generally recommended that oral anticoagulation should be considered in patients with a CHA2DS2VASc of greater than or equal to 2 (Class I Indication, Level of Evidence B) with either Coumadin or a direct oral anticoagulant. In patients with a CHA2DS2VASc score of greater than or equal to 1 oral anticoagulation, aspirin or no antithrombotic therapy can be considered (Class IIb Indication, Level of Evidence C). For patients with a CHA2DS2VASc of 0 no antithrombotic therapy is generally recommended. In general, female gender in a patient with no other risk factor for stroke would not result in the institution of oral anticoagulation although this clearly has to be reviewed with increasing age. It should also be remembered that each individual risk factor does not confer an equal percentage risk for stroke.

Although CHA2DS2VASc is more sensitive for predicting low event rates in low-risk patients, it is only modestly effective in terms of its positive predictive value with an area under the

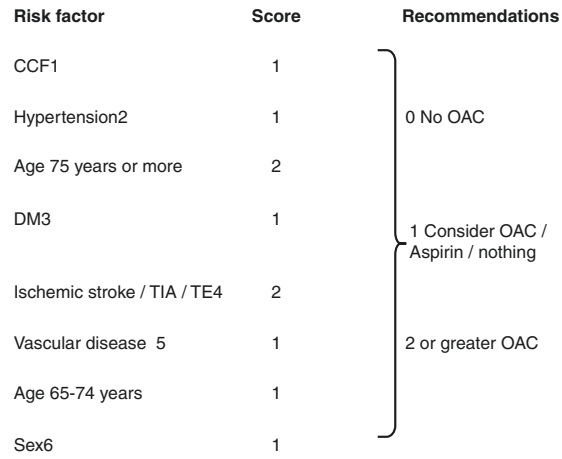

1 Signs/symptoms of LV/RV/Biventricular dysfunction confirmed with objective testing
2 Resting SBP > 140 mmHg and/or DBP > 90 mmHg on 2 or more measurements or patients receiving antihypertensive medication
3 Fasting plasma glucose greater than or equal to 7.0mmol/L /126 mg/dL or treatment with oral hypoglycemic agent or insulin
4 Ischemic stroke is defined as a sudden focal neurological deficit diagnosed by a neurologist and found to be due to an ischemic orgin lasting greater than 24 hours
TIA is a sudden focal neurological deficit diagnosed by a neurologist and lasting less than 24 hours
5 Vascular disease is considered a prior MI/PVD/aortic plaque
6 Female gender with no other risk factors is not considered sufficient for commencing OAC

Fig. 8.2 Summarizing the CHA2DS2VASc Scoring system for Non-Valvular AF. *SBP* systolic blood pressure, *DBP* diastolic blood pressure, *TIA* transient ischemic attack, *TE* thromboembolism, *MI* myocardial infarction, *PVD* peripheral vascular disease

receiver-operating characteristic curve of approximately 0.6 (Troughton and Crozier 2013).

Additional factors which have been examined in order to help calculate the risk of stroke include the use of biomarkers as well as LAA morphology. Biomarkers such as NT-pro-BNP, von Willebrand levels, d-dimers and troponin have been studied. Although they appear to have some merit they have yet to be incorporated into the guidelines. LAA morphology appears to correlate to an extent with the risk of thromboembolism. It has been proposed that an increase in trabeculations, number of bends and narrowness of the LAA orifice may also increase the risk of thrombus formation. Although this can be documented on TEE or CT, this is not recommended for decision making regarding oral anticoagulation therapy.

Vitamin K Antagonist

Warfarin acts by inhibiting the cyclic interconversion of vitamin K and vitamin K epoxide, thereby reducing the vitamin K-dependent clotting factors II, VII, IX and X. When compared with placebo, adjusted dose warfarin maintaining an INR or 2.0–2.9 results in an absolute reduction in ischemic and hemorrhagic strokes of 2.7% per year (Hart et al. 2007). Warfarin has also been shown to be superior to aspirin in patients considered to be at an increased risk of stroke.

Several major limitations concerning warfarin exist. The time within the therapeutic range is often less than 75% exposing patients to the risk of thrombo-embolism for significant periods of time. Warfarin administration is associated with several drug-drug interactions; therefore, food and dose adjustments are frequently required. Despite these considerations, there is still a role for warfarin in clinical practice particularly in patients with valvular heart disease and AF. The non-vitamin K antagonist agents are contraindicated in the presence of valvular AF and also need to be used with extreme caution in the setting of renal impairment. The widespread use of warfarin combined with antiplatelet agents has been clinically documented and the ability to monitor the effect of the drug may provide a reasonable indication of patient compliance. Warfarin is also relatively easily, albeit slowly, reversed with vitamin K.

Non-vitamin K Antagonist Oral Anticoagulation Therapy (OAC's)

These agents act by either directly suppressing thrombin or the conversion of prothrombin to thrombin by blocking the activated Xa factor. They have several theoretical advantages over warfarin such as a rapid onset and offset of action, reasonably predictable pharmacokinetics that do not require ongoing monitoring, and fewer interactions overall. It is important to monitor renal function particularly in patients where the baseline eGFR is below normal limits.

Direct Thrombin Inhibitors

Direct thrombin inhibitors bind to both soluble and fibrin-bound thrombin. The most commonly used agent in this group is the pro-drug dabigatran etexilate which was evaluated against warfarin in the RELY study. This prospective, randomized trial compared either 150 mg or 110 mg twice daily with warfarin (INR 2.0–3.0) for the prevention of stroke and systemic embolism in patients with non-valvular AF (Connolly et al. 2009).

Dabigatran at a dose of 150 mg has been shown to be superior to warfarin with no significant difference in the primary safety endpoint of major bleeding. At a dose of 110 mg, dabigatran was non-inferior to warfarin, with fewer major bleeds. The incidence of intracranial haemorrhage and haemorrhagic stroke were lower with both doses of dabigatran.

Based on these results, dabigatran etexilate has been approved by the Food and Drug Administration (FDA) at 150 mg twice daily with 75 mg twice daily in patients with renal impairment. The European Medicines Association (EMA) has approved both doses of 110 mg twice

daily and 150 mg twice daily in patients with non-valvular AF.

Factor Xa Inhibitors

The three available factor Xa inhibitors in clinical practice are edoxaban, apixaban and rivaroxaban.

Edoxaban has been shown to be noninferior to warfarin in the largest of all the clinical trials and also appears to have a very favorable side effect profile when compared with warfarin.

Rivaroxaban has a plasma half life of 7–11 h with a flat dose response resulting in a once daily administration. Rivaroxaban was compared with warfarin for the prevention of stroke or systemic embolism among patients with nonvalvular AF who were at moderate-to-high risk for stroke in the Rocket AF Trial (Patel et al. 2011). This double-blind trial compared rivaroxaban 20 mg once daily (15 mg daily for those with an estimated creatinine clearance of 30–49 mL/min) with warfarin in 14,264 patients. Rivaroxaban was found to be noninferior compared with warfarin for the primary endpoint of stroke and systemic embolism with a significant reduction in haemorrhagic stroke and intracranial haemorrhage. Rivaroxaban has a distinct advantage in being a once daily preparation. Additionally, the ROCKET AF study enrolled older patients (mean age 73 years), with at least two risk factors (congestive heart failure, hypertension, stroke or TIA), higher mean values of CHADS2 score (3.5) and lower median values for therapeutic INR's compared to other trials which are more comparable to real life conditions.

Approximately one-third of active rivaroxaban is renally excreted and a dose reduction from 20 mg once daily to 15 mg once daily is recommended for patients with moderate to severe renal impairment with periodic monitoring of renal function. A sub-study of the ROCKET AF study demonstrated that this lower dose was safe and effective in patients with a creatinine clearance between 30 and 49 mL min^{-1}. Rivaroxaban has been approved by both the FDA and the EMA for stroke prevention in non-valvular AF.

Apixaban has been shown to reduce the risk of stroke (predominantly through its effects on a reduction in hemorrhagic stroke) or systemic embolism, major bleeding and mortality in comparison with warfarin (Granger et al. 2011). Moreover, in patients for whom vitamin K antagonist therapy was considered unsuitable, apixaban compared with aspirin, reduced the risk of stroke or systemic embolism without a significant increase in the risk of major bleeding (Connolly et al. 2011). Apixaban has gained clinical approval with the FDA and EMA in patients with nonvalvular AF. Although the usual dose is 5 mg BiD, this should be reduced to 2.5 mg BiD if two out of the following three criteria are present: age greater than or equal to 80 years, weight less than or equal to 60 kg or a serum creatinine greater than or equal to 133 mmol/L. The details associated with the major trials in the NOACs are summarized on Table 8.1.

HAS-BLED Score

This is a scoring system used to predict the 1-year risk of major bleeding defined as intracranial bleeding, hospitalization, blood transfusion or a drop in hemoglobin of greater than 2 g/L. The components of this scoring system are:

Hypertension: uncontrolled systolic blood pressure >160 mm Hg

Abnormal renal or liver function: a serum creatinine greater than 200 mmol/L, need for long-term dialysis or history of a renal transplant. Abnormal liver function is defined as an elevation of transaminases greater than three times the upper limit of normal or a history of chronic liver disease

Stroke

Bleeding

Labile INR: in the therapeutic range less than 60% of the time

Elderly

Drugs or alcohol: the use of non-steroidal anti-inflammatory or antiplatelet agents

Table 8.1 Showing a summary of randomized clinical trial data supporting NOAC's

Parameter	Dabigatran (Rely)	Rivaroxaban (Rocket-AF)	Apixaban (Averroes)	Edoxaban (Engage AF)
Drug Dose	150 mg BID or 110 mg BID versus Warfarin (INR 2.0–3.0)	20 mg QD 15 mg QD in patients with creatinine clearance 30–49 mL/min) versus Warfarin (INR 2.0–3.0)	5 mg BID versus Aspirin 81–315 mg OD	60 mg Edoxaban versus Warfarin or 30 mg Edoxaban OD
Study Design	Randomized, open label	Randomized double-blind, double Dummy	Randomized, double-blind	Randomized double blind
Inclusion Criteria	AF within 6 mths + 1 risk factor	AF within 6 mths + 2 risk factors	AF within 6 mths + 1 risk factor	AF within 12 mths + 2 risk factors
Number of Patients	18,113	14,000	5600	21,105
Mean Age	71.5 years	73 years	70 years	72 years
Prior Stroke/TIA	20%	55%	13.5%	28.5%
Mean CHADS2 score	2.1	3.5	2.1	2.8
Stroke and Systemic Embolism (percent/year)	1.71% warfarin 1.54% dabigatran 110 mg ($p = 0.34$) 1.11% dabigatran 150 mg ($p < 0.001$)	2.42% warfarin 2.12% rivaroxaban ($p = 0.117$)	3.9% aspirin 1.7% apixaban ($p < 0.001$)	1.50% warfarin 1.18% Edoxaban
Major Bleeding	3.57% warfarin 2.87% dabigatran 110 mg ($p = 0.003$) 3.32% dabigatran 150 mg ($p = 0.31$)	3.45% warfarin 3.6% rivaroxaban ($p = 0.576$)	1.2% aspirin 1.4% apixaban ($p = 0.33$)	3.43% warfarin 2.75% edoxaban ($p < 0.001$)
Intracranial Haemorrhage Rate (percent/year)	0.74% warfarin 0.23% dabigatran 110 mg ($p < 0.001$) 0.3% dabigatran 150 mg ($p < 0.001$)	0.74% warfarin 0.49% rivaroxaban ($p = 0.019$)	0.3% aspirin 0.4% apixaban ($p = 0.83$)	0.85% warfarin 0.39% edoxaban ($p < 0.001$)

The maximum score is 9 with a score of ≥3 indicative of a high bleeding risk, where increased caution and regular review should be performed. This scoring system should not be used solely to exclude administration of oral anticoagulation therapy but may be used to highlight patients at a higher risk of bleeding for the modification of controllable risk factors.

Catheter Ablation for AF

Catheter ablation for the treatment of AF emerged as a viable treatment option when it was discovered that ectopic foci, which originate from sleeves of myocardium extending into the pulmonary veins, may initiate AF (Haissaguerre et al. 1998). This resulted in the concept that isolation of these foci by catheter ablation may reduce the likelihood of developing AF. Although the foci themselves were initially targeted, this resulted in a high incidence of pulmonary vein stenosis, which has now been largely replaced with wide antral circumferential ablation (WACA). This technique has been shown to be associated with a lower incidence of arrhythmia recurrence compared with segmental antral ablation (Proietti et al. 2014). This may be due to the isolation of regions of the left atrial PV junction where micro re-entry may occur. Additionally, WACA may have a greater effect on the elimination of other non-PV triggers in the posterior LA wall, debulk the left atrium, and have a greater effect on autonomic denervation.

Pulmonary vein isolation (PVI) is currently considered the mainstream catheter approach for

paroxysmal AF. It also is a very reasonable approach for the management of persistent AF, albeit, with the need for additional options to be considered. Some centers perform PVI in all patients with a history of persistent AF followed by an electrical cardioversion for the first ablation procedure. If the patient presents with further AF, then either linear lesions, CFAE ablation or rotor ablation can be considered at that stage. Other centers perform more ablation for the first procedure although this may increase the potential for developing AT.

Risks of Catheter Ablation of AF

The risk of a significant complication associated with an AF ablation is approximately 2.9% (Gupta et al. 2013). The most common complication is vascular (approximately 1%) which is largely related to groin hematoma and occasionally femoral pseudoaneurysm formation. The risk of stroke and TIA is 0.6%, cardiac tamponade (1%) and clinically evident PV stenosis 0.5%. The incidence of phrenic nerve palsy is approximately 0.4% and although esophageal injury is common, atrio-oesophageal fistula is unusual occurring in 0.1% of cases. The overall mortality is 0.06%.

How to Perform a PVI

Patient Preparation

A PVI can be performed either with the patient under general anesthesia or with intravenous sedation and analgesia. There are several advantages to either strategy. General anesthesia often results in a quicker procedure with less patient discomfort and less patient movement. However, this may not always be available, and some operators prefer sedation as there is more patient feedback during the procedure.

A TEE may be performed in order to rule out a LAA thrombus particularly in patients who are in AF and have not been anticoagulated prior to the procedure. In most cases where the patient is receiving warfarin, this can be continued throughout the procedure with an upper INR cut off of 3.5 above which the risk of bleeding is increased by a factor of 6 (Kim et al. 2013).

If the patient is receiving a non vitamin K antagonist OAC (NOAC), a decision must be made whether to stop the agent or not.

Some data suggests that uninterrupted dabigatran compared with uninterrupted warfarin is associated with an increased risk of bleeding and thrombo-embolic complications (Lakkireddy et al. 2012). Dabigatran increases the effects of heparin often doubling the effects, an effect not seen to the same degree with rivaroxaban and apixaban (Walenga and Adiguzel 2010). It is therefore, standard practice to interrupt dabigatran prior to performing an AF ablation. The decision of when to hold dabigatran is dependent on the patient's renal function. In patients with normal renal function, the drug may be held either the morning of the procedure or the evening prior but not for more than 24 h pre-procedure (Providência et al. 2014). Dabigatran should be stopped earlier if renal function is reduced.

In patients with normal renal clearance, the best option may be drug suspension on the morning of the procedure, or the night before, but always <24 h before the procedure. A target ACT of greater than 350 s should be achieved during the procedure. Dabigatran can then be recommenced 3–4 h following removal of the sheaths (Providência et al. 2014). The dosage of dabigatran following this should be based on renal function and the potential risk of bleeding.

Recent data has shown that uninterrupted rivaroxaban therapy appears to be as efficacious as uninterrupted warfarin in preventing thromboembolic and bleeding complications in patients undergoing AF ablation (Lakkireddy et al. 2014). If the decision is made to hold rivoroxaban for an AF ablation, the dose on the morning of the procedure may be held. There is currently limited data regarding the use of apixaban in patients undergoing an AF ablation although it may seem reasonable to hold a dose the morning of or the evening before the procedure.

It is common practice to administer the final dose of the OAC 24 h prior to the ablation and

perform a pre-procedure TEE. Heparin is then administered throughout the procedure and the OAC is recommenced 3 h following removal of the venous sheaths which are removed at the end of the case with no reversal of heparin.

If the patient is receiving a general anesthetic the TEE probe can be left in position in order to help facilitate the transseptal access and monitor for pericardial effusion.

Venous access is generally achieved via the femoral vein with two 8 Fr sheaths and a 6 Fr sheath. A decapolar is positioned in the coronary sinus to help with the transseptal puncture and may also be useful for mapping and pacing particularly if an AT develops during the procedure.

Two transseptal sheaths are then positioned over 0.032 wires into the superior vena cava and flushed with heparinized saline. Heparin is then administered at a dose of 100 iu/kg in order to achieve an ACT of greater than 300 s in patients who are either not on warfarin or have an INR less than 2.0 (Calkins et al. 2012). For patients who are receiving warfarin and have a therapeutic INR 75 iu/kg of heparin should be administered in order to achieve an ACT of greater than 300 s. ACT should be checked every 20 min at which time, either further boluses or an infusion can be administered.

Transseptal Access

A posterior location in the fossa ovalis is chosen in order to facilitate access to all regions around the pulmonary veins. Although his can be performed under fluoroscopic guidance the addition of echocardiographic data is oftentimes helpful particularly if the fossa is difficult to cross or is aneurysmal.

A range of sheaths and transseptal needles are available. A BRK1 needle often results in a good location and is useful in patients who have enlarged atria. If this is tenting the fossa without crossing, then the flexion can be slightly reduced or a BRK or Baylis needle can be considered. Transseptal access can generally be achieved using a combination of a PA, left lateral, RAO and LAO views. Generally, for PVI, standard sheaths are sufficient although deflectable sheaths may help with contact and occasionally with access to the right superior pulmonary vein. Deflectable sheaths may be useful for a linear lesion joining the mitral isthmus to the left inferior pulmonary vein. If a non-standard sheath is to be switched to a deflectable sheath, a 0.032 wire can be extended out to the left superior pulmonary vein for an over the wire switch.

Notwithstanding the choice of sheath, it is very important that the side arms are flushed with heparinized saline in a closed circuit and that no air bubbles enter the system.

Anatomic Reconstruction of the Left Atrium

The anatomy of the LA is generally constructed using a multipolar circular catheter. This may be merged with a pre-procedure CT, which could be helpful in determining the presence of aberrant pulmonary veins as well as the presence of variants such as common ostia. MRI of the LA can also be performed but is more time consuming. Either of these modalities can be merged with the electroanatomic image. Carto-Merge (Biosense Webster) uses fiducial points taken from selected anatomical structures such as the pulmonary vein ostia. The image is then rotated in order to compare the anatomic shells of both structures for comparison. If there is a difference between the two images further points can be taken on the electro anatomic map.

NavX Fusion (St Jude Medical) can also be used to integrate the electroanatomic map onto a baseline CT scan. Following acquisition of the anatomic shell, this system utilizes a field scaling algorithm which adjusts for the non-linearity of the geometry and takes into account the measured inter-electrode spacing for all locations within the geometry. Four fiducial points are then taken on the CT and the electroanatomic map and secondary fusion is used to reduce mismatch between the two images (Brooks et al. 2008).

Although these systems may be helpful the LA dimensions vary with rhythm status and are also dependent on the intravascular volume.

Overall, there remains no convincing data to suggest that image integration increases success or reduces complications. IT may, however, reduce fluoroscopy times.

Ablation Technique

Following anatomic reconstruction of the LA, a circular mapping catheter is positioned within the ostia in one of the pulmonary veins where it should record nearfield pulmonary vein potentials and farfield left atrial potentials. If a contact force catheter is being used for ablation, this should be positioned in the middle of the left atrium where there is no contact and a zero is set on the catheter.

The catheter should then be positioned so that it is on the atrial side of the pulmonary vein ostia. The ostia can be difficult to locate precisely on fluoroscopy or even on an electroanatomic map and there is an overlap between left atrial myocytes extending into the pulmonary veins and venous tissue extending into the left atrium. If the demarcation is unclear, the ablation catheter can be placed on the venous side of the ostia while pacing and capturing the pulmonary veins. The point at which pulmonary vein capture no longer occurs is a reasonable estimate of the ostia.

Point by point ablation is generally performed using a 3.5–4.0 mm irrigated catheter. Power is delivered at 30–35 W anterior to the pulmonary veins and 25–30 W along the posterior wall in order to limit energy delivery to the esophagus and branches of the vagus nerve. A target temperature of less than 40 °C and irrigation at 17 mL/min are set. If contact force is used, then a minimum of 10 g of force should be targeted. The catheter is typically moved every 30–60 s.

Certain regions around the pulmonary veins may be technically more challenging than others and require different catheter manipulations. The ridge between the left pulmonary veins and the left atrial appendage is an infolding of the lateral atrial wall (Fig. 8.3). It is at its narrowest at the border of the left superior pulmonary vein measuring 2.2–6.3 mm to its broadest aspect at the boundary of the left inferior pulmonary vein measuring 6.2–12.3 mm (Ho et al. 2012). It is at its thickest at the anterosuperior region.

In order to ablate along the ridge, the ablation catheter can be withdrawn from the left superior pulmonary vein with counterclockwise rotation so that the catheter is moving anterior in the direction of the LAA. This should maximize contact with this region. Excess counterclockwise torque results in the catheter moving into the LAA, which often needs to be counteracted with clockwise rotation. Given the significant autonomic innervation of the lateral ridge, ablation in this region commonly results in a slowing of the sinus rate.

Flexion and extension of the ablation catheter is required for ablation inferior and superior to the left sided PV's. Ablation starting on the roof superior to the left superior pulmonary vein often results in separation of local pulmonary vein signals and LAA farfield signals.

Ablation superior and inferior to the right sided PV's can be performed often with a combination of rotation with flexion and extension of the catheter. Occasionally a deflectable sheath may be useful in these regions although the use of a bidirectional catheter through a standard sheath is generally suitable to reach all regions. When ablation is performed inferior to the right inferior pulmonary vein within a small left atrium, it is important to flex with an acute angle in order to minimize the risk of losing transseptal access.

Ablation may be required in the carina between the pulmonary veins despite WACA being performed. This may be explained by endocardial to epicardial connections in this region resulting in continued conduction. Additionally, connections exist between ipsilateral PV's resulting in several isthmuses which may be an important consideration when performing PVI and may in part explain why segmental ablation was previously shown to have limited efficacy (Cabrera et al. 2009).

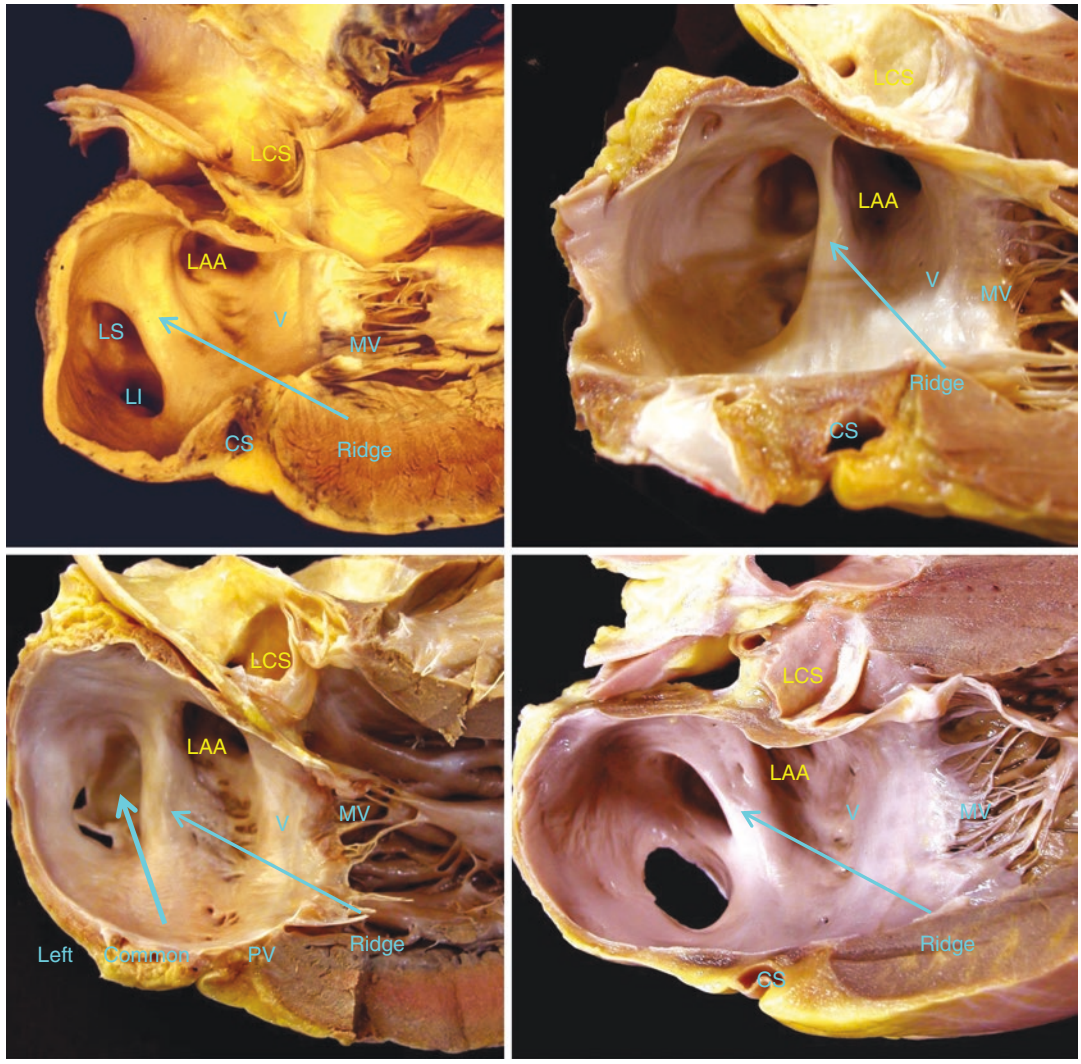

Fig. 8.3 The ridge between the left superior (LS) pulmonary vein, the left inferior (LI) pulmonary vein and the left atrial appendage (LAA). This ridge can vary significantly from being broad and extending anterior to the LS and LI pulmonary veins (top left image) to a more narrow structure (top right image) or may be anterior to a left common pulmonary vein (bottom left) or may be broad and move anterior as it extends inferior so as to have less of a direct relationship with the LI pulmonary vein. Also seen in these images are the mitral valve (MV), the vestibule of the mitral valve (V) and the coronary sinus (CS)

Pulmonary Vein Potentials and Farfield Signals

Electrograms recorded from the ostia of the pulmonary veins show an initial non circumferential lower amplitude atrial signal followed by an isoelectric period and finally, by sharp pulmonary vein potentials (Patel et al. 2003). Depending on the overlap between the left atrium and the surrounding structures as well as the orientation of the mapping catheter there is a variable delay between the farfield electrogram and the pulmonary vein potentials. An example of this is shown in Fig. 8.4 in which the first component is farfield left atrial followed by an isoelectric line followed by a PVP which is a sharp high frequency signal.

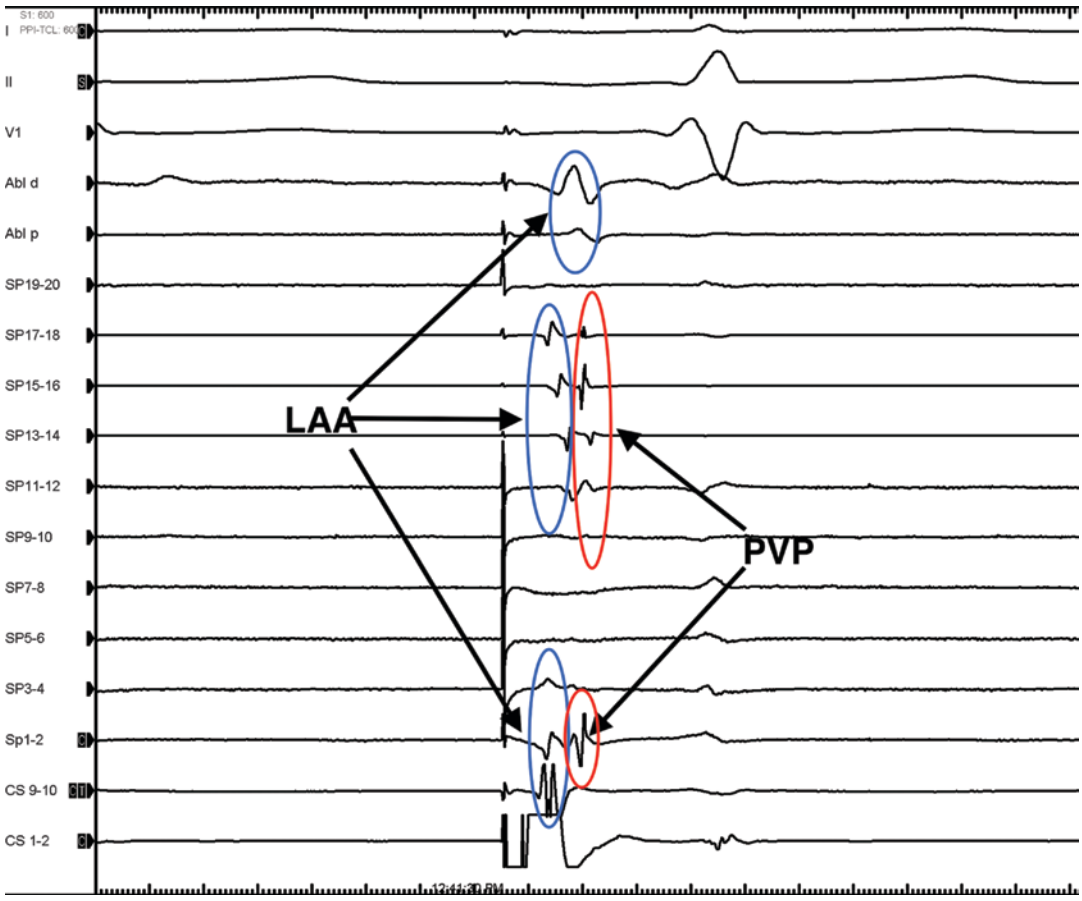

Fig. 8.4 The circular catheter (SP 1–20) is in the left superior pulmonary vein. Pacing is performed from the distal coronary sinus (CS 1–2). The first deflection is farfield from the left atrial appendage (circled in blue) followed by an isoelectric line followed by a sharp pulmonary vein potential (circles in red)

The LAA is anterior to the left superior pulmonary vein. As a result, sharp pulmonary vein potentials can often be merged within LAA signals. In order to separate LAA signals from PV potentials, CS pacing can be used as shown in Fig. 8.4. Additionally, direct pacing may be performed from the LAA. For the left superior and inferior pulmonary veins, pacing from the distal coronary sinus or left atrial appendage can be performed in order to increase the isoelectric line between the farfield and nearfield signals. Although pacing from the distal coronary sinus is reasonably simple, it is somewhat dependent on the variable connections between the coronary sinus and the left atrium. Left ventricular farfield may also be recorded in the left inferior pulmonary vein.

This cannot be performed if the patient is in AF as differentiation of farfield LAA signals from local PV potentials can be somewhat more complex. An example of isolation of the LSPV during AF is shown in Fig. 8.5. In this example the circular catheter is positioned in the LSPV during ablation along the ridge between the LAA and the vein. The earliest activation is recorded on poles 13–14 where ablation is performed. This results in isolation of the vein with farfield LAA potentials being recorded on poles 9–10, 11–12 and 19–20 which are all in anterior locations. Another example of isolation of the RSPV is

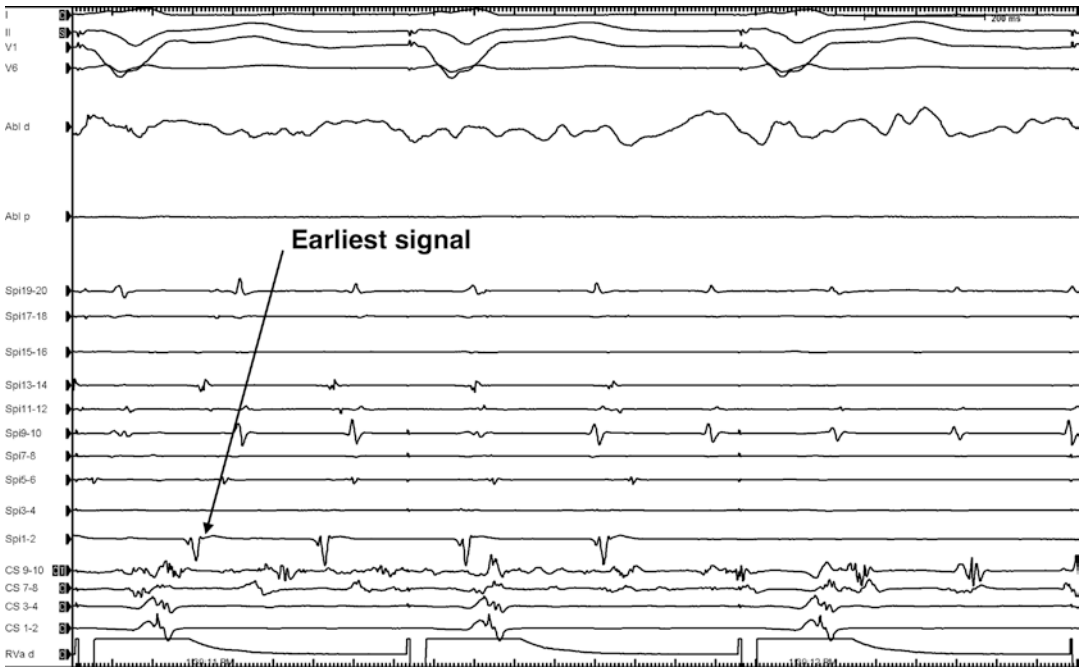

Fig. 8.5 Isolation of the LSPV. The circular catheter is positioned in the LSPV. The earliest nearfield activation is recorded on Spi poles 1–2 followed by 13–14. These poles are almost overlapping and are located along the lower junction between the LSPV and the LAA along the ridge (near to where the ablation catheter is positioned). Ablation in this region results in isolation of the vein with only LAA farfield recorded on the circular catheter. (CS 9–10 is in the proximal coronary sinus and CS 1–2 is in the distal CS). Ventricular pacing from the RV apex is performed as the patient became bradycardic during RF ablation

shown in Fig. 8.6. As ablation is performed, local PVP's in the vein slow considerably and then disappear with only farfield atrial activation recorded.

As shown in the anatomic image in Fig. 8.7, the superior vena cava is anterior to the right superior pulmonary vein. In order to differentiate superior vena cava potentials from pulmonary vein potentials, the signal can be measured relative to the surface p wave. As the superior vena cava is so close to the sinus node, signals will be very early if they originate from the superior vena cava. If this is within 30 ms of the onset of the p wave, it is likely to reflect superior vena cava activity. There is generally no significant farfield recorded in the right inferior PV. The PV potentials recorded on the circular catheter have slowed considerably during ablation. Further ablation results in loss of PV potentials with only farfield atrial signals.

Confirming Pulmonary Vein Isolation

PVI may be confirmed by proving bidirectional block with or without the administration of intravenous adenosine as well as pacing along the ablation line around the pulmonary veins. Of note, **entrance block without exit block may occur in up to 40% of the patients** (Takahashi et al. 2002).

Entrance block may be observed either during normal sinus rhythm or with atrial pacing during sinus rhythm. The circular catheter is positioned in the PV antra just distal to the line of ablation. The most important principle is to distinguish between PV potentials and LA or RA signals detected as farfield on the circular catheter. Although PV potentials are sharp and of a much higher frequency than farfield atrial potentials, they may be superimposed. Pacing the structure or close to the structure where the atrial signals

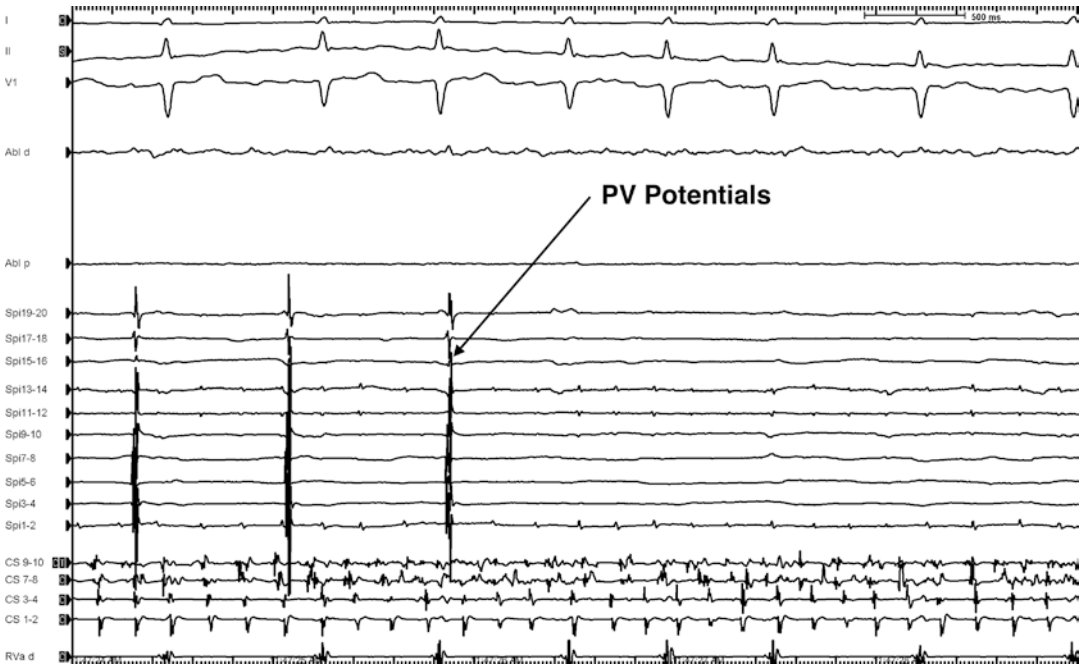

Fig. 8.6 Loss of local PV potentials during isolation of the RSPV. These signals are slowed considerably during ablation and following further ablation only farfield atrial signals are detected. The spiral (Spi) catheter is located in the RSPV. (CS 9–10 is positioned in the proximal coronary sinus and CS 1–2 is located in the distal CS)

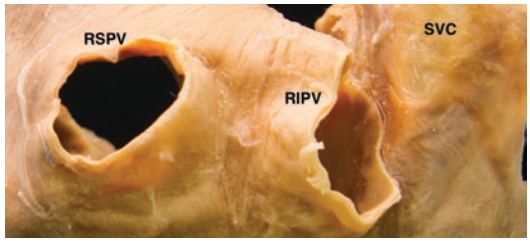

Fig. 8.7 Anatomic specimen showing a posterior view of the right superior pulmonary vein (RSPV) and right inferior pulmonary vein (RIPV). The superior vena cava (SVC) is anterior and close to both of these structures and farfield electrical activity from the SVC may be detected when mapping these veins

are originating from should result in these signals becoming earlier if they are originating from that structure. For potentials coming from the LAA either the LAA can be paced directly or the distal CS if the catheter is positioned appropriately. An example of 2:1 conduction from the left atrium to the LSPV is seen in Fig. 8.8 in which a potential with the vein is recorded after every second atrial electrogram. This represents slow conduction with conduction through SP 3–4, which was positioned posterior to the LSPV. Ablation in this region resulted in isolation of the vein.

In order to prove exit block, the ablation catheter can be positioned in the same pulmonary vein as the circular mapping catheter. Although pacing can be performed from either the ablation catheter alone or the circular catheter alone, it is often easier to discern pulmonary vein potentials from a separate catheter which has closely spaced poles without superimposed pacing artifact. Pacing can be performed using a decremental output until there is only pulmonary vein capture. This avoids capture of adjacent structures, which may mimic intact conduction. Lack of conduction from the pulmonary veins to the left atrium proves that the ablation line is resulting in conduction block. An example of this is shown in Fig. 8.9.

Although the presence of dissociated PV potentials is a useful indicator of exit block, conduction may still be present in 10% of patients

Fig. 8.8 2:1 conduction from the left atrium to the left superior pulmonary vein. A potential is recorded in the vein after every second atrial electrogram. This signified continued conduction in the posterior region of the LSPV (SP 3–4) which required further ablation for isolation of the vein

who display these (Europace 2009). An example of dissociated potentials from the RIPV is shown in Fig. 8.10. Pacing is performed from the high right atrium (HRA). Farfield atrial potentials are seen on the circular catheter with intermittent PV potentials which are not conducted to the atrium.

Another useful technique to help confirm an intact line around the pulmonary veins is to assess for unexcitability to pacing. Following ablation, the catheter is positioned along the line during sinus rhythm at an output of 10 mA and a pulse width of 2 ms (Steven et al. 2013). If lack of local capture occurs, the catheter is moved a further 5 mm along the line and pacing is repeated. If local capture occurred, then further ablation was performed in this region and pacing is performed at the same output.

The administration of intravenous adenosine appears to be of some use in assessing for dormant conduction following isolation of the PV's due to the hyperpolarization of myocytes which have been acutely ablated. This can be administered after a period of monitoring post-ablation whereby further ablation should be performed if there is any evidence of dormant conduction. An example of this is shown in Fig. 8.11.

Assessing for Non PV Triggers

Non pulmonary vein triggers may contribute to AF in some cases and are worth examining particularly in redo ablations where the pulmonary veins have remained isolated. As shown in Fig. 8.12, potential locations include the superior vena cava, coronary sinus, crista terminalis, fossa ovalis, ligament of Marshall and left atrial appendage.

In order to map for non pulmonary vein triggers a multipolar catheter is positioned in the coronary sinus and another along the posterolareral right atrium extending into the superior vena cava. Intravenous isoprenaline is administered in incremental doses from 3 to 20 μg/min. If AF is not inducible, decremental atrial pacing can be performed. Using the earliest sites of activation,

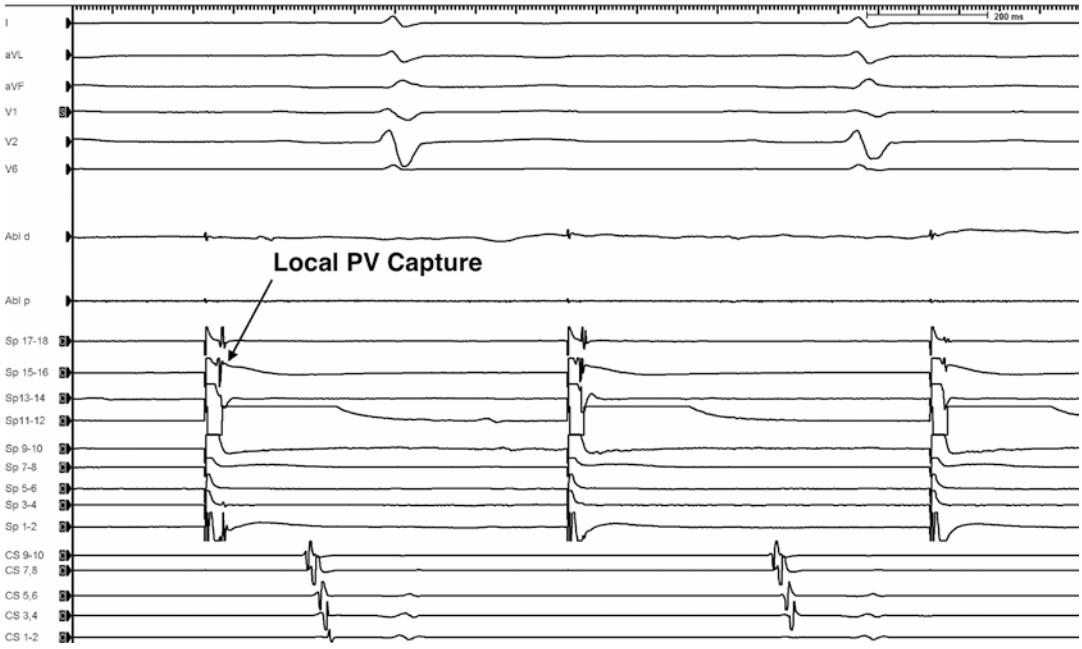

Fig. 8.9 Circular catheter (SP 1–18) in the right superior pulmonary vein with pacing from poles 15–16 showing local capture with sharp local PV potentials which do not capture the left atrium. (CS 9–10 is located in the proximal coronary sinus while CS 1–2 is located in the distal coronary sinus)

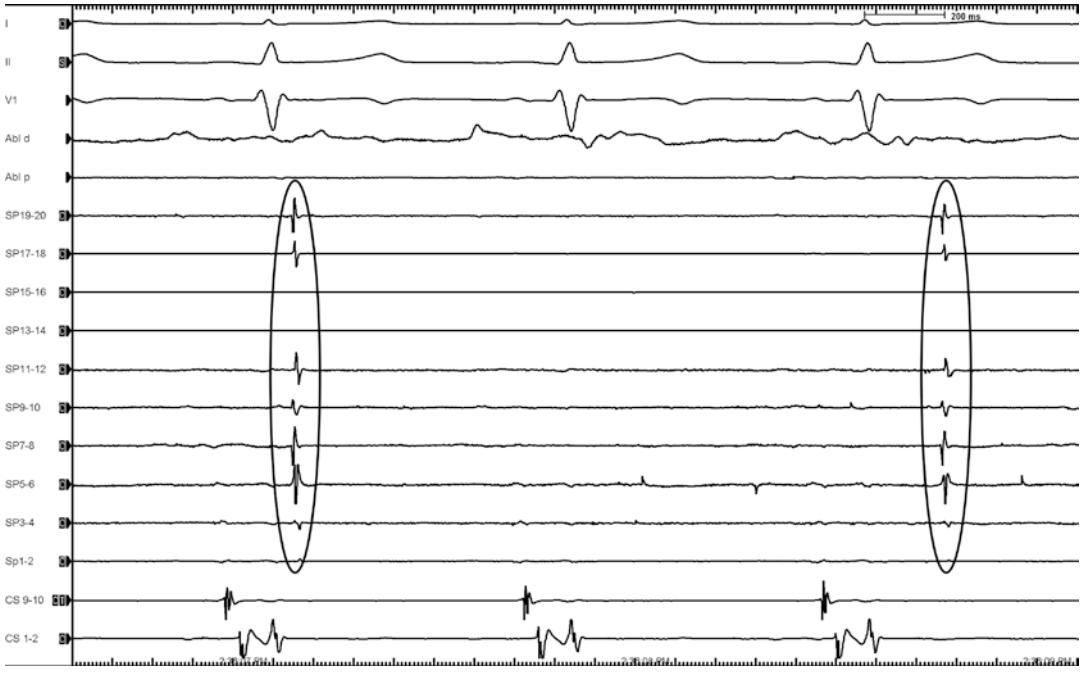

Fig. 8.10 Dissociated PV potentials (circled) recorded on a circular catheter (Sp 1–20) positioned in the right superior pulmonary vein (RSPV). Pulmonary vein potentials are seen which do not conduct into the left atrium. The ablation catheter is positioned in the RSPV. CS 9–10 is in the proximal CS while CS 1–2 is in the distal CS

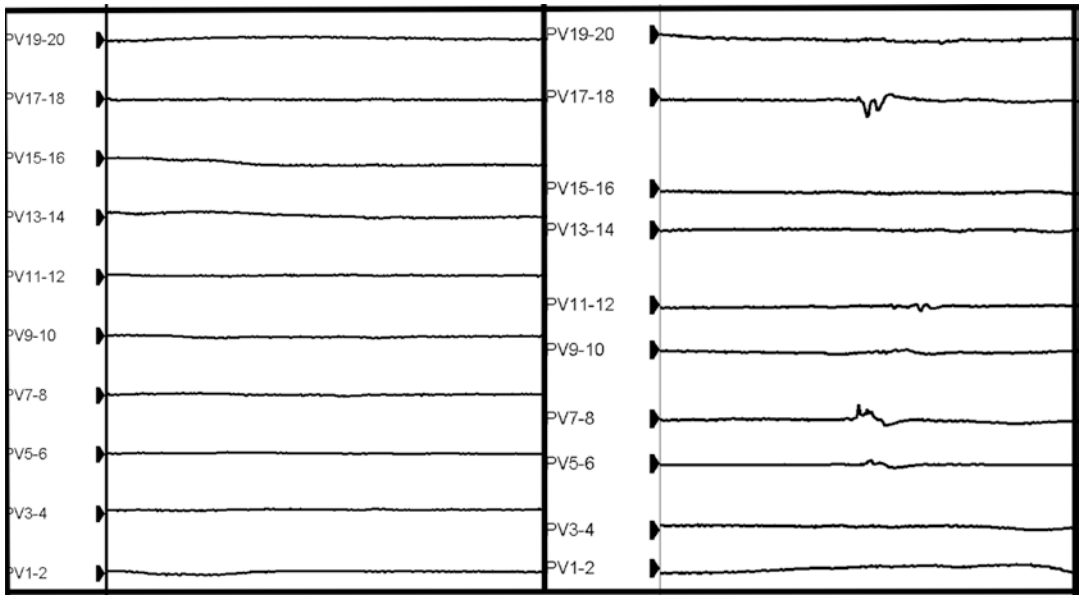

Fig. 8.11 The circular catheter (PV 1–20) is in the right superior pulmonary vein. The image on the right shows the potentials recorded following ablation and before the administration of adenosine. The pulmonary vein appears to be isolated. The image on the right is recorded following the administration of adenosine. This shows early activation in PV 7–8 followed by 5–6, 17–18, 9–10 and 11–12. This region was anterior to the right superior pulmonary vein at the level of the carina. Further ablation was delivered here and the vein was retested with adenosine and found to be isolated

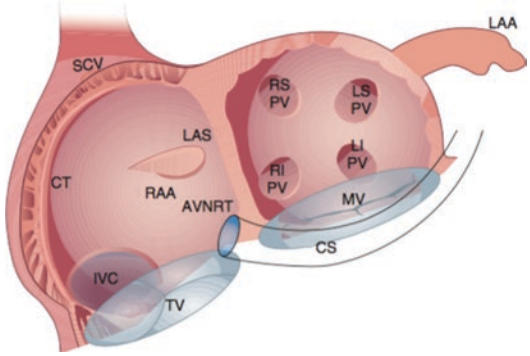

Fig. 8.12 Potential locations of Non-Pulmonary Venous Triggers (*RSPV* right superior pulmonary vein, *RIPV* right inferior pulmonary vein, *LSPV* left superior pulmonary vein, *LIPV* left inferior pulmonary vein, *MV* mitral valve, *CS* coronary sinus, *LAA* left atrial appendage, *LAS* left anterior septum, *RAA* right atrial appendage, *AVNRT* AV nodal re-entry tachycardia, *TV* tricuspid valve, *SVC* superior vena cava, *IVC* inferior vena cava)

focal ablation can be performed and further triggers can then be mapped. Given the increasing width of WACA, many triggers may be incorporated into the original lesions.

Cryoablation

Cryoablation utilizes a system (Arctic Front Cardiac CryoAblation, Medtronic, Inc) which pumps the refrigerant N20 into an inflatable balloon as shown in Fig. 8.13. This is positioned at the PV orifice. Contrast is injected into the PV in order to assess for good contact and applications are generally performed over a period of 4 min. A circular catheter assesses for electrical isolation of the PV's and further applications are performed if required. This procedure generally requires a single transseptal access with a 15 Fr sheath. The balloon is advanced over a guidewire and positioned at the PV ostia. The balloon diameter is available in either 23 or 28 mm. The size can be determined on CT or ICE. Cryoablation has been shown to be non-inferior to point by point RF ablation with regards to freedom from AF and an absence of persistent complications (Luik et al. 2015). The second generation cryoballoon has an inner mapping guidewire and an increased number of emission ports.

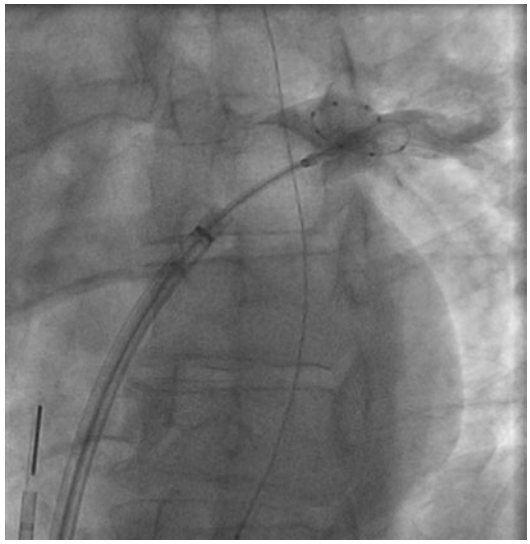

Fig. 8.13 Showing the new generation Cryoballoon used for antral pulmonary vein isolation. On this fluoroscopic image the cryoballoon is positioned in the left superior pulmonary vein. (© Medtronic plc 2015)

Hybrid Ablation of AF

Surgical ablation for AF has evolved from the Cox Maze procedure to a minimally invasive epicardial approach. These methods can be used to deliver RF around the PV antra as well as create a roof and floor line resulting in a posterior box lesion. Although this holds moderate effectiveness in cases of paroxysmal AF, freedom from AF for cases of persistent AF is relatively low due to complex AF propagation patterns which arise from progressive AF modeling. As a result, a hybrid approach combining endocardial and epicardial ablation has been developed. During hybrid ablation, thoracoscopic isolation of the PVs may be confirmed using circular mapping catheters. These endocardial catheters can verify the completeness and transmurality of the epicardial lesions and identify any macro or microreentrant circuits that may be treated through the creation of additional ablation lines. Although endocardial-epicardial ablation can be performed at the same time it is often considered reasonable to delay endocardial ablation for several months in order to assess conduction block after a period of time. This may be a useful option in patients with persistent AF and dilated atria.

Ablation of Persistent AF

Ablation strategies in persistent AF are imperfect. Several techniques have been developed for ablation for persistent AF. Linear lesions may be performed until sinus rhythm is restored or until an electrical cardioversion is performed and the lines checked for conduction block. CFAE ablation may be performed in the left and right atria and rotors ("drivers") may be mapped either invasively or non-invasively and selectively targeted.

Linear Lesions

Following isolation of the pulmonary veins, linear lesions can be performed. The most common of these involve a linear lesion along the left atrial roof joining the right superior pulmonary vein to the left superior pulmonary vein. A mitral isthmus line may also be performed although it may be difficult to achieve successful and permanent block as the wall may be relatively thick and require epicardial ablation via the coronary sinus (at a lower power). Rather than performing linear lesions in all cases of AF, these are often performed in cases where the patient develops an atrial flutter either during the ablation or has a documented history of an atrial flutter which is then induced. In such cases the CTI is often mapped first followed by the pulmonary veins. If these are silent then entrainment in certain anatomic locations can then be performed as well as mapping of local signals. The most common locations to map are the mitral annulus and the LA roof as the majority of macro re-entry atrial flutters involve these regions. If there is a significant variability in the tachycardia cycle length (greater than 15%) then the mechanism is more likely to represent a focal AT. In our experience both a focal AT and a macro re-entry atrial flutter may have a tachycardia cycle length less than

15% and therefore, this may not serve as a reliable discriminator.

Roof Dependent Left Atrial Flutter

In order to map roof dependent left atrial flutter, the catheter is positioned anterior to the roof and then more inferiorly close to the anterior mitral annulus. This is repeated by positioning the ablation catheter along the roof in the posterior direction and then towards the coronary sinus which generally marks the general direction of the posterior mitral annulus. If the activation is in the reverse direction (i.e. earlier inferior than superior on the anterior wall and earlier superior to inferior on the posterior wall or vice versa), this is likely to be a roof dependent atrial flutter. If entrainment is performed in the anterior and posterior regions of the roof, then a PPI-TCL <30 ms further helps to confirm roof dependent atrial flutter. In the setting of a prior roof line or PVI with WACA mapping of fractionated potentials in the region of the roof is also helpful. An example of an activation map of roof dependent atrial flutter is shown in Fig. 8.14.

A roof line connecting the LSPV and the RSPV should be performed in the setting of a macro re-entry atrial tachycardia circulating around the PV's and involving the roof. In order to perform this, the sheath is directed towards the right superior pulmonary vein while the catheter is flexed over to the left superior PV. Using 30–35 W the catheter flexion can then be slowly released staying at each point for approximately 30–60 s. A superior and a PA view help to ensure that the line is performed along the roof rather than the posterior wall. In order to evaluate the roof line, the LAA is paced during sinus rhythm. Roof line block is demonstrated by the presence of double potentials along the line during pacing as well as caudocranial activation of the posterior wall.

Mitral Isthmus Dependent Atrial Flutter

This is a relatively common cause of post PVI atrial arrhythmias and generally occurs as a result of slow conduction inferior to the LIPV from a prior mitral isthmus ablation or PVI. With this arrhythmia, CS activation is either proximal to

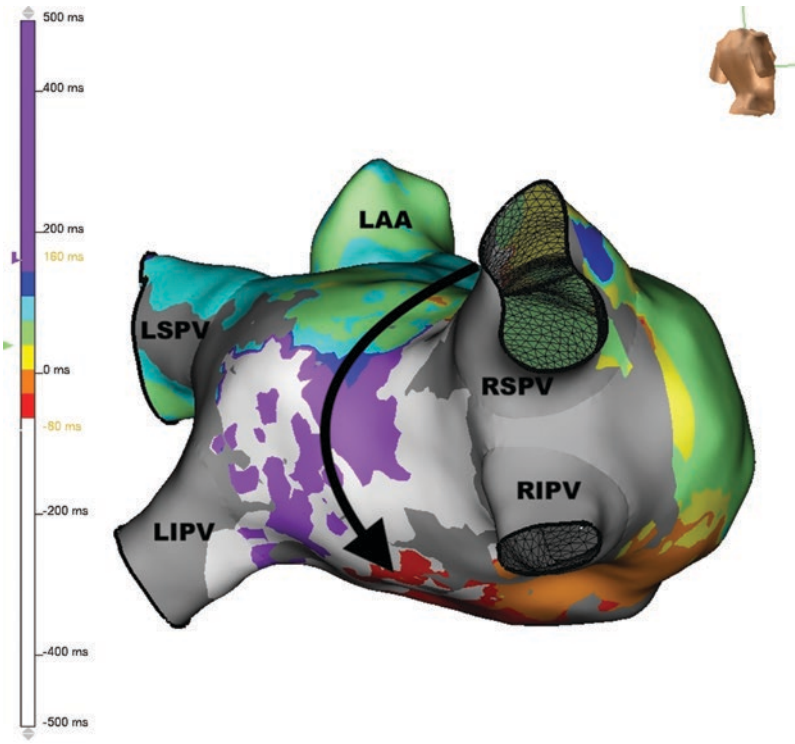

Fig. 8.14 Activation map of roof dependent atrial flutter showing propagation of early (white) at the inferior posterior wall of the left atrium to red, yellow, green indigo, navy and then purple which is the latest region (*LSPV* left superior pulmonary vein, *LIPV* left inferior pulmonary vein, *LAA* left atrial appendage, *RSPV* right superior pulmonary vein, *RIPV* right inferior pulmonary vein)

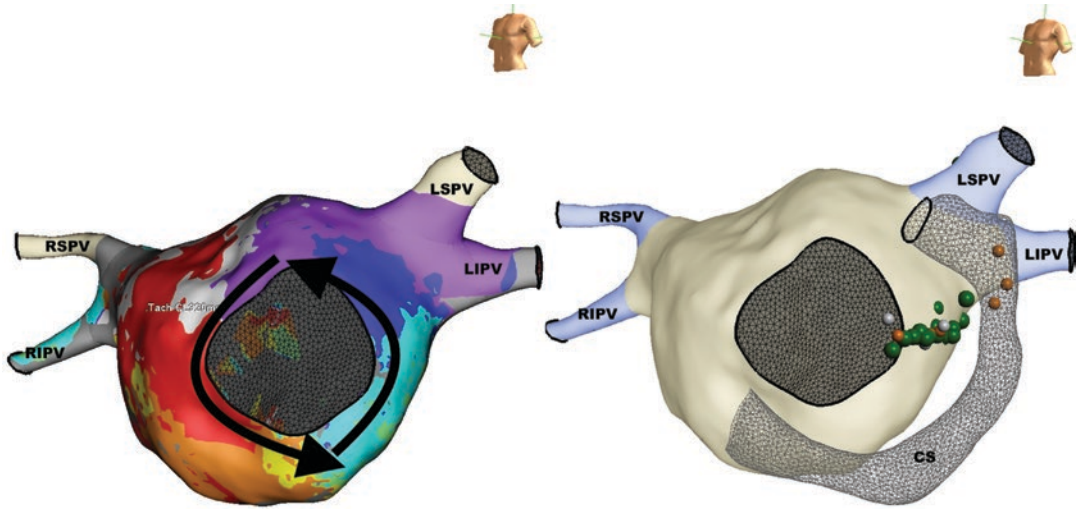

Fig. 8.15 Activation map (left image) showing counter-clockwise mitral isthmus atrial flutter with endocardial ablation (green lesions on right image) and epicardial ablation (brown lesions) within the coronary sinus (CS) resulting in termination of mitral isthmus dependent atrial flutter with block along the line of ablation (*RSPV* right superior pulmonary vein, *RIPV* right inferior pulmonary vein, *LSPV* left superior pulmonary vein, *LIPV* left inferior pulmonary vein)

distal or distal to proximal. It is useful to use the ablation catheter to map the anterior mitral annulus. If CS activation is proximal to distal then anterior activation should be from lateral to septal. If the CS activation is distal to proximal, then the anterior mitral annular activation should be from septal to lateral.

A posterior mitral isthmus line may be performed which connects the LIPV to the posterior mitral annulus close to the coronary sinus. A deflectable sheath is used and the ablation catheter is positioned at the ventricular side of the lateral mitral annulus with an AV ratio of either 1:1 or 2:1 (Jais et al. 2004).

During proximal CS pacing the catheter and sheath are then rotated clockwise towards the left inferior PV with delivery at 30 W for 90–120 s applied at each location. The catheter is moved whenever there is splitting of the local electrograms. The mitral isthmus varies in thickness along its length being thinner at the annular end and thicker at the medial end.

In order to prove block for a posterior mitral isthmus line, pacing is performed from the CS and activation is measured in the LAA. Normally pacing from the distal CS should result in a shorter conduction time to the LAA than pacing from a less distal pole. In the event of posterior mitral isthmus block the more distal location will take longer to travel to the LAA. The presence of double potentials along the entire ablation line with coronary sinus pacing is also a useful endpoint. As shown in Fig. 8.15 ablation sometimes has to be performed at 20 W from the coronary sinus in order to block epicardial activation. An alternative approach is to perform an anterior mitral isthmus line joining the anterior mitral annulus to the LSPV.

CFAE Mapping and Ablation

CFAE's are defined as local electrograms which are fractionated with at least two components and with cycle lengths less than 120 ms recorded during AF and lasting for at least 10 s (Nademanee et al. 2004). These are frequently recorded during AF within the regions of the LA close to the pulmonary vein antral regions and therefore may be ablated and electrically isolated during a pulmonary vein isolation.

In persistent atrial fibrillation, CFAE's may be located anywhere within the left and right atrium with a propensity for the septum, inferoposterior wall of the LA and the LAA.

There are various theories as to what CFAE's actually represent with suggestions such as anchor points in rotors, regions of conduction slowing or autonomic activation. The long-term results of CFAE ablation are not impressive and certainly this does not appear to represent a very effective strategy for the treatment of persistent AF.

Re-Entry Mapping

A rotor is defined as an unexcited core, termed a phase singularity, resulting in reverberations which radiate at very high velocity into the surrounding tissue (Pandit and Jalife 2013). Phase singularities are surrounded by different phases of the cardiac action potential and may be considered useful targets for ablation as they may be considered regions of tissue which can support rotors. They may occur on the endocardium, mid myocardium or epicardium or indeed span all layers. The theory is that following initiation of atrial fibrillation from PV and non-PV sources, rotors result in maintenance of atrial fibrillation.

Rotors differ from re-entry circuits in several ways. In a rotor, the core is the active component with secondary spiral activity. The rotor core is functional and does not appear to be related to a detectable structural obstacle. Rotors are not stationary and may move over a considerable area (Narayan et al. 2013a). Spiral waves also collide with each other altering the overall activation pattern. Additionally, there does not appear to be a close correlation between rotors and CFAE's (Narayan et al. 2013a).

Some of these features actually make mapping of rotors very complex. Rotor activation is complex, can change during the mapping process and may involve different regions of the endocardium, myocardium and epicardium. There are currently two systems which may be used for mapping rotors. These involve either invasive mapping using a multi-electrode basket catheter called the Focal Impulse and Rotor Modulation system and a non-invasive multi electrode vest which is superimposed on a cardiac CT.

Focal Impulse and Rotor Modulation of Atrial Fibrillation

This system uses a 64-electrode basket with eight splines which is positioned in either the right, left or both atria as shown in Fig. 8.16. If the patient is in atrial fibrillation the unipolar electrograms are recorded and exported for analysis. If the patient is in sinus rhythm, atrial fibrillation is induced with rapid atrial pacing and the signals are then recorded and analyzed after 10 min of sustained atrial fibrillation. It is critical that there is excellent electrode contact. The correct size of basket should be chosen, and this may prove to be difficult in larger atria. Catheter orientation should be optimized on fluoroscopy and with the aid of a 3-D mapping system in order to record vital areas of the left atrium including the pulmonary veins and the left atrial appendage as well as septal, roof, anterior and posterior activity.

The signals are then processed using RhythmView™ (Topera Inc.). This system is based on restitution monophasic action potential data acquired during rapid atrial pacing and atrial fibrillation. This displays the activation signals on a 2-dimensional image where the operator can then visualize potential rotors or focal sources. The image of each atria is opened so that for the right atrium the tricuspid annulus is inferior with the septal component to the right of the image and the lateral component to the left. For the left atrium the mitral annulus is at the bottom of the image and is divided. The electrodes of interest where a rotor core is believed to exist can then be referenced off an electroanatomic system and ablation can then be performed.

It has been shown that focal sources and rotors may be recorded in almost all patients with atrial fibrillation. Approximately one third of these can be recorded in the right atrium (Narayan et al. 2012), and more than one half of all rotors are recorded outside of the regions where a wide area circumferential ablation would be performed (Narayan et al. 2013b). Results suggest that the addition of ablation of rotors using this technique

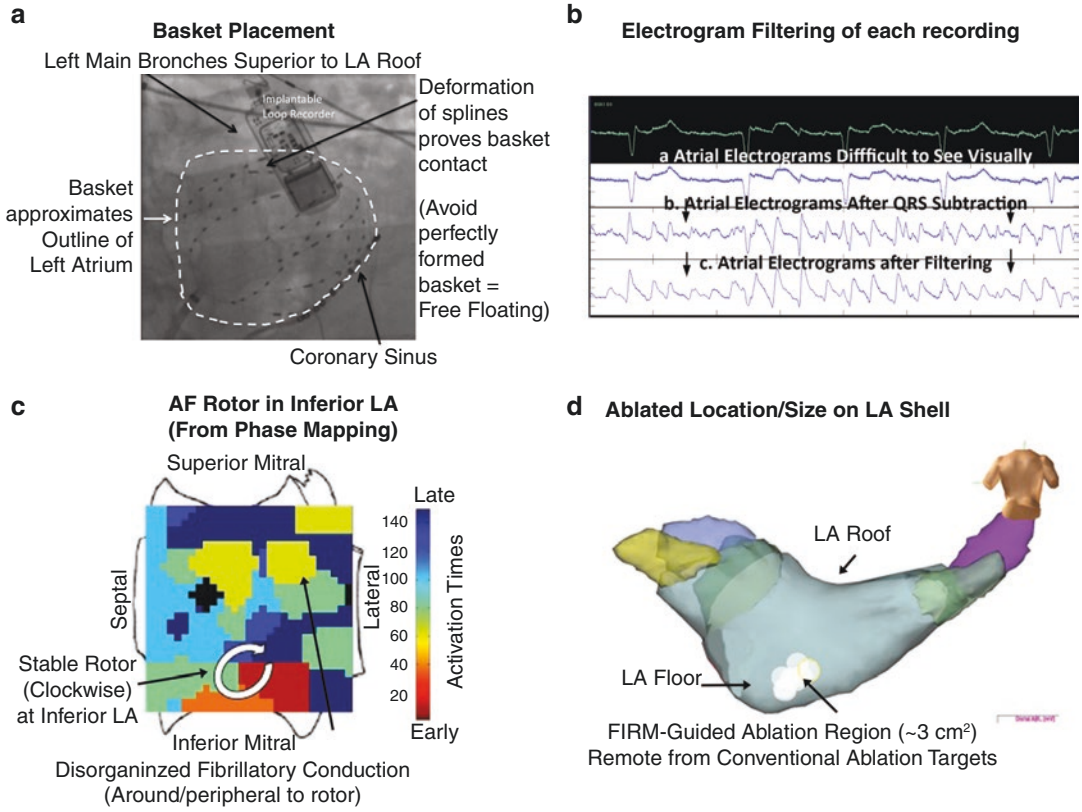

Fig. 8.16 Approach to FIRM (Focal Impulse and Rotor Mapping) Guided Ablation of Atrial Fibrillation. (Courtesy of Dr. Sanjiv Narayen). (**a**) **Baskets placed in left atrium (shown)** and also in right atrium to map both chambers sequentially. Good positioning results in deformation of the highly compliant basket, proving electrode contact, and splines that approximate the LA roof and floor. In contrast, a spherical shape when deployed indicates an undersized basket with poor contact. (**b**) **Electrogram filtering** using well-established methods enables detection of atrial signals which are sometimes difficult to identify visually. (**c**) **Rotor during human AF in left atrium**, revealed by spatial phase mapping of filtered atrial electrograms, depicted as clockwise 'snapshot' (isochrone) where early and late activation meet, surrounded by fibrillatory disorganization. Phase mapping is used since activation mapping during dynamically changing activation in AF is challenging. Intraprocedurally, diagnosis is actually made from animated 'FIRM movies" which better convey rotor precession and their dynamic interaction with the fibrillatory milieu. (**d**) **FIRM-guided ablation zone,** in inferior left atrium guided by map, typically of ≈3 cm^2 areas

increases the success when compared with pulmonary vein isolation alone.

Non-Invasive Multi Electrode Mapping

Using this technique a 252 electrode vest (CardioInsight, © Medtronic plc 2015) is applied to the patient during AF. This is used to record unipolar surface potentials. Anatomic data is then acquired by performing a noncontrast cardiac CT with the vest in place so that each electrode position can be calculated relative to the cardiac chambers. The system then performs a calculation in order to calculate and display electrical data on the surface of the heart from the surface unipolar electrograms. Activation sequences are then calculated by looking at the most negative dV/dT. This can then be displayed on a 3-D reconstruction of the right and left atria using colors to animate various phases of depolarization

and repolarization as shown in Fig. 8.16. This can be analyzed for focal sources as well as rotors. There are several advantages of this system since it simultaneously maps both atria and therefore can help to differentiate between active rotors and passive activation. It also does not rely on contact to record the electrograms. Given that data is acquired prior to an ablation there may be a question of changes in activation or changes related to the ablation itself.

Important Points to Remember

1. AF is classified as paroxysmal, persistent, longstanding persistent or permanent. Paroxysmal AF is defined as two or more episodes of AF each of which terminate within 7 days and commonly within 24 h. Persistent AF is sustained generally for greater than 7 days (or less if a cardioversion was performed in this time) and requires chemical or electrical cardioversion for termination of the arrhythmia. Longstanding persistent refers to cases in which AF has been present for more than 1 year and previously may have been designated as being permanent; however, an electrical cardioversion or ablation strategy is being pursued and therefore sinus rhythm may be achieved. Permanent AF also continues for more than 7 days and cannot be terminated anymore thus a rhythm control strategy has been unsuccessful or is not appropriate.
2. The main cardiovascular causes of AF are hypertension, coronary artery disease and valvular heart disease. Metabolic causes of AF include thyroid dysfunction and diabetes mellitus while lifestyle risk factors include obesity, excessive alcohol and obstructive sleep apnea. AF is frequently seen in an acute setting in post operative patients as well as those who have infection, or in association with pulmonary embolism, pericarditis and myocarditis. AF may also occur in association with other supraventricular arrhythmias, such as AV nodal re-entry tachycardia, AV re-entry tachycardia and atrial flutter.
3. PVI is considered to be a reasonable strategy in patients with paroxysmal AF in whom medication has been ineffective, poorly tolerated or in cases of patient preference. This may be performed using a point-by-point technique or a ‘single shot’ device. PVI may also be useful in patients with persistent AF as a method of isolating the potential triggers.
4. Electrograms recorded from the ostia of the pulmonary veins show an initial non circumferential lower amplitude atrial signal followed by an isoelectric period and finally by sharp pulmonary vein potentials. Depending on the overlap between the left atrium and the surrounding structures as well as the orientation of the mapping catheter there is a variable delay between the farfield electrogram and the pulmonary vein potentials. For the LSPV and to a lesser degree the LIPV, farfield electrograms from the LAA may be recorded. These can be separated from the PV potentials by pacing from the LAA or the distal CS. For the RSPV farfield electrograms may be recorded from the SVC. If the signal is within 30 ms of the onset of the p-wave then these are likely to represent SVC farfield.
5. Entrance block may be observed either during normal sinus rhythm or with atrial pacing during sinus rhythm. The circular catheter is positioned in the PV antra just distal to the line of ablation.

6. In order to prove exit block the ablation catheter can be positioned in the same pulmonary vein as the circular mapping catheter. Although pacing can be performed from either the ablation catheter alone or the circular catheter alone it is often easier to discern pulmonary vein potentials from a separate catheter which has closely spaced poles without a superimposed pacing artifact.
7. An additional useful technique to help prove an intact line around the pulmonary veins is to assess for unexcitability to pacing. Following ablation, the catheter is positioned along the line during sinus rhythm at an output of 10 mA and a pulse width of 2 ms. If lack of local capture occurs the catheter is moved a further 5 mm along the line and pacing repeated. If local capture occurred, then further ablation was performed in this region and pacing performed at the same output.
8. In some cases, non pulmonary vein triggers may contribute to AF. Potential locations include the superior vena cava, coronary sinus, crista terminalis, fossa ovalis, ligament of Marshall and left atrial appendage.
9. Post-PVI atrial arrhythmias may involve the CTI, gaps around the PV's, the mitral annulus or the LA roof. Activation mapping using the ablation catheter relative to a stable CS electrogram may help to distinguish these.
10. Newer mapping techniques including the potential mapping of rotors may help to further understand the mechanism for AF.

References

Abed HS, Wittert GA, Leong DP, et al. Effect of weight reduction and cardiometabolic risk factor management on symptom burden and severity in patients with atrial fibrillation: a randomized clinical trial. JAMA. 2013;310:2050–60.

Benjamin EJ, Levy D, Vaziri SM, et al. Independent risk factors for atrial fibrillation in a population-based cohort. The Framingham Heart Study. JAMA. 1994;271:840–4.

Brooks AG, Wilson L, Kuklik P, et al. Image integration using NavX fusion: initial experience and validation. Heart Rhythm. 2008;5:526–35.

Cabrera A, Ho SY, Climent V, et al. Morphological evidence of muscular connections between contiguous pulmonary venous orifices: relevance of the interpulmonary isthmus for catheter ablation in atrial fibrillation. Heart Rhythm. 2009;6(8):1192–8.

Calkins H, Kuck KH, Cappato R, et al. 2012 HRS/EHRA/ECAS expert consensus statement on catheter and surgical ablation of atrial fibrillation: recommendations for patient selection, procedural techniques, patient management and follow-up, definitions, endpoints, and research trial design: a report of the heart rhythm society (HRS) task force on catheter and surgical ablation of atrial fibrillation. Heart Rhythm. 2012;9:632–96.

Chen YH, Xu SJ, Bendahhou, et al. KCNQ1 gain-of-function mutation in familial atrial fibrillation. Science. 2003;299(5604):251–4.

Chinitz JS, Gerstenfeld EP, Marchlinski FE, et al. Atrial fibrillation is common after ablation of isolated atrial flutter during long-term follow-up. Heart Rhythm. 2007;4:1029–33.

Chugh SS, Havmoeller R, Narayanan K, et al. Worldwide epidemiology of atrial fibrillation: a Global Burden of Disease Study 2010. Circulation. 2014;129:837–47.

Chung MK, Martin DO, Sprecher D, Wazni O, Kanderian A, Carnes CA, et al. C-reactive protein elevation in patients with atrial arrhythmias: inflammatory mechanisms and persistence of atrial fibrillations. Circulation. 2001;104:2886–91.

Colish J, Walker JR, Elmayergi N, Almutairi S, Alharbi F, Lytwyn M, Francis A, Bohonis S, Zeglinski M, Kirkpatrick ID, Sharma S, Jassal DS. Obstructive sleep apnea: effects of continuous positive airway pressure on cardiac remodeling as assessed by cardiac biomarkers, echocardiography, and cardiac MRI. Chest. 2012;141:674–81.

Connolly SJ, Ezekowitz MD, Yusuf S, et al. Dabigatran versus warfarin in patients with atrial fibrillation. N Engl J Med. 2009;361:1139–51.

Connolly SJ, Eikelboom J, Joyner C, et al. Apixaban in patients with atrial fibrillation. N Engl J Med. 2011;364:806–17.

Dagenais GR, Pogue J, Fox K, Simoons ML, Yusuf S. Angiotensin-converting-enzyme inhibitors in stable vascular disease without left ventricular systolic dysfunction or heart failure, a combined analysis of three trials. Lancet. 2006;368:581–8.

Darbar D, Herron KJ, Ballew JD, Jahangir A, Gersh BJ, Shen WK, Hammill SC, Packer DL, Olson TM. Familial atrial fibrillation is a genetically heterogeneous disorder. J Am Coll Cardiol. 2003;41: 2185–92.

Di Carli MF, Bianco-Batlles D, Landa ME, et al. Effects of autonomic neuropathy on coronary blood flow in patients with diabetes mellitus. Circulation. 1999;100:813–991.

Dimmer C, Tavernier R, Gjorgov N, et al. Variations of autonomic tone preceding onset of atrial fibrillation after coronary artery bypass grafting. Am J Cardiol. 1998;82:22–5.

Dublin S, Glazer NL, Smith NL, et al. Diabetes mellitus, glycemic control, and risk of atrial fibrillation. J Gen Intern Med. 2010;25:853–8.

Ellinor PT, Lunetta KL, Glazer NL, et al. Common variants in KCNN3 are associated with lone atrial fibrillation. Nat Genet. 2010;42(3):240–4.

Electrophysiological evaluation of pulmonary vein isolation. Europace. 2009;11:1423–33.

Fein A, Shvilkin A, Shah D, et al. Treatment of obstructive sleep apnea reduces the risk of atrial fibrillation recurrence–after catheter ablation. JACC. 2013;62(4):300–5.

Fox CS, Parise H, D'Agostino RB Sr, Lloyd-Jones DM, Vasan RS, Wang TJ, Levy D, Wolf PA, Benjamin EJ. Parental atrial fibrillation as a risk factor for atrial fibrillation in offspring. JAMA. 2004;291:2851–5.

Frey WC, Pilcher J. Obstructive sleep-related breathing disorders in patients evaluated for bariatric surgery. Obes Surg. 2003;13:676–83.

Frost L, Hune LJ, Vestergaard P. Overweight and obesity as risk factors for atrial fibrillation or flutter: the Danish Diet, Cancer, and Health Study. Am J Med. 2005;118:489–95.

Frustaci A, Chimenti C, Bellocci F, Morgante E, Russo MA, Maseri A. Histological substrate of atrial biopsies in patients with lone atrial fibrillation. Circulation. 1997;96:1180–4.

Fuster V, Ryden LE, Cannom DS, et al. 2011 ACCF/AHA/HRS focused updates incorporated into the ACC/AHA/ESC 2006 guidelines for the management of patients with atrial fibrillation: a report of the American College of Cardiology Foundation/American Heart Association Task Force on Practice Guidelines. Circulation. 2011;123:e269–367.

Goette A, Bukowska A, Dobrev D, et al. Acute atrial tachyarrhythmia induces angiotensin II type receptor-mediated oxidative stress and microvascular flow abnormalities in the ventricles. Eur Heart J. 2009;30:1411–20.

Granger CB, Alexander JH, McMurray JJV, et al. Apixaban versus warfarin in patients with atrial fibrillation. N Engl J Med. 2011;365:981–92.

Gupta A, Perera T, Ganesan A, et al. Complications of catheter ablation of atrial fibrillation. Circ Arrhythm Electrophysiol. 2013;6:1082–8.

Haissaguerre M, Jais P, Shah DC, Takahashi A, Hocini M, Quiniou G, Garrigue S, Le Mouroux A, Le Metayer P, Clementy J. Spontaneous initiation of atrial fibrillation by ectopic beats originating in the pulmonary veins. N Engl J Med. 1998;339:659–66.

Hart RG, Pearce LA, Aguilar MI. Meta-analysis: antithrombotic therapy to prevent stroke in patients who have nonvalvular atrial fibrillation. Ann Intern Med. 2007;146:857–67.

Healey JS, Baranchuk A, Crystal E, et al. Prevention of atrial fibrillation with angiotensin converting enzyme inhibitors and angiotensin receptor blockers. A meta-analysis. J Am Coll Cardiol. 2005;45:1832–9.

Ho SY, Cabrera A, Sanchez-Quintana D. Left atrial anatomy revisited. Circulation. 2012;5:220–8.

Jais P, Hocini M, Hsu LF, et al. Technique and results of linear ablation at the mitral isthmus. Circulation. 2004;110:2996–3002.

Kim JS, Jongnarangsin K, Latchamsetty R, et al. The optimal range of international normalized ratio for radiofrequency catheter ablation of atrial fibrillation during therapeutic anticoagulation with warfarin. Circ Arrhythm Electrophysiol. 2013;6:302–9.

Lakkireddy D, Reddy YM, Di Biase L. Feasibility and safety of dabigatran versus warfarin for periprocedural anticoagulation in patients undergoing radiofrequency ablation for atrial fibrillation: results from a multicenter prospective registry. J Am Coll Cardiol. 2012;59:1168–74.

Lakkireddy D, Reddy YM, Di Biase L, et al. Feasibility & safety of uninterrupted rivaroxaban for periprocedural anticoagulation in patients undergoing radiofrequency ablation for atrial fibrillation: results from a multicenter prospective registry. J Am Coll Cardiol. 2014;63:982–8.

Liu L, Nattel S. Differing sympathetic and vagal effects on atrial fibrillation in dogs: role of refractoriness heterogeneity. Am J Phys. 1997;273:805–16.

Luik A, Radzewitz A, Kieser M, et al. Cryoballoon versus open irrigated radiofrequency ablation in patients with paroxysmal atrial fibrillation: the prospective, randomised, controlled, non-inferiority freeze AF study. Circulation. 2015;132:1311–9.

Magnani JW, Johnson VM, Sullivan LM, Gorodeski EZ, Schnabel RB, Lubitz SA, Levy D, Ellinor PT, Benjamin EJ. P wave duration and risk of longitudinal atrial fibrillation in persons >/= 60 years old

(from the Framingham Heart Study). Am J Cardiol. 2011;107:917–21.

Magnani JW, Lopez FL, Soliman EZ, Maclehose RF, Crow RS, Alonso A. P wave indices, obesity, and the metabolic syndrome: the atherosclerosis risk in communities study. Obesity. 2012;20:666–72.

Miyasaka Y, Barnes ME, Gersh BJ. Secular trends in incidence of atrial fibrillation in Olmsted County, Minnesota, 1980 to 2000, and implications on the projections for future prevalence. Circulation. 2006;12:114–9.

Munger TM, Dong YX, Masaki M, et al. Electrophysiological and hemodynamic characteristics associated with obesity in patients with atrial fibrillation. J Am Coll Cardiol. 2012;60:851–60.

Nademanee K, McKenzie J, Kosar E, et al. A new approach for catheter ablation of atrial fibrillation: mapping of the electrophysiologic substrate. J Am Coll Cardiol. 2004;43:2044–53.

Narayan SM, Krummen DE, Shivkumar K, et al. Treatment of atrial fibrillation by the ablation of localized sources-CONFIRM (Conventional ablation for atrial fibrillation with or without focal impulse and rotor modulation) trial. J Am Coll Cardiol. 2012;60:628–3.

Narayan SM, Shivkumar K, Krummen DE, et al. Panoramic electrophysiological mapping but not electrogram morphology identifies stable sources for human atrial fibrillation: stable atrial fibrillation rotors and focal sources relate poorly to fractionated electrograms. Circ Arrhythm Electrophysiol. 2013a;6:58–67.

Narayan SM, Krummen DE, Clopton P, et al. Direct or coincidental elimination of stable rotors or focal sources may explain successful AF ablation: on-treatment analysis of the CONFIRM trial. J Am Coll Cardiol. 2013b;60:138–47.

Otto ME, Belohlavek M, Romero-Corral A, Gami AS, Gilman G, Svatikova A, Amin RS, Lopez-Jimenez F, Khandheria BK, Somers VK. Comparison of cardiac structural and functional changes in obese otherwise healthy adults with versus without obstructive sleep apnea. Am J Cardiol. 2007;99:1298–302.

Pandit SV, Jalife J. Rotors and the dynamics of cardiac fibrillation. Circ Res. 2013;112:849–62.

Patel N, Kay GN, Sanchez J, Ideker RE, Smith WM. Discrimination of left atrial and pulmonary vein potentials in patients with paroxysmal atrial fibrillation. J Cardiovasc Electrophysiol. 2003;14:698–704.

Patel D, Mohanty P, Di Biase L, et al. Safety and efficacy of pulmonary vein antral isolation in patients with obstructive sleep apnea–the impact of continuous positive airway pressure. Circ Arrhythm Electrophysiol. 2010;3:445–51.

Patel MR, Mahaffey KW, Garg J, et al. Rivaroxaban versus warfarin in nonvalvular atrial fibrillation. N Engl J Med. 2011;365:883–91.

Pathak R, Middeldorp M, Lau D, et al. Aggressive risk factor reduction study for atrial fibrillation and implications for the outcome of ablation. The ARREST-AF study. JACC. 2014;64(21):2222–31.

Pop-Busui R, Kirkwood I, Schmid H, et al. Sympathetic dysfunction in type 1 diabetes: association with impaired myocardial blood flow reserve and diastolic dysfunction. J Am Coll Cardiol. 2004;4:2368–74.

Proietti R, Santangeli P, Di Biase L, et al. Comparative effectiveness of wide antral versus ostial pulmonary vein isolation: a systematic review and meta-analysis. Circ Arrhythm Electophysiol. 2014;7:39–45.

Providência R, Albenque JP, Combes S, et al. Safety and efficacy of dabigatran versus warfarin in patients undergoing catheter ablation of atrial fibrillation: a systematic review and meta-analysis. Heart. 2014;100:324–35.

Sacre JW, Franjic B, Jellis CL, et al. Association of cardiac autonomic neuropathy with subclinical myocardial dysfunction in type 2 diabetes. JCMG. 2010;3:1207–15.

Schneider R, Lauschke J, Tischer T, et al. Pulmonary vein triggers play an important role in the initiation of atrial flutter: initial results from the prospective randomized Atrial Fibrillation Ablation in Atrial Flutter (Triple A) trial. Heart Rhythm. 2015;12:865–71.

Steven D, Sultan A, Reddy V, et al. Benefit of pulmonary vein isolation guided by loss of pace capture on the ablation line: results from a prospective 2-center randomized trial. J Am Coll Cardiol. 2013;62:44–50.

Stritzke J, Markus MR, Duderstadt S, Lieb W, Luchner A, Döring A, Keil U, Hense HW, Schunkert H, MONICA/KORA Investigators. The aging process of the heart: obesity is the main risk factor for left atrial enlargement during aging the MONICA/KORA (monitoring of trends and determinations in cardiovascular disease/cooperative research in the region of Augsburg) study. J Am Coll Cardiol. 2009;54:1982–9.

Takahashi A, Iesaka Y, Takahashi Y, et al. Electrical connections between pulmonary veins: implication for ostial ablation of pulmonary veins in patients with paroxysmal atrial fibrillation. Circulation. 2002;105:2998–3003.

Tesfaye S, Chaturvedi N, Eaton SE, et al. Vascular risk factors and diabetic neuropathy. N Engl J Med. 2005;352:341–50.

Troughton RW, Crozier I. Fine tuning risk stratification for atrial fibrillation. J Am Coll Cardiol. 2013;61(22):2285–7.

Walenga JM, Adiguzel C. Drug and dietary interactions of the new and emerging oral anticoagulants. Int J Clin Pract. 2010;64:956–67.

Wolf PA, Abbott RD, Kannel WB. Atrial fibrillation as an independent risk factor for stroke: the Framingham Study. Stroke. 1991;22:983–8.

Zacharias A, Schwann TA, Riordan CJ, Durham SJ, Shah AS, Habib RH. Obesity and risk of new-onset atrial fibrillation after cardiac surgery. Circulation. 2005;112:3247–55.

Ventricular Tachycardia

9

Justin Hayase, Benedict M. Glover, Pedro Brugada, and Jason S. Bradfield

Abstract

Ventricular tachycardia is defined as an arrhythmia which originates from the ventricles consisting of at least three or more consecutive beats at a rate of greater than 100/min and independent of AV or atrial conduction. If this terminates spontaneously within less than 30 s it is defined as non-sustained. If it lasts greater than 30 s or requires treatment for termination it is defined as sustained. Most commonly VT is associated with structural heart disease such as scar related re-entry in patients who have had a prior MI. Occasionally it may be associated with a structurally normal heart and is termed idiopathic. This is most commonly seen in the right ventricular outflow tract, coronary cusps, coronary veins or around the valve annuli.

Introduction

Ventricular tachycardia (VT) is defined as an arrhythmia originating from the ventricles consisting of at least three or more consecutive beats at a rate of greater than 100 beats/min. Sustained VT is defined as lasting longer than 30 s or requiring treatment for termination. Non-sustained VT is defined as self-terminating within less than 30 s. Most commonly VT is associated with structural heart disease and is due to macroreentry in patients who have myocardial scar. Occasionally VT can occur in a structurally normal heart and can be termed idiopathic. Idiopathic VT most commonly arises in the outflow tracts, papillary muscles, coronary veins or around the valve annuli.

Mechanism

Monomorphic VT can be due to either a macro re-entrant circuit or a focal mechanism within the ventricles. In the presence of structural heart disease, physical barriers such as myocardial fibrosis create regions of slow conduction that serve as critical isthmuses to sustain macro-reentrant VT (Fig. 9.1). Focal mechanisms can be due to either enhanced automaticity or triggered activity and are more common with idiopathic VTs such as outflow tract VTs or papillary muscle arrhythmias in structurally normal hearts.

J. Hayase · J. S. Bradfield (✉)
UCLA Cardiac Arrhythmia Center, Ronald Reagan UCLA Medical Center, Los Angeles, CA, USA
e-mail: JBradfield@mednet.ucla.edu

B. M. Glover
Division of Cardiology, Department of Medicine, University of Toronto, Toronto, Ontario, Canada

P. Brugada
University Hospital of Brussel, Brussels, Belgium
e-mail: pedro@brugada.org

B. M. Glover, P. Brugada (eds.), *Clinical Handbook of Cardiac Electrophysiology*,
https://doi.org/10.1007/978-3-030-74319-2_9

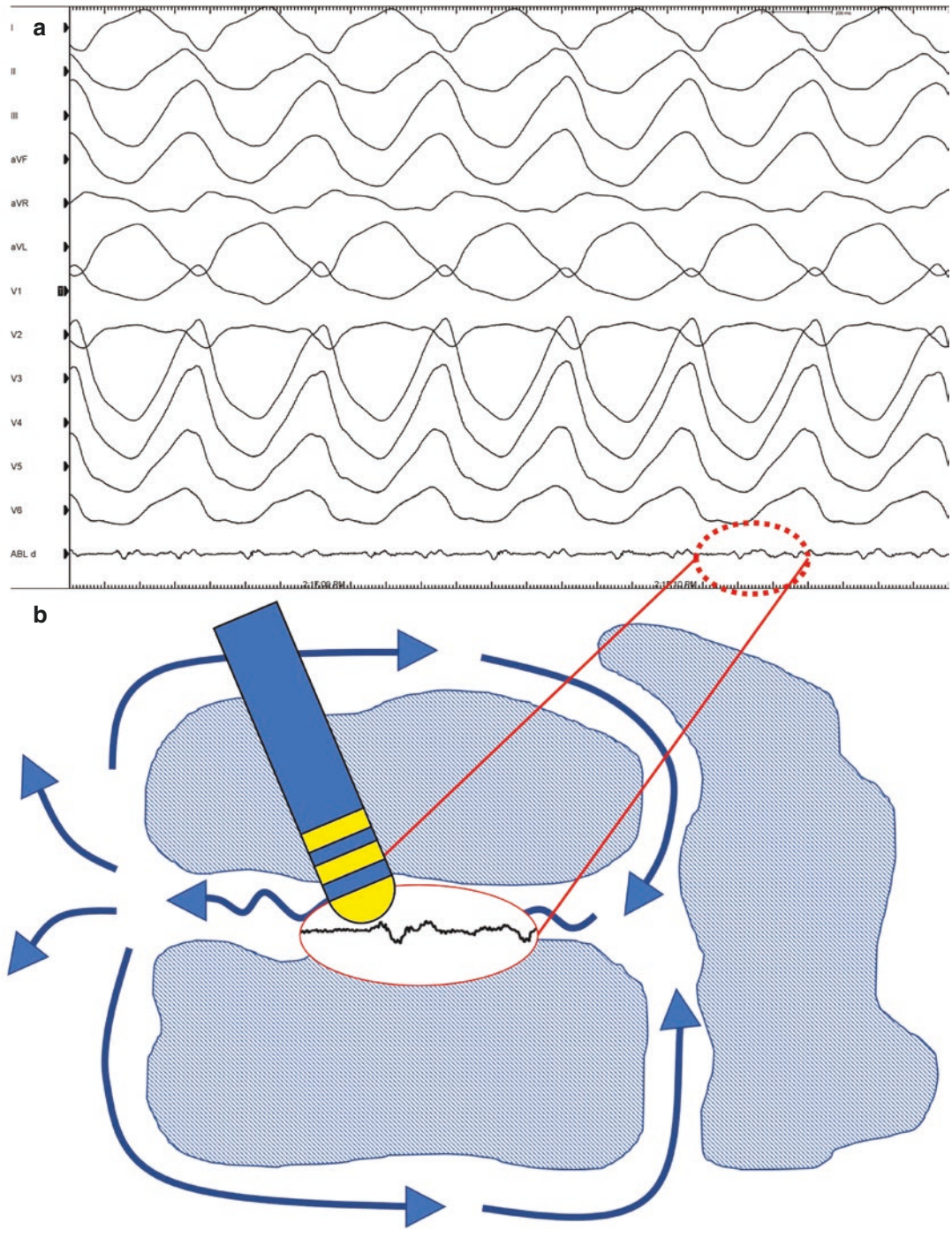

Fig. 9.1 (**a**) Catheter mapping during scar related re-entry VT showing long fractionated signals on the distal ablation catheter (ABLd) during diastole. (**b**) Illustrative diagram correlating the diastolic fractionated signals seen on the ablation catheter. In many cases mid-diastolic potentials correlate with a critical isthmus within islands of scar (shaded regions) surrounding a central area of slow conduction. Ablation in this region resulted in termination of the tachycardia with no further inducible arrhythmia. Adapted from Stevenson, et al. "Exploring postinfarction reentrant ventricular tachycardia with entrainment mapping." JACC 1997

Diagnosis

The most important diagnostic tool for VT is the 12-lead ECG obtained during the arrhythmia. Multiple criteria have been developed to distinguish VT from alternate mechanisms such as supraventricular tachycardia with aberrancy (Fig. 9.2). The surface ECG is also important for identifying the site or origin of the arrhythmia within the ventricles, which will be discussed in the following sections.

The Brugada criteria employ a stepwise approach to identify VT with high sensitivity and specificity. These criteria were originally developed by examining 348 cases of VT and comparing these with 170 cases of SVT with abberancy (Brugada et al. 1991). The classical Wellens criteria for VT in leads V1–V2 as well as V6 are also applied in this algorithm to characterize morphological features which favor VT diagnosis (Wellens et al. 1978). These morphology criteria analyze different features within V1–V2 and V6 which distinguish typical bundle branch block patterns that can suggest SVT with aberrancy versus those which are more likely to indicate VT.

Another algorithm utilizing only lead aVR has been developed for VT diagnosis by Vereckei and colleagues (Vereckei et al. 2008). As shown in Fig. 9.2 the presence of an initial R-wave, the width of an initial r- or q-wave greater than 40 ms, the presence of notching on the initial downstroke of a predominantly negative QRS complex and a V_i/V_t less than or equal to one are more indicative of VT.

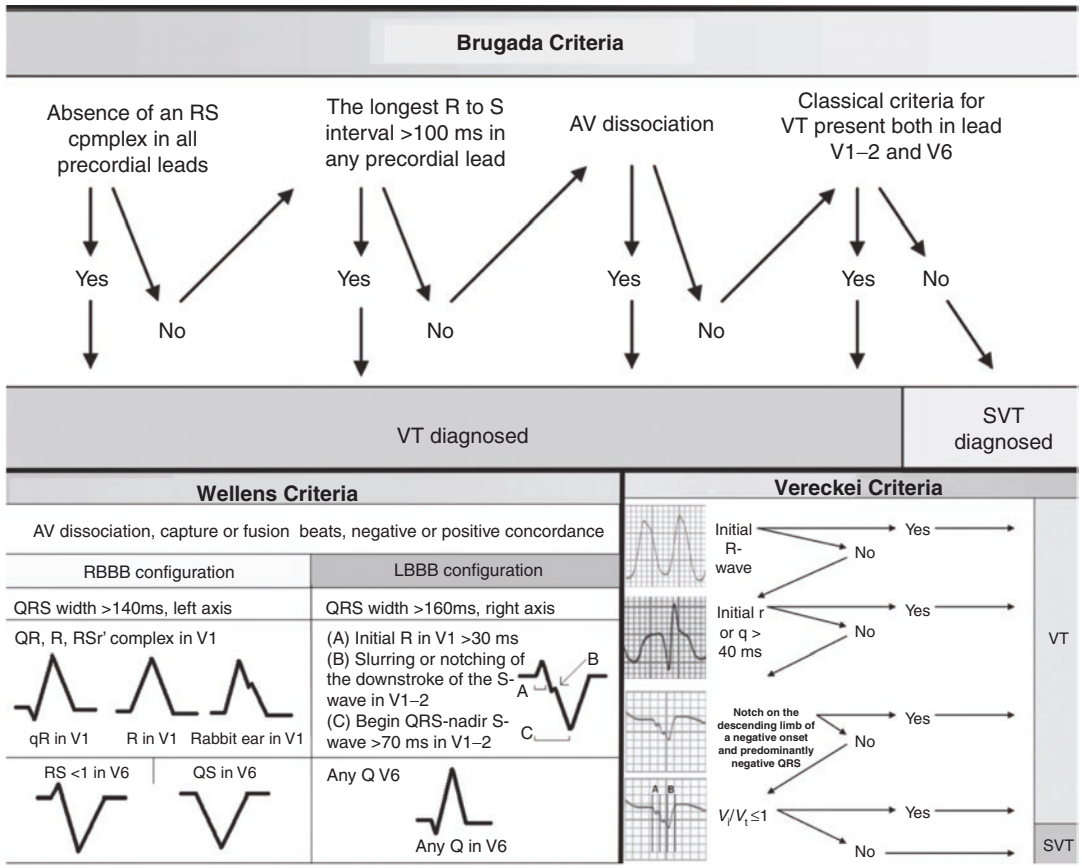

Fig. 9.2 ECG diagnostic criteria for VT diagnosis. (Reproduced with permission from Alzand BS, Crijns HJ. Diagnostic criteria of broad QRS complex tachycardia: decades of evolution. Europace 2011; 13:465–72. Oxford University Press)

Surface ECG Features

Localization

Through analysis of various features of the QRS complexes during VT, the 12-lead ECG is a crucial tool that can identify the site of origin or more specifically the exit site of the arrhythmia (Josephson and Callans 2005) (Fig. 9.3). The bundle branch block pattern generally indicates an origin from the contralateral side. Right bundle branch block pattern typically indicates left ventricular origin, and left bundle branch block pattern points toward a right ventricular source; however, septal exits can also give left bundle branch block patterns. The limb lead axis helps to establish the coronal plane origin with an inferior axis indicating a superior source and vice versa. The precordial leads guide the localization within the Z-plane with predominantly RS complexes (positive concordance) identifying a basal exit and predominantly QS complexes (negative concordance) pointing towards an apical site. QRS width can also be helpful as narrower complexes can suggest a location close to the conduction system such as the septum. A very broad QRS with a prolonged intrinsicoid deflection generally indicates a site far from the conduction system such as the epicardium (discussed in further detail later). It should be noted there are a number of factors that impact the interpretation of the 12-lead ECG for VT, such as myocardial scar, antiarrhythmic medications, metabolic abnormalities, presence of hypertrophy, or the orientation of the heart within the chest cavity.

Outflow Tract Anatomy and the ECG

Both the right and left ventricular outflow tracts are superior structures. Arrhythmias arising from these regions generate a vector from superior to inferior resulting in a positive QRS axis in leads II, III and aVF and negative in aVR and aVL. Differentiating right versus left ventricular outflow tract origin based on the ECG can occasionally be more complex.

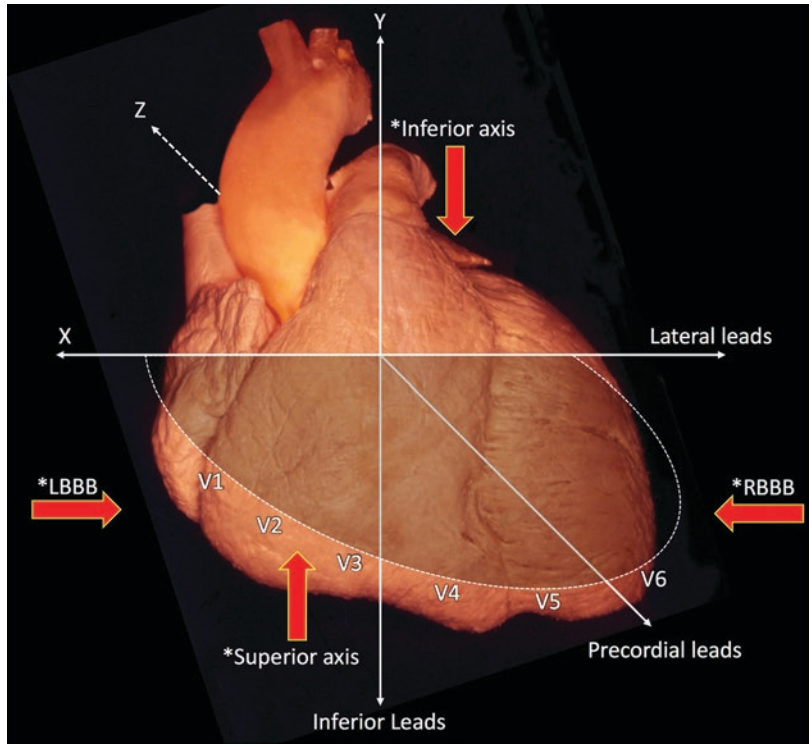

Fig. 9.3 General localization of ventricular arrhythmias based on 12-lead QRS morphology. The X and Y (coronal) plane can be determined by the bundle branch block pattern as well as the limb lead axis. The Z plane is localized by the predominant forces as well as the transition pattern within the precordial leads (predominantly positive forces indicate basal and negative forces indicate apical exit). Courtesy of UCLA Cardiac Arrhythmia Center, McAlpine Collection

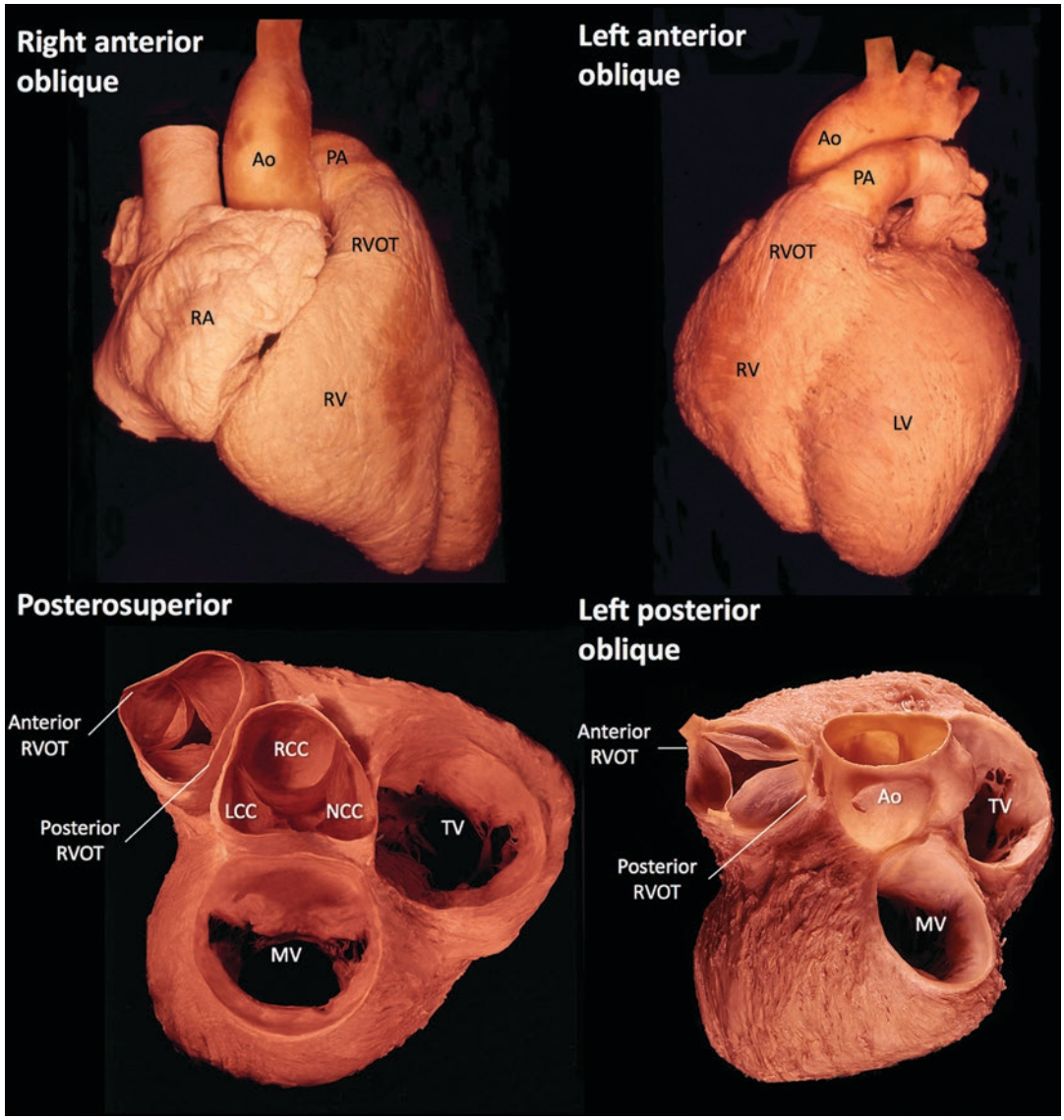

Fig. 9.4 Gross anatomy specimen showing the relationship of the outflow tracts. (Top) Right anterior oblique view on the left and left anterior oblique view on the right. The right ventricular outflow tract can be appreciated as starting inferiorly on the right then coursing superiorly leftward. The RVOT is anterior to the LVOT. The LVOT cannot be appreciated without further dissection. (Bottom) The right and left atria have been removed and the great vessels transected above the aortic and pulmonary valves. The spiral relationship of the LVOT and RVOT are well appreciated in the posterosuperior and left posterior oblique views as the RVOT wraps anteriorly around the LVOT. Courtesy of UCLA Cardiac Arrhythmia Center, McAlpine Collection (*Ao* aorta, *PA* pulmonary artery, *RA* right atrium, *RV* right ventricle, *LV* left ventricle, *RVOT* right ventricular outflow tract, *RCC* right coronary cusp, *LCC* left coronary cusp, *NCC* non-coronary cusp, *MV* mitral valve, *TV* tricuspid valve)

As shown in Fig. 9.4 the right ventricular outflow tract (RVOT) is anterior to the left ventricular outflow tract (LVOT). As the RVOT courses superiorly, it also moves to the left of the LVOT such that the pulmonary valve is actually to the left of the aortic valve.

As a result of the anatomical relationship between the outflow tracts, ventricular activation

from the RVOT generally spreads from anterior to posterior. This results in a negative QRS in V1 with a LBBB type pattern on the ECG, typically with a later precordial transition. If the precordial transition occurs at lead V4 or later then the origin is likely RVOT.

In general, an earlier precordial transition suggests LVOT origin; however, localization becomes more challenging when the precordial transition occurs at or close to V3 or when there is an R wave in the early precordial leads. An R wave in V1–V2 may be present in posterior RVOT or anterior LVOT foci. In order to help estimate the location several algorithms have been developed.

The V2 transition ratio is a surface ECG tool that was developed to distinguish RVOT versus LVOT origin (Betensky et al. 2011). The transition ratio is calculated by dividing the percentage R wave in V2 (R/R+S) during VT to the percentage R wave in V2 during sinus rhythm. A value of 0.6 or greater can distinguish an LVOT origin with high specificity and sensitivity. Similarly, the V2S/V3R index can also help distinguish between a RVOT and LVOT origin in outflow tract arrhythmias (Yoshida et al. 2014). As shown in Fig. 9.5 the amplitude of the S wave in lead V2 is divided by the amplitude of the R wave in lead V3. A value of less than or equal to 1.5 has been shown to be suggestive of a LVOT origin while a value greater than 1.5 represents a likely RVOT origin.

Having ascertained whether the origin is located in either the RVOT or LVOT, further ECG analysis can help estimate the specific location within the respective outflow tract. As demonstrated in Fig. 9.6 a lateral lead such as lead I may be useful in further ascertaining the origin of an outflow tract tachycardia. In an RVOT tachycardia a negative QRS in lead I is indicative of a more leftward origin close to or above the pulmonary valve. A positive QRS in lead I indicates a more rightward structure such as the RVOT freewall. Posteroseptal and anterior origins often are biphasic in lead I.

A final point of emphasis is in regards to leads aVR and aVL. These are almost always negative for outflow tract tachycardias. However, if aVL is isoelectric or positive, the inferior portion of the RVOT close to the bundle of His and right bundle should be considered, which has implications for potential catheter ablation and procedural risk assessment.

ECG Characteristics Suggestive of Epicardial Involvement

In general, the QRS during VT originating from or exiting the epicardium results in a significantly wider QRS due to the greater distance from the His Purkinje system. For epicardial VT with a RBBB morphology thought to have an exit site in the region of the left ventricle several parameters can be measured which may suggest epicardial involvement (Berruezo et al. 2004; Valles et al. 2010; Bazan et al. 2006). Table 9.1 shows validated ECG criteria which suggest epicardial origin for VT.

Figure 9.7 shows an example of an epicardial VT meeting several ECG criteria. It should be noted, however, that concurrent use of antiarrhythmic medications limits the reliability of these criteria (Berruezo et al. 2004).

Mapping and Ablation of Scar Related VT

In patients with structural heart disease, catheter ablation for VT is effective for reducing arrhythmic events. In patients with ICDs, this is particularly important for reducing ICD shocks, which are associated with increased morbidity and mortality (Delacretaz et al. 2013). Per guideline recommendations, ablation should be offered to patients with VT refractory to, or who prefer to avoid, medical management (Al-Khatib et al. 2018). In particular, patients who continue to have VT in spite of amiodarone therapy benefit from catheter ablation (Sapp et al. 2016).

Mapping and ablation strategies for VT depend in large part on whether or not the arrhythmia can be induced in the EP lab and whether it is hemodynamically tolerated. If sustained VT can be induced and tolerated without

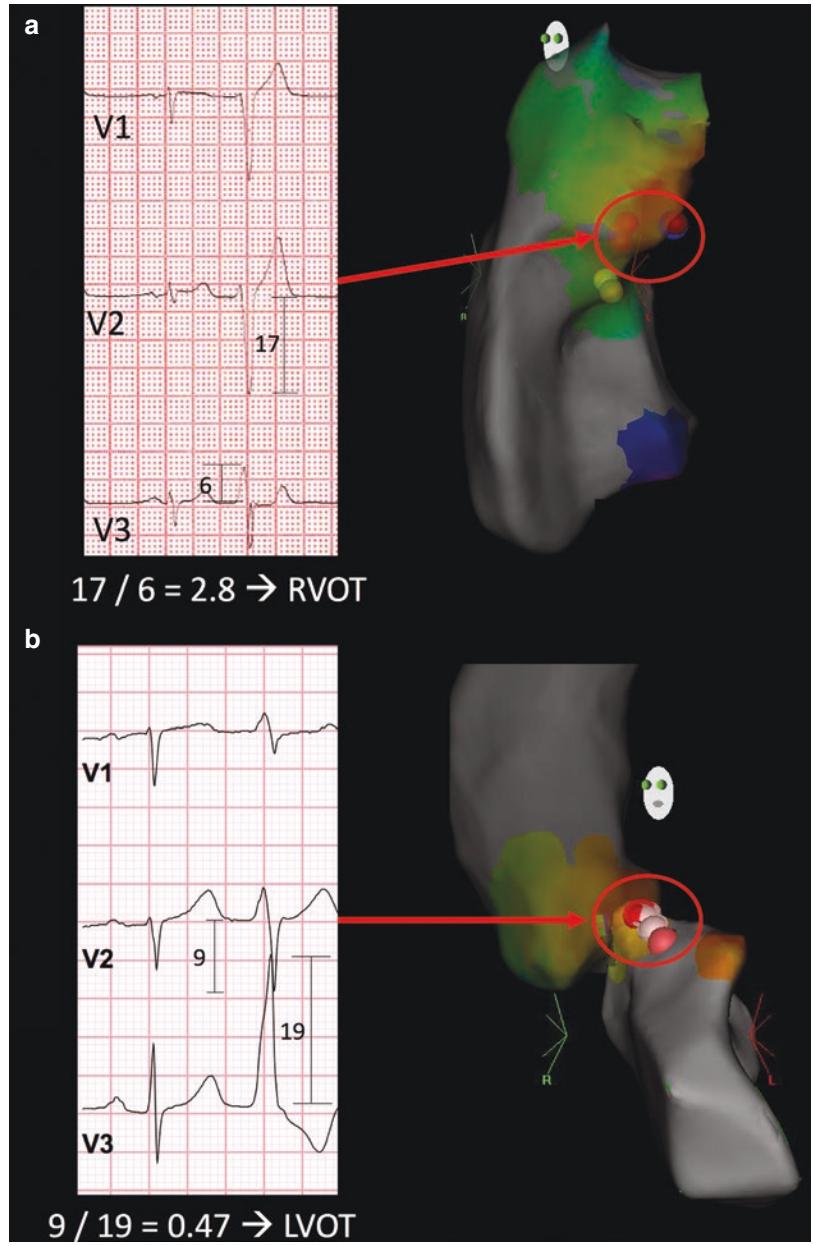

Fig. 9.5 Measurement and calculation of the V2S/V3R ratio outflow tract premature ventricular complexes (PVCs). (**a**) The S wave in lead V2 is 17, while the R wave in V3 is 6 resulting in a V2S/V3R of 2.8 which is indicative of an RVOT origin. The PVC in this patient was mapped to the posterior RVOT and successfully ablated in this region shown on the Carto (Biosense Webster, Irvine, CA, USA) electroanatomic map. (**b**) The S wave in lead V2 is 9, while the R wave in V3 is 19 resulting in a V2S/V3R of 0.47 which is indicative of an LVOT origin. The PVC in this patient was mapped to just below the right and left coronary cusp junction in the LVOT and successfully ablated at this location

hemodynamic collapse, this allows for activation mapping and entrainment maneuvers. In activation mapping, local electrograms are compared to a reference time point such as the surface QRS which are then tagged to an electroanatomic map to create a visual representation of the activation wavefronts. The activation map can often suggest either a macro-reentrant versus a focal mechanism based on the pattern (e.g., "early meets late"). Similarly, overdrive pacing can help distinguish re-entrant from focal mechanisms. The presence of progressive fusion (paced QRS morphology becomes increasingly similar to the paced complex at increasing rates) points toward a re-entrant mechanism. Entrainment can also be a powerful tool in evaluating the pacing location relative to the re-entrant VT circuit (Stevenson et al. 1997). A post-pacing interval difference of

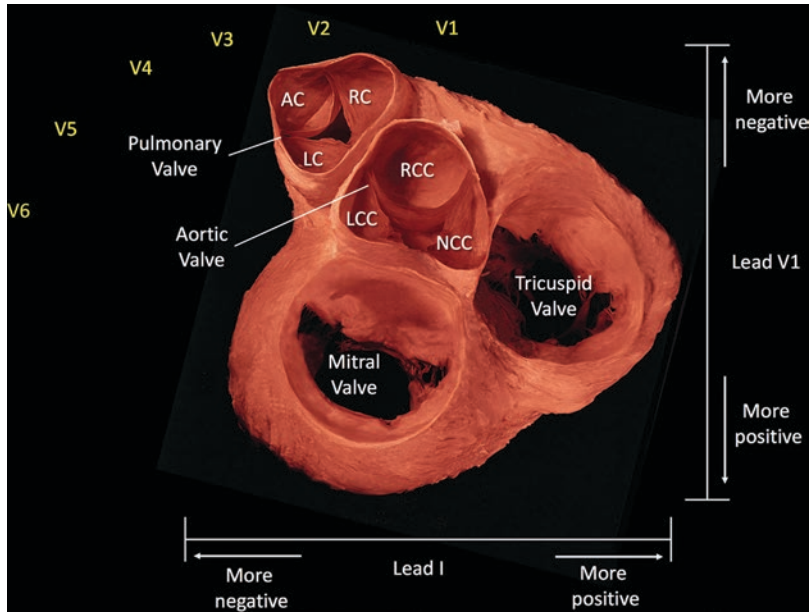

Fig. 9.6 Showing the anatomic relationship of the precordial lead V1 and lead I to the outflow tracts (*AC* anterior cusp, *RC* right cusp, *LC* left cusp, *RCC* right coronary cusp, *LCC* left coronary cusp, *NCC* non-coronary cusp)

Table 9.1 Validated 12-lead ECG criteria for ischemic and non-ischemic cardiomyopathy which suggest an epicardial site of origin for VT (Berruezo et al. 2004; Valles et al. 2010)

Ischemic cardiomyopathy	Non-ischemic cardiomyopathy
1. Pseudo-delta wave >34 ms in any precordial lead **2. Intrinsicoid deflection time >85 ms.** The time from the onset of the QRS to the peak of the R wave measured in V2. **3. RS complex duration ≥121 ms** in any precordial lead of	**1. Presence of inferior Q waves** **2. Pseudo-delta ≥75 ms** in any precordial lead **3. Maximum deflection index (MDI) ≥0.59**, defined as the interval measured from QRS onset to the maximum deflection divided by the total QRS duration (in the precordial lead with the shortest time) **4. Presence of Q wave in lead I**

less than 30 ms relative to the tachycardia cycle length typically indicates close proximity to the circuit. The presence of concealed entrainment, a stim-QRS interval similar to the local EGM-QRS interval during VT, and a stim-QRS divided by the VT cycle length between 0.3–0.7, then these features can further support the location of the catheter as being at a critical isthmus site.

If VT is non-inducible or not hemodynamically tolerated, activation mapping and entrainment cannot be easily utilized. In these cases, pace mapping and substrate modification can be performed. In pace mapping, the catheter is placed in a region of interest and pacing performed at the lowest output required to capture the myocardium. The surface ECG of the paced QRS complex is then compared to the clinical VT or premature ventricular complex (PVC) and an identical match indicates that the catheter location is near the exit site of the arrhythmia. A long stimulus to QRS with a good pace map is often a reasonable sign of being close to the isthmus. Pacing at certain sites of low voltage, fractionation, or late potentials can occasionally result in multiple different QRS morphologies or even induce ventricular tachycardia. These pacing responses indicate multiple exit sites within areas of complex scar or pacing within what is potentially a critical isthmus, and ablation in these regions can result in improved outcomes (Tung et al. 2012).

A number of local electrogram features during sinus rhythm can indicate abnormal tissue which may serve as targets for ablation. **Local abnormal ventricular activities (LAVA)** represent poorly coupled fibers surrounded by normal myocardial tissue (Jais et al. 2012). An example

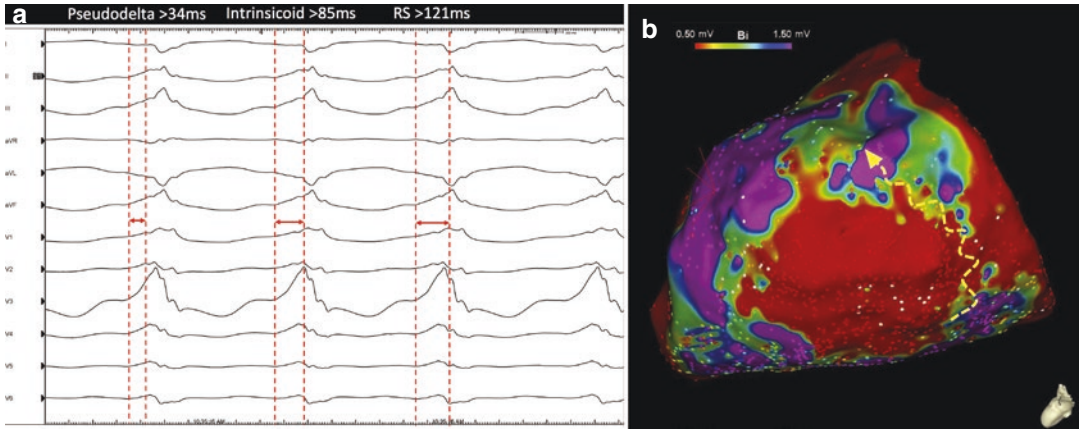

Fig. 9.7 (**a**) ECG of VT with exit site at basal lateral left ventricular epicardium in a patient with ischemic cardiomyopathy. The QRS is broad and satisfies multiple epicardial criteria with a pseudodelta wave of >34 ms, an instrinsicoid deflection of >85 ms to the peak of the R wave in lead V2, and an RS complex duration of >121 ms in any precordial lead. (**b**) Epicardial voltage map in a patient with non-ischemic cardiomyopathy using Carto (Biosense Webster, Irvine, CA, USA) at standard voltage settings 0.5–1.5 mV with likely VT isthmus indicated by hatched yellow arrow

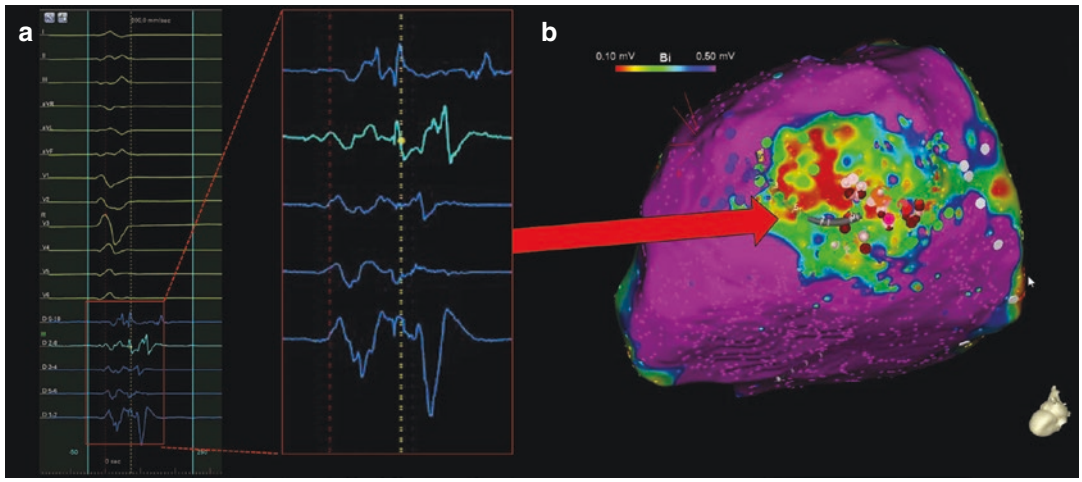

Fig. 9.8 (**a**) Taken from the same patient as Fig. 9.7. Intracardiac electrogram recordings from a decapolar catheter placed at the lateral epicardial left ventricle demonstrating extensive local abnormal ventricular activities (LAVA) during sinus rhythm. (**b**) Inferolateral Carto epicardial voltage map at dense scar settings 0.1–0.5 mV with an area of dense scar at the lateral epicardial left ventricle where LAVAs were encountered. This area was targeted for extensive substrate ablation

of LAVAs are shown in Fig. 9.8. The classical features of LAVA during sinus rhythm are: (1) high frequency often double (or more) potentials separated by a low amplitude baseline (2) separate from and often (but not always) following ventricular far-field, and (3) may require pacing at the site in order to distinguish LAVA from ventricular farfield. As previously discussed, if ventricular pacing at these sites results in different morphologies this indicates that the pacing substrate is complex. Targeting and ablation of LAVA have demonstrated improved outcomes (Jais et al. 2012). Aside from LAVA, **late potentials (LP)** are discrete, isolated electrogram components occurring after the surface QRS complex. They are a marker of slow conduction, which can

potentially indicate critical isthmuses. The ablation of late potentials can also provide an endpoint for patients with unmappable or unstable VT (Vergara et al. 2012; Arenal et al. 2003).

An important consideration is that the timing and features of LAVA and LP depend on a number of factors including their anatomic location (septal versus lateral, endocardial versus epicardial) and the directionality of the activation wavefront (Komatsu et al. 2013; Tung et al. 2016). It is therefore important to perform pacing, potentially from multiple different sites, in order to separate out local fractionated potentials from farfield ventricular activation and improve sensitivity.

A substrate-homogenization approach may also be effective. This strategy begins with a comprehensive voltage map to guide ablation. In general, normal myocardial tissue is defined as a bipolar peak-to-peak voltage greater than 1.5 mV and dense scar is a voltage less than 0.5 mV. Voltage between 0.5 and 1.5 mV is defined as borderzone tissue. Additionally, the use of unipolar voltage mapping can suggest the presence of epicardial scar with a cutoff of <8.27 mV indicating potential abnormal tissue (Hutchinson et al. 2011). Mapping and ablation of epicardial VT will be discussed in detail later in the chapter. Some trial data suggest that the elimination of all abnormal voltage signals with radiofrequency ablation can have superior outcomes (Di Biase et al. 2015). Another strategy consists of ablation around the border of abnormal tissue as a means of "core isolation" of the arrhythmogenic substrate (Tzou et al. 2015). While these techniques can be effective for some patients, they require extensive ablation and may not always be feasible depending on patient substrate, anatomy, hemodynamic stability, or extent of scar.

Macro-Reentrant VT Involving the Conduction System

Bundle Branch Re-Entry

Bundle branch re-entrant VT typically occurs in patients with structural heart disease who have a damaged His-Purkinje system. Under normal circumstances antegrade conduction through the His Purkinje network is relatively rapid. Since the tissue then remains refractory for more prolonged periods of time this generally prevents re-entry from occurring between the right and the left bundle branches. In cases where conduction is slowed or transiently blocked in either the antegrade or retrograde directions, re-entry may occur. As shown in Fig. 9.9 this may result in antegrade conduction down the right bundle with retrograde conduction up the left bundle resulting in a left bundle branch block morphology during VT. The reverse, though less common, may also occur with antegrade conduction down the left bundle and retrograde conduction up the right bundle resulting in a right bundle branch block morphology during VT.

EP Study and Ablation for Bundle Branch Re-Entry VT

In patients with bundle branch re-entry the baseline ECG during normal sinus rhythm often shows first degree AV block with some variant of intraventricular conduction delay or an incomplete bundle branch block. The baseline EP study generally demonstrates a prolonged HV interval during sinus rhythm of greater than 60 ms. (Blanck et al. 1993) Tachycardia may be induced with either atrial or ventricular pacing. The morphology is more commonly a LBBB than a RBBB. The diagnosis is made by the presence of a His signal before every QRS with a HV interval typically slightly shorter than during sinus rhythm. The His signal is generally followed by the right bundle potential or less commonly a left bundle potential depending on the direction of the circuit. As these are all vital components in the circuit, a change in either the H-H, RB-RB or LB-LB intervals prolongs the tachycardia cycle length. Entrainment may be possible by pacing from the right ventricular apex. A difference of less than 30 ms is suggestive of bundle branch re-entry (Merino et al. 2001).

In general ablation of the right bundle branch is performed. In order to map this the His is located and a more distal location with a right

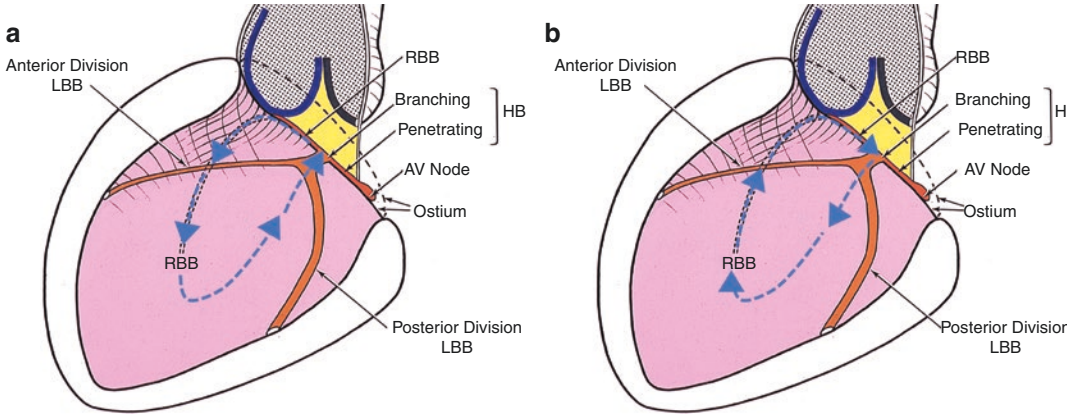

Fig. 9.9 Showing the Potential Circuits Involved in bundle branch re-entry. Illustration shown is in a left posterior oblique view of the interventricular septum. (**a**) The more common scenario where antegrade conduction occurs along the right bundle and retrogradely along the left bundle providing a left bundle branch block morphology on ECG. (**b**) The less common antegrade conduction along the left bundle with retrograde conduction along the right bundle which gives a right bundle branch block morphology on ECG. *RBB* right bundle branch, *LBB* left bundle branch, *HB* his bundle. Courtesy UCLA Cardiac Arrhythmia Center, McAlpine Collection

bundle electrogram and no atrial signal is chosen along the superobasal region.

Fascicular Re-Entry VT

Fascicular re-entry VT is sometimes referred to as either verapamil sensitive or Belhassen VT and can occur in either structurally normal or abnormal hearts. Whereas in bundle branch re-entry VT the His activation occurs before left bundle activation in fascicular re-entry His activation tends to occur after left bundle activation and with a much shorter HV interval during tachycardia. The QRS in fascicular VT although prolonged, is generally less than 140 ms and therefore is not as prolonged as many other types of VT. Upper septal re-entry tends to be narrower and may even be confused with SVT. Three different types of fascicular VT exist (Nogami 2011).

The most common type is left posterior fascicular in which the antegrade component to the circuit involves slowly conducting, decremental verapamil-sensitive Purkinje fibers extending from the base of the interventricular septum towards the LV apex. The retrograde circuit then propagates along the posterior fascicle with an exit site in the inferoposterior septum resulting in a RBBB morphology with a superior directed axis. Less common is left anterior fascicular in which the retrograde activation occurs along the anterior fascicle with an exit along the anterolateral wall of the LV resulting in a RBBB morphology QRS during tachycardia with an inferior directed axis.

In upper septal VT the left posterior and left anterior fascicles both act as the antegrade limbs resulting in a relatively narrow QRS often with a RBBB morphology although occasionally there is a LBBB pattern with an inferior or normal axis. Diagrammatic representation of these is shown in Fig. 9.10.

EP Study and Ablation for Fascicular VT

EP evaluation and catheter ablation may be performed successfully in the majority of patients. Given that the circuit is located in the left ventricle access can be achieved either retrograde aortic or through a transseptal approach. The risks are therefore similar to those for all left ventricular ablations with the additional potential risk of the development of LBBB and AV block.

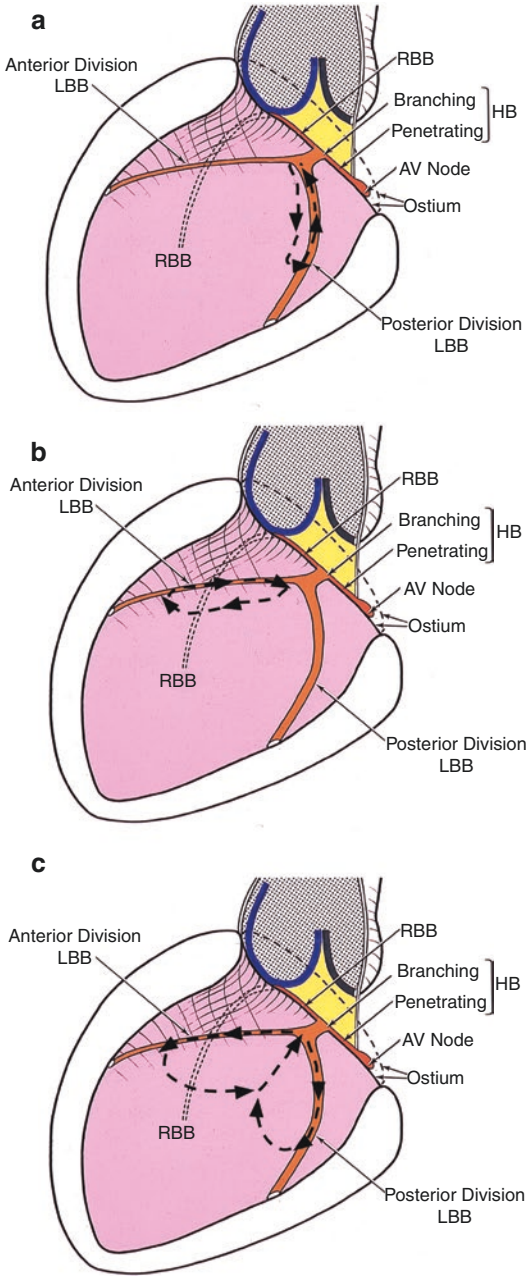

Fig. 9.10 Potential Circuits Involved in fascicular reentry. Illustration shown is in a left posterior oblique view of the interventricular septum. (**a**) Posterior fascicular circuit with posterior fascicle as antegrade limb. This is the most common form of fascicular VT. ECG will demonstrate RBBB and superior axis. (**b**) Anterior fascicular circuit with anterior fascicle as the antegrade limb. ECG will demonstrate RBBB and inferior axis. (**c**) Upper septal circuit with both anterior and posterior fascicles as the simultaneous antegrade circuit. QRS is often narrow <120 ms with normal or RBBB morphology. *RBB* right bundle branch, *LBB* left bundle branch, *HB* his bundle. Courtesy UCLA Cardiac Arrhythmia Center, McAlpine Collection

One of the hallmark features of this type of VT is that it can be induced and entrained by performing atrial pacing. If pacing is insufficient for the induction of VT then isoprenaline can be helpful. During normal sinus rhythm and during tachycardia a sharp high frequency Purkinje potential can be recorded prior to the onset of the QRS. During sinus rhythm a lower frequency potential may be recorded after the QRS which is known as a late diastolic potential. During tachycardia, however, this electrogram precedes the Purkinje potential as it forms the verapamil sensitive antegrade limb of the circuit; and therefore, is also known as the pre-Purkinje potential. As the mapping catheter is moved further from the base of the interventricular septum towards the LV apex the pre-purkinje potential becomes later during tachycardia. The area of slow conduction tends to occur at the junction of the fascicle and the antegrade limb where the purkinje potential is at its earliest and the pre-purkinje potential is at its latest (Nogami et al. 2000).

Ablation is generally performed during tachycardia when possible. A region close to the exit site can be targeted approximately one third of the way from the LV apex to the base where the earliest purkinje potential precedes the QRS**.** The late diastolic potential tends to occur after the QRS in this region. An alternative approach where the earliest late diastolic potential can be targeted until VT is terminated thus cutting off all downstream fascicular activation. This appears to be associated with a slightly higher risk of AV block or LBBB. If VT cannot be induced nor sustained and the suspicion is that of a left posterior fascicular VT then a linear lesion can be made 1 cm proximal to the exit site (Lin et al. 2005). The exit site can be identified by careful pace mapping. If the linear lesion is successful, the purkinje potential jumps from before to after the QRS complex.

It is also possible to have a focal arrhythmia originating from the purkinje network which results in a RBBB morphology QRS with either a superior or inferior directed axis. As a focal arrhythmia, it tends not to be initiated or entrained from pacing in the atrium or ventricles. In focal fascicular VT, the earliest site of activation should be targeted.

Mapping and Ablation of Focal Ventricular Arrhythmias

The main indications for the ablation of focal ventricular arrhythmias are either symptoms which cannot be effectively treated with pharmacological agents or frequent arrhythmias resulting in left ventricular dysfunction. Less commonly, frequent PVCs can induce episodes of ventricular fibrillation, and ablation of the triggers can be an effective treatment (Haissaguerre et al. 2002). If there are minimal symptoms, often no treatment is required. Pharmacological therapy is often of modest efficacy if symptoms persist and includes beta blockers, calcium channel blockers, and class 1C antiarrhythmic agents.

Strategies for ablation of focal ventricular arrhythmias differ from scar-related macroreentrant VT in multiple ways. In contrast to reentrant arrhythmias, overdrive pacing will not demonstrate progressive fusion in focal VT. Mapping relies predominantly on activation and pace mapping techniques. Local electrograms more than 20 ms pre-QRS can indicate catheter location near the site of origin. Unipolar electrogram recordings are also useful as a QS complex can be seen at the focal source due to the centrifugal activation wavefront. As previously discussed, pace mapping is also a useful tool, though again, this identifies the exit sites of the arrhythmia and not necessarily the true origin. (Fig. 9.11) Specific considerations for different types of focal ventricular arrhythmias will be discussed in the following sections.

If possible, all antiarrhythmic drugs should be discontinued for at least five half-lives prior to the procedure. One of the most common challenges arises from the inability to induce the tachycardia at the start of the case. Intravenous sedation should be minimized. If there is no spontaneous ectopy, rapid atrial or ventricular pacing can be performed, or isoprenaline or epinephrine can be infused at the start of the case. The circadian pattern of PVC burden based on ambulatory monitoring can help predict whether sympathomimetic agents will be helpful in PVC induction, either during infusion or washout (Hamon et al. 2018). If there are very infrequent episodes of ectopy then careful pace mapping can be performed using the minimum output to result in local capture until a suitable site can be identified.

If there are no focal regions of early activation but rather a general area either on time with or slightly ahead of the onset of the QRS then adjacent anatomical structures should be mapped. These will be discussed in further detail in the following sections.

Following ablation, it is reasonable to monitor the patient for 30 min. If there is a recurrence of ectopy with similar morphology, then further mapping and ablation should be performed. It is possible that the exit site of an ectopic focus may be shifted by ablation, thus altering 12-lead ECG morphology. If pharmacological agents were required for initiation of the ectopy at baseline, then these should be administered following ablation.

The Outflow Tracts

The most common locations for idiopathic VT and PVCs are within the right and left ventricular outflow tracts. Isolated PVC's in the setting of normal left ventricular function are generally low-risk. Non-sustained and sustained focal VT may also originate from the outflow tracts and is more commonly found in the right ventricular outflow tract (RVOT) compared with the left ventricular outflow tract (LVOT). Acute termination can be performed with the administration of intravenous adenosine which acts by blocking the beta-adrenergic activation of intracellular calcium (Lerman 2007).

To access the RVOT, the ablation catheter is positioned in the right atrium then flexed and advanced into the right ventricle. From this point, the catheter can be carefully rotated clockwise to direct the tip towards the RVOT. The anterior RVOT and free wall of the right ventricle are vulnerable, thin-walled structures, so vigilant use of fluoroscopy, intracardiac echocardiography, and electroanatomic mapping are important to avoid injury. A curl in the tip of the catheter often makes advancement less traumatic with a lower chance

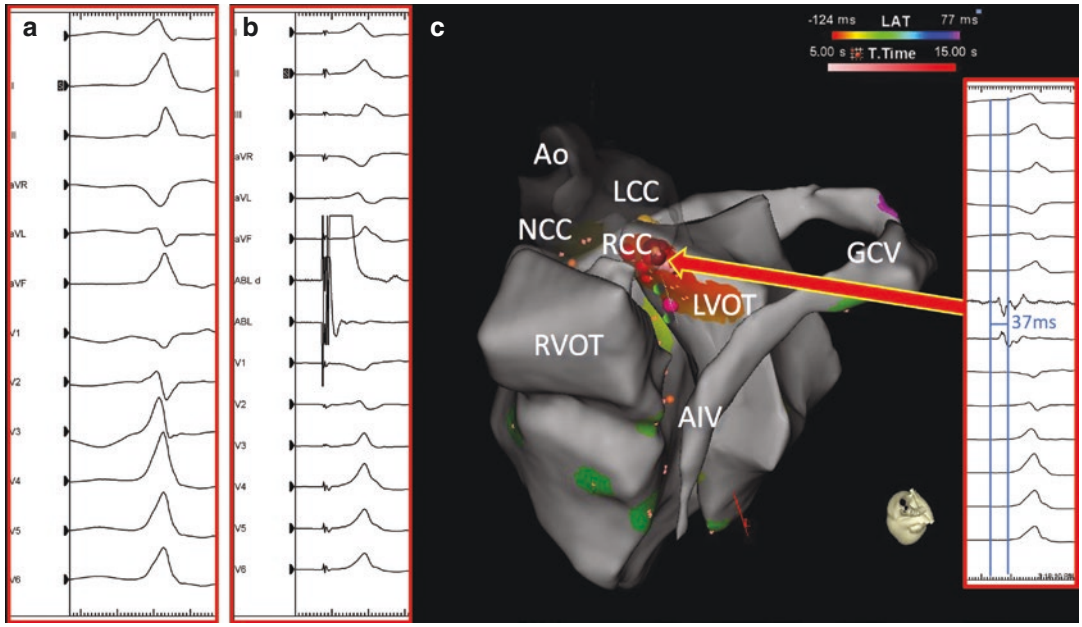

Fig. 9.11 (**a**) Surface 12-lead ECG of a patient with symptomatic PVCs. The clinical PVC demonstrated inferior axis, left-bundle branch block morphology, and V3 transition consistent with outflow tract morphology. (**b**) Pace map with the ablation catheter (ABL) from a location just below the right and left coronary cusps. Pace maps in this region can be deceiving due to preferential conduction (Yamada et al. 2007) (**c**) Left anterior oblique cranial view of a Carto (Biosense Webster, Irvine, CA, USA) activation map demonstrating earliest signal –37 ms pre-QRS below the right and left coronary cusps. Ablation in this region abolished this patient's PVCs. *Ao* aorta, *NCC* non-coronary cusp, *LCC* left coronary cusp, *RCC* right coronary cusp, *LVOT* left ventricular outflow tract, *RVOT* right ventricular outflow tract, *AIV* anterior interventricular vein, *GCV* great cardiac vein

of right ventricular outflow tract perforation. In order to access the LVOT, either a retrograde aortic or trans-septal approach can be employed. However, mapping of the supra-valvular aortic sinus of Valsalva cannot be easily done via a transeptal approach unless utilizing remote magnetic navigation. Remote magnetic navigation technology can also be used for outflow tract arrhythmias with data demonstrating success rates similar to manually controlled catheters but reduced fluoroscopy times (Shauer et al. 2018).

During the delivery of RF in a successful region there is often an episode of non-sustained VT or frequent unifocal ventricular ectopy followed by normal rhythm for the remainder of the ablation. The occurrence of impedance drop by approximately 10 Ohms and ST segment elevation in the unipolar electrogram is generally a good sign of local tissue injury.

A number of considerations must be kept in mind for safe performance of outflow tract arrhythmias. If the focus is inferior and septal then caution must be taken to ensure no damage to the His bundle conduction system. For ablations in the more superior posterior RVOT it must be remembered that the left main coronary artery is often only 5 mm from the site of the ablation catheter, and a coronary angiogram should be considered (Vaseghi et al. 2006). The RVOT is relatively thin in many regions and care must be taken not to use excess power or force so as to minimize perforation risk.

The overall acute success for catheter ablation of outflow tract tachycardia is approximately 90%. Two predictors of recurrence are shorter earliest activation times targeted for ablation or reliance on pace mapping as the only procedural strategy (Chung et al. 2014). Pace mapping is particularly limited by the preferential conduction properties of the outflow tract tissues, which can create misleading pace maps at sites of origin, possibly due to insulated myocardial fibers

leading to unexpected breakout locations during pacing (Yamada et al. 2007).

The Atrioventricular Valve Annuli

The mitral and tricuspid valve annuli are other anatomic regions where focal ventricular arrhythmias can arise (Tada et al. 2005, 2007). For mitral annular sites, positive precordial concordance is typically present for these arrhythmias due to their basal origin, and the inferior leads can determine whether the origin is superior or inferior on the annulus. More septal origins tend to be narrower (typically <140 ms) than LV free wall locations (Tada et al. 2005). For the tricuspid annulus, a left bundle branch pattern is universally present in lead V1 with no negative component in lead I. Septal locations are typically more common than free wall origins, although effective ablation in these areas can be limited due to close proximity to the His-Purkinje system (Tada et al. 2007). Ablation of a tricuspid annular PVC is shown in Fig. 9.12.

The Purkinje Fibers and Papillary Muscles

As previously mentioned, the Purkinje fiber conduction system can be a common source of PVCs. These sources can originate within the fascicles along the left ventricular septum, and ablation of these initiating triggers can provide therapeutic benefit in some patients with idiopathic ventricular fibrillation (Haissaguerre et al. 2002). The anterolateral and inferomedial papillary muscles are also common locations for focal ventricular arrhythmias within the left ventricle (Santoro et al. 2014). In the right ventricle, the moderator band can also be a site of origin, which shares similar anatomic challenges for ablation as the papillary muscles (Sadek et al. 2015). Catheter stability and contact can be a significant obstacle to performing effective radiofrequency ablation. For radiofrequency energy delivery, the use of contact-force technology in conjunction with intracardiac echocardiography can help inform proper catheter positioning (Seiler et al. 2009). Cryoablation is another tool that can be utilized which can aid catheter stability during lesion formation on these intracardiac structures (Rivera et al. 2016).

The Left Ventricular Summit

The summit is the most superior portion of the left ventricle within the attitudinally oriented heart. The summit is bounded by the bifurcation of the left coronary arteries, which is a triangular-shaped region between the left anterior descending (LAD) and circumflex (LCx) arteries (McAlpine 1975). Ventricular arrhythmias originating from the LV summit can be particularly challenging due to a number of anatomic factors. The close proximity of multiple vessels including the LAD and LCx as well as the greater cardiac vein (GCV) can limit the efficacy of performing ablation in this region. The GCV can provide a means of access to this site; however, this can pose technical difficulties. If ablation is performed in the cardiac venous system, then power is generally limited to 20–25 W using an irrigated catheter. The issues in these regions may include the possibility of coronary artery damage and the possibility of impedance rises due to poor flow. Additionally, the epicardial surface of the LV summit is typically insulated by adipose, which further limits the efficacy of ablation, particularly via an epicardial access approach. The critical sites for these arrhythmias can also be intramural, which can be difficult to access via any percutaneous approach (Fig. 9.13). It is not uncommon for successful ablation of LV summit arrhythmias to require ablation from multiple different approaches (e.g., endocardial, coronary venous system, epicardial) (Yamada et al. 2010; Chung et al. 2020).

Challenging Ablation Sites

As discussed in the prior section the LV summit is an anatomically difficult region to access with an ablation catheter. For similar sites that are

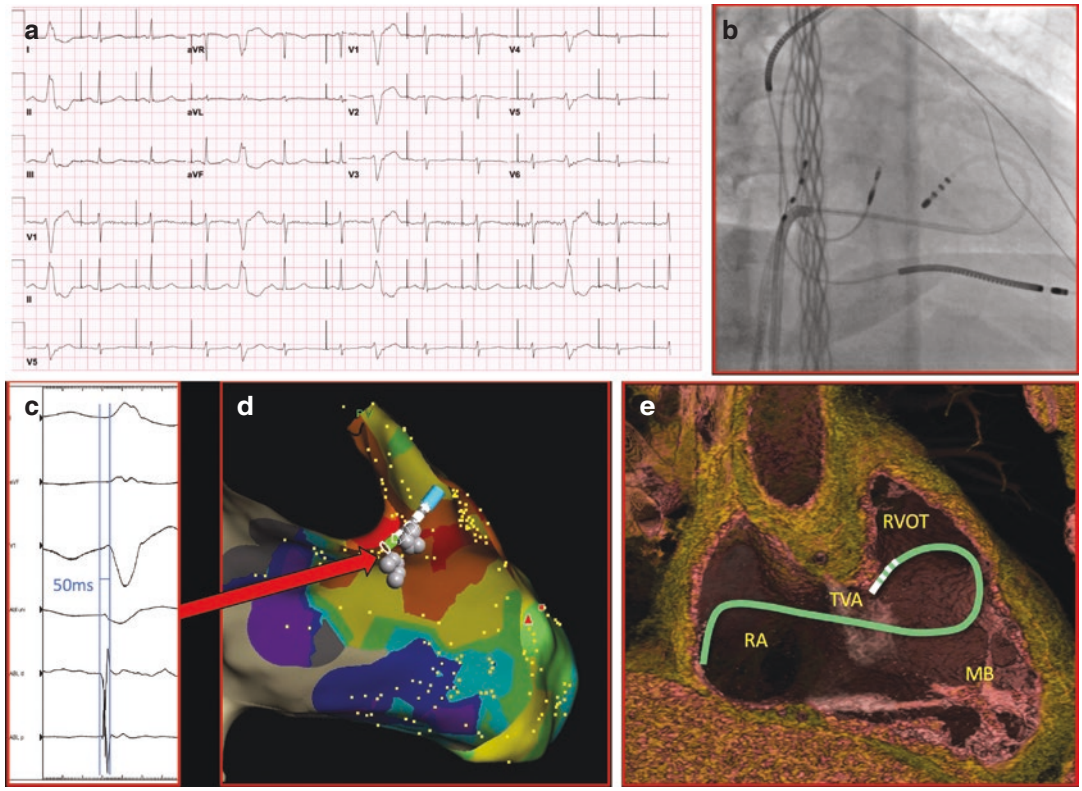

Fig. 9.12 (**a**) 12-lead ECG of a patient with frequent symptomatic PVCs with left bundle branch block morphology, inferior axis, with positivity in lead I. (**b**) Right anterior oblique fluoroscopic image during ablation procedure demonstrating ablation catheter position in a "candy-cane" formation targeting the superior tricuspid annulus. (**c**) Intracardiac ablation catheter early signal 50 ms pre-QRS at the successful lesion site. (**d**) NavX (Abbott Medical, St. Paul, MN, USA) activation map of the right ventricle in right anterior oblique view demonstrating successful ablation site. (**e**) Computed tomography 3-D anatomical reconstruction with cartoon superimposition demonstrating ablation catheter orientation within the heart at the successful ablation site. Image courtesy of Shumpei Mori, MD, PhD. *RA* right atrium, *TVA* tricuspid valve annulus, *RVOT* right ventricular outflow tract, *MB* moderator band

Fig. 9.13 LV summit ablation. (**a**) 12-lead ECG morphology of clinical PVC in a patient with non-ischemic cardiomyopathy and bi-ventricular ICD. Pacing artifact can be appreciated due to the device being programmed to asynchronous pacing mode during the case. Intracoronary wire pace mapping was performed in the mid-septal, first septal, proximal left anterior descending, and left circumflex arteries with good, but not perfect pacemap matches. The intracoronary wires allow for unipolar recordings at the tip of the wire with the body of the wire insulated with an uninflated angioplasty balloon. (**b**) Left anterior oblique caudal image of intracoronary wires placed within the LAD and LCx. (**c**) Left anterior oblique fluoroscopic image of successful ablation site which was achieved via retrograde aortic approach on the endocardial aspect at the LV summit with the ablation catheter in a candy cane configuration. (**d**) Gross anatomy specimen from a superior viewpoint with transection of the great vessels demonstrating the location of the LV summit, which is a triangular region (yellow shading) bounded by the proximal LAD and LCx arteries. (**e**) Gross anatomy specimen from a right anterior oblique view with transection vertically through the ascending aorta, left ventricle, right atrium, and right ventricle. LV summit region indicated by yellow shaded region. Copyright UCLA Cardiac Arrhythmia Center, McAlpine Collection

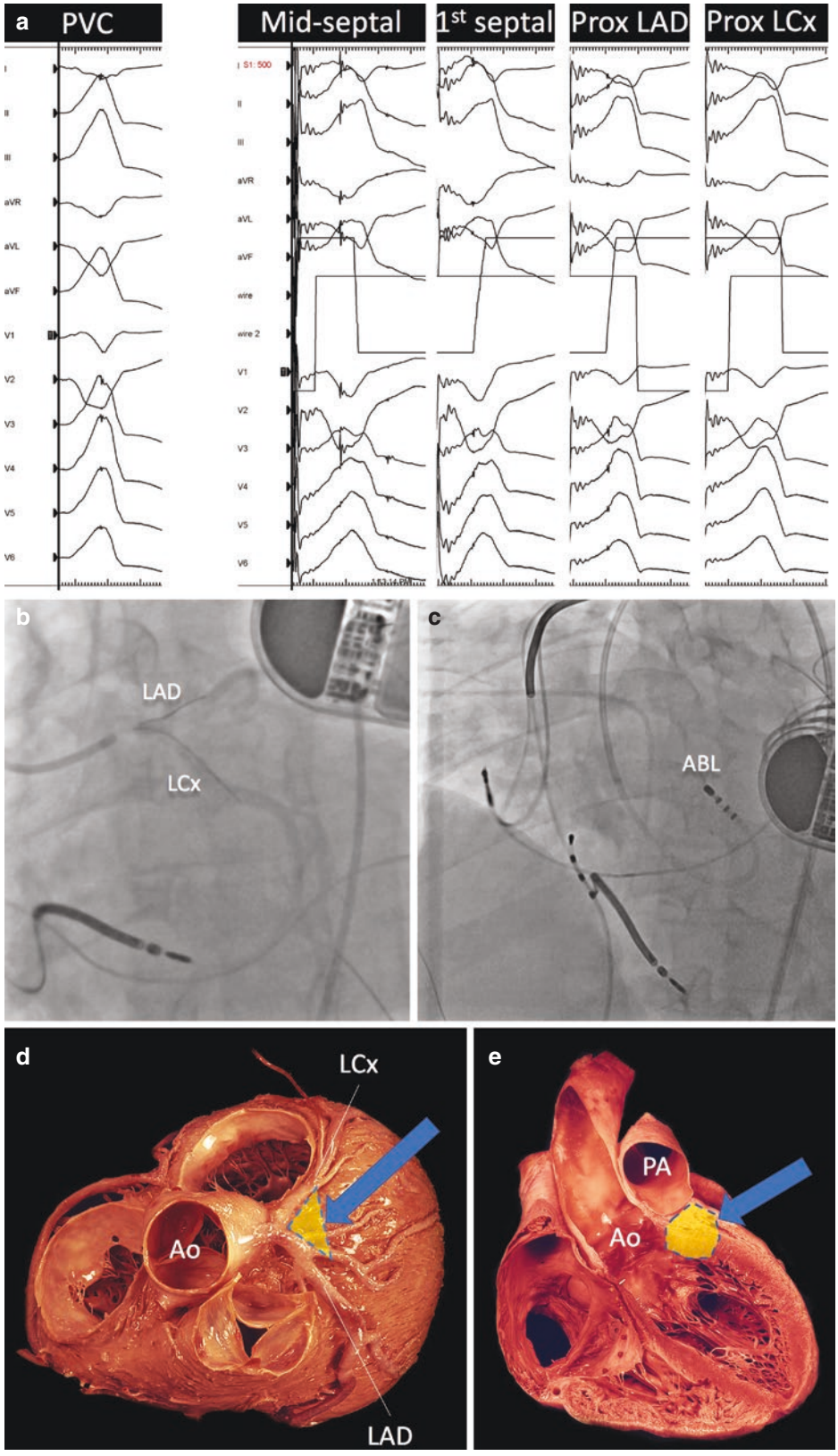
a
PVC
Mid-septal
1st septal
Prox LAD
Prox LCx
I
II
III
aVR
aVL
aVF
V1
V2
V3
V4
V5
V6
wire
wire 2
b
LAD
LCx
c
ABL
d
LCx
Ao
LAD
e
PA
Ao

intramural or intraseptal, it can also be difficult to create an effective lesion at the desired location. A number of different techniques can be utilized to achieve success.

The use of half-normal saline for irrigation results in decreased charge density and increased impedance around the catheter tip, thus directing greater current delivery to the myocardial tissue. The off-label application of half-normal radiofrequency ablation has been demonstrated to create larger lesions and can be utilized in select cases (Nguyen et al. 2018). A higher incidence of steam pops has been reported with this technique, however.

Another strategy to create larger, deeper lesions is the use of two catheters on either side of the region of the interest with one serving as the active electrode and the other as the ground. The clinical application of this technique has been employed with some success, particularly in the ablation of intraseptal sites of origin with bipolar catheters placed on either side of the interventricular septum (Nguyen et al. 2016). Alternative modalities to reach intraseptal locations include the use of ethanol (via either coronary arterial or venous system) (Sacher et al. 2008; Kreidieh et al. 2016), coil embolization of the coronary septal branches (Tholakanahalli et al. 2013), or the use of intramyocardial wires to deliver radiofrequency energy (Romero et al. 2018).

Epicardial Access and Ablation

Scar related monomorphic VT circuits may involve the endocardium, mid myocardium and epicardium. This is more commonly but not exclusively seen in non-ischemic VT. Certain cases may require epicardial access in order to successfully target the critical components of the circuit. This may be determined according to the underlying substrate, by using imaging with cardiac MRI or PET-Ct which may help visualize scar distribution, in cases where ablation was unsuccessful from the endocardium and in cases where the ECG may exhibit certain characteristics as discussed previously.

Epicardial Access

For the proper entry point, it is important to identify the left sternocostal triangle, also known as Larrey's space, which is a relatively avascular region allowing for the safe performance of epicardial access (Baudoin et al. 2003). Most commonly, a 17-gauge Tuohy needle is introduced at a 45° angle initially until it has passed through the diaphragm and then a slightly shallower angle so as to minimize risk of collateral injury to organs such as liver or colon. The direction of the needle can be visualized in the RAO view aiming towards the medial one third of the RV (where there are no major coronary vessels) while the depth is most easily seen in a left lateral projection.

As the tip of the needle enters the epicardial space a sensation of a 'give' is felt followed by a cardiac pulsation. Contrast can be injected which will layer within the pericardial space if in the appropriate location. Additionally, a long wire can be advanced through the needle. If this is truly in the pericardial space it should not follow the course of any cardiac chamber. If this is in the RV it will tend to pass towards the RVOT and into the pulmonary truck often with significant ectopy. Alternatively, the pressure from the needle can be recorded, which will change from a flat line as the needle is advanced through tissue to a sudden negative pressure as the tip of the needle passes into the pericardial space (Di Biase et al. 2017). Entering the right ventricle will demonstrate an RV pressure waveform. In general as long as only the needle tip and wire enter the ventricle, a fresh attempt can be made with close hemodynamic monitoring.

As soon as it is confirmed that the needle and wire are in the epicardium then a sheath and dilator can be introduced. It is important that a catheter is left in the sheath to avoid laceration of the ventricular wall with the tip of the sheath. The relevant anatomy pertaining to epicardial access is shown on anatomical image and the CT image in Fig. 9.14.

In certain patients epicardial access is not possible or extremely limited due to pericardial adhesions. This is particularly common in

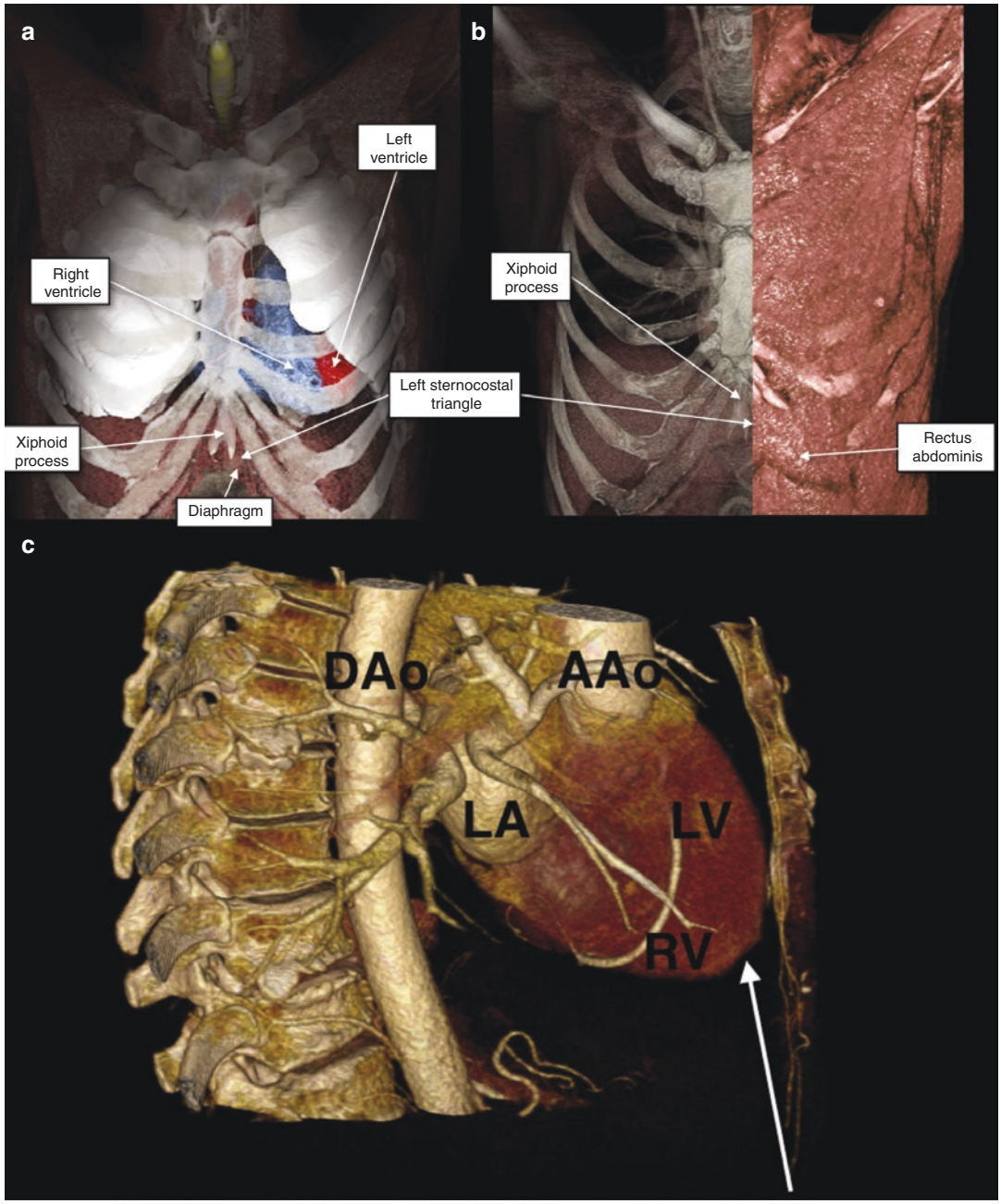

Fig. 9.14 Anatomical image showing the relevant anatomy from an anterior view for epicardial access in panel (**a**) and with superimposed soft tissue in panel (**b**). The left sternocostal triangle (also known as Larrey's space) is generally a safe access point due to the relative paucity of vascularity in this region. (**c**) A lateral sagittal view shown on a 3D CT reconstruction with white arrow indicating appropriate course of the needle for epicardial access. (*LA* left atrium, *RA* right atrium, *LV* left ventricle, *RV* right ventricle, *AAo* ascending aorta, *Dao* descending aorta)

patients who have had prior cardiac surgery as well as some patients with a prior history of pericarditis. In these cases surgical exposure can be performed with either a subxiphoid window or lateral thoracotomy, depending on the suspected origin or VT (Li et al. 2018).

Epicardial Mapping and Ablation

An irrigated catheter is commonly used for mapping and ablation. The general principles of mapping are the same as for endocardial mapping. An important issue which may arise is the differentiation of scar from epicardial fat. In general fat greater than 5 mm results in a reduction in the amplitude of the local electrogram. The degree of fractionation is helpful and is reasonably specific for local scar rather than fat (Tung et al. 2010). If a region of low amplitude signals follows the distribution of a coronary vessel, then it is likely to represent epicardial fat.

The fact that ablation catheters deliver circumferential radiofrequency energy means that there is always a degree of damage to surrounding structures. This is generally the pericardium and pleura which accommodate this with no major problems. The main structures to avoid when delivering RF to the epicardial surface are the coronary arteries and the phrenic nerves. In general either a CT is merged at the start of the procedure with the locations of the coronary arteries or a coronary angiogram is performed prior to ablation. A minimum distance of 5 mm should be maintained between the site of ablation and the coronary artery in order to prevent coronary artery spasm or acute thrombosis.

As there is no flow in the pericardium, irrigation is utilized. This should be periodically aspirated from the side arm of the sheath to prevent cardiac tamponade. RF can be delivered at a power ranging from 25–50 W. A higher power of 50 W can typically be used given limited risk from steam pops in this space. An alternative ablation modality consists of cryoablation which can be particularly useful in cases of surgical epicardial access where cardiac motion and impedance limitations can pose challenges with RF delivery.

In most cases the phrenic nerve course should be determined prior to performing ablation so as to minimize risk of injury. Different methods can help reduce risk of phrenic nerve injury if ablation in close proximity is required, such as injection of saline and air into the pericardial space (Di Biase et al. 2009) or the inflation of a balloon catheter (Buch et al. 2007) to separate the phrenic nerve from the ablation site.

Symptoms of pericarditis are common and can develop in up to 30% of patients after ablation. Following epicardial access for catheter procedures, intrapericardial corticosteroids may be administered based on animal model data and limited patient series data (d'Avila et al. 2007; Maxwell and Crouch 2010).

Important Points

1. Ventricular tachycardia is defined as an arrhythmia which originates from the ventricles consisting of at least three of more consecutive beats at a rate of greater than 100 beats/min and can be due to macro-reentrant or focal mechanism
2. The majority of macro-reentrant VT is due to an area of slow conduction surrounded by islands of a structural barrier which is most commonly scar.
3. The surface 12-lead ECG is critical to identifying the site of origin or exit site of VT depending on bundle branch block pattern, limb lead axis, and precordial lead morphology.
4. Outflow tract VT exhibits left bundle branch block with inferior axis, and precordial lead criteria can aid in differentiating right versus left ventricular outflow tract origin.
5. A number of ECG criteria can identify epicardial origin for VT, primarily relating to the delayed activation that

occurs due to the remoteness from the His-Purkinje system.
6. The strategies used to perform mapping and ablation of scar-related VT such as activation, entrainment, substrate, or pace mapping depend on whether VT is inducible and hemodynamically tolerated.
7. Bundle branch and fascicular re-entry VT are macro-reentrant arrhythmias which can be successfully targeted with catheter ablation of the appropriate conduction system limb.
8. Mapping and ablation of focal VT generally targets sites of earliest activation, with common anatomic regions being the outflow tracts, mitral valve annulus, tricuspid valve annulus, papillary muscles, and Purkinje fibers.
9. The LV summit is a notoriously difficult region for ablation due to challenges in accessibility. Successful ablation may require multiple anatomic approaches as well as multiple ablation modalities.
10. Epicardial access for VT ablation can be safely performed with a comprehensive understanding of anatomy guiding the access approach.

Conflict of Interest
None.

References

Al-Khatib SM, Stevenson WG, Ackerman MJ, Bryant WJ, Callans DJ, Curtis AB, Deal BJ, Dickfeld T, Field ME, Fonarow GC, Gillis AM, Hlatky MA, Granger CB, Hammill SC, Joglar JA, Kay GN, Matlock DD, Myerburg RJ, Page RL. 2017 AHA/ACC/HRS guideline for management of patients with ventricular arrhythmias and the prevention of sudden cardiac death: executive summary: a report of the American College of Cardiology/American Heart Association Task Force on Clinical Practice Guidelines and the Heart Rhythm Society. Circulation. 2018;138:e210–71.

Arenal A, Glez-Torrecilla E, Ortiz M, Villacastin J, Fdez-Portales J, Sousa E, del Castillo S, Perez de Isla L, Jimenez J, Almendral J. Ablation of electrograms with an isolated, delayed component as treatment of unmappable monomorphic ventricular tachycardias in patients with structural heart disease. J Am Coll Cardiol. 2003;41:81–92.

Baudoin YP, Hoch M, Protin XM, Otton BJ, Ginon B, Voiglio EJ. The superior epigastric artery does not pass through Larrey's space (trigonum sternocostale). Surg Radiol Anat. 2003;25:259–62.

Bazan V, Bala R, Garcia FC, Sussman JS, Gerstenfeld EP, Dixit S, Callans DJ, Zado E, Marchlinski FE. Twelve-lead ECG features to identify ventricular tachycardia arising from the epicardial right ventricle. Heart Rhythm. 2006;3:1132–9.

Berruezo A, Mont L, Nava S, Chueca E, Bartholomay E, Brugada J. Electrocardiographic recognition of the epicardial origin of ventricular tachycardias. Circulation. 2004;109:1842–7.

Betensky BP, Park RE, Marchlinski FE, Hutchinson MD, Garcia FC, Dixit S, Callans DJ, Cooper JM, Bala R, Lin D, Riley MP, Gerstenfeld EP. The V(2) transition ratio: a new electrocardiographic criterion for distinguishing left from right ventricular outflow tract tachycardia origin. J Am Coll Cardiol. 2011;57:2255–62.

Blanck Z, Dhala A, Deshpande S, Sra J, Jazayeri M, Akhtar M. Bundle branch reentrant ventricular tachycardia: cumulative experience in 48 patients. J Cardiovasc Electrophysiol. 1993;4:253–62.

Brugada P, Brugada J, Mont L, Smeets J, Andries EW. A new approach to the differential diagnosis of a regular tachycardia with a wide QRS complex. Circulation. 1991;83:1649–59.

Buch E, Vaseghi M, Cesario DA, Shivkumar K. A novel method for preventing phrenic nerve injury during catheter ablation. Heart Rhythm. 2007;4:95–8.

Chung FP, Chong E, Lin YJ, Chang SL, Lo LW, Hu YF, Tuan TC, Chao TF, Liao JN, Huang YC, Chi PC, Chan CS, Chen YY, Huang HK, Chen SA. Different characteristics and electrophysiological properties between early and late recurrences after acute successful catheter ablation of idiopathic right ventricular outflow tract arrhythmias during long-term follow-up. Heart Rhythm. 2014;11:1760–9.

Chung FP, Lin CY, Shirai Y, Futyma P, Santangeli P, Lin YJ, Chang SL, Lo LW, Hu YF, Chang HY, Marchlinski FE, Chen SA. Outcomes of catheter ablation of ventricular arrhythmia originating from the left ventricular summit: a multicenter study. Heart Rhythm. 2020;17:1077–83.

d'Avila A, Neuzil P, Thiagalingam A, Gutierrez P, Aleong R, Ruskin JN, Reddy VY. Experimental efficacy of pericardial instillation of anti-inflammatory agents during percutaneous epicardial catheter ablation to prevent postprocedure pericarditis. J Cardiovasc Electrophysiol. 2007;18:1178–83.

Delacretaz E, Brenner R, Schaumann A, Eckardt L, Willems S, Pitschner HF, Kautzner J, Schumacher B, Hansen PS, Kuck KH, Group VS. Catheter ablation

of stable ventricular tachycardia before defibrillator implantation in patients with coronary heart disease (VTACH): an on-treatment analysis. J Cardiovasc Electrophysiol. 2013;24:525–9.

Di Biase L, Burkhardt JD, Pelargonio G, Dello Russo A, Casella M, Santarelli P, Horton R, Sanchez J, Gallinghouse JG, Al-Ahmad A, Wang P, Cummings JE, Schweikert RA, Natale A. Prevention of phrenic nerve injury during epicardial ablation: comparison of methods for separating the phrenic nerve from the epicardial surface. Heart Rhythm. 2009;6:957–61.

Di Biase L, Burkhardt JD, Lakkireddy D, Carbucicchio C, Mohanty S, Mohanty P, Trivedi C, Santangeli P, Bai R, Forleo G, Horton R, Bailey S, Sanchez J, Al-Ahmad A, Hranitzky P, Gallinghouse GJ, Pelargonio G, Hongo RH, Beheiry S, Hao SC, Reddy M, Rossillo A, Themistoclakis S, Dello Russo A, Casella M, Tondo C, Natale A. Ablation of stable VTs versus substrate ablation in ischemic cardiomyopathy: the VISTA randomized multicenter trial. J Am Coll Cardiol. 2015;66:2872–82.

Di Biase L, Burkhardt JD, Reddy V, Romero J, Neuzil P, Petru J, Sadiva L, Skoda J, Ventura M, Carbucicchio C, Dello Russo A, Csanadi Z, Casella M, Fassini GM, Tondo C, Sacher F, Theran M, Dukkipati S, Koruth J, Jais P, Natale A. Initial international multicenter human experience with a novel epicardial access needle embedded with a real-time pressure/frequency monitoring to facilitate epicardial access: Feasibility and safety. Heart Rhythm. 2017;14:981–8.

Haissaguerre M, Shoda M, Jais P, Nogami A, Shah DC, Kautzner J, Arentz T, Kalushe D, Lamaison D, Griffith M, Cruz F, de Paola A, Gaita F, Hocini M, Garrigue S, Macle L, Weerasooriya R, Clementy J. Mapping and ablation of idiopathic ventricular fibrillation. Circulation. 2002;106:962–7.

Hamon D, Abehsira G, Gu K, Liu A, Blaye-Felice Sadron M, Billet S, Kambur T, Swid MA, Boyle NG, Dandamudi G, Maury P, Chen M, Miller JM, Lellouche N, Shivkumar K, Bradfield JS. Circadian variability patterns predict and guide premature ventricular contraction ablation procedural inducibility and outcomes. Heart Rhythm. 2018;15:99–106.

Hutchinson MD, Gerstenfeld EP, Desjardins B, Bala R, Riley MP, Garcia FC, Dixit S, Lin D, Tzou WS, Cooper JM, Verdino RJ, Callans DJ, Marchlinski FE. Endocardial unipolar voltage mapping to detect epicardial ventricular tachycardia substrate in patients with nonischemic left ventricular cardiomyopathy. Circ Arrhythm Electrophysiol. 2011;4:49–55.

Jais P, Maury P, Khairy P, Sacher F, Nault I, Komatsu Y, Hocini M, Forclaz A, Jadidi AS, Weerasooryia R, Shah A, Derval N, Cochet H, Knecht S, Miyazaki S, Linton N, Rivard L, Wright M, Wilton SB, Scherr D, Pascale P, Roten L, Pederson M, Bordachar P, Laurent F, Kim SJ, Ritter P, Clementy J, Haissaguerre M. Elimination of local abnormal ventricular activities: a new end point for substrate modification in patients with scar-related ventricular tachycardia. Circulation. 2012;125:2184–96.

Josephson ME, Callans DJ. Using the twelve-lead electrocardiogram to localize the site of origin of ventricular tachycardia. Heart Rhythm. 2005;2:443–6.

Komatsu Y, Daly M, Sacher F, Derval N, Pascale P, Roten L, Scherr D, Jadidi A, Ramoul K, Denis A, Jesel L, Zellerhoff S, Lim HS, Shah A, Cochet H, Hocini M, Haissaguerre M, Jais P. Electrophysiologic characterization of local abnormal ventricular activities in postinfarction ventricular tachycardia with respect to their anatomic location. Heart Rhythm. 2013;10:1630–7.

Kreidieh B, Rodriguez-Manero M, Schurmann P, Ibarra-Cortez SH, Dave AS, Valderrabano M. Retrograde coronary venous ethanol infusion for ablation of refractory ventricular tachycardia. Circ Arrhythm Electrophysiol. 2016;9:e004352.

Lerman BB. Mechanism of outflow tract tachycardia. Heart Rhythm. 2007;4:973–6.

Li A, Hayase J, Do D, Buch E, Vaseghi M, Ajijola OA, Macias C, Krokhaleva Y, Khakpour H, Boyle NG, Benharash P, Biniwale R, Shivkumar K, Bradfield JS. Hybrid surgical versus percutaneous access epicardial ventricular tachycardia ablation. Heart Rhythm. 2018;15(4):512–9.

Lin D, Hsia HH, Gerstenfeld EP, Dixit S, Callans DJ, Nayak H, Russo A, Marchlinski FE. Idiopathic fascicular left ventricular tachycardia: linear ablation lesion strategy for noninducible or nonsustained tachycardia. Heart Rhythm. 2005;2:934–9.

Maxwell CB, Crouch MA. Intrapericardial triamcinolone for acute pericarditis after electrophysiologic procedures. Am J Health Syst Pharm. 2010;67:269–73.

McAlpine WA. Heart and coronary arteries: an anatomical atlas for clinical diagnosis, radiological investigation, and surgical treatment. Berlin; New York: Springer-Verlag; 1975.

Merino JL, Peinado R, Fernandez-Lozano I, Lopez-Gil M, Arribas F, Ramirez LJ, Echeverria IJ, Sobrino JA. Bundle-branch reentry and the postpacing interval after entrainment by right ventricular apex stimulation: a new approach to elucidate the mechanism of wide-QRS-complex tachycardia with atrioventricular dissociation. Circulation. 2001;103:1102–8.

Nguyen DT, Tzou WS, Brunnquell M, Zipse M, Schuller JL, Zheng L, Aleong RA, Sauer WH. Clinical and biophysical evaluation of variable bipolar configurations during radiofrequency ablation for treatment of ventricular arrhythmias. Heart Rhythm. 2016;13:2161–71.

Nguyen DT, Tzou WS, Sandhu A, Gianni C, Anter E, Tung R, Valderrabano M, Hranitzky P, Soeijma K, Saenz L, Garcia FC, Tedrow UB, Miller JM, Gerstenfeld EP, Burkhardt JD, Natale A, Sauer WH. Prospective multicenter experience with cooled radiofrequency ablation using high impedance irrigant to target deep myocardial substrate refractory to standard ablation. JACC Clin Electrophysiol. 2018;4:1176–85.

Nogami A. Purkinje-related arrhythmias part I: monomorphic ventricular tachycardias. Pacing Clin Electrophysiol. 2011;34:624–50.

Nogami A, Naito S, Tada H, Taniguchi K, Okamoto Y, Nishimura S, Yamauchi Y, Aonuma K, Goya M, Iesaka Y, Hiroe M. Demonstration of diastolic and presystolic Purkinje potentials as critical potentials in a macroreentry circuit of verapamil-sensitive idiopathic left ventricular tachycardia. J Am Coll Cardiol. 2000;36:811–23.

Rivera S, Ricapito Mde L, Tomas L, Parodi J, Bardera Molina G, Banega R, Bueti P, Orosco A, Reinoso M, Caro M, Belardi D, Albina G, Giniger A, Scazzuso F. Results of cryoenergy and radiofrequency-based catheter ablation for treating ventricular arrhythmias arising from the papillary muscles of the left ventricle, guided by intracardiac echocardiography and image integration. Circ Arrhythm Electrophysiol. 2016;9:e003874.

Romero J, Diaz JC, Hayase J, Dave RH, Bradfield JS, Shivkumar K. Intramyocardial radiofrequency ablation of ventricular arrhythmias using intracoronary wire mapping and a coronary reentry system: description of a novel technique. Heart Rhythm Case Rep. 2018;4:285–92.

Sacher F, Sobieszczyk P, Tedrow U, Eisenhauer AC, Field ME, Selwyn A, Raymond JM, Koplan B, Epstein LM, Stevenson WG. Transcoronary ethanol ventricular tachycardia ablation in the modern electrophysiology era. Heart Rhythm. 2008;5:62–8.

Sadek MM, Benhayon D, Sureddi R, Chik W, Santangeli P, Supple GE, Hutchinson MD, Bala R, Carballeira L, Zado ES, Patel VV, Callans DJ, Marchlinski FE, Garcia FC. Idiopathic ventricular arrhythmias originating from the moderator band: electrocardiographic characteristics and treatment by catheter ablation. Heart Rhythm. 2015;12:67–75.

Santoro F, Di Biase L, Hranitzky P, Sanchez JE, Santangeli P, Perini AP, Burkhardt JD, Natale A. Ventricular fibrillation triggered by PVCs from papillary muscles: clinical features and ablation. J Cardiovasc Electrophysiol. 2014;25:1158–64.

Sapp JL, Wells GA, Parkash R, Stevenson WG, Blier L, Sarrazin JF, Thibault B, Rivard L, Gula L, Leong-Sit P, Essebag V, Nery PB, Tung SK, Raymond JM, Sterns LD, Veenhuyzen GD, Healey JS, Redfearn D, Roux JF, Tang AS. Ventricular tachycardia ablation versus escalation of antiarrhythmic drugs. N Engl J Med. 2016;375:111–21.

Seiler J, Lee JC, Roberts-Thomson KC, Stevenson WG. Intracardiac echocardiography guided catheter ablation of incessant ventricular tachycardia from the posterior papillary muscle causing tachycardia—mediated cardiomyopathy. Heart Rhythm. 2009;6:389–92.

Shauer A, De Vries LJ, Akca F, Palazzolo J, Shurrab M, Lashevsky I, Tiong I, Singh SM, Newman D, Szili-Torok T, Crystal E. Clinical research: remote magnetic navigation vs. manually controlled catheter ablation of right ventricular outflow tract arrhythmias: a retrospective study. Europace. 2018;20:ii28–32.

Stevenson WG, Friedman PL, Sager PT, Saxon LA, Kocovic D, Harada T, Wiener I, Khan H. Exploring postinfarction reentrant ventricular tachycardia with entrainment mapping. J Am Coll Cardiol. 1997;29:1180–9.

Tada H, Ito S, Naito S, Kurosaki K, Kubota S, Sugiyasu A, Tsuchiya T, Miyaji K, Yamada M, Kutsumi Y, Oshima S, Nogami A, Taniguchi K. Idiopathic ventricular arrhythmia arising from the mitral annulus: a distinct subgroup of idiopathic ventricular arrhythmias. J Am Coll Cardiol. 2005;45:877–86.

Tada H, Tadokoro K, Ito S, Naito S, Hashimoto T, Kaseno K, Miyaji K, Sugiyasu A, Tsuchiya T, Kutsumi Y, Nogami A, Oshima S, Taniguchi K. Idiopathic ventricular arrhythmias originating from the tricuspid annulus: prevalence, electrocardiographic characteristics, and results of radiofrequency catheter ablation. Heart Rhythm. 2007;4:7–16.

Tholakanahalli VN, Bertog S, Roukoz H, Shivkumar K. Catheter ablation of ventricular tachycardia using intracoronary wire mapping and coil embolization: description of a new technique. Heart Rhythm. 2013;10:292–6.

Tung R, Nakahara S, Ramirez R, Lai C, Fishbein MC, Shivkumar K. Distinguishing epicardial fat from scar: analysis of electrograms using high-density electroanatomic mapping in a novel porcine infarct model. Heart Rhythm. 2010;7:389–95.

Tung R, Mathuria N, Michowitz Y, Yu R, Buch E, Bradfield J, Mandapati R, Wiener I, Boyle N, Shivkumar K. Functional pace-mapping responses for identification of targets for catheter ablation of scar-mediated ventricular tachycardia. Circ Arrhythm Electrophysiol. 2012;5:264–72.

Tung R, Josephson ME, Bradfield JS, Shivkumar K. Directional influences of ventricular activation on myocardial scar characterization: voltage mapping with multiple wavefronts during ventricular tachycardia ablation. Circ Arrhythm Electrophysiol. 2016;9:e004155.

Tzou WS, Frankel DS, Hegeman T, Supple GE, Garcia FC, Santangeli P, Katz DF, Sauer WH, Marchlinski FE. Core isolation of critical arrhythmia elements for treatment of multiple scar-based ventricular tachycardias. Circ Arrhythm Electrophysiol. 2015;8:353–61.

Valles E, Bazan V, Marchlinski FE. ECG criteria to identify epicardial ventricular tachycardia in nonischemic cardiomyopathy. Circ Arrhythm Electrophysiol. 2010;3:63–71.

Vaseghi M, Cesario DA, Mahajan A, Wiener I, Boyle NG, Fishbein MC, Horowitz BN, Shivkumar K. Catheter ablation of right ventricular outflow tract tachycardia: value of defining coronary anatomy. J Cardiovasc Electrophysiol. 2006;17:632–7.

Vereckei A, Duray G, Szenasi G, Altemose GT, Miller JM. New algorithm using only lead aVR for differential diagnosis of wide QRS complex tachycardia. Heart Rhythm. 2008;5:89–98.

Vergara P, Trevisi N, Ricco A, Petracca F, Baratto F, Cireddu M, Bisceglia C, Maccabelli G, Della Bella P. Late potentials abolition as an additional technique for reduction of arrhythmia recurrence in scar

related ventricular tachycardia ablation. J Cardiovasc Electrophysiol. 2012;23:621–7.

Wellens HJ, Bar FW, Lie KI. The value of the electrocardiogram in the differential diagnosis of a tachycardia with a widened QRS complex. Am J Med. 1978;64:27–33.

Yamada T, Murakami Y, Yoshida N, Okada T, Shimizu T, Toyama J, Yoshida Y, Tsuboi N, Muto M, Inden Y, Hirai M, Murohara T, McElderry HT, Epstein AE, Plumb VJ, Kay GN. Preferential conduction across the ventricular outflow septum in ventricular arrhythmias originating from the aortic sinus cusp. J Am Coll Cardiol. 2007;50:884–91.

Yamada T, McElderry HT, Doppalapudi H, Okada T, Murakami Y, Yoshida Y, Yoshida N, Inden Y, Murohara T, Plumb VJ, Kay GN. Idiopathic ventricular arrhythmias originating from the left ventricular summit: anatomic concepts relevant to ablation. Circ Arrhythm Electrophysiol. 2010;3:616–23.

Yoshida N, Yamada T, McElderry HT, Inden Y, Shimano M, Murohara T, Kumar V, Doppalapudi H, Plumb VJ, Kay GN. A novel electrocardiographic criterion for differentiating a left from right ventricular outflow tract tachycardia origin: the V2S/V3R index. J Cardiovasc Electrophysiol. 2014;25:747–53.

Anti-Arrhythmic Drugs

10

Kathryn L. Hong, Benedict M. Glover, and Paul Dorian

Abstract

Anti-arrhythmic drugs (AAD's) alter the electrical properties of the heart principally by either prolonging the cardiac action potential, decreasing conduction velocity, reducing focal automaticity or a combination of these effects. Despite the fact that a large number of AAD's were initially developed for ventricular arrhythmias the most common current indication is currently atrial fibrillation (AF).

Although the majority of these drugs act relatively specifically on certain targets or receptors, the overall general distribution of these receptors throughout the ventricular and atrial myocardium may result in unwanted effects such as Torsades de Pointes (TdP) predominantly with class IA and class III drugs, and prolongation of AV conduction, QRS widening and monomorphic VT with class IC drugs. The toxicity profile of AADs is varied, leading to severe adverse effects and discontinuation of treatment in 12–19% of patients. Therefore, the choice of AAD must depend on the presence of comorbidities, cardiovascular risk and patient preference, proarrhythmic potential, toxic effects, and symptom burden.

A meta-analysis of 44 trials involving 11,322 patients showed that all AAD's were associated with an increased risk of proarrhythmia with the exception of amiodarone and propafenone (Lafuente-Lafuente et al. 2006). Although amiodarone is a very useful agent in the treatment of both atrial and ventricular arrhythmias its use is often limited as a result of its potential for long-term non-cardiac side effects (Rothenberg et al. 1994).

More recently, "atrial selective" AAD's have been developed which may have improved efficacy with better side effect profile. Additionally, some drugs (such as renin-angiotensin aldosterone inhibitors and anti-inflammatory agents) may affect the underlying substrate and be indirectly antiarrhythmic.

Mechanisms of Action: An Overview

Although the majority of AAD's have multiple effects on either the AP directly or by autonomic modulation, their actions can generally be classified into groups according to the predominant

K. L. Hong (✉) · B. M. Glover
Division of Cardiology, Department of Medicine, University of Toronto, Toronto, Ontario, Canada

P. Dorian
Department of Medicine, University of Toronto, Toronto, ON, Canada
e-mail: dorianp@smh.ca

B. M. Glover, P. Brugada (eds.), *Clinical Handbook of Cardiac Electrophysiology*,
https://doi.org/10.1007/978-3-030-74319-2_10

mechanism or resulting electrophysiological effect. This classification is called the Vaughan Williams system which was subsequently modified by Singh and Harrison (Table 10.1). It should be remembered that most AAD's have properties belonging to more than one group; it is therefore more appropriate to refer to 'classes of antiarrhythmic drug action', rather than to drugs belonging to a particular class.

Drugs with Class I action act by blocking the rapidly activating sodium channels that are responsible for phase 0 of the AP thus affecting its slope and amplitude. These drugs are subdivided according to the rate of binding and dissociation from the sodium channel. Class IB mechanism of action is associated with the most rapid onset of action and dissociation, IA has intermediate activities and IC the slowest (Fig. 10.1).

These variances in action result in clinically relevant differences as a function of heart rate - drugs with the slowest rates of binding and unbinding have "rate dependent properties" with the effect of greater slowing of conduction velocity (manifest on the surface ECG as greater degree of QRS prolongation) at higher heart rates, not seen with the class 1b mechanism of action. As well as their effects on the slope of rapid depolarization, agents with class I properties also have different effects on repolarization (and APD) and thus refractory periods. Class IA property is generally associated with an increase, Class IB with a shortening and Class IC with no effect on the APD.

Class II agents act by blocking beta adrenergic receptors, antagonizing the effect of circulating, neurally or locally released catecholamines, with effects on all cardiac tissues. Additionally, they prolong the phase 2 and 3 (after chronic use) of the AP and thus lengthen the effective refractory period.

Agents with Class III properties such as sotalol and amiodarone prolong the APD principally by inhibition of the potassium channels (although these drugs also have other electrophysiologic properties-see below).

Class IV action inhibits the slow calcium current and therefore depress phase II and III of the AP in certain tissues primarily the SAN and AV nodes).

Antiarrhythmics with Class IA Properties

Procainamide is conjugated to the active metabolite N-acetylprocainamide at a rate determined by whether the patient is a rapid acetylator (Jusko et al. 1980; Atkinson and Ruo 1986). Although it was previously used for the treatment of atrial and ventricular arrhythmias its use is now largely reserved for the treatment of VT. It is also used for the acute management of haemodynamically stable, pre-excited AF in the WPW syndrome (Class IIb indication) (Fuster et al. 2006). Proarrhythmia occurs in up to 9% of cases (Podrid et al. 1987) and like all class IA drugs its

Table 10.1 Classification of current anti-arrhythmic drug actions as well as inotropic effects on the ventricle and potential pro-arrhythmic effects

Class	Examples	Mechanism	Inotropic Effect	Pro-arrhythmia
Ia	Procainamide Quinidine	Inhibition of Intermediate Na^+ Channel	Negative	QRS Widening and VT (Torsades)
Ib	Lidocaine Mexilitine	Inhibition of fast Na^+ Channel	Negative	Asystole
Ic	Flecainide, Propafenone	Inhibition of slow Na^+ Channel	Negative	1:1 AV Conduction of atrial atrial arrhythmias slowed by the drug
II	B Blockers	B Adrenoceptor Blockade	Negative	Bradycardia
III	Amiodarone Sotalol	K^+ Channel Blockade	Neutral	Sotalol: Bradycardia, ↑QT, Torsades
IV	Ca Channel Blockers	Ca^{2+} Channel Blockade	Negative	Bradycardia

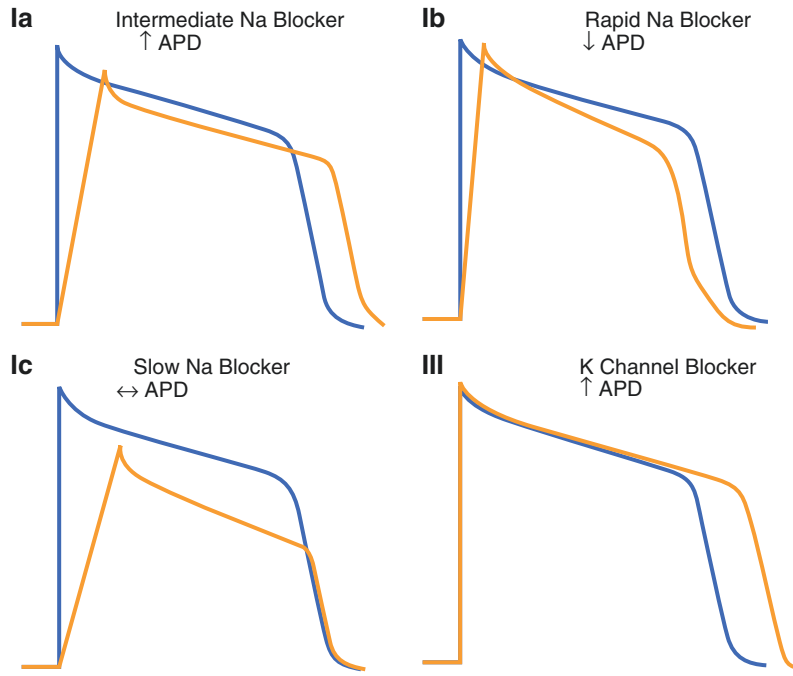

Fig. 10.1 Schematic of the effects of Class Ia, Ib, Ic and Class III effects on the Cardiac AP

use has been severely restricted due to the associated risk of TdP particularly in patient with bradycardia and left ventricular hypertrophy (LVH) (Yap and Camm 2003). In general terms the risk of TdP for all class IA and some class III AAD's include a long baseline QT interval, a family history of Td, female gender, bradycardia, renal impairment (for renally excreted drugs) and a low potassium or magnesium (Camm 2008).

Procainamide can also increase the ventricular rate in patients with uncontrolled AF or flutter (Class IA effect). This occurs as a result of slowing the fibrillation or flutter rate as well as increasing the likelihood that a given impulse will pass through the AV node due to the direct vagolytic action of procainamide. Thus, conduction through the AV node must be slowed and the ventricular response controlled before therapy with procainamide is initiated in these disorders. Nearly all patients will develop a positive antinuclear antibody, with a lupus-like syndrome in approximately one-third of patients taking the drug for more than 1 year (Brogan and Olsen 2003). Severe neutropaenia has been reported with long term use of oral procainamide (Katkov and Ellrodt 1985). In patients with structural heart defects, evidence suggests that procainamide may be more effective than lidocaine in the termination of monomorphic VT, although further reports are still lacking (Komura et al. 2010). It is also commonly used for pharmacological testing in Brugada risk stratification.

Quinidine has similar properties and side effects to procainamide, but owing to its additional effect on the transient outward current, there has been some limited interest in this drug in patients with Brugada syndrome. Although there is some evidence to support a degree of efficacy in maintaining sinus rhythm following an electrical cardioversion for AF (Coplen et al. 1990) it carries significant pro-arrhythmic side effects with an increased associated mortality (Reimold et al. 1992). The incidence of TdP reported with quinidine use varies from 0.5% to 8% (Grace and Camm 1998) and like all class IA drugs the QT prolongation tends to occur early and therefore it is recommended that it should be initiated in the hospital under continuous ECG monitoring (Thibault and Nattel 1999). Modest QT prolongation is relatively common while excessive prolongation is unusual and generally indicates toxicity. As with all AAD's

in this group, it is contraindicated in the presence of structural heart disease and LVH and is not recommended as first-line agent for the long-term management of any atrial arrhythmia. One of the more common reasons for discontinuation of the drug are the associated gastrointestinal side effects such as nausea, reduced appetite, an abnormal bitter taste and abdominal discomfort are relatively common occurring in approximately one third of patients. Quinidine has been reported to be effective in patients with ventricular tachycardia (Viskin et al. 2019) and Brugada syndrome (Belhassen et al. 2004), as well as with idiopathic ventricular fibrillation (Tsai et al. 1998).

Disopyramide has marked anticholinergic effects and thus in theory may prove useful in vagally mediated AF (Fuster et al. 2006). The evidence for disopyramide in AF however is very weak involving a small study involving 90 patients following a successful electrical cardioversion from AF to sinus rhythm (Karlson et al. 1988). Following 1 month 70% of patients receiving disopyramide were in sinus rhythm versus 39% in the placebo group. It is considered a second- or third-line agent for suppression of atrial and ventricular arrhythmias and conversion of AF to normal sinus rhythm. Due to its negative inotropic effect it has been used in the treatment of hypertrophic cardiomyopathy in order to reduce the outflow tract gradient and improve symptoms (Pollick 1982) Other than the proarrhythmic and negative inotropic effects characteristic to this group the other main adverse effects are related to its anticholinergic effects, including urinary retention, blurred vision, constipation and dry mouth. This drug is therefore rarely used clinically.

Antiarrhythmics with Class IB Properties

The two main drugs in Class IB are lidocaine and mexiletine both of which act predominantly on the ventricular myocardium.

Lidocaine is a short acting intravenous antiarrhythmic which has been used extensively for the management and prophylaxis of ventricular arrhythmias. The initial clinical data for the use of lidocaine was in its ability to suppress PVC's and prevent VF after an acute myocardial infarction (Lie et al. 1974). However this practice was halted after data showed an associated increased mortality most likely related to bradyarrhythmias and hypotension (MacMahon et al. 1988). Although one trial has shown an increased prehospital survival with lidocaine (Herlitz et al. 1997) other randomised trial comparing lidocaine with amiodarone have shown amiodarone to be superior in terms of return of spontaneous circulation (Dorian et al. 2002) as well as a lower rate of asystole (Weaver et al. 1990). As a result of this the ALS (UK) guidelines recommend the use of lidocaine only as an alternative if amiodarone is not available.

Mexiletine is structurally similar to lidocaine but has a much higher oral bioavailability and therefore, is available as an oral preparation. Its main activity occurs in the His Purkinje and ventricular myocardium with minimal effects on the sinus node, atrium and AV node (Roos et al. 1976; McCornish et al. 1977). The most frequent side effects are related to GI disturbances and CNS toxicity. Cardiovascular side effects include hypotension, sinus bradycardia, and worsening of ventricular arrhythmias in 10–15% of cases (McCornish et al. 1977). Use of mexiletine has been reported to be associated with an increased mortality (Campbell 1987) but may be used in patients who cannot tolerate amiodarone; or in combination with amiodarone in electrical storm.

Class IC AAD's

The class IC drugs flecainide and propafenone have the slowest onset of action in sodium inhibition and have no direct effect on action potential duration.

Current guidelines recommend flecainide as a first-line agent for the conversion of existing AF and prevention of recurrences in patients with intermittent episodes of AF, in patients without structural heart disease. Although its use in this subset of patients is well-established, its clinical

use continues to be limited predominantly due to the potential risk of ventricular proarrythmia (Preliminary report 1989). The exact mechanism underlying flecanide's ventricular proarrhythmic potential remains unknown.

Cardiac arrhythmia is more likely in the presence of myocardial ischaemia, suggesting that it may be due to excessive conduction slowing in ischemic tissue. Both flecainide and propafenone have been shown to be relatively similar in terms of efficacy in the management of symptomatic paroxysmal AF in two randomized control trials (Chimienti et al. 1996; Aliot and Denjoy 1996). However, a recent meta-analysis of randomized studies found the overall AF conversion rate within 2 h to be higher with the use of flecainide (66%) when compared with any other antiarrhythmic agent (46%) (Markey et al. 2018). Indeed, in cases of recent onset AF, IV flecainide has been shown to be effective in termination of the arrhythmia in 90% of cases (Fernández-Martinez et al. 2000). Oral flecainide has been shown to be as effective as the intravenous preparation for acute chemical cardioversion although obviously with a slower onset of action (Alp et al. 2000).

This fact combined with the large degree of use dependence has led to the regimen called 'pill in the pocket' (PiP) in which patients with symptomatic paroxysmal AF self-administer a single oral dose of flecainide (generally with a beta blocker or rate slowing calcium blocker) for chemical cardioversion. Although this has been shown to be effective in up to 94% of cases with no significant adverse effects (Alboni et al. 2004), this strategy has only been employed in highly selected patients who can reliably self-identify symptomatic episodes and is not ideal for many patients with paroxysmal AF. In general, if this strategy is to be used, patients are usually tested with the identical regimen in hospital to assess for side effects and potential arrhythmias. Despite this precaution, 5% of patients still experience problems such as presyncope, syncope and sinus arrest.

Despite the efficacy of class IC drugs, their use has been largely limited by safety concerns. They may occasionally convert AF to atrial flutter with 1:1 AV conduction and thus result in a paradoxical increase in ventricular response rate. This tachycardia occasionally can be confused with VT particularly when there is QRS widening (also due to the drug). Given that they have minimal effects on AV conduction, it is recommended that they be used in the presence of an AV nodal blocker such as a beta blocker. However, the major concerns regarding these drugs arose from a series of trials showing an increase in cardiovascular mortality in patients with ventricular arrhythmias in the setting of coronary artery disease and other structural heart disease. The Cardiac Arrhythmia Suppression Trial (CAST) compared flecainide, encainide, moricine and placebo for the suppression of PVC's in 1498 post MI patients (Preliminary report 1989). The trial was prematurely terminated after showing an increased mortality in patients receiving flecainide and encainide (subsequently withdrawn) primarily due to the incidence of arrhythmias.

Although propafenone may have a relatively better side effect profile given its additional beta adrenergic blocking effects, the Cardiac Arrest Survival in Hamburg (CASH) study showed a significant increase in mortality in patients receiving propafenone. The CASH trial was designed to compare survival with an ICD as compared to antiarrhythmic drug therapy with amiodarone, propafenone or metoprolol, in 349 survivors of cardiac arrest due to documented VT (Kuck et al. 2000).

For these reasons, these drugs are contraindicated in the setting of prior myocardial infarction or a history of VT, and relatively contraindicated in the setting of structural heart disease.

Class II Antiarrhythmics

This class of drugs act by inhibiting sympathetic activity, primarily via beta-adrenergic blockade, and is subdivided based on the specific adrenergic blockade profile and associated properties. Propranolol is a first-generation non-selective beta-blocker with equal affinity for the β1 and β2 receptors. At high doses, propranolol may also block sodium channels. Despite its proven effi-

cacy in reducing ventricular rate in AF, propranolol has not been shown to be useful as an atrial anti-arrhythmic (Tsolakas et al. 1964).

Metoprolol and bisoprolol are second-generation beta-blockers, which preferentially inhibit β2 receptors and may have more useful atrial antiarrhythmic effects than propranolol. Bisoprolol has been shown to be similar to sotalol in the maintenance of sinus rhythm at 12 months following an electrical cardioversion (Plewan et al. 2001). Metoprolol has also been shown to be superior to placebo in maintenance of sinus rhythm as well as a slower ventricular rate during a recurrence (Kuhlkamp et al. 2000).

Beta adrenergic blockers have been shown to reduce mortality owing to a reduction in arrhythmic death in most cases, in patients with long QT syndrome (Sauer et al. 2007), survivors of cardiac arrest (Hallstrom et al. 1991), post myocardial infarction (Freemantle et al. 1999) and in patients with impaired LV systolic function (McAlister et al. 2009).

Class III

Class III AAD's exert their action by blocking potassium channels, thereby prolonging repolarization, the APD, and the refractory period. These changes are manifested on the surface ECG by prolongation of the QT interval. This group includes sotalol, amiodarone, dofetilide, vernakalant and ibutilide.

Sotalol consists of 2 isomers, D and L, each of which contribute to its antiarrhythmic properties. The D isomer blocks the rapid component of the delayed rectifier potassium current (IKr channel) during phase 3 of the AP and thus prolongs the AP duration. The L isomer also prolongs the cardiac AP, while having a degree of beta-adrenergic blocking activity. Although a preparation of the D isomer has been developed, it has been shown to be associated with an increase in the risk of mortality in patients with impaired LV function and a recent MI or heart failure with a history of prior MI (Waldo et al. 1996).

Sotalol has been shown to be effective in maintaining sinus rhythm and reducing the incidence of episodes of AF, although not as effectively as amiodarone. The CTAF study randomised patients with a history of AF to sotalol, amiodarone or propafenone (Roy et al. 2000). After a mean follow-up of 16 months similar percentages of patients receiving sotalol and propafenone had a recurrence of AF while significantly fewer receiving amiodarone experienced AF recurrences.

In clinical practice, sotalol is generally used for the control of paroxysmal AF as a second- or third-line agent after flecainide/propafenone and amiodarone. It has also been shown to reduce the recurrence of sustained ventricular arrhythmias (Mason 1993), albeit less than amiodarone (Connolly et al. 2006), and can also be considered after amiodarone in terms of reducing ICD discharges.

The most significant risk associated with sotalol is the risk of TdP particularly at slower heart rates, which has been reported as approximately 2.5% at a median follow up of 164 days (Lehmann et al. 1996) This risk is increased in females, patients with a history of heart failure, patients with renal impairment and at high doses of sotalol (greater than 320 mg/day) (Lehmann et al. 1996).

Amiodarone was first used as an anti-anginal drug in the 1960's, and its anti-arrhythmic properties were first reported in 1970. The predominant mode of action is class III by blocking the IKr and IKs channels. This results in a reduction in dispersion of refractoriness, re-entry and pro-arrhythmia and overall a prolongation of myocardial repolarization homogeneously. Additionally, it also blocks sodium channels (Class I effects) and thus reduces conduction velocity, has non-selective beta adrenergic blocking effects (Class II) and inhibits the L type calcium channel (Class IV). It causes use dependent potassium channel blockade meaning that as the heart rate increases the refractory period increases incrementally (Singh et al. 1994).

The onset and mode of action depends on the type of administration. If given intravenously the onset of action is several hours and there is minimal AP prolongation except in the AV node. The oral preparation takes several days and the

overall effects are more pronounced after chronic usage.

Amiodarone has been shown to be the most efficacious AAD in the treatment of both AF and VT. The Canadian Trial of AF, in which patients with at least one episode of AF were randomized to various antiarrhythmic medications, showed that 35% of patients randomized to amiodarone had a recurrence of AF versus 63% of patients randomized to either sotalol or propafenone (Waldo et al. 1996). There was no significant difference in the maintenance of sinus rhythm between those who received either sotalol or propafenone. Given its multichannel effects and minimal negative inotropic effects, it is considered relatively safe in patients with impaired LV function and is recommended as first line therapy for the treatment of ventricular arrhythmias unless there is a contraindication (MacMahon et al. 1988). Although amiodarone prolongs the QT interval the risk of torsades de pointes VT is less than 1% (Goldschlager et al. 2007).

The most common and significant side effects which limit the long-term use of amiodarone are generally non cardiac, with adverse effects reported as high as 15% within the first year of treatment and 50% during long term therapy (Goldschlager et al. 2007). It is therefore important that the patient is monitored for side effects as shown in Fig. 10.2.

Amiodarone induced hypothyroidism is more common than thyrotoxicosis. Within the first 3 months of therapy there is an increase in thyroid stimulating hormone (TSH), free T4 and a reduction in free T3. TSH then normalises while T4 and T3 may remain abnormal. The importance of this is that it is generally not useful to check thyroid function within the first 3 months and following this the most useful measure is TSH (Goldschlager et al. 2007). Amiodarone induced thyrotoxicosis is less predictable and can occur relatively suddenly at any time during treatment. It can be due either to aggravation of pre-existing thyroid disease or thyroiditis, although often it is difficult to distinguish between these. It is generally recommended that all patients being commenced on long term amiodarone therapy should have baseline TFT's which should be rechecked after 3 months to establish a new baseline and then every 6 months or sooner if clinically indicated (Goldschlager et al. 2007).

Lung toxicity has been reported as occurring in up to 2% of patients (Goldschlager et al. 2007). Risk factors for pulmonary fibrosis are a prior history of lung disease and a daily dose of amiodarone greater than 400 mg/day (Vassallo and Trohman 2007). It may present anytime from 1 week following initiation of the drug and is relatively unpredictable. Therefore, although pulmonary function tests are frequently performed, they are of limited value in this case.

There is no conclusive evident that pulmonary functions tests are useful in anticipating or diagnosing amiodarone long toxicity. However, close clinical surveillance for symptomatic adverse effects of amiodarone is critical in order to detect the early onset of neurological symptoms including vivid dreams, tremor, postural instability, incoordination.

These and other non cardiac side effects of amiodarone have subsequently led to the development of the noniodinated benzofuran derivative, dronedarone.

The dose of dronedarone was established in the Dronedarone Atrial Fibrillation Study after Electrical Cardioversion (DAFNE) (Touboul et al. 2003). Three different doses (800, 1200, or 1600 mg) of dronedarone daily were compared with placebo in patients following a successful electrical cardioversion. A dose of 800 mg/day delayed the time to recurrence of AF; 35% dronedarone versus 10% placebo at 6 months. While higher doses of dronedarone resulted in better ventricular rate control in patients who converted to atrial fibrillation, higher doses were also associated with increases in the QT interval albeit with no cases of torsades de pointes. Additionally, dronedarone administered at any dose was not associated with any thyroid, pulmonary or ocular side effects. The most important side effects associated with the use of dronedarone were gastrointestinal disturbance. Based on these results, the dose of 400 mg twice daily was chosen and was subsequently studied in patients with either atrial fibrillation or atrial flutter in the twin studies called The European Trial in Atrial Fibrillation or Flutter Patients Receiving

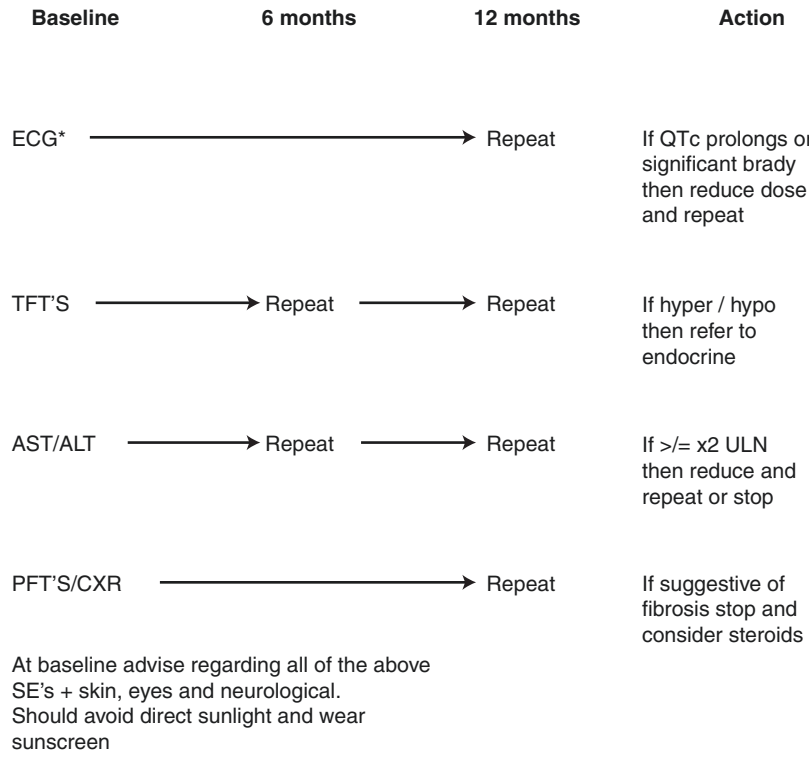

Fig. 10.2 Suggested Monitoring for the Side Effects of Long Term Amiodarone (*Evidence of QTc prolongation, sinus node or AV node conduction abnormalities should prompt close monitoring)

Dronedarone for the Maintenance of Sinus Rhythm (EURIDIS) and the American- Australian-African Trial with Dronedarone in Atrial Fibrillation or Flutter Patients for the Maintenance of Sinus Rhythm (ADONIS) (Singh et al. 2007). These trials randomised patients with a history of paroxysmal atrial fibrillation or atrial flutter to receive either dronedarone or placebo. Dronedarone increased the time to first recurrence of atrial fibrillation from 53 to 116 days, when patients receiving placebo were compared to those administered dronedarone. Furthermore, in patients who had a recurrence of atrial fibrillation dronedarone significantly reduced the ventricular rate. A post hoc analysis revealed a 27% reduction of relative risk of hospitalization and death with dronedarone treatment.

The effect of dronedarone in ventricular rate control for patients with permanent AF was studied in the Efficacy and Safety of Dronedarone for Control of Ventricular Rate (ERATO) (Davy et al. 2008). The addition of dronedarone (800 mg/day) to standard rate-control therapy reduced the ventricular rate by 11.7 beats/min after 2 weeks of treatment and by a mean of 24.5 bpm during exercise.

Dronedarone was studied in patient with moderate to severe left ventricular impairment irrespective of the rhythm in the Antiarrhythmic Trial with Dronedarone in Moderate-to- Severe Congestive Heart Failure Evaluating Morbidity Decrease (ANDROMEDA) (Kober et al. 2008). Patients had a left ventricular ejection fraction less than 35% and had been hospitalized with new or worsening heart failure. In addition, they also needed to present with at least one episode of shortness of breath on minimal exertion or at rest (NYHA III or IV) or paroxysmal nocturnal dyspnoea within the month prior to admission. There was no restriction related to renal function.

After a median follow up period of 2 months, a significantly higher mortality rate was reported with dronedarone treatment (8.1%) as compared with placebo (3.8%). Worsening left ventricular function corresponding with a higher the risk of death and has led to the avoidance of dronedarone in patients with severe LV dysfunction and heart failure.

To help address some of these issues a further study was carried out looking at patients with stable AF and at least one cardiovascular risk factor. The Assess the Efficacy of Dronedarone for the Prevention of Cardiovascular Hospitalization or Death from Any Cause in Patients with Atrial Fibrillation/Atrial Flutter (ATHENA) (Hohnloser et al. 2009) had the composite primary end point of all-cause mortality and cardiovascular hospitalization. 4628 patients with a history of paroxysmal or persistent AF/atrial flutter were randomised to dronedarone 400 mg twice a day versus placebo with 12 months of follow-up. The use of dronedarone was associated with a significant 27% reduction in the primary end point of death or cardiovascular hospitalization. The most frequently reported adverse effect of dronedarone was gastrointestinal, principally nausea and diarrhoea that led to drug discontinuation in several cases. The overall reduction in hospitalisations was a principle reason for dronedarone gaining clinical approval in North America and more recently, led to a second draft guidance by the National Institute for Clinical Excellence (NICE). A recent retrospective analysis comparing patients receiving a first prescription of dronedarone versus other AADs (amiodarone, flecainide, propafenone, or sotalol) found that patients receiving dronedarone was associated had a decreased risk of myocardial infarction and stroke (Ehrlich et al. 2019). These results are consistent with DATA from post hoc studies of the ATHENA trial, which correlated dronedarone administration to a reduced risk of first acute coronary syndrome and stroke as compared to placebo (Connolly et al. 2009; Pisters et al. 2014). It is therefore recommended that dronedarone should be administered as second-line treatment in patients with additional cardiovascular risk factors whose AF has not been controlled by first-line therapy (usually including beta blockers).

Class IV

Verapamil and diltiazem block the L-type calcium channel and principally prolong the atrioventricular nodal refractory period. The VERDICT study showed no benefit in maintenance of sinus rhythm of verapamil over digoxin (Van Noord et al. 2001). Two large trials which examined the use of verapamil in the maintenance of sinus rhythm following an electrical cardioversion both showed verapamil combined with quinidine was similar in efficacy to sotalol with a higher incidence of TdP in the sotalol group (Patten et al. 2004; Fetsch et al. 2004). Due to its negative inotropic effects verapamil should be used cautiously in patients with left ventricular dysfunction. Additionally, verapamil should also be avoided in sick sinus syndrome as it suppresses sinus node automaticity. Both verapamil and diltiazem are similar in efficacy and side effects (other than constipation associated with verapamil). Calcium channel blockade may be a reasonable choice of drug for ventricular rate control in patients with preserved LV function and can be considered as an alternative to ß-blockers.

AAD's Not in the Vaughan Williams Classification

Some drugs such as digoxin, adenosine and ivabradine do not fit into the traditional Vaughan Williams classification.

Digoxin acts directly on the myocardium in order to increase the concentration of intracellular sodium and exert its positive inotropic effects. However, in addition to its vagotonic effects, this may shorten the atrial effective refractory period and therefore increase its potential to develop AF in patients who are in sinus rhythm (Sticherling et al. 2000). Its predominant role in AF is therefore to slow AV conduction (through its vagotonic effects) and thereby reduce the ventricular rate. It is not an ideal drug for acute ventricular rate control as the onset of action is 4–6 h and may not be as effective if the rate is partially sympathetically driven. Data consistently suggests that it may have deleterious effects and therefore it is relatively used as a monotherapy. Nonetheless, it continues to have an important role in the management of AF and is particularly effective when combined with a beta-adrenergic blocker due to

synergistic effects (Fuster et al. 2006). Most recently, data based on the outcomes of the AF-CHF trial found that digoxin use amongst patients with combined heart failure and reduced ejection fraction and AF was associated with increased all-cause mortality (Elayi et al. 2020).

Adenosine is a metabolite of adenosine triphosphate which results in slowing of AV nodal conduction, shortening of the atrial myocardial refractory period and depression of sinus node automaticity (Lerman and Belardinelli 1991). Adenosine is highly effective in terminating supraventricular arrhythmias in which the AV node forms part of the reentrant circuit, such as in the cases of AV nodal reentry and orthodromic reciprocating tachycardia.

Additionally, it can be used for diagnostic purposes such as transiently slowing AV conduction in SVT to identify the underlying rhythm and may also be helpful in differentiating SVT from VT (although very rarely adenosine may terminate a specific type of VT). Side effects such as facial flushing (due to cutaneous vasodilation), dyspnoea, and chest pressure have been reported to occur in about 30% of patients (Platia et al. 1990). Given the short half-life of adenosine, these side effects generally last less than 60 s. The downside to this short duration of action is that in some cases, arrhythmias recur after several minutes following termination with adenosine (DiMarco et al. 1985).

Ivabradine is a novel selective inhibitor of the I_f channel in the SA node, therefore reducing the sinus rate with no effect on either the AV node or intraventricular conduction times (Di Francesco and Camm 2004). Although its principle use is for symptom relief in patients with chronic stable angina, it may also have a clinical role in patients with an inappropriate sinus tachycardia. A recent study examining its use in 18 symptomatic patients with an inappropriate sinus tachycardia (defined as a nonparoxysmal tachyarrhythmia with a P-wave morphology and endocardial activation identical to sinus rhythm and an excessive increase of heart rate in response to minimal physical activity and emotional stress, and nocturnal normalization) showed a significant reduction in heart rate on Holter and exercise stress tests (Calo et al. 2010). Despite the study's small sample size, there may be a role for this drug in these patients where other drug therapies can be relatively ineffective and ablation therapy may carry significant risks.

The Future: Novel AAD's

Given the significant cardiac and non-cardiac side effects associated with current AAD's there has been a huge interest in the development of novel 'atrial selective' drugs for the treatment of AF. These drugs can be broadly divided into amiodarone derivatives such as dronedarone, PM101 and budiodarone; selective Iks blockers such as HMR1556; atrial repolarization-delaying agents such as vernakalant; and sodium channel blockers such as ranolazine.

Atrial Repolarization Delaying Agents: Vernakalant

Vernakalant is a relatively new anti-arrhythmic drug which works by predominantly targeting early-activating K+ channels and frequency-dependent Na+ channels in the atria. It has showed efficacy and safety in recent-onset AF, demonstrating an efficacy of 52% in the acute conversion of recent onset AF compared to a 4% success rate with placebo (Roy et al. 2008). More recently, the results of the randomized double-blind multicentre AVRO trial showed that vernakalant has a higher efficacy for the conversion of AF as well as a greater rate of symptom relief (51.7% converted with vernakalant versus 5.2% with amiodarone) in 254 adult patients with AF. Treatment with vernakalant resulted in a rapid conversion to sinus rhythm, with a median conversion time of 11 min. Most recently, a large meta-analysis of 1358 participants comparing vernakalant to another drug or placebo for the

pharmacological cardioversion of AF deemed vernakalant a viable first-line treatment option for patients with haemodynamically stable recent-onset AF without severe structural heart disease (McIntyre et al. 2019). While the authors raised moderate concern over suspected publication bias, vernakalant appeared to be well tolerated and relatively safe with no cases of ventricular arrhythmias or drug related deaths. The main side effects associated with its use appear to be dysgeusia (30%), transient sneezing (17%), hypotension (5%) and bradycardia (5%). Currently, the use of vernakalant is approved in Europe and Canada and is indicated in patients with AF (⩽7 days) and no heart disease (Class I, level A) or in patients with mild or moderate structural heart disease (Class IIb, level B). Vernakalant may also be considered for recent-onset AF (⩽3 days) following cardiac surgery (class IIb, level B).

Sodium Channel Blockers: Ranolazine

Ranolazine has been shown to be effective as an anti-anginal agent when added to standard medical therapy most likely through various mechanisms but predominantly through its ability to inhibit the inward sodium current. In a similar mechanism it has been postulated that this may have anti-arrhythmic effects in the atria where rapid atrial rates during AF may result in oxidative stress and atrial myocardial ischaemia. The Metabolic Efficiency with Ranolazine for Less Ischaemia in Non-ST-elevation acute coronary syndrome— Thrombolysis in Myocardial Infarction (MERLINTIMI 36) trial compared ranolazine with placebo in 6560 patients hospitalized with acute coronary syndromes. A significant reduction in tacharrhythmias (SVT and VT) was noted on 7-day continuous cardiac monitoring in patients commenced on ranolazine versus placebo (Scirica et al. 2007). There was no effect on sustained arrhythmias such as AF and VT and no overall effect on mortality or recurrent ischaemia. Further clinical studies are required to assess the clinical utility of ranolazine as an AAD.

Important Points

1. Anti-arrhythmic drugs alter the electrical properties of the heart principally by either prolonging the cardiac AP (thus prolonging refractoriness), decreasing conduction velocity, reducing focal automaticity or a combination of these effects.
2. The Vaughan Williams classification categorizes anti-arrhythmic drugs action into groups according to the main mechanism of action. These are:

Class I action block the fast sodium channels which are responsible for phase 0 of the action potential thus affecting its slope and amplitude. These drugs are subdivided according to the rate of binding and dissociation from the sodium channel. Class IB mechanism of action is associated with the most rapid onset of action and dissociation, IA has intermediate activities and IC the slowest.

Class II action block beta adrenergic receptors prolonging the phase 2 and 3 (after chronic use) of the action potential and thus lengthen the effective refractory period.

Class III action refers to prolongation of the action potential duration, principally by inhibition of the potassium channels.

Class IV action inhibits the slow calcium current and therefore depress phase II and III of the AP in certain tissues primarily the SN and AV nodes).

References

Alboni P, Botto GL, Baldi N, et al. Outpatient treatment of recent-onset atrial fibrillation with the "pill-in-the-pocket" approach. N Engl J Med. 2004;351:2384–91.

Aliot E, Denjoy I. Comparison of the safety and efficacy of flecainide versus propafenone in hospital outpatients with symptomatic paroxysmal atrial fibrillation/flutter. The Flecainide AF French Study Group. Am J Cardiol. 1996;77:66A–71A.

Alp NJ, Bell JA, Shahi M. Randomised double blind trial of oral versus intravenous flecainide for the cardioversion of acute atrial fibrillation. Heart. 2000;84:37–40.

Atkinson A, Ruo T. Pharmacokinetics of N-acetylprocainamide. Angiology. 1986;37:959–67.

Belhassen B, Glick A, Viskin S. Efficacy of quinidine in high-risk patients with Brugada syndrome. Circulation. 2004;110:1731–7.

Brogan BL, Olsen NJ. Drug-induced rheumatic syndromes. Curr Opin Rheumatol. 2003;15:76.

Calo L, Rebecchi M, Sette A, et al. Efficacy of ivabradine administration in patients affected by inappropriate sinus tachycardia. Heart Rhythm. 2010;7:1318–23.

Camm AJ. Safety considerations in the pharmacological management of atrial fibrillation. Int J Cardiol. 2008;127:299–306.

Campbell RW. Mexiletine. N Engl J Med. 1987;316:29–34.

Chimienti M, Cullen MT, Casadei G. Safety of long-term flecainide and propafenone in the management of patients with symptomatic paroxysmal atrial fibrillation: report from the Flecainide and Propafenone Italian Study Investigators. Am J Cardiol. 1996;77:60A–75A.

Connolly SJ, Dorian P, Roberts RS, et al. Comparison of β-blockers, amiodarone plus β-blockers, or sotalol for prevention of shocks from implantable cardioverter defibrillators: the OPTIC study: a randomized trial. JAMA. 2006;295(2):165–71. https://doi.org/10.1001/jama.295.2.165.

Connolly SJ, Crijns H, Torp-Pedersen C, et al. Analysis of stroke in ATHENA: a placebo-controlled, double-blind, parallel-arm trial to assess the efficacy of dronedarone 400 mg BID for the prevention of cardiovascular hospitalization or death from any cause in patients with atrial fibrillation/atrial flutter. Circulation. 2009;120:1174–80.

Coplen SE, Antman EM, Berlin JA, et al. Efficacy and safety of quinidine therapy for maintenance of sinus rhythm after cardioversion. A meta-analysis of randomized control trials. Circulation. 1990;82:1106–16.

Davy JM, Herold M, Hoglund C, et al. Dronedarone for the control of ventricular rate in permanent atrial fibrillation: the Efficacy and safety of dRonedArone for the cOntrol of ventricular rate during atrial fibrillation (ERATO) study. Am Heart J. 2008;156:527–9.

Di Francesco D, Camm JA. Heart rate lowering by specific and selective If current inhibition with ivabradine: a new therapeutic perspective in cardiovascular disease. Drugs. 2004;64:1757–65.

DiMarco JP, Sellers TD, Lerman BB, et al. Diagnostic and therapeutic use of adenosinein patients with supraventricular tachyarrhythmias. J Am Coll Cardiol. 1985;6:417–25.

Dorian P, Cass D, Schwartz B, et al. Amiodarone as compared with lidocaine for shock-resistant ventricular fibrillation. N Engl J Med. 2002;346:884–90.

Ehrlich JR, Look C, Kostev K, et al. Impact of dronedarone on the risk of myocardial infarction and stroke in atrial fibrillation patients followed in general practices in Germany. Int J Cardiol. 2019;278:126–32.

Elayi CS, Shohoudi A, Moodie E, et al. Digoxin, mortality, and cardiac hospitalizations in patients with atrial fibrillation and heart failure with reduced ejection fraction and atrial fibrillation: an AF-CHF analysis. Int J Cardiol. 2020;313:48–54.

Fernández-Martinez, Marcos FJ, Garcia-Garmendia JL, et al. Comparison of intravenous flecainide, propafenone, and amiodarone for conversion of acute atrial fibrillation to sinus rhythm. Am J Cardiol. 2000;86:950–3.

Fetsch T, Bauer P, Engberding R, et al. Prevention of atrial fibrillation after cardioversion: results of the PAFAC trial. Eur Heart J. 2004;25:1385–94.

Freemantle N, Cleland J, Young P, et al. Beta Blockade after myocardial infarction: systematic review and meta regression analysis. BMJ. 1999;318:1730–7.

Fuster V, Ryden LE, Cannom DS, et al. European Heart Rhythm Association, Heart Rhythm Society, ACC/AHA/ESC 2006 guidelines for the management of patients with atrial fibrillation--executive summary: a report of the American College of Cardiology/American Heart Association Task Force on Practice Guidelines and the European Society of Cardiology Committee for Practice Guidelines (Writing Committee to Revise the 2001 Guidelines for the Management of Patients With Atrial Fibrillation). J Am Coll Cardiol. 2006;48:854–906.

Goldschlager N, Epstein AE, Naccarelli G, et al. Practical guidelines for clinicians who treat patients with amiodarone. Heart Rhythm. 2007;4:1250–9.

Grace AA, Camm AJ. Quinidine. N Engl J Med. 1998;338:35–45.

Hallstrom AP, Cobb LA, Yu BH, et al. An antiarrhythmic drug experience in 941 patients resuscitated from an initial cardiac arrest between 1970 and 1985. Am J Cardiol. 1991;68:1025–31.

Herlitz J, Bang A, Holmberg M, et al. Rhythm changes during resuscitation from ventricular fibrillation inrelation to delay until defibrillation, number of shocks delivered andsurvival. Resuscitation. 1997;34:17–22.

Hohnloser SH, Crijns H, Eickels M, et al. Effect of dronedarone on cardiovascular events in atrial fibrillation. N Engl J Med. 2009;360:668–78.

Jusko W, Evans W, Schentag J. Applied pharmacokinetics: principles of therapeutic drug monitoring. San Francisco: Applied Therapeutics; 1980. p. 618–38.

Karlson BW, Torstensson I, Abjorn C, et al. Disopyramide in the maintenance of sinus rhythm after electroconversion of atrial fibrillation. A placebo-controlled one-year follow-up study. Eur Heart J. 1988;3:284–90.

Katkov W, Ellrodt AG. Neutropenia and procainamide. Am Heart J. 1985;110:1321–2.

Kober L, Torp-Pedersen C, McMurray JJ, et al. Increased mortality after dronedarone therapy for severe heart failure. N Engl J Med. 2008;358:2678–87.

Komura S, Chinushi M, Furushima H, et al. Efficacy of procainamide and lidocaine in terminating sustained monomorphic ventricular tachycardia. Circ J. 2010;74(5):43–6.

Kuck KH, Cappato R, Siebels J, Ruppel R. Randomized comparison of antiarrhythmic drug therapy with implantable defibrillators in patients resuscitated from cardiac arrest: the Cardiac Arrest Study Hamburg (CASH). Circulation. 2000;102:748–54.

Kuhlkamp V, Schirdewan A, Stangl K, et al. Use of metoprolol CR/XL to maintain sinus rhythm after conversion from persistent atrial fibrillation: a randomized, double-blind, placebo-controlled study. J Am Coll Cardiol. 2000;36:139–46.

Lafuente-Lafuente C, Mouly S, Longas-Tejero MA, et al. Antiarrhythmic drugs for maintaining sinus rhythm after cardioversion of atrial fibrillation: a systematic review of randomized controlled trials. Arch Intern Med. 2006;166:719–28.

Lehmann MH, Hardy S, Archibald D, et al. Sex difference in risk of torsade de pointes with d,l-sotalol. Circulation. 1996;94:2535–4251.

Lerman BB, Belardinelli L. Cardiac electrophysiology of adenosine. Basic and clinical concepts. Circulation. 1991;83:1499–509.

Lie KI, Wellens HJ, van Capelle FJ, Durrer D. Lidocaine in the prevention of primary ventricular fibrillation: a double-blind, randomized study of 212 consecutive patients. N Engl J Med. 1974;291:1324–6.

MacMahon S, Collins R, Peto R, et al. Effects of prophylactic lidocaine in suspected acute myocardial infarction. An overview of results from the randomized, controlled trials. JAMA. 1988;260:1910–6.

Markey GC, Salter N, Ryan J. Intravenous flecainide for emergency department management of acute atrial fibrillation. J Emerg Med. 2018;54:320–7.

Mason JW. A comparison of seven antiarrhythmic drugs in patients with ventricular tachyarrhythmias. Electrophysiologic Study versus Electrocardiographic Monitoring Investigators. Engl J Med. 1993;329:452–8.

McAlister FA, Wiebe N, Ezekowitz JA, et al. Meta-analysis: beta-blocker dose, heart rate reduction, and death in patients with heart failure. Ann Intern Med. 2009;150:784–94.

McCornish M, Robinson C, Kitson D, et al. Clinical electrophysiologic effects of mexiletine. Postgrad Med. 1977;33 (Suppl):85.

McIntyre WF, Healey JS, Bhatnagar AK, et al. Vernakalant for cardioversion of recent-onset atrial fibrillation: a systematic review and meta-analysis. Europace. 2019;21(8):1159–66. https://doi.org/10.1093/europace/euz175.

Patten M, Maas R, Bauer P, et al. Suppression of paroxysmal atrial tachyarrhythmias—results of the SOPAT trial. Eur Heart J. 2004;25:1395–404.

Pisters R, Hohnloser SH, Connolly SJ, et al. Effect of dronedarone on clinical end points in patients with atrial fibrillation and coronary heart disease: insights from the ATHENA trial. Europace. 2014;16:174–81.

Platia E, McGovern B, Scheinman MM, et al. Adenosine for paroxysmal supraventricular tachycardia: dose ranging and comparison with verapamil. Ann Intem Med. 1990;113:104–10.

Plewan A, Lehmann G, Ndrepepa G, et al. Maintenance of sinus rhythm after electrical cardioversion of persistent atrial fibrillation; sotalol vs bisoprolol. Eur Heart J. 2001;22:1504–10.

Podrid PJ, Lampert S, Graboys TB, et al. Aggravation of arrhythmia by antiarrhythmic drugs--incidence and predictors. Am J Cardiol. 1987;59:38E–44E.

Pollick C. Muscular subaortic stenosis: hemodynamic and clinical improvement after disopyramide. N Engl J Med. 1982;307:997–9.

Preliminary report. Effect of encainide and flecainide on mortality in a randomized trial of arrhythmia suppression after myocardial infarction. The Cardiac Arrhythmia Suppression Trial (CAST) Investigators. N Engl J Med. 1989;321:406–12.

Reimold SC, Chalmers TC, Berlin JA, Antman EM. Assessment of the efficacy and safety of antiarrhythmic therapy for chronic atrial fibrillation: observations on the role of trial design and implications of drug-related mortality. Am Heart J. 1992;124:924–32.

Roos JC, Paalman ACA, Dunning AJ. Electrophysiologic effects of mexiletine in man. Br Heart J. 1976;38:62.

Rothenberg F, Franklin JO, DeMaio SJ. Use, value, and toxicity of amiodarone. Heart Dis Stroke. 1994;3:19–23.

Roy D, Talajic M, Dorian P, et al. Amiodarone to prevent recurrence of atrial fibrillation. Canadian Trial of Atrial Fibrillation Investigators. N Engl J Med. 2000;342:913–20.

Roy D, Pratt CM, Torp-Pedersen C, et al. Atrial Arrhythmia Conversion Trial Investigators. Vernakalant hydrochloride for rapid conversion of atrial fibrillation: a phase 3, randomized, placebo-controlled trial. Circulation. 2008;117:1518–25.

Sauer AJ, Moss AJ, McNitt S, et al. Long QT syndrome in adults. J Am Coll Cardiol. 2007;49:329–37.

Scirica BM, Morrow DA, Hod H, et al. E. Effect of ranolazine, an antianginal agent with novel electrophysiological properties, on the incidence of arrhythmias in patients with non ST-segment elevation acute coronary syndrome: results from the Metabolic Efficiency With Ranolazine for Less Ischemia in Non ST-Elevation Acute Coronary Syndrome Thrombolysis in Myocardial Infarction 36 (MERLIN-TIMI 36) randomized controlled trial. Circulation. 2007;116:1647–52.

Singh BN, Wellens HJ, Hockings BE. Electropharmacological control of cardiac arrhythmias. New York, NY: Futura Publishing Co; 1994.

Singh BN, Connolly SJ, Crijns HJ, et al. Dronedarone for maintenance of sinus rhythm in atrial fibrillation or flutter. N Engl J Med. 2007;357:987–99.

Sticherling C, Oral H, Horrocks J, et al. Effects of digoxin on acute, atrial fibrillation–induced changes in atrial refractoriness. Circulation. 2000;102:2503–8.

Thibault B, Nattel S. Optimal management with Class I and Class III antiarrhythmic drugs should be done in the outpatient setting: protagonist. J Cardiovasc Electrophysiol. 1999;10:472–81.

Touboul P, Brugada J, Capucci A, et al. Dronedarone for prevention of atrial fibrillation: a dose-ranging study. Eur Heart J. 2003;24:1481–7.

Tsai CF, Chen SA, Tai CT, et al. Idiopathic ventricular fibrillation: clinical, electrophysiologic characteristics and long-term outcomes. Int J Cardiol. 1998;64:47–55.

Tsolakas TC, Davies JP, Oram S. Propranolol in attempted maintenance of sinus rhythm after electrical defibrillation. Lancet. 1964;18:1064.

Van Noord T, Van Gelder IC, Tieleman RG, et al. VERDICT: the verapamil versus digoxin cardioversion trial: a randomized study on the role of calcium lowering for maintenance of sinus rhythm after cardioversion of persistent atrial fibrillation. J Cardiovasc Electrophysiol. 2001;12:766–9.

Vassallo P, Trohman RG. Prescribing amiodarone. An evidence-based review of clinical indications. JAMA. 2007;298:1312–22.

Viskin S, Chorin E, Viskin D, et al. Quinidine-responsive polymorphic ventricular tachycardia in patients with coronary Heart Disease. Circulation. 2019;139(20):2304–14.

Waldo AL, Camm AJ, de Ruyter H, et al. Effect of d-sotalol on mortality in patients with left ventricular dysfunction after recent and remote myocardial infarction. The SWORD Investigators. Survival with oral d-Sotalol. Lancet. 1996;348:7–12.

Weaver WD, Fahrenbruch CE, Johnson DD, et al. Effect of epinephrine and lidocaine therapy on outcome after cardiac arrest due to ventricular fibrillation. Circulation. 1990;82:2027–34.

Yap YG, Camm AJ. Drug induced QT prolongation and torsades de pointes. Heart. 2003;89:1363–72.

Index

B. M. Glover, P. Brugada (eds.), *Clinical Handbook of Cardiac Electrophysiology*,
https://doi.org/10.1007/978-3-030-74319-2